RS-8232-21 67154 8524

cy 1   P. W. Dean

Interpretations of Single-Well Hydraulic Tests Conducted At and Near The Waste Isolation Pilot Plant (WIPP) Site, 1983-1987

8232-2//067154

00000001   -

Richard L. Beauheim

INTERPRETATIONS OF SINGLE-WELL HYDRAULIC TESTS CONDUCTED AT AND NEAR THE WASTE ISOLATION PILOT PLANT (WIPP) SITE, 1983-1987

Richard L. Beauheim
Earth Sciences Division
Sandia National Laboratories

ABSTRACT

Both single-well and multiple-well hydraulic tests have been performed in wells at and near the WIPP site as part of the site hydrogeologic-characterization program. The single-well tests conducted from 1983 to 1987 in 23 wells are the subject of this report. The stratigraphic horizons tested include the upper Castile Formation; the Salado Formation; the unnamed, Culebra, Tamarisk, Magenta, and Forty-niner Members of the Rustler Formation; the Dewey Lake Red Beds; and Cenozoic alluvium. Tests were also performed to assess the integrity of a borehole plug isolating a pressurized brine reservoir in the Anhydrite III unit of the Castile Formation. The types of tests performed included drillstem tests (DST's), rising-head slug tests, falling-head slug tests, pulse tests, and pumping tests.

The Castile and Salado testing was performed at well WIPP-12 to try to define the source of high pressures measured at the WIPP-12 wellhead between 1980 and 1985. The tests of the plug above the Castile brine reservoir indicated that the plug may transmit pressure, but if so the apparent surface pressure from the underlying brine reservoir is significantly lower than the pressure measured at the wellhead. The remainder of the upper Castile did not show a pressure response differentiable from that of the plug. All attempts at testing the Salado in WIPP-12 using a straddle-packer DST tool failed because of an inability to locate good packer seats. Four attempts to test large sections of the Salado using a single-packer DST tool and a bridge plug were successful. All zones tested showed pressure buildups, but none

showed a clear trend to positive surface pressures. The results of the WIPP-12 testing indicate that the source of the observed high pressures is within the Salado Formation rather than within the upper Castile Formation, and that this source must have a very low flow capacity and can only create high pressures in a well shut in over a period of days to weeks.

DST's performed on the lower siltstone portion of the unnamed lower member of the Rustler Formation at H-16 indicated a transmissivity for the siltstone of about 2.4×10^{-4} ft²/day. The formation pressure of the siltstone is higher than that of the overlying Culebra at H-16 (compensated for the elevation difference), indicating the potential for vertical leakage upward into the Culebra. However, the top of the tested interval is separated from the Culebra by over 50 ft of claystone, halite, and gypsum.

The Culebra Dolomite Member of the Rustler Formation was tested in 22 wells. In 12 of these wells (H-4c, H-12, WIPP-12, WIPP-18, WIPP-19, WIPP-21, WIPP-22, WIPP-30, P-15, P-17, ERDA-9, and Cabin Baby-1), falling-head slug tests were the only tests performed. Both falling-head and rising-head slug tests were performed in H-1, and only a rising-head slug test was performed in P-18. DST's were performed in conjunction with rising-head slug tests in wells H-14, H-15, H-16, H-17, and H-18. At all of these wells except H-18, the indicated transmissivities were 1 ft²/day or less and single- porosity models fit the data well. At H-18, the Culebra has a transmissivity of about 2 ft²/day. The apparent single-porosity behavior of the Culebra at H-18 may be due to the small spatial scale of the tests rather than to the intrinsic nature of the Culebra at that location. Pumping tests were performed in the other 3 Culebra wells. The Culebra appears to behave hydraulically like a double-porosity medium at wells H-8b and DOE-1, where transmissivites are 8.2 and 11 ft²/day, respectively. The Culebra transmissivity is highest, 43 ft²/day, at the Engle well. No double-porosity behavior was apparent in the Engle drawdown data, but the observed single-porosity behavior may be related more to wellbore and near-wellbore conditions than to the true nature of the Culebra at that location.

The claystone portion of the Tamarisk Member of the Rustler Formation was tested in wells H-14 and H-16. At H-14, the pressure in the claystone failed to stabilize in three days of shut-in testing, leading to the conclusion that the transmissivity of the claystone is too low to measure in tests performed on the time scale of days. Similar behavior at H-16 led to the abandonment of testing at that location as well.

The Magenta Dolomite Member of the Rustler Formation was tested in wells H-14 and H-16. At H-14, examination of the pressure response during DST's revealed that the Magenta had taken on a significant overpressure skin during drilling and Tamarisk-testing activities. Overpressure-skin effects were less pronounced during the drillstem and rising-head slug tests performed on the Magenta at H-16. The transmissivity of the Magenta at H-14 is about 5.5×10^{-3} ft²/day, while at H-16 it is about 2.7×10^{-2} ft²/day. The static formation pressures calculated for the Magenta at H-14 and H-16 are higher than those of the other Rustler members.

The Forty-niner Member of the Rustler Formation was tested in wells H-14 and H-16. Two portions of the Forty-niner were tested at H-14: the medial claystone and the upper anhydrite. DST's and a rising-head slug test were performed on the claystone, indicating

4

a transmissivity of about 7×10^{-2} ft^2/day. A buildup test of the Forty-niner anhydrite revealed a transmissivity too low to measure on a time scale of days. A pulse test, DST's, and a rising-head slug test of the Forty-niner clay at H-16 indicated a transmissivity of about 5.3×10^{-3} ft^2/day. Formation pressures estimated for the Forty-niner at H-14 and H-16 are lower than those calculated for the Magenta (compensated for the elevation differences), indicating that water cannot be moving downwards from the Forty-niner to the Magenta at these locations.

The lower portion of the Dewey Lake Red Beds, tested only at well H-14, has a transmissivity lower than could be measured in a few days' time. No information was obtained pertaining to the presence or absence of a water table in the Dewey Lake Red Beds at H-14.

The hydraulic properties of Cenozoic alluvium were investigated in a pumping test performed at the Carper well. The alluvium appears to be under water-table conditions at that location. An estimated 120 ft of alluvium were tested, with an estimated transmissivity of 55 ft^2/day.

The database on the transmissivity of the Culebra dolomite has increased considerably since 1983. At that time, values of Culebra transmissivity were reported from 20 locations. This report and other recent reports have added values from 18 new locations, and have significantly revised the estimated transmissivities reported for several of the original 20 locations. In general, locations where the Culebra is fractured, exhibits double-porosity hydraulic behavior, and has a transmissivity greater than 1 ft^2/day are usually, but not always, correlated with the absence of halite in the unnamed member beneath the Culebra. This observation has led to a hypothesis that the dissolution of halite from the unnamed member causes subsidence and fracturing of the Culebra. This hypothesis is incomplete, however, because relatively high transmissivities have been measured at DOE-1 and H-11 where halite is still present beneath the Culebra, and low transmissivity has been measured at WIPP-30 where halite is absent beneath the Culebra.

Recent measurements of the hydraulic heads of the Rustler members confirm earlier observations that over most of the WIPP site, vertical hydraulic gradients within the Rustler are upward from the unnamed lower member to the Culebra, and downward from the Magenta to the Culebra. New data on hydraulic heads of the Forty-niner claystone show that present hydraulic gradients are upwards from the Magenta to the Forty-niner, effectively preventing precipitation at the surface at the WIPP site from recharging the Magenta or deeper Rustler members.

TABLE OF CONTENTS

FIGURES

TABLES

INTERPRETATIONS OF SINGLE-WELL HYDRAULIC TESTS CONDUCTED AT AND NEAR THE WASTE ISOLATION PILOT PLANT (WIPP) SITE, 1983-1987

1. INTRODUCTION

This report presents the results of single-well hydraulic tests performed in 23 wells in the vicinity of the Waste Isolation Pilot Plant (WIPP) site in southeastern New Mexico (Figure 1-1) between 1983 and 1987. The WIPP is a U.S. Department of Energy research and development facility designed to demonstrate safe disposal of transuranic radioactive wastes resulting from the nation's defense programs. The WIPP facility will lie in bedded halite in the lower Salado Formation. The tests reported herein were conducted in the Salado Formation, in the underlying Castile Formation, and in the overlying Rustler Formation, Dewey Lake Red Beds, and Cenozoic alluvium. These tests were performed under the technical direction of Sandia National Laboratories, Albuquerque, New Mexico.

Most of the tests discussed in this report were performed in the Culebra Dolomite Member of the Rustler Formation. The Culebra was tested at wells H-1, H-4c, H-8b, H-12, H-14, H-15, H-16, H-17, H-18, WIPP-12, WIPP-18, WIPP-19, WIPP-21, WIPP-22, WIPP-30, P-15, P-17, P-18, ERDA-9, Cabin Baby-1, DOE-1, and Engle. The Forty-niner, Magenta, and Tamarisk Members of the Rustler were tested in H-14 and H-16. The unnamed lower member of the Rustler Formation was tested in H-16. The Dewey Lake Red Beds were tested in well H-14. Alluvium of Cenozoic age was tested in the Carper well. The Castile and Salado Formations were tested in WIPP-12. With the exception of additional testing performed at DOE-2 that has been previously reported by Beauheim (1986), this report discusses all single-well testing initiated by Sandia and its subcontractors at the WIPP site from 1983 through 1987.
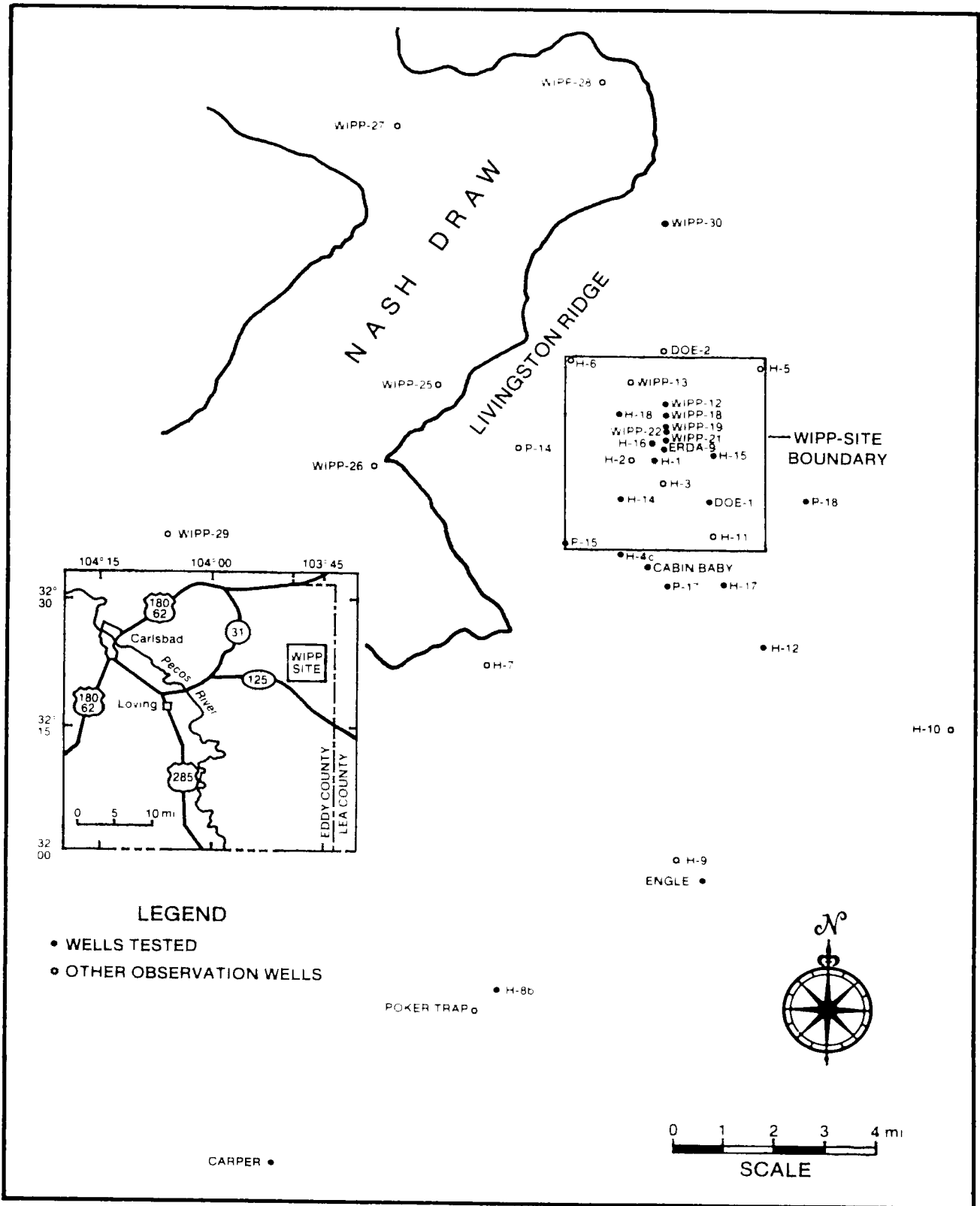
Figure 1-1. Locations of the WIPP Site and Tested Wells

2. SITE HYDROGEOLOGY

The WIPP site is located in the northern part of the Delaware Basin in southeastern New Mexico. WIPP-site geologic investigations have concentrated on the upper seven formations typically found in that part of the Delaware Basin. These are, in ascending order, the Bell Canyon Formation, the Castile Formation, the Salado Formation, the Rustler Formation, the Dewey Lake Red Beds, the Dockum Group, and the Gatuna Formation (Figure 2-1). All of these formations are of Permian age, except for the Dockum Group, which is of Triassic age, and the Gatuna, which is a Quaternary deposit. Of these formations, the Bell Canyon and the Rustler contain the most-transmissive, regionally continuous saturated intervals.

SYSTEM	SERIES	GROUP	FORMATION	MEMBER
RECENT	RECENT		SURFICIAL DEPOSITS	
QUATER-NARY	PLEISTO-CENE		MESCALERO CALICHE	
			GATUNA	
TRIASSIC		DOCKUM	UNDIVIDED	
PERMIAN	OCHOAN		DEWEY LAKE RED BEDS	
			RUSTLER	Forty-niner
				Magenta Dolomite
				Tamarisk
				Culebra Dolomite
				unnamed
			SALADO	Vaca Triste Sandstone
				Cowden Anhydrite
			CASTILE	
	GUADALUPIAN	DELAWARE MOUNTAIN	BELL CANYON	
			CHERRY CANYON	
			BRUSHY CANYON	

Figure 2-1.   WIPP-Area Stratigraphic Column

The Castile Formation at the WIPP site is composed of five informal members (in ascending order): Anhydrite I, Halite I, Anhydrite II, Halite II, and Anhydrite III. Apart from isolated brine reservoirs sometimes found in fractured portions of the upper Castile anhydrites (Popielak et al., 1983), little is known about Castile hydrology because of the extremely low permeabilities of the unfractured anhydrite and halite units (Mercer, 1987).

The Salado Formation is approximately 2000 ft thick at the WIPP site, and is composed largely of halite, with minor amounts of interspersed clay and polyhalite. The Salado also contains interbeds of anhydrite, polyhalite, clay, sylvite, and langbeinite. Jones et al. (1960) labeled several of the anhydrite and/or polyhalite interbeds that are traceable over most of the Delaware Basin "Marker Beds" and numbered them from 101 to 145, increasing downward. The WIPP facility horizon lies between Marker Beds 138 and 139. Because of the extremely low permeability of halite, few hydraulic tests have been attempted in the Salado, and little is known about Salado hydrology (Mercer, 1987).

At the locations where the Rustler Formation was tested, its top lies from 231 (P-15) to 692 ft (H-15) below ground surface, and its bottom lies from 542 (P-15) to 1088 ft (P-18) deep. At these locations, the Rustler consists of five mappable members (in ascending order): the unnamed lower member, the Culebra Dolomite Member, the Tamarisk Member, the Magenta Dolomite Member, and the Forty-niner Member. The unnamed lower member is composed of a layered sequence of clayey siltstone, anhydrite, and halite (absent on the western side of the WIPP site) ranging from 95 (WIPP-30) to 150 ft (P-18) thick. The Culebra is a light olive-gray, fine-grained, vuggy, silty dolomite, 21 (WIPP-18) to 29 ft (P-18) thick. The Tamarisk Member is composed of two anhydrite and/or gypsum units with a silty-claystone interbed which contains halite along the southern and central portions of the eastern boundary of the WIPP site. The Tamarisk has a total thickness of 84 (WIPP-19, ERDA-9, DOE-1) to 179 ft (P-18). The Magenta Dolomite Member consists of a silty, gypsiferous, laminated dolomite, 22 (H-8b) to 27 ft (P-15) thick. The Forty-niner Member consists of two anhydrite/gypsum units separated by a silty claystone interbed which contains halite east of the

WIPP site. The aggregate thickness of the Forty-niner varies between 55 (DOE-1) and 76 ft (P-18).

All of the Rustler members are believed to be saturated. The Culebra dolomite is the most transmissive member, and is considered to be the most important potential groundwater-transport pathway for radionuclides which may escape from the WIPP facility to reach the accessible environment. Hence, the vast majority of hydrologic tests performed at the WIPP site have examined the hydraulic properties of the Culebra. The Magenta dolomite is generally considered to be the second-most transmissive Rustler member, and has been tested at numerous locations by the U.S. Geological Survey (Mercer, 1983). Magenta hydraulic heads are generally higher than those of the Culebra. The other members of the Rustler are believed to have low permeabilities; few hydraulic tests have beenperformed on them and little is known about their hydraulic properties.

The Dewey Lake Red Beds consist of siltstone with claystone and sandstone interbeds. Numerous bedding-plane breaks and fractures at various angles to the bedding are filled with secondary selenite. A well H-14, the Dewey Lake Red Beds are 320 ft thick, lying from 40 to 360 ft below ground surface. Continuous zones of saturation have not been observed within the Dewey Lake where it overlies the underground WIPP facility, although some minor, possibly perched, moist zones have been noted (Mercer, 1983). The Dewey Lake does provide small quantities of water to wells south and southwest of the WIPP site (Mercer, 1983).

Cenozoic alluvium forms aquifers in much of the Delaware Basin, particularly in northern Texas. The alluvium consists of fluvial deposits, caliche, gypsite, conglomerates, aeolian sands, terrace deposits, and playa deposits (Richey et al., 1985). The alluvium is thickest in depressions caused by dissolution of the Salado. In southeastern Eddy County, the alluvium occurs past the erosional limit of the Dewey Lake Red Beds, and rests on an erosional/dissolution surface that moves progressively downsection from east to west from the Rustler to the Castile (Bachman, 1984).

3. TEST WELLS

Most of the wells discussed in this report were drilled from 1974 to 1987 for a variety of purposes. Many of them have been recompleted one or more times since the original drilling. Some of the wells are, or were, open holes through the strata tested, while others are cased and perforated to the tested intervals. The following sections contain brief histories of the wells, along with descriptions of their configurations at the times of testing. Unless otherwise indicated, all depths listed below are referenced to ground surface.

3.1 H-1

Well H-1 was drilled in May and June 1976 as the first hydrologic test hole for the Rustler Formation at the WIPP site. After drilling, selected coring, and open-hole testing, the well was reamed to a diameter of 9.875 inches to a total depth of 856 ft (Mercer and Orr, 1979). Seven-inch casing was installed and cemented from 848 ft to the surface, and a cement plug was left in the casing at a depth of 831 ft. Three sections of the casing were subsequently perforated using jet shots: the Rustler/Salado contact zone between 803 and 827 ft; the interval between 675 and 703 ft, including the Culebra from 676 to 699 ft; and the interval between 562 and 590 ft, including the Magenta from 563 to 589 ft. Following testing in 1977, a retrievable bridge plug was set in the casing at about 790 ft, and a production-injection packer (PIP) was set on 2.375-inch tubing at about 651 ft. This configuration allowed monitoring of the Culebra water level through the 2.375-inch tubing, and monitoring of the Magenta water level in the annulus between the well casing and the tubing. The PIP was replaced with a similar PIP in July 1987 set from 645.0 to 649.4 ft on 2.375-inch tubing. The Culebra interval was developed by bailing on August 27, September 1, and September 15, 1987 in preparation for slug testing (Stensrud et al., 1988). A small-diameter minipacker was set in the tubing temporarily at about 600 ft for use in the slug testing. The configuration of H-1 at the time of the 1987 testing is shown in Figure 3-1.
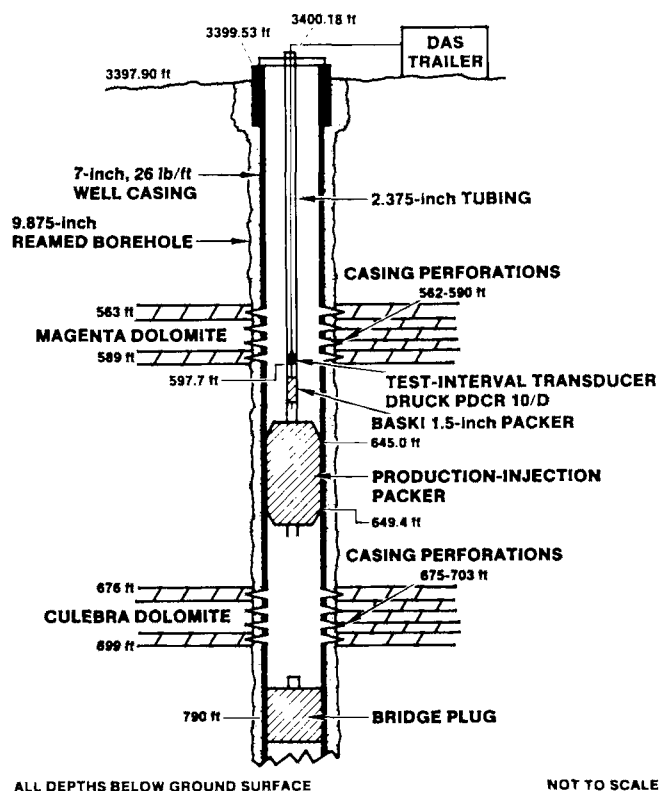
Figure 3-1.   Well Configuration for H-1 Slug Tests

3.2 H-4c

Well H-4c was originally drilled in April and May 1978 to serve as a Rustler-Salado contact monitoring well. A 7.875-inch hole was drilled and reamed to a depth of 609.5 ft, and 5.5-inch casing was cemented from that depth to the surface. A 4.75-inch hole was then cored to a total depth of 661 ft, about 35 ft into the Salado Formation (Mercer et al., 1981). In February 1981, a retrievable bridge plug was set in the casing at a depth of about 530 ft. The depth interval from 494 to 520 ft was then shot-perforated to provide access to the Culebra. Mercer et al. (1981) report the Culebra at H-4c as lying between 490 and 516 ft

deep. The gamma-ray log used to guide the perforation shows the Culebra from 489 to 515 ft deep, which indicates that the upper 4 to 5 ft of the Culebra are apparently not perforated at H-4c. For slug testing, a PIP was temporarily set in the casing from 479.2 to 483.6 ft deep on 2.375-inch tubing. Figure 3-2 shows the configuration of H-4c during the 1986 slug test.
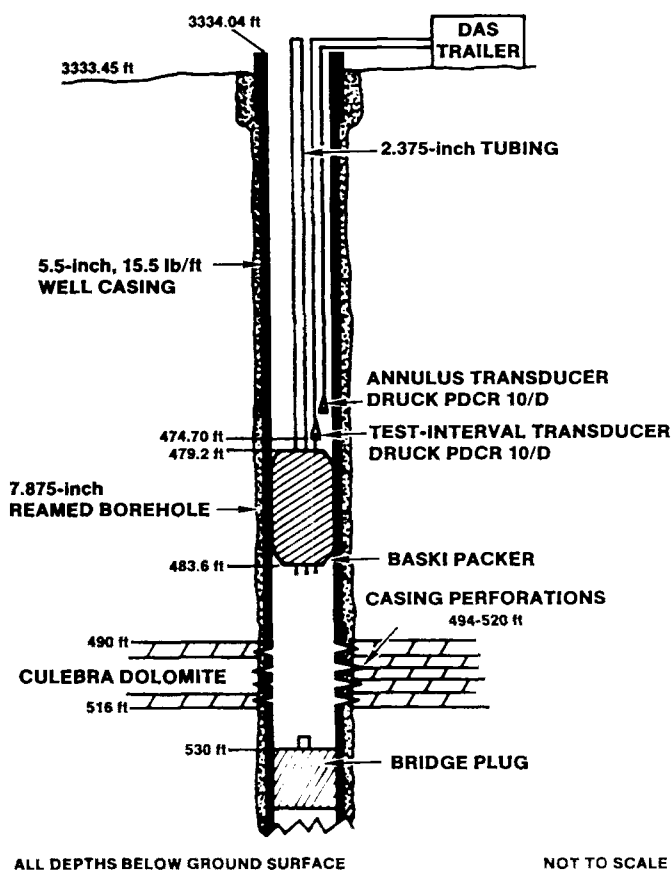
Figure 3-2. Well Configuration for H-1 Slug Tests

3.3 H–8b

Well H-8b was drilled in August 1979 by the USGS as one of 3 wells in the H-8 borehole complex (Figure 3-3). The hole was drilled and reamed to a diameter of 9.75 inches down to 575 ft, and 7-inch casing was set and cemented from 574 ft to the surface. A 6.125-inch hole was then cored to a total

depth of 624 ft. The Culebra at H-8 lies from 588 to 614 ft below land surface (Wells and Drellack, 1982). The open interval in H-8b includes, therefore, the lower 13 ft of the Tamarisk Member, which consists of anhydrite and gypsum, the entire Culebra dolomite, and the upper 10 ft of the unnamed lower member of the Rustler, which consists of mudstone and gypsum. Only the Culebra portion of this interval is believed to have significant permeability. For testing in 1985, a pump was installed in the well below a packer set from 557.7 to 561.9 ft on 1.5-inch galvanized pipe. The configuration of the well at the time of the December 1985 pumping test is shown in Figure 3-4.
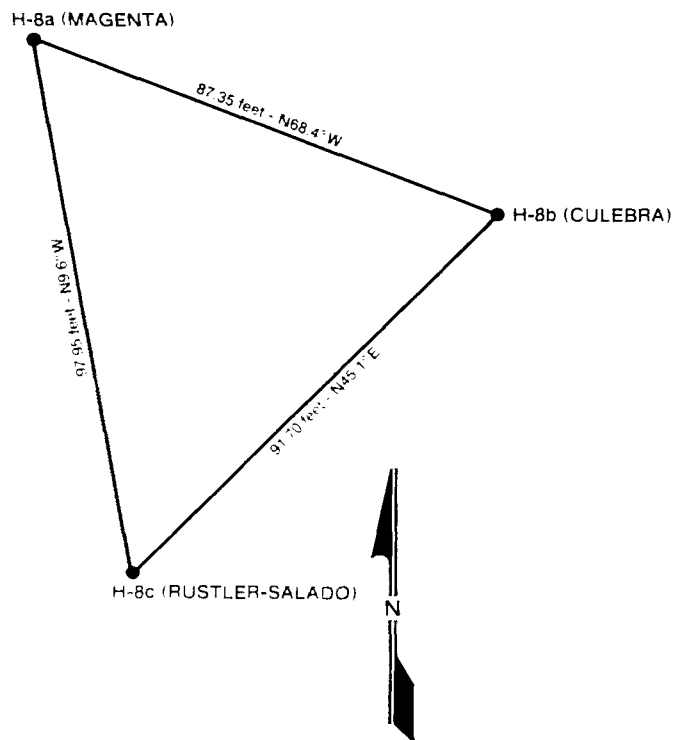
Figure 3-3.   Plan View of the Wells at the H-8 Hydropad

3.4 H–12

Well H-12 was drilled in October 1983 to provide hydrologic and stratigraphic data southeast of the WIPP site. The hole was cored and reamed to a diameter of 7.875 inches to a depth of 820 ft, and
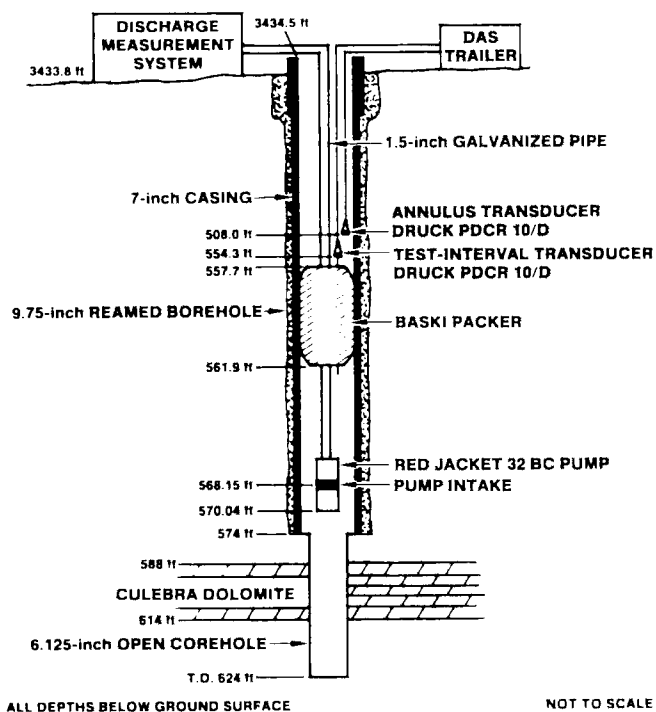
Figure 3-4. Well Configuration for H-8b Pumping Test

Figure 3-5. Well Configuration for H-12 Slug Tests

5.5-inch casing was cemented from that depth to the surface (HydroGeoChem, 1985). The hole was then deepened to 1001 ft, 21 ft into the Salado Formation, by coring and reaming to a diameter of 4.75 inches. The bottom of the hole was plugged back with cement to a depth of 890 ft. As a result, the well is open to the lower 3 ft of the Tamarisk from 820 to 823 ft, the Culebra from 823 to 850 ft, and the unnamed lower member of the Rustler from 850 to 890 ft. The well was developed by bailing on July 10, 13, 15, and 17, 1987 in preparation for slug testing (Stensrud et al., 1988). A PIP on 2.375-inch tubing was set in the well casing from 810.3 to 814.7 ft from August to September 1987 to aid in testing. In addition, a minipacker was set in the tubing at about 484 ft. The configuration of H-12 at the time of testing is shown in Figure 3-5.

3.5 H-14

H-14 was drilled in October 1986 to provide a Culebra monitoring well in the southwest quadrant of the WIPP site where no other Culebra wells existed (see Figure 1-1). A 7.875-inch hole was drilled and reamed to a depth of 533 ft, stopping about 12 ft above the Culebra. After the Tamarisk, Magenta, Forty-niner, and Dewey Lake Red Beds were tested, 5.5-inch casing was set and cemented from 532 ft to the surface. A 4.5-inch hole was then cored to 574 ft. Following Culebra tests, the hole was reamed to 4.75 inches, and deepened to the final depth of 589 ft. Stratigraphic depths of the formation encountered and the final as-built configuration of H-14 are shown in Figure 3-6.

Figure 3-6 (Well H-14)

Diagram labels (left to right):

3345.48 ft
3347.11 ft

13 ft HOLOCENE DEPOSITS
GATUÑA FORMATION
40 ft

DEWEY LAKE RED BEDS

359.5 ft

RUSTLER FORMATION

FORTY-NINER MEMBER
ANHYDRITE/GYPSUM
390 ft CLAYSTONE
405 ft ANHYDRITE/GYPSUM
424 ft MAGENTA DOLOMITE MEMBER
448 ft

TAMARISK MEMBER
ANHYDRITE/GYPSUM
517 ft CLAYSTONE
525 ft ANHYDRITE/GYPSUM
545 ft

CULEBRA DOLOMITE MEMBER
571 ft UNNAMED LOWER MEMBER

12.25-inch HOLE
8.625-inch, 28 lb/ft CONDUCTOR CASING
39 ft
7.875-inch REAMED BOREHOLE
5.5-inch, 15.5 lb/ft WELL CASING
532 ft
4.75-inch OPEN HOLE
TOTAL DEPTH 589 ft

ALL DEPTHS BELOW GROUND SURFACE   NOT TO SCALE

Figure 3-6. As-Built Configuration for Well H-14

Figure 3-7 (Well H-15)

Diagram labels (left to right):

3480.22 ft
3481.63 ft

18 ft HOLOCENE DEPOSITS
GATUÑA
42 ft DOCKUM GROUP
168 ft

DEWEY LAKE RED BEDS

692 ft

RUSTLER FORMATION

FORTY-NINER MEMBER

748 ft MAGENTA DOLOMITE MEMBER
773 ft

TAMARISK MEMBER

861 ft CULEBRA DOLOMITE MEMBER
883 ft UNNAMED LOWER MEMBER

12.25-inch HOLE
8.625-inch, 28 lb/ft CONDUCTOR CASING
39 ft
7.875-inch REAMED BOREHOLE
5.5-inch, 15.5 lb/ft WELL CASING
853 ft
4.75-inch OPEN HOLE
TOTAL DEPTH 900 ft

ALL DEPTHS BELOW GROUND SURFACE   NOT TO SCALE

Figure 3-7. As-Built Configuration for Well H-15

3.6 H-15

H-15 was drilled in November 1986 to provide a Culebra monitoring well in the east-central portion of the WIPP site where no other Culebra wells existed (see Figure 1-1). A 7.875-inch hole was drilled to a depth of 854 ft, about 7 ft above the top of the Culebra, and 5.5-inch casing was set and cemented from 853 ft to the surface. The hole was then cored and reamed through the Culebra to about 891 ft to a diameter of 4.75 inches. Following tests of the Culebra, the hole was deepened at a diameter of 4.75 inches to its final depth of 900 ft. Stratigraphic depths of the formations encountered and the final as-built configuration of the well are shown in Figure 3-7.

3.7 H-16

H-16 was drilled in July and August 1987 to provide a location to monitor the hydraulic responses of the members of the Rustler during construction of the WIPP Air-Intake Shaft. A hole was rotary-drilled and reamed to a diameter of 9.625 inches to a depth of 470 ft, and 7-inch casing was installed and cemented in place from the surface to a depth of 469 ft. The hole was deepened in five steps to its final total depth of 850.9 ft. Each member of the Rustler was successively cored and reamed to a 4.75-inch diameter. Drillstem, slug, and/or pulse tests were performed on each member before the next member was cored. After all testing was finished, the hole

was reamed to a final diameter of 6.125 inches. The well was completed by installing a 5-packer system that isolates each of the Rustler members and allows monitoring of fluid pressure in each member. Stratigraphic depths of the formations encountered and the 5-packer completion of the well are shown in Figure 3-8.

3.8 H-17

Well H-17 was drilled from September to November 1987 to investigate an area south of the WIPP site that was believed, on the basis of computer modeling (Haug et al., 1987) and surface geophysical surveys (Bartel, in preparation), to have high transmissivity in the Culebra. A 7.875-inch hole was drilled to a depth of about 510 ft, just below the top of the Rustler Formation. The hole was then cored to a depth of 693 ft, about 13 ft above the top of the Culebra. After reaming to 9.625 inches, 7-inch casing was set and cemented from 692 ft to the surface. The hole was then cored and reamed through the Culebra to about 735 ft to a diameter of 4.75 inches. Following testing of the Culebra, the hole was cored to 870.3 ft for stratigraphic information, reamed to 6.125 inches for geophysical logging, and then plugged back to 773 ft with cement. Stratigraphic depths of the formations encountered and the final as-built configuration of the well are shown in Figure 3-9.

3.9 H-18

Well H-18 was drilled in October and November 1987 to investigate an area in the northwest portion of the WIPP site where large changes in Culebra transmissivity and water quality occur. A 9.625-inch hole was cored and reamed to a depth of 674 ft, about 15 ft above the top of the Culebra, and 7-inch casing was set and cemented from 673 ft to the surface. The hole was then cored and reamed through the Culebra to about 714 ft to a diameter of 4.75 inches. Following testing of the Culebra, the hole was cored to 830.5 ft for stratigraphic information, reamed to 6.125 inches for geophysical logging, and then plugged back to 766 ft with cement. Stratigraphic depths of the formations

encountered and the final as-built configuration of the well are shown in Figure 3-10.

3.10 WIPP-12

Drilling began at WIPP-12 in November 1978. The hole was drilled and reamed to a diameter of 12.25 inches to a depth of about 1003 ft, and 9.625-inch casing was set and cemented from 1002 ft to the surface. The hole was then cored and reamed to a diameter of 7.875 inches to a total depth of about 2774 ft, approximately 48 ft into the Castile Formation (Sandia and D'Appolonia, 1982). As the borehole was being deepened in 1981, a pressurized brine reservoir was encountered at a depth of about 3017 ft in the lower portion of the Anhydrite III unit of the Castile (Popielak et al., 1983). The hole was deepened at a diameter of 7.875 inches to about 3107 ft, from which point the diameter was reduced to 6 inches for the balance of the hole down to the total depth of 3927.5 ft in the upper part of the Anhydrite I unit of the Castile (Black, 1982). In June 1983, the upper part of the wellbore was isolated from the brine reservoir by setting a bridge plug in the hole from 3000 to 3005 ft deep, putting 27 ft of sand on top of the bridge plug, and putting a 189-ft cement plug on top of the sand (D'Appolonia, 1983). Key stratigraphic horizons and the well configuration at the time of the August-September 1985 testing are shown in Figure 3-11.

On October 12, 1985, a retrievable bridge plug was set in the WIPP-12 casing between the depths of 984.0 and 989.4 ft. Two days later, gamma-ray logging was performed which indicated that the Culebra interval extended from 815 to 840 ft below ground surface, and that interval was then shot-perforated. All stratigraphic contacts shown on this log are approximately 5 ft deeper than those reported by Sandia and D'Appolonia (1982). This discrepancy may be due to the 1978 and 1985 logging surveys having used different datums to "zero" their depth counters. Inasmuch as the 1985 gamma-ray log and the perforation were run off the same depth counter and used the same datum, the correct Culebra interval should have been perforated.
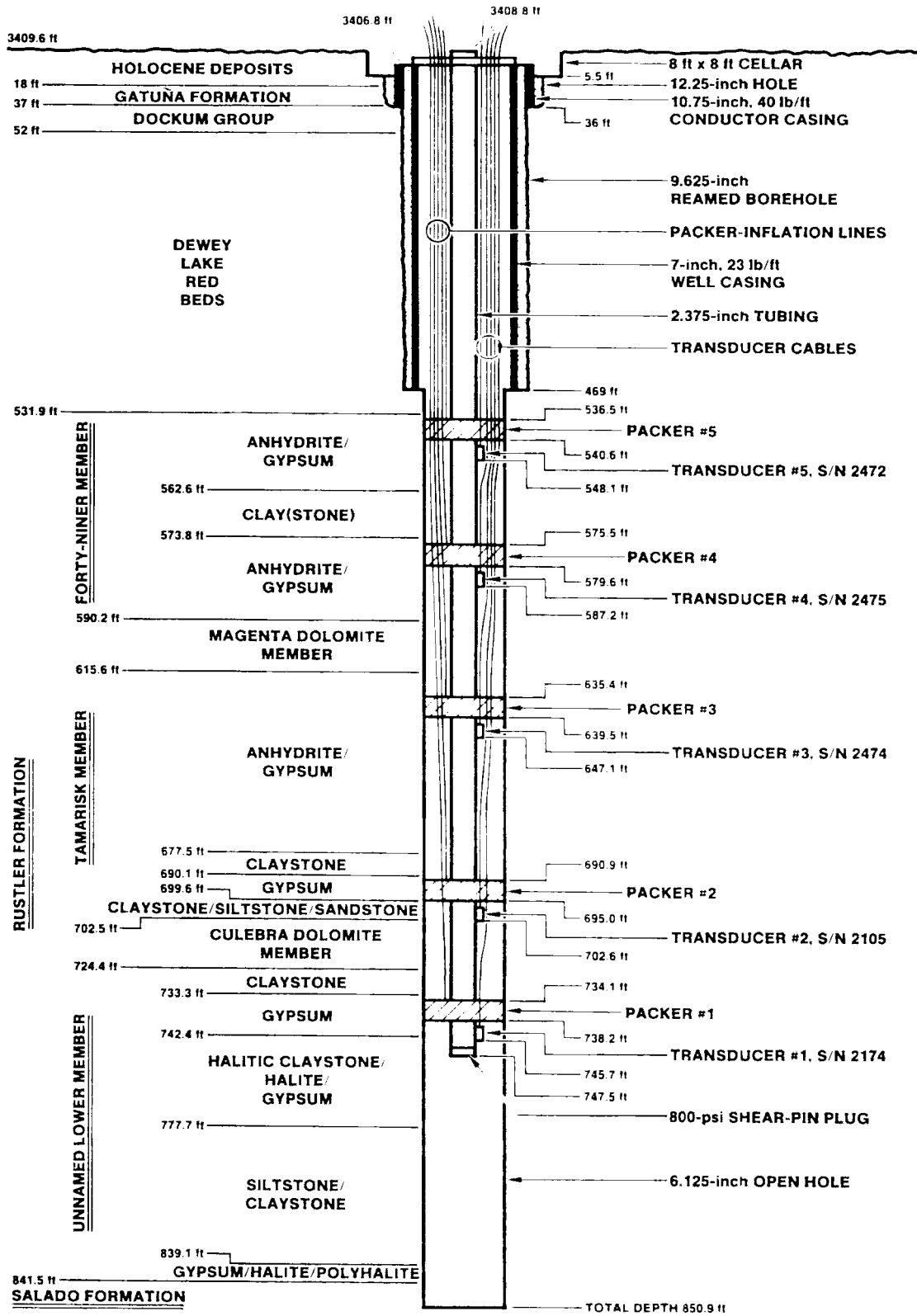
Figure 3-8. As-Built Configuration and 5-Packer Completion for Well H-16

ALL DEPTHS BELOW GROUND SURFACE

NOT TO SCALE

26
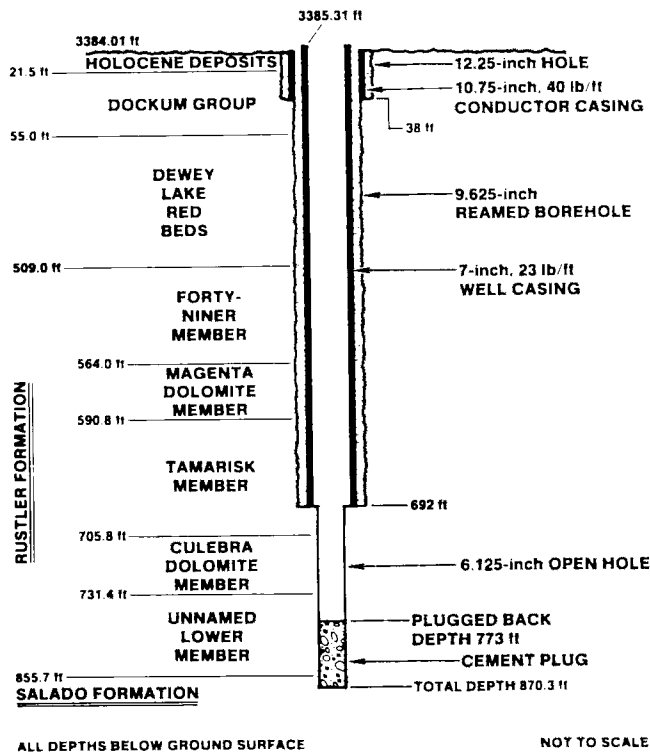
Figure 3-9. As-Built Configuration for Well H-17

Figure 3-10. As-Built Configuration for Well H-18

WIPP-12 was pumped briefly on May 1, 1986 to develop the perforations and to provide information useful in designing a testing program (Saulnier et al., 1987). The well yielded very little water, indicating low transmissivity and/or a poor hydraulic connection between the well and the formation. In an effort to improve the effectiveness of the casing perforations in connecting the well with the formation, the well was acidized on May 21, 1986. About 50 gallons of a 20% hydrochloric-acid solution were injected into the perforations under a surface pressure of 300 to 500 psig over 95 minutes. Because the acid solution was not readily injected, 500 gallons of the acid solution were placed at and above the Culebra perforations, and further well-development work was deferred.

The spent acid solution and other wellbore fluids were bailed from WIPP-12 on August 27 and 28, 1987. After the fluid level recovered, a pump was set

in the well and all fluids were pumped from the well on 3 occasions in October and November 1987. The pump was then removed, and the well was bailed again on December 8, 1987. The fluid removed on this occasion was used to inflate a PIP set in the well casing on 2.375-inch tubing from 794.4 to 796.0 ft on December 16, 1987. A small-diameter minipacker was set in the tubing from 601.0 to 602.8 ft. The PIP, tubing, and minipacker were removed from the well at the conclusion of testing. The configuration of WIPP-12 during the 1987 Culebra slug tests is shown in Figure 3-12.

3.11 WIPP-18

WIPP-18, WIPP-19, WIPP-21, and WIPP-22 were originally drilled in 1978 in the north-central portion of the WIPP site to investigate the structure of near-surface formations after preliminary interpretations of seismic-survey data indicated the potential existence

27
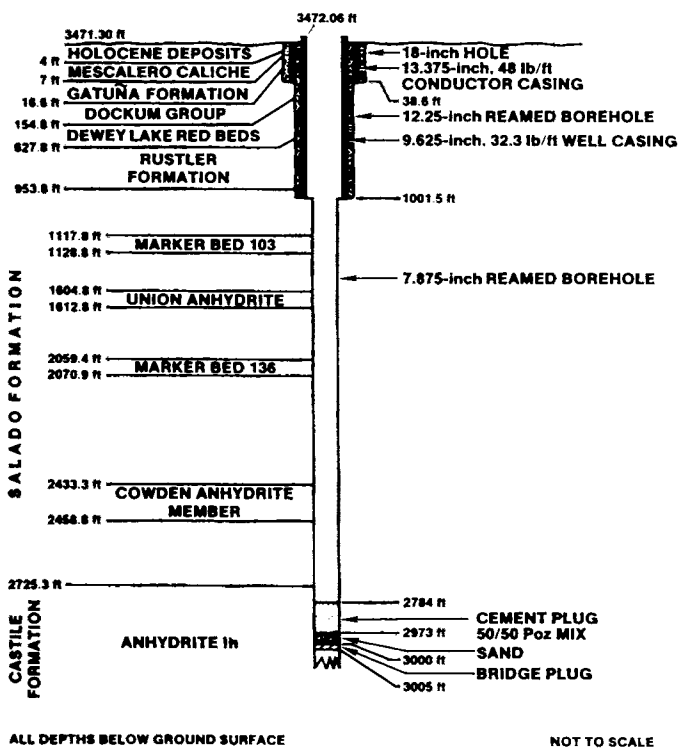
Figure 3-11.   Well Configuration for WIPP-12
                Castile and Salado Testing

Figure 3-12.   Well Configuration for WIPP-12
                Culebra Slug Tests

of a fault in that vicinity (Sandia and USGS, 1980a). WIPP-18 was drilled to a total depth of 1060 ft, 132 ft into the Salado Formation, and no evidence of a fault was found. WIPP-18 was abandoned in an open-hole condition filled with brine mud until October 1985, when the hole was recompleted to serve as a Culebra observation well. To this end, the hole was reamed to a diameter of 7.875 inches, and 5.5-inch casing was installed and cemented from the surface to a depth of 1050 ft. The Culebra interval was then shot-perforated from 784 to 806 ft deep, based on gamma-ray logging performed to locate the Culebra. Sandia and USGS (1980a) report the Culebra at WIPP-18 as being from 787 to 808 ft deep. The discrepancy in depths was probably caused by the 1978 and 1985 logging surveys using different datums to zero the tools. From May 10 to 14, 1986, WIPP-18 was developed by pumping and surging (Saulnier et al., 1987). For slug testing, a PIP was temporarily set in the well casing on 2.375-inch

tubing from 769.7 to 774.0 ft. The configuration of the well at the time of testing is shown in Figure 3-13.

3.12 WIPP-19

WIPP-19 was drilled as part of the same program as WIPP-18 in 1978 (Sandia and USGS, 1980b). The hole was continuously cored to a total depth of 1038.2 ft, 143.2 ft into the Salado Formation. WIPP-19 was then abandoned in an open-hole condition filled with brine mud until October 1985, when the hole was recompleted to serve as a Culebra observation well. The borehole was reamed to a diameter of 7.875 inches, and 5.5-inch casing was installed and cemented from the surface to a depth of 1036.6 ft. The Culebra interval was then shot-perforated from 754 to 780 ft deep, based on gamma-ray logging performed to locate the Culebra. Sandia and USGS (1980b), by comparison, report the Culebra as being 756 to 779 ft deep. From May 28 to
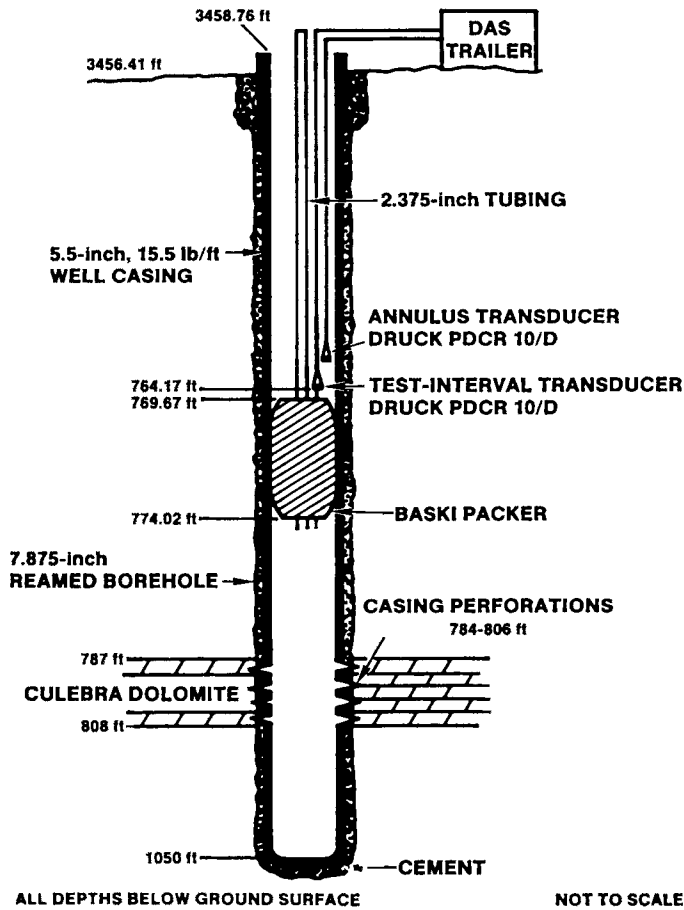
Figure 3-13. Well Configuration for WIPP-18 Slug Test

Figure 3-14. Well Configuration for WIPP-19 Slug Test

29, 1986, the well was developed by pumping and surging (Saulnier et al., 1987). For slug testing, a PIP was temporarily set in the well casing from 737.5 to 741.8 ft on 2.375-inch tubing. The configuration of the well at the time of testing is shown in Figure 3-14.

3.13 WIPP-21

WIPP-21 was drilled as part of the same program as WIPP-18 and WIPP-19 in 1978 (Sandia and USGS, 1980c). The hole was drilled to a total depth of 1046 ft, 178 ft into the Salado Formation. WIPP-21 was then abandoned in an open-hole condition filled with brine mud until October 1985, when the hole was recompleted to serve as a Culebra observation well. The borehole was reamed to a diameter of 7.875 inches, and 5.5-inch casing was installed and

cemented from the surface to a depth of 1013.7 ft. The Culebra interval was then shot-perforated from 727 to 751 ft deep, based on gamma-ray logging performed to locate the Culebra. Sandia and USGS (1980c) report the Culebra lies 2 ft lower, from 729 to 753 ft deep, probably because of difference in the datums from which depths were measured. From June 28 to July 1, 1986, the well was developed by pumping and surging (Saulnier et al., 1987). For slug testing, a PIP was temporarily set in the well casing from 705.9 to 711.8 ft on 2.375-inch tubing. The configuration of the well at the time of testing is shown in Figure 3-15.

3418.96 ft

3417.08 ft

DAS TRAILER

2.375-inch TUBING

5.5-inch, 15.5 lb/ft
WELL CASING

ANNULUS TRANSDUCER
DRUCK PDCR 10/D

700.65 ft
705.85 ft

TEST-INTERVAL TRANSDUCER
DRUCK PDCR 10/D

7.875-inch
REAMED BOREHOLE

711.73 ft

BASKI PACKER

CASING PERFORATIONS
727-751 ft

729 ft

CULEBRA DOLOMITE

753 ft

1013.72 ft

CEMENT

ALL DEPTHS BELOW GROUND SURFACE   NOT TO SCALE
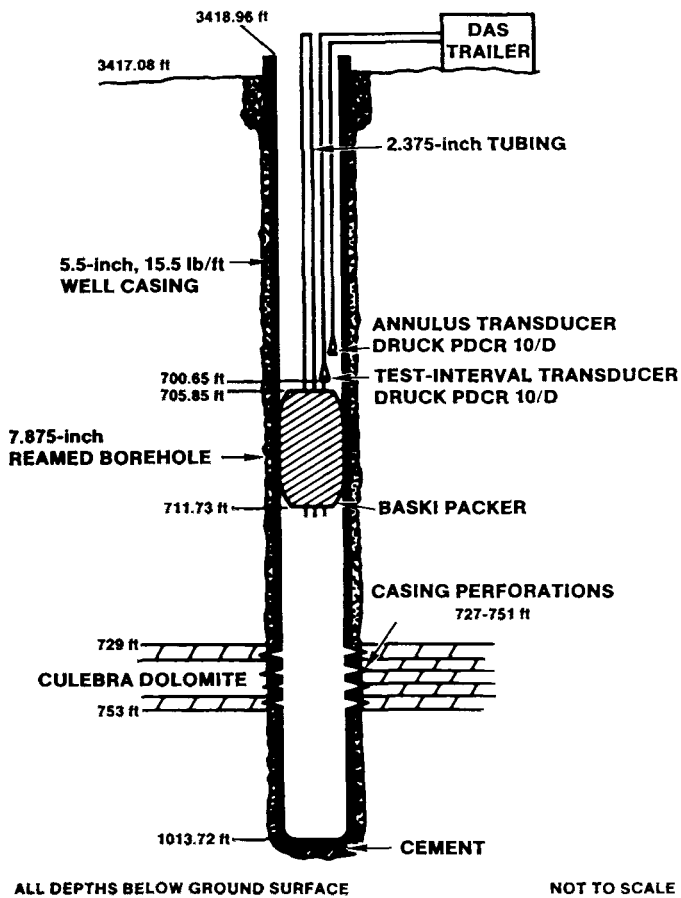
Figure 3-15. Well Configuration for WIPP-21 Slug Test

3.14 WIPP-22

WIPP-22 was drilled as part of the same program as WIPP-18, WIPP-19, and WIPP-21 in 1978 (Sandia and USGS, 1980d). The hole was drilled to a total depth of 1448 ft, 565 ft into the Salado Formation. WIPP-22 was then abandoned in an open-hole condition filled with brine mud until October 1985, when the hole was recompleted to serve as a Culebra observation well. The borehole was reamed to a diameter of 7.875 inches, and 5.5-inch casing was installed and cemented from the surface to a depth of 949.8 ft. The Culebra interval was then shot-perforated from 748 to 770 ft deep, based on gamma-ray logging performed to locate the Culebra. Sandia and USGS (1980d) report the Culebra 6 ft higher, from 742 to 764 ft deep. The source of the 6-ft discrepancy between the 1978 and 1985 surveys is unknown.

The depth discrepancy may be due to one of the two surveys having incorrectly "zeroed" a depth counter. Inasmuch as the 1985 survey and the subsequent perforation were run using the same depth counter and the same datum, the correct interval was probably perforated, whatever its true absolute depth. From June 11 to 17, 1986, WIPP-22 was developed by pumping and surging (Saulnier et al., 1987). For slug testing, a PIP was temporarily set in the well casing from 738.1 to 742.5 ft on 2.375-inch tubing. The configuration of the well at the time of testing is shown in Figure 3-16.

3428.12 ft

3425.79 ft

DAS TRAILER

2.375-inch TUBING

5.5-inch, 15.5 lb/ft
WELL CASING

ANNULUS TRANSDUCER
DRUCK PDCR 10/D

733.59 ft
738.09 ft

TEST-INTERVAL TRANSDUCER
DRUCK PDCR 10/D

7.875-inch
REAMED BOREHOLE

742.49 ft

BASKI PACKER

CASING PERFORATIONS
748-770 ft

742 ft

CULEBRA DOLOMITE

764 ft

949.82 ft

CEMENT

ALL DEPTHS BELOW GROUND SURFACE   NOT TO SCALE
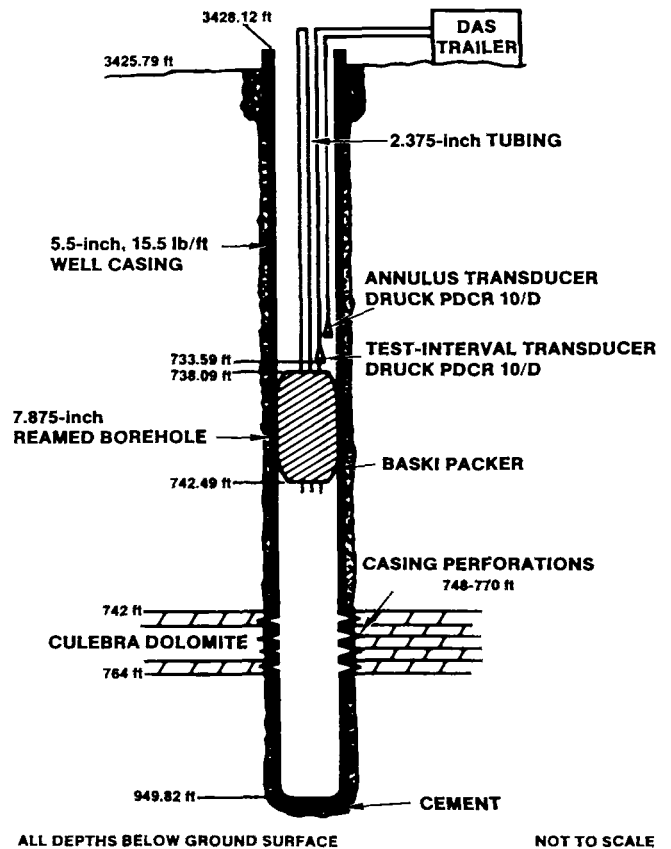
Figure 3-16. Well Configuration for WIPP-22 Slug Test

3.15 WIPP-30

Well WIPP-30 was drilled in September 1978 as one of six wells drilled to evaluate dissolution of near-surface rocks in and adjacent to Nash Draw (Sandia and USGS, 1980). WIPP-30 was cored and reamed to

a diameter of 8.75 inches to a depth of 246 ft, and then deepened to 913 ft by coring and reaming to a diameter of 7.875 inches. Casing (5.5-inch) was installed and cemented from 912 ft to the surface. In March, July, and September 1980, three sections of the casing were perforated: the Rustler/Salado contact zone from 731 to 753 ft; the interval from 631 to 654 ft which includes the Culebra from 631 to 653 ft; and the interval from 510 to 540 ft which includes the Magenta from 513 to 537 ft (Seward, 1982). Retrievable bridge plugs were set at depths of 688.5 and 590.7 ft in September 1980. In August 1983, the upper bridge plug was replaced with a PIP set on 2.375-inch tubing at a depth of 570 ft to allow monitoring of the Culebra water level through the tubing, and the Magenta water level through the annulus between the casing and tubing.

In October 1987, the PIP was removed and the casing was reperforated between the depths of 629 and 655 ft to improve the hydraulic connection between the Culebra and the well. In November 1987, the well was bailed once and pumped 4 times (with both the Culebra and Magenta open to the well) to develop the perforations. On December 8, 1987, the well was pumped a final time to provide water for use in the subsequent slug tests, and a PIP was set from 613.1 to 617.5 ft in the well on 2.375-inch tubing. A minipacker was installed in the tubing from 599.4 to 601.1 ft, and was removed after testing was completed. The configuration of WIPP-30 at the time of testing is shown in Figure 3-17.

3.16 P-15

Well P-15 was drilled in October 1976 as part of a 21-well evaluation program to investigate the potash resources in the Salado Formation at the proposed location of the WIPP site (Jones, 1978). P-15 was drilled and reamed to a diameter of 7.875 inches to a depth of 637 ft, and 4.5-inch casing was installed and cemented from 635 ft to the surface. The hole was deepened by coring at a 4-inch diameter to 1465 ft, and the bottom of the hole was plugged back to 620 ft with cement (Mercer and Orr, 1979). In January and April 1977, two sections of the casing were perforated: the Rustler/Salado contact zone from 532 to 556 ft deep; and the interval from 410 to 438 ft which includes the Culebra from 413 to 435 ft.
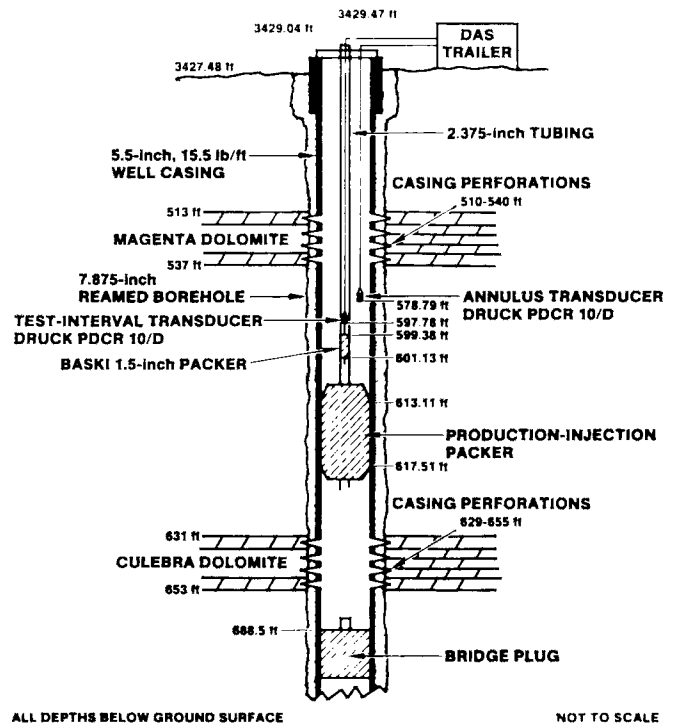
Figure 3-17.   Well Configuration for WIPP-30 Slug Tests

A PIP was set in the casing at a depth of 512 ft on 2.375-inch tubing to allow monitoring of Rustler/Salado and Culebra water levels. The PIP was determined to be leaking in May 1985, and was replaced on June 6, 1985 with a retrievable bridge plug set from 441 to 447 ft deep.

P-15 was developed by bailing on March 27, April 7, 16, and 21, 1987 in preparation for slug testing (Stensrud et al., 1988). A PIP on 2.375-inch tubing was set in the well casing temporarily from 389.6 to 393.9 ft in May 1987 to aid in the testing. The configuration of P-15 at the time of testing is shown in Figure 3-18.

3.17 P-17

P-17 was drilled in October 1976 as part of the potash-resource evaluation program at the proposed location for the WIPP site (Jones, 1978). The hole was first rotary drilled at a diameter of 7.875-inches to a depth of 755 ft, approximately 40 ft into the Salado

31
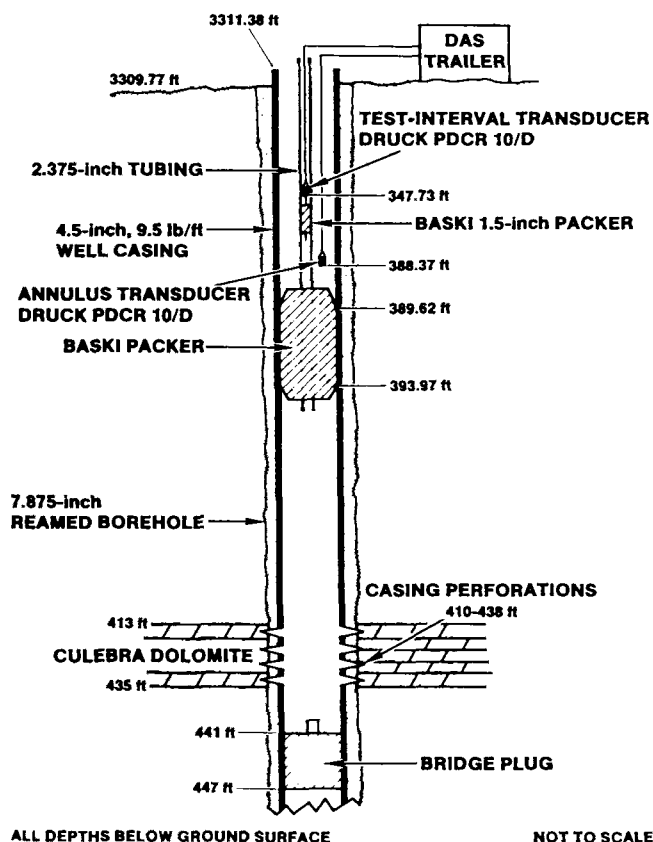
Figure 3-18. Well Configuration for P-15 Slug Tests

Figure 3-19. Well Configuration for P-17 Slug Tests

Formation. Casing (4.5-inch diameter) was then set and cemented from 741 ft to the surface, and the hole was deepened at a 4-inch diameter to a total depth of 1660 ft. After coring was completed, the hole was plugged back to a depth of 731 ft with cement. In January and April 1977, two sections of the casing were perforated: the Rustler/Salado contact zone between 702 and 726 ft; and the interval from 558 to 586 ft, which includes the entire Culebra from 558 to 583 ft (Mercer and Orr, 1979). A PIP was set in the casing at 683 ft on 2.375-inch tubing to allow monitoring of Rustler/Salado and Culebra water levels. In March 1983, the PIP was replaced with a retrievable bridge plug set from 674 to 679 ft. For testing in 1986, a PIP was temporarily set in the casing from 532.3 to 536.6 ft deep on 2.375-inch tubing. The configuration of the well at the time of testing is shown in Figure 3-19.

3.18 P-18

Well P-18 was drilled in October and November 1976 as part of the potash-resource evaluation program at the proposed WIPP site (Jones, 1978). The hole was drilled and reamed to a depth of 1139 ft at a diameter of 7.875 inches, and 4.5-inch casing was cemented from 1138 ft to the surface. The hole was then drilled and cored at a 4-inch diameter to a depth of 1998 ft, and plugged back to 1125 ft with cement. In January and April 1977, two sections of the casing were perforated: the Rustler/Salado contact zone between 1076 and 1100 ft; and the interval from 912 to 940 ft, which includes most of the Culebra which lies between 909 and 938 ft (Mercer and Orr, 1979). In May 1977, a PIP was set on 2.375-inch tubing at a depth of 1061 ft to allow monitoring of Rustler/Salado and Culebra water levels. In early 1983, the PIP was removed and a bridge plug was set from 997 to

1002 ft deep to allow testing of the Culebra. Testing consisted of a pressure-pulse test and a slug test, both of which indicated very low transmissivity, but were otherwise inconclusive.

On June 12, 1987, the P-18 casing was reperforated from 909 to 938 ft to improve the hydraulic connection between the Culebra and the well. On June 16, 1987, a PIP was set in the well from 895.9 to 899.2 ft deep on 2.375-inch tubing, and all fluid was bailed from the tubing. The tubing was bailed again on August 26, 1987, after the fluid level in the tubing had recovered. A minipacker was then installed in the tubing from 780.4 to 782.2 ft for use in subsequent testing. The configuration of the well at the time of testing is shown in Figure 3-20.
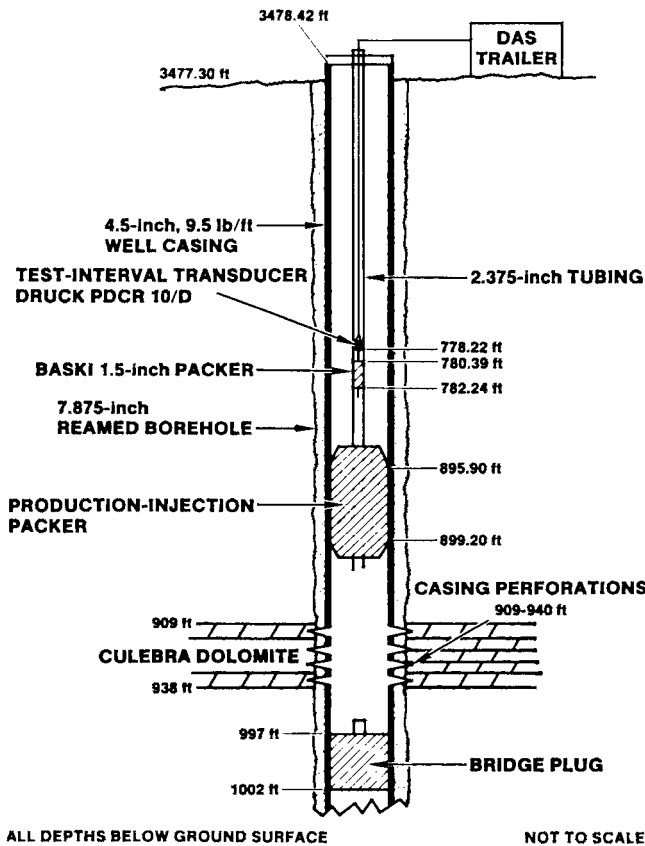
Figure 3-20. Well Configuration for P-18 Slug Test

3.19 ERDA-9

ERDA-9 was the first exploratory borehole for the proposed WIPP. It was drilled between April and June 1976 to provide stratigraphic and structural information on the Permian evaporites, as well as to provide core samples for further testing. When the bottom of the 15-inch hole was 1078 ft deep, 10.75-inch casing was installed and cemented from the surface to a depth of 1033 ft, approximately 185 ft into the Salado Formation. After the hole was drilled to its final total depth of about 2877 ft at a diameter of 9.875 inches, it was completed by installing 7-inch casing from the surface to a depth of 2871 ft, and cementing only the lower 343 ft of that casing in place (Sandia and USGS, 1983). The hole was then left filled with a diesel-fuel-based drilling mud.

ERDA-9 remained in this configuration until October 1986, when it was recompleted as a Culebra observation well. During the recompletion, the upper 980 ft of the 7-inch casing were cut off from the lower section and removed from the hole. A retrievable bridge plug was then set in the 10.75-inch casing from 758.9 to 760.6 ft deep, and the Culebra interval between 705.5 and 728.5 ft deep, as determined from a gamma-ray log, was shot-perforated using 4 shots/ft. Sandia and USGS (1983) reported the Culebra 1.5 ft higher, probably indicating that the two geophysical surveys did not use the same datum. From October 27 to November 14, 1986, ERDA-9 was developed by pumping and surging. Additional recompletion and development information is contained in Stensrud et al. (1987). For slug testing, a PIP was temporarily set in the well casing from 672.7 to 674.5 ft on 2.375-inch tubing, and a minipacker was set in the tubing from 641.0 to 642.8 ft. The configuration of the well at the time of testing is shown in Figure 3-21.

3.20 Cabin Baby-1

Cabin Baby-1 was drilled by a private company in 1974 and 1975 to explore the potential for natural-gas production from the upper Bell Canyon Formation. The borehole was cased from the surface to about 650 ft deep with 13.375-inch casing. The U.S. Department of Energy assumed control over the well after it was found to be a "dry hole." The hole was reentered and deepened in 1983 to a depth of about 4291 ft at a diameter of 9.875 inches to allow hydrologic testing of sandstone units in the upper Bell Canyon (Beauheim et al., 1983). Following those tests, a PIP was set at the base of the Castile
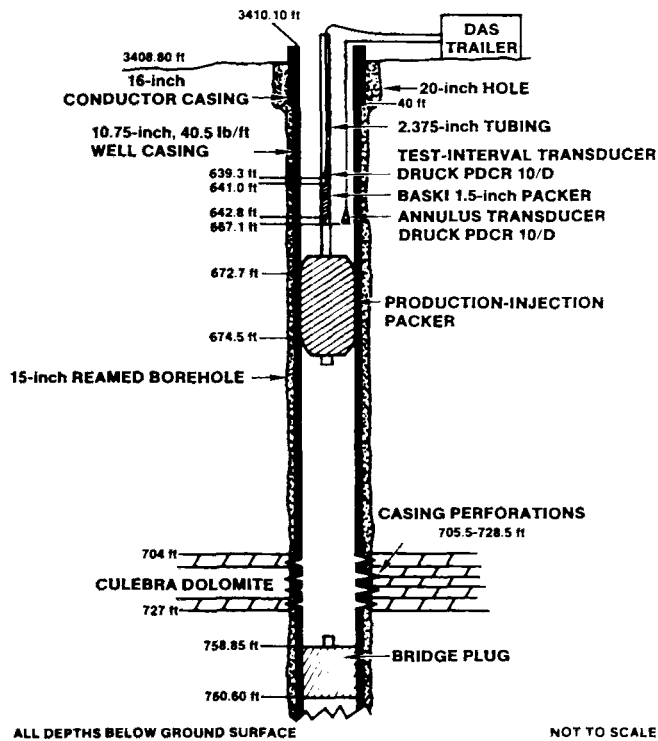
Figure 3-21. Well Configuration for ERDA-9
Slug Tests

Formation. Tubing attached to the PIP provided access for Bell Canyon hydraulic-head measurements, while the annulus between the tubing and the borehole wall was open to the Castile and Salado Formations.

In September 1986, Cabin Baby-1 was recompleted as a Culebra observation well. The PIP at the base of the Castile was replaced by a retrievable bridge plug, and another retrievable bridge plug was set in the well casing from about 585.4 to 588.4 ft deep. The casing was perforated between the depths of 503 and 529 ft, which coincides with the Culebra interval identified from a gamma-ray log run immediately before perforation (all Cabin Baby-1 stratigraphic depths above the Salado reported in Beauheim et al. (1983) are incorrect). Following the recompletion, the well was developed between September 23 and October 3, 1986 by repeatedly pumping most of the water from the well and allowing the water level to recover. Additional recompletion and well-development information is contained in Stensrud et al. (1987). To facilitate the 1987 slug testing, a PIP

was temporarily set in the well casing from 492.2 to 494.8 ft deep on 2.375-inch tubing, and a minipacker was set in the tubing from 459.6 to 460.1 ft deep. The configuration of Cabin Baby-1 at the time of testing is shown in Figure 3-22.
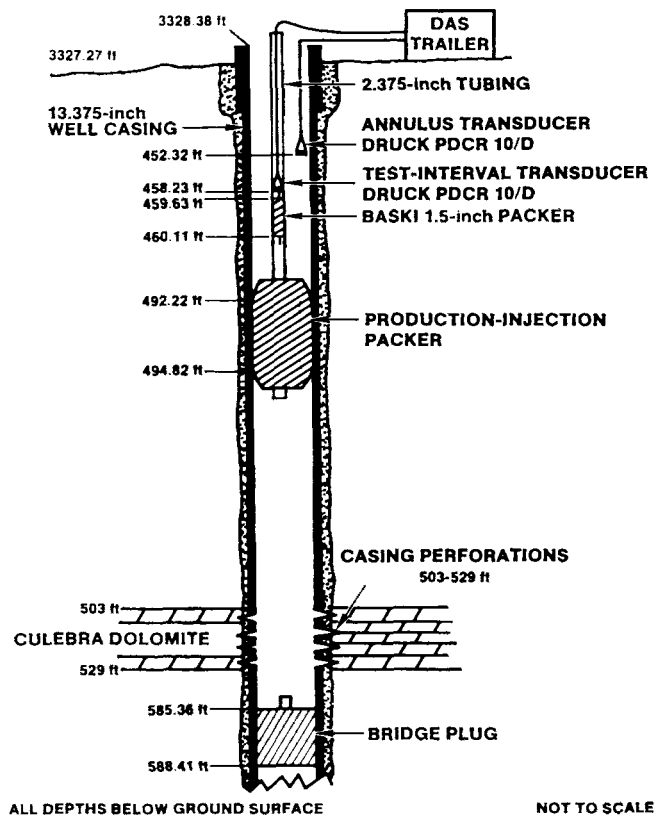
Figure 3-22. Well Configuration for Cabin Baby-1
Slug Tests

3.21 DOE-1

DOE-1 was drilled in July 1982 to investigate a structural anomaly in the Castile Formation inferred from seismic-reflection surveys. The well was drilled at a 14.75-inch diameter to a depth of 1122.5 ft, and 10.75-inch casing was set and cemented from about 1118 ft to the surface. A 7.875-inch hole was then drilled to a total depth of about 4057 ft (Freeland, 1982). In March 1983, a retrievable bridge plug was set in the casing at a depth of about 858 ft, and an interval encompassing the Culebra from 820 to 843 ft deep was shot-perforated using 4 shots/ft (HydroGeoChem, 1985). The well was developed

between March 30 and April 29, 1983, by bailing and pumping using a pump jack. The configuration of DOE-1 at the time of the 1983 pumping test is shown in Figure 3-23.
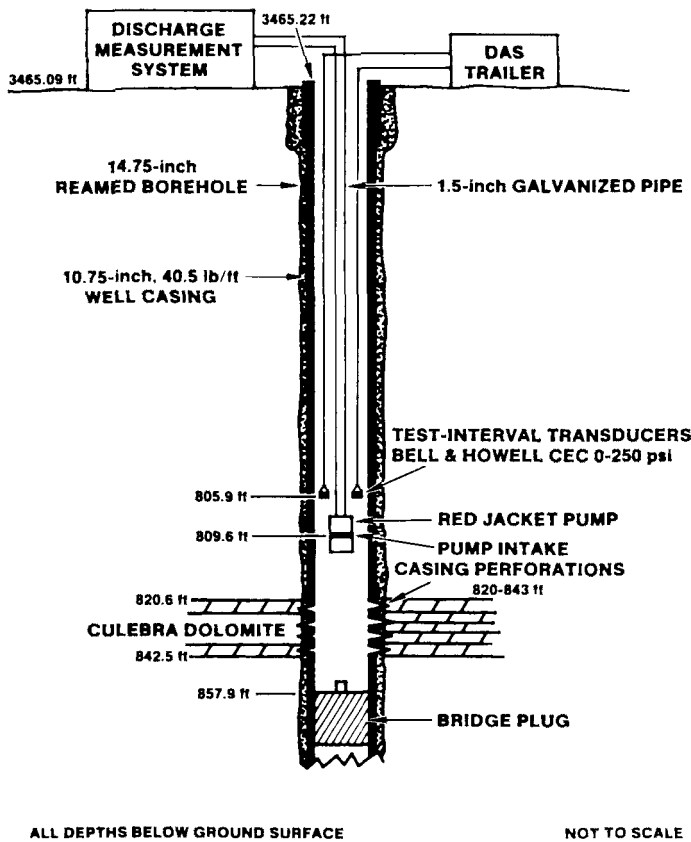
Figure 3-23.   Well Configuration for DOE-1 Pumping Test

3.22 Engle

The Engle well is a livestock-watering well equipped with a windmill. Little is known about the history of the Engle well. The following information was obtained from unpublished geophysical logs run in the Engle well by the USGS in November 1983. The well has a total depth of about 683 ft, and is cased with 7-inch casing from about 648 ft to the surface. The Culebra lies from 659 to 681 ft deep. The open hole through the Culebra appears to have been drilled to a 7-inch diameter, although a caliper log indicates that it has washed out or caved to an average diameter of about 7.4 inches. The configuration of the well during the November 1983 pumping test is shown in Figure 3-24.
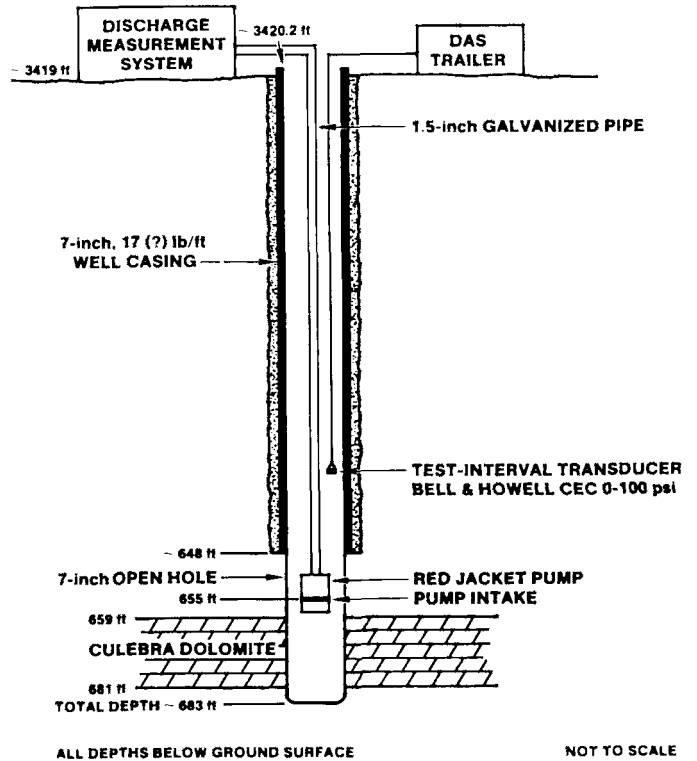
Figure 3-24.   Well Configuration for Engle Pumping Test

3.23 Carper

The Carper well is an oil test hole converted to a livestock-watering well equipped with a windmill. The well is in the northwest quarter of Section 7, Township 25 South, Range 30 East, in the Poker Lake area described by Borns and Shaffer (1985), among others. Cooper and Glanzman (1971) reported that the well was cased to 250 ft, and plugged at a depth of 385.6 ft. Recent measurements indicate that the casing has a 5.5-inch outside diameter. The production zone is reported by Cooper and Glanzman (1971) as being undifferentiated Quaternary and Tertiary deposits. Richey et al. (1985) refer to these deposits as Cenozoic alluvium. In March 1959, the depth to water was 263.3 ft. The static water level before the February 1984 pumping test was about 262.8 ft below ground surface. Figure 3-25 shows the configuration of the Carper well during the February 1984 pumping test.
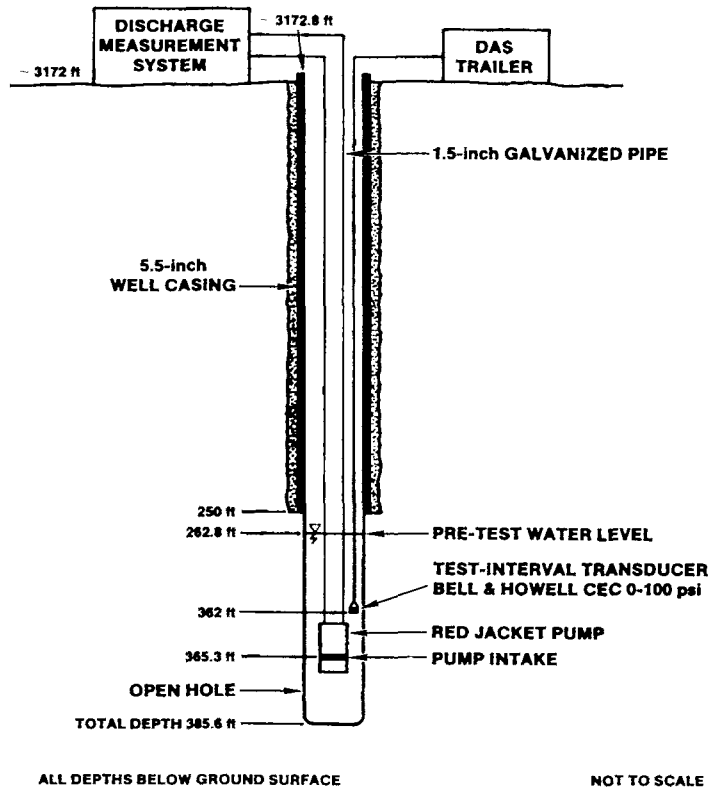
Figure 3-25. Well Configuration for Carper Pumping Test

4. TEST METHODS

A variety of testing methods were employed for single-well tests at the WIPP site because of the wide range of permeabilities encountered and because of the different types of well completions. Drillstem tests (DST's), rising-head slug tests, falling-head slug tests, pressure-pulse tests, and pumping tests were all employed in the course of these investigations. Generalized procedures for each type of test are presented below. The techniques used to interpret the data from these tests are discussed in detail in Appendix A.

4.1 Drillstem Tests

DST's are generally performed shortly after a well has been drilled and before the well has been completed, when all of the units penetrated are still accessible for testing and little is known about their hydraulic properties. DST's (and slug and pressure-pulse tests) require a packer assembly mounted at the bottom of a tubing string in the hole which isolates the interval to be tested. For a test of the lower portion of the hole, a single packer may be used. To test a discrete zone in a hole, a straddle-packer arrangement is required. Other necessary equipment includes a shut-in tool to isolate the test interval from the tubing, pressure transducers to measure fluid pressures above, between, and below the packers, and a data-acquisition system.

The first step in a DST is to select the interval to be tested and establish the appropriate packer separation. Next, the packer assembly, including transducers, is installed in the hole at the desired depth, and the packers are inflated. The test interval is then shut-in (isolated from the tubing above), and the fluid in the tubing above the tool is removed by swabbing while the pressure in the test interval stabilizes.

The actual DST begins with opening the shut-in tool, which allows the fluid in the isolated interval to enter the tubing. Due to the large pressure differential normally existing between the evacuated tubing and the isolated interval, water under the initial stabilized formation pressure flows towards the borehole and

up the tubing string. This is the first flow period (FFL; see Figure 4-1). This period begins with a drop in pressure from pre-test conditions (shut-in tool closed) to a pressure corresponding to the weight of the water remaining in the tubing (after swabbing) above the transducer. As water rises up the tubing string, the pressure exerted downward on the isolated interval increases, reducing the pressure differential and thus the flow rate.

When the flow rate has decreased by no more than about fifty percent from its initial value, the shut-in tool is closed, stopping the flow of water up the tubing. This is the beginning of the first pressure buildup period (FBU). The fluid pressure in the test interval, which was increasing relatively slowly during the FFL, builds up toward the pre-test formation pressure more quickly after the interval is once again isolated. Initially, the fluid pressure builds up rapidly because of the differential between the pressure in the test interval at the end of the FFL and that in the surrounding formation. As this pressure differential decreases, the rate of pressure buildup decreases. On an arithmetic plot of fluid pressure versus time, the slope of the data curve decreases with time and the curve becomes asymptotic to the static formation pressure (Figure 4-1). The longer the first buildup period, the more definitive the data become for estimating formation hydraulic parameters, and conditions become more ideal for the start of the second flow period. In practical terms, the FBU should generally last at least four times as long as the FFL. In very low permeability formations, an FBU duration more than ten times as long as the FFL may be necessary to provide adequate data for analysis.

Following the FBU, the shut-in tool is reopened to initiate the second flow period (SFL). The water level in the tubing will not have changed since the end of the FFL, so a pressure differential will remain between the test interval and the tubing. If the remaining pressure differential is less than desired, the tubing can be swabbed again before beginning the SFL. The SFL typically lasts somewhat longer than the FFL, but again the flow rate is only allowed to decrease by no more than about fifty percent. At
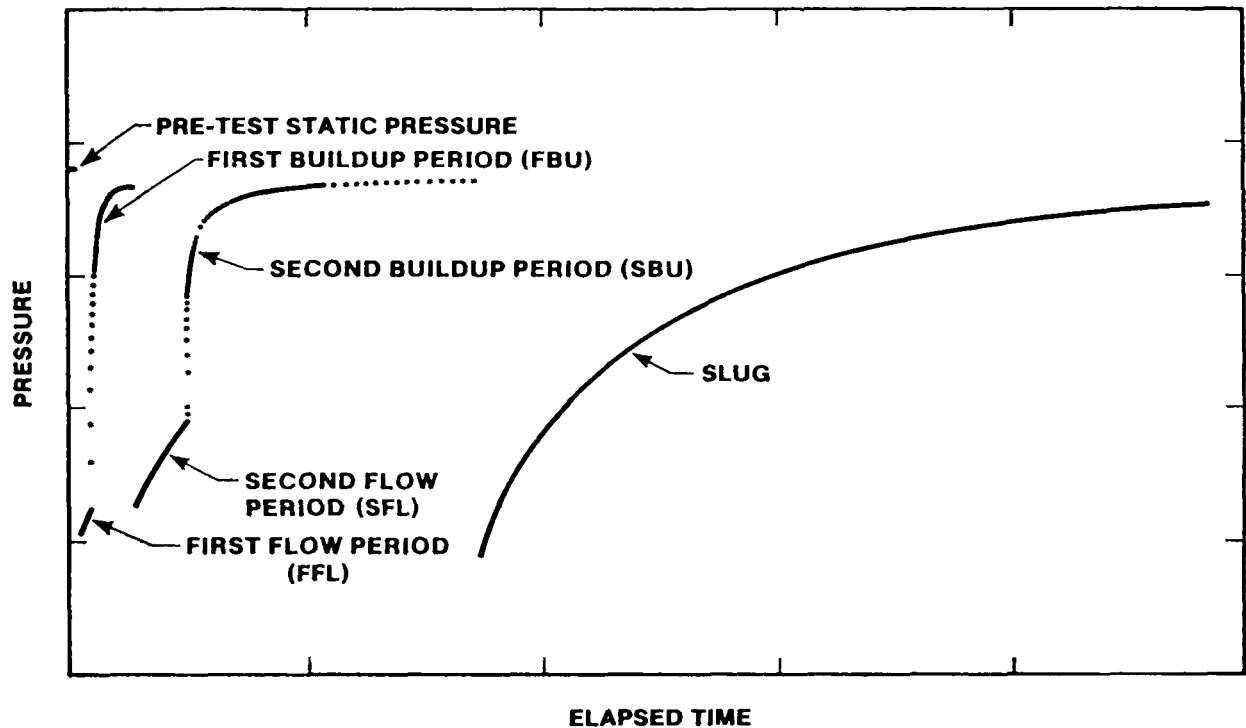
Figure 4-1. Components of a DrillStem Test and Slug Test

the conclusion of the SFL, the shut-in tool is closed and the second buildup period (SBU) begins. Like the FBU, the SBU continues until the pressure-vs.-time data curve becomes asymptotic to the static formation pressure. As with the FBU, the data become more definitive the longer the SBU continues, and conditions improve for the next phase of testing. These four periods, the FFL, FBU, SFL, and SBU, generally constitute a complete DST cycle. On occasion, however, DST's may include additional flow and buildup periods.

DST flow rates are calculated rather than measured directly. The calculations are based on observed pressure changes over time caused by fluid filling the tubing, the known or estimated specific gravity of the fluid, and the size of the tubing. Because buildup-test analysis relies on the preceding flow rate(s) being approximately constant, the actual rates during DST flow periods must be converted to one or more equivalent constant rates. This is done by dividing the total flow period into shorter time periods encompassing less flow-rate variation, and calculating the average rate over each time period.

DST's were performed at well H-14 in the lower Dewey Lake Red Beds and in the Forty-niner, Magenta, and Culebra Members of the Rustler Formation; in the Culebra at well H-15; in the Forty-niner, Magenta, Culebra, and unnamed lower members of the Rustler at well H-16; in the Culebra at well H-17; in the Culebra at well H-18; and in the upper Castile Formation and Salado Formation at well WIPP-12.

4.2 Rising–Head Slug Tests

Rising-head slug tests are most easily performed following DST's, while the DST tool is still in the hole. Following the second buildup of the DST, and while the shut-in tool is still closed, the fluid is swabbed out of the tubing. The shut-in tool is then opened to initiate the test. A rising-head slug test is performed in exactly the same manner as the DST flow periods, except that the test is not terminated after the flow rate changes by fifty percent (Figure 4-1). Ideally, the slug test should continue until the initial pressure differential has decreased by ninety percent or more. Practically, forty percent recovery generally provides

adequate data for analysis, particularly if log-log plotting techniques are used (Ramey et al., 1975).

Rising-head slug tests can also be performed with a production-injection packer (PIP) set in a well on a tubing string. The water is swabbed from the tubing, and a small-diameter minipacker is quickly inserted into the tubing and inflated a short distance below the water level existing at that time. A transducer monitors the pressure below the minipacker. When the pressure stabilizes, the minipacker is deflated rapidly, stimulating flow from the formation into the relatively underpressurized tubing. The water-level or fluid-pressure rise in the tubing is monitored to provide the data needed to analyze the test.

Rising-head slug tests were performed in the Culebra at wells H-1, H-14, H-15, H-16, H-17, H-18, and P-18; in the Magenta at well H-16; and in the Forty-niner clay(stone) at H-14 and H-16.

4.3 Falling–Head Slug Tests

Falling-head slug tests are commonly performed after a well has been completed, when only one water-bearing unit is in communication with the wellbore. They are generally performed in low-productivity wells that cannot sustain a pumping test. To prepare for a falling-head slug test, a packer is lowered into the well (or into tubing if a PIP is being used to isolate the test zone from other water-producing zones) below the water surface and inflated. Additional water is then added to the well (or tubing) above the packer. After pressures above and below the packer have stabilized, the packer is deflated as rapidly as possible. This connects the overlying slug of water with the formation below, marking the beginning of the test. As with a rising-head slug test, a falling-head slug test should be continued until the pressure differential caused by the added slug of water dissipates to ten percent or less of its initial value. Frequently, almost complete dissipation of the pressure differential can be obtained.

Falling-head slug tests were performed in the Culebra at wells H-1, H-4c, H-12, WIPP-12, WIPP-18, WIPP-19, WIPP-21, WIPP-22, WIPP-30, P-15, P-17, ERDA-9, and Cabin Baby-1.

4.4 Pressure–Pulse Tests

In water-bearing units whose transmissivities are so low (i.e., < 0.1 ft²/day) that slug tests would take days to months to complete, pressure-pulse tests can be performed to determine the near-well hydraulic properties of the units. Pressure-pulse tests are most easily performed using a DST tool, and can take the form of either pulse-withdrawal or pulse-injection tests. For either type, the test interval is first shut-in and the pressure allowed to stabilize. The tubing string is either swabbed for a pulse-withdrawal test, or filled to the surface or otherwise pressurized for a pulse-injection test. The shut-in tool is then opened only long enough for the underpressure (pulse-withdrawal) or overpressure (pulse-injection) to be transmitted to the test zone, and then the shut-in tool is closed. In practical terms, it typically takes about one minute to open the tool, verify over several pressure readings that the pressure pulse has been transmitted, and close the tool. The dissipation of the resultant pressure differential between the test zone and the formation is then monitored for the actual test. As with a slug test, the pressure differential should be allowed to decrease by ninety percent or more. However, pressure-pulse tests proceed much more rapidly than slug tests, because equilibration is caused by compression/expansion of fluid rather than by filling/draining a volume of tubing, and hence attaining almost complete recovery is generally practical during a pressure-pulse test.

Pressure-pulse tests were performed in the Forty-niner clay at well H-16, and in the lower Dewey Lake Red Beds at well H-14.

4.5 Pumping Tests

When wells are sufficiently productive to sustain a constant pumping rate over a period of days to weeks, pumping tests are the preferred method of determining the hydraulic properties of water-bearing zones. Pumping tests are performed by lowering a pump into a well, isolating the interval to be tested with packers (if necessary), and pumping water from the formation at a nominally constant rate while monitoring the decline in water level or pressure in the well. Durations of pumping periods are highly variable, and are primarily a function of what volume

(or areal extent) of the aquifer one wishes to test. Following the pumping period, the recovery (rise) of the water level or pressure in the well is monitored, typically for a period twice as long as the pumping period.

Pumping tests were performed in the Culebra at wells H-8b, DOE-1, and Engle, and in Cenozoic alluvium at the Carper well.

4.6 Isolation Verification

Pressures above and below the tested interval are monitored whenever possible during tests so that any leakage around packers or other types of flow into or out of the test interval from/to above or below can be detected. Slow, uniform pressure changes of a few psi in the borehole intervals above and below the test interval are not uncommon, as fluids from these intervals may seep into the adjacent formations or formation fluids may flow into relatively underpressurized intervals. Abrupt, higher magnitude pressure changes may indicate faulty packer seats or equipment malfunctions.

Even when inflated to 2000 psi above ambient borehole pressures, packers exhibit a degree of compliance, or "give". Because some shut-in tools require an up or down movement of the tubing string with several tons of force, packers may shift very slightly upward or downward. In an isolated interval of the borehole, such as below the bottom packer, the increase or decrease in volume caused by the packer compliance is translated into a detectable pressure change. Packer-compliance effects should not be confused with pressure changes having other causes. Differentiation is possible because packer compliance typically causes abrupt pressure changes at the time of tool movements or following packer inflation, followed by a return to the pre-disturbance pressure, whereas packer leaks or bad seals between packers and the borehole or casing wall usually result in continuous pressure changes or equilibration between test-interval pressure and annulus or bottomhole pressure.

5. TEST OBJECTIVES AND INTERPRETATIONS

The single-well tests of the different stratigraphic units had different objectives. Some tests were exploratory in the sense of trying to determine if some seldom-tested units had appreciable permeabilities or measurable pressures. Other tests, particularly those of the Culebra, were designed to provide additional quantitative information on the hydraulic properties of units extensively tested at other locations. The following sections describe the objectives to be met by testing each stratigraphic horizon, and present interpretations of the test data.

Detailed descriptions of the different sets of instrumentation used in the different single-well hydraulic tests, as well as the raw test data, are contained in the series of Hydrologic Data Reports prepared semi-annually for Sandia's WIPP hydrology program (e.g., INTERA Technologies, 1986). Specific references for each test accompany the test descriptions.

5.1 Castile and Salado Formations

The Castile and Salado Formations were tested only in well WIPP-12. The original 1978 completion of WIPP-12 left the upper 48 ft of the Castile Formation and all but the upper 48 ft of the Salado Formation in hydraulic communication with the wellbore. A standard oilfield wellhead was welded to the top of the well casing, and a pressure gauge was attached to the wellhead, which was otherwise sealed. In 1980, wellhead pressures of up to 472 psig were observed at WIPP-12 (Sandia and D'Appolonia, 1982). When WIPP-12 was deepened in 1981, a brine reservoir was encountered in the upper Castile Formation. The highest pressure recorded at the wellhead from the brine reservoir was 208 psig (Popielak et al., 1983). Just before setting the plug above the brine reservoir in 1983 (Section 3.10), the wellhead pressure was 169 psig (D'Appolonia, 1983). Pressure measurements made at the wellhead after plugging revealed a pressure buildup reaching 288 psig in July 1985.

The purpose of reentering WIPP-12 in August 1985 was to try to determine whether the pressures most-

recently observed at the wellhead originated in the brine reservoir, in which case the plug emplaced in 1983 (Section 3.10) had to be leaking or bypassed, or in either the upper Castile or the Salado Formation. Several sets of tests were planned to meet this objective. First, tests were to be performed with a DST tool as close to the plug in the Castile as possible to evaluate the integrity of the plug. Second, tests of the majority of the exposed Castile were planned to attempt to determine whether any high-pressure sources were present. Third, tests of various zones within the Salado were planned to determine if the Salado was the source of the observed pressures. The tests were not intended to provide quantitative information on the permeability of the Castile and Salado Formations. They were intended simply to identify any zones that, when isolated, would rapidly pressurize to levels comparable to those measured at the wellhead. Detailed information on the WIPP-12 test equipment and data is contained in Stensrud et al. (1987).

Before testing began, gamma-ray and caliper logging was performed in the WIPP-12 borehole. These logs were used to identify stratigraphic intervals and select potential packer seats. In general, the geophysical "signatures" of the various stratigraphic units were found to be 4 to 5 ft lower than reported by Sandia and D'Appolonia (1982) based on 1978 geophysical logs. This discrepancy is believed to have been caused by the two geophysical surveys "zeroing" their depth counters at different elevations, perhaps reflecting modifications made to the drilling pad between 1978 and 1985. The 1985 testing relied on the interpretations from the 1985 geophysical logs, while the well configuration illustrated in Figure 3-11 reflects the 1978 logs and land-surface survey.

5.1.1 Plug Tests.
To evaluate the effectiveness of the brine-reservoir plug, DST's were performed with a single packer set from about 2770.8 to 2774.5 ft below ground surface, approximately 9 ft above the plug. Figure 5-1 shows the pressures measured during the testing. After setting the packer, the tubing was swabbed to lower the pressure in the test
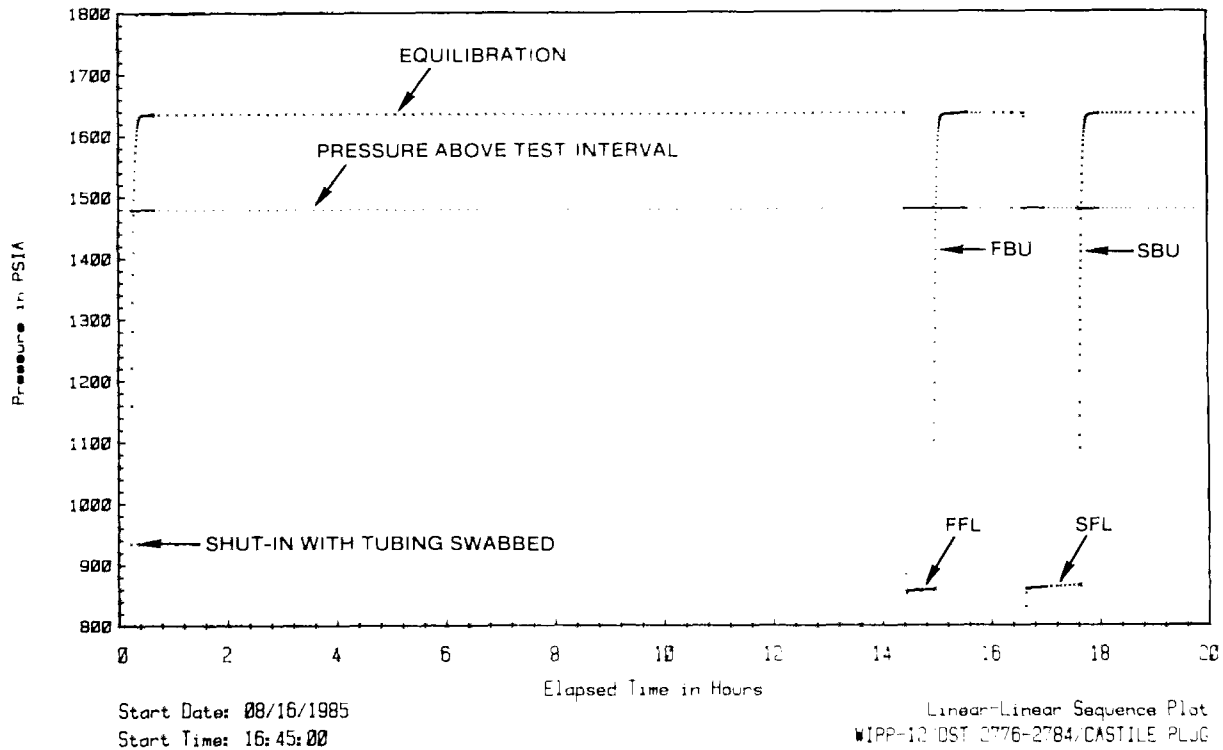
Figure 5-1. WIPP-12/Brine Reservoir Plug Test Linear-Linear Sequence Plot

zone, and the test interval was then shut in overnight to allow the pressure to equilibrate. As can be seen in Figure 5-1, the pressure stabilized very rapidly at a pressure of about 1635 psia. The following morning, August 17, 1985, DST's consisting of two flow and two buildup periods were performed. The first flow period lasted about 31 minutes, and was followed by a 100-minute buildup period. During the buildup period, the pressure rapidly reached 1635 psia and stabilized. The second flow period lasted about 59 minutes, and was followed by a 128-minute buildup period. Again, the pressure rapidly reached 1635 psia during the buildup period and stabilized.

The transducer was set at a depth of 2760.4 ft during these tests. The fluid in the well was a saturated brine having a specific gravity of about 1.2. Corrected for depth, specific gravity, and atmospheric pressure, 1635 psia corresponds to a pressure of about 190 psig at the surface. This pressure is well below the 288 psig measured before testing began, but intermediate between the maximum brine-reservoir pressure recorded

(208 psig) and the brine-reservoir pressure measured just before the plug was set in 1983 (169 psig).

The speed with which a constant pressure of 1635 psia was repeatedly reached during these tests indicates the presence of a constant-pressure source. This source is most likely the brine reservoir. The brine-reservoir plug is apparently not a perfect seal; pressure seems to be transmitted through the plug fairly readily. The fact that WIPP-12 wellhead pressures were higher than the pressure coming through the plug, however, indicates two things. First, the brine reservoir is not the source of the pressures measured at the surface. Second, any flow through the plug would be driven downwards into the brine reservoir by the higher pressures present above the plug.

5.1.2 Castile Tests. Following the plug tests, the DST tool was raised 39 ft and reset at the top of the Castile Formation. The bottom of the packer at this time was at a depth of 2735.5 ft. Figure 5-2 shows
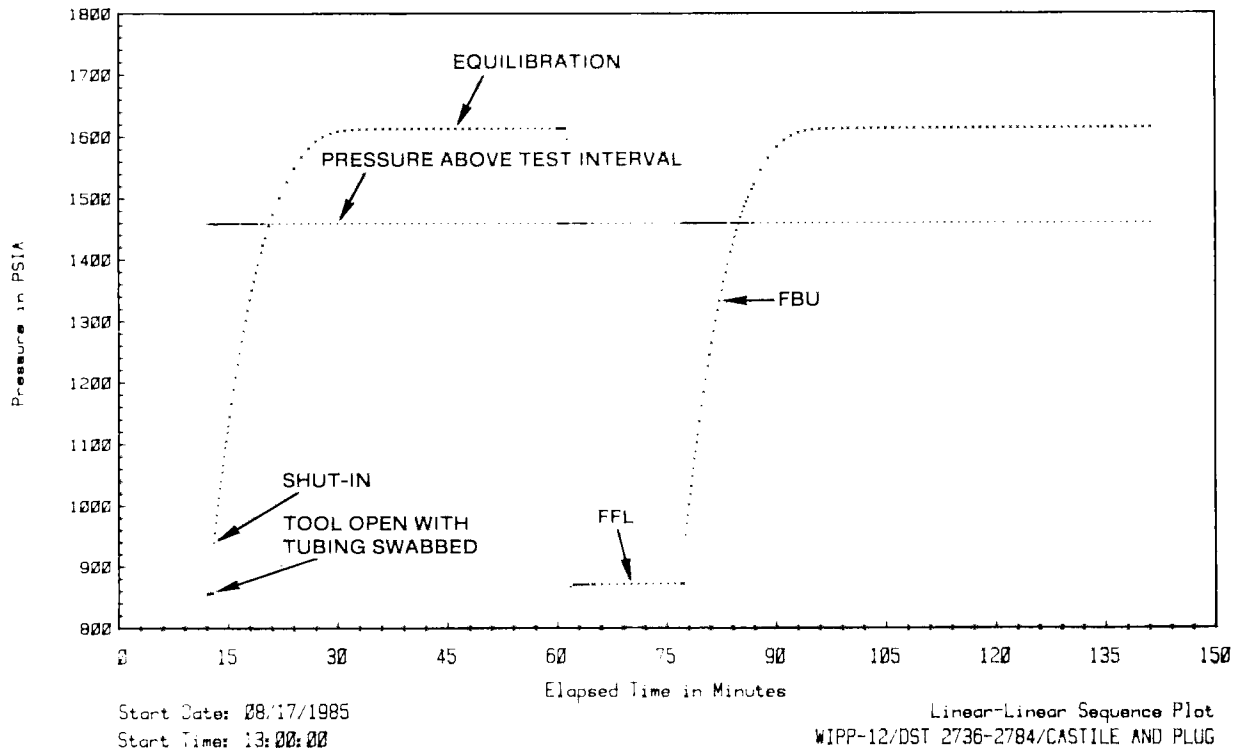
Figure 5-2. WIPP-12/Upper Castile and Plug Test Linear-Linear Sequence Plot

the pressures measured during the subsequent testing. The tubing was swabbed to decrease the pressure in the test interval, and the test interval was then shut in to allow the pressure to equilibrate. In less than an hour, the pressure was near stabilization at a value of almost 1614 psia. After a 15-minute flow period, the test interval was again shut in for a 64-minute buildup period. Again, the pressure was rapidly stabilizing at almost 1614 psia.

The results of these tests are virtually identical to the results of the plug tests discussed in Section 5.1.1. The pressure in these tests stabilized about 21 psi lower than in the previous tests, but that was caused by the transducer being positioned 39 ft higher in the hole for these tests. Pressure transmitted from the brine reservoir through the plug appeared to be the dominating factor in these tests. No other pressure sources were noted in the upper Castile.

5.1.3 Salado Tests. The Salado tests were originally meant to be performed using a double-

(straddle-) packer DST tool with a 100-ft separation between packers. Hole conditions proved to be such, however, that two good packer seats 100 ft apart could not be found. From August 19 to 23, 1985, 17 attempts were made to set the DST tool and perform tests at depth intervals ranging from 1005 to 2200 ft. All of these attempts failed as fluid was able to bypass one or both packers. Only a single packer seat, from 1115 to 1120 ft deep between Marker Beds 102 and 103, was unequivocally good. During the course of these attempts, the DST tool was pulled up into the well casing and tested on four separate occasions. Each time, both packers set successfully with no apparent fluid leakage around them. Between the ninth and tenth attempts at testing, the tool was brought to the surface and all components were either replaced or rehabilitated. Our tentative conclusion from these failures is that hole closure since the original drilling in 1978 has caused fracturing in the rock around the hole that allows fluid to bypass any packer blocking the hole itself.

Once straddle tests proved impossible, our testing strategy changed. We believed that various anhydrite beds within the Salado, such as the Cowden and Union anhydrites and various marker beds, would provide adequate individual packer seats. Hence, we decided to use a retrievable bridge plug set in an anhydrite bed to define the bottom of a test interval, and a DST tool with a single packer set in a higher anhydrite to define the top of the interval.

For the first test, the bridge plug was set in the Anhydrite III unit of the Castile Formation from 2750 to 2754 ft deep. A single-packer DST tool was then set in the Cowden anhydrite from 2450 to 2454 ft deep (see Figure 3-11), and the lower Salado between the Cowden and the Castile was tested. Following the test of the infra-Cowden portion of the Salado, the bridge plug was reset in the Cowden and left there for the balance of testing in WIPP-12. The DST-tool packer was then set in Marker Bed 136 from 2066 to 2070 ft deep, but the packer seat failed. A good packer seat was obtained 4 ft lower between 2070 and 2074 ft deep, and testing proceeded. The next five attempts at testing failed, as fluid bypassed the packer at two settings in the Union anhydrite, two settings in Marker Bed 124, and one setting in Marker Bed 123. We then returned to the one good packer seat found during the first attempts at straddle testing, 1115 to 1120 ft deep, between Marker Beds 102 and 103. Again, this location provided a good seat and we were able to test from there down to the Cowden. The final test was performed with the DST-tool packer set at the base of the well casing between 1001 and 1005 ft deep. In summary, out of 10 attempts to test using a bridge plug and single-packer DST tool, 4 were successful. These are discussed below.

5.1.3.1 Infra–Cowden. The infra-Cowden portion of the Salado Formation was tested between the depths of 2454 and 2750 ft (see Figure 3-11). Inasmuch as the objective of the testing was to identify sources of high pressure rather than to provide data for quantitative permeability analysis, no effort was made to allow the test-interval pressure to stabilize before testing began. As the DST-tool packer was set, the expansion of the packer compressed the fluid in the test interval slightly, raising the test-interval pressure above that in the

well annulus above the packer. This pressure decayed slightly over about 32 minutes while the tubing was being swabbed and other preparations were being made for the test (Figure 5-3). The test interval was then opened to the tubing for almost 12 minutes for a flow period. Very little fluid entered the tubing during this period. Following the flow period, the test interval was shut in for a buildup lasting about 127 minutes. The pressure buildup was slow, and showed no signs of trending towards a positive surface pressure. At the end of the buildup period, the pressure was rising at a rate slightly less than 25 psi/hr, and the rate was constantly decreasing.

Figure 5-4 shows a Horner plot of the buildup data. A precise determination of the static formation pressure (p*) cannot be made because the data curve is continuing to steepen at the end of the test. Extrapolation from the last two data points to infinite time provides a minimum static pressure estimate of 925 psia. The curve would have to continue to steepen considerably, however, to ever extrapolate to the approximately 1567 psia that, with the transducer at a depth of 2439.6 ft, would correspond to the 288 psig measured at the WIPP-12 wellhead. The test of the infra-Cowden, therefore, gave no clear indication of that portion of the Salado being the source of the high pressures measured at the WIPP-12 wellhead.

5.1.3.2 Marker Bed 136 to Cowden Anhydrite. The Salado between Marker Bed 136 and the Cowden anhydrite, 2074 to 2450 ft deep, was tested on August 28 and 29, 1985. Testing consisted of a flow period lasting almost 13 minutes followed by a 15-hr buildup period (Figure 5-5). As was the case during the infra-Cowden test, very little fluid entered the tubing during the flow period. The pressure buildup proceeded slowly, at an ever-decreasing rate, and showed no signs of trending towards a positive surface pressure. At the end of the buildup period, the pressure was rising less than 10 psi/hr.

Figure 5-6 is a Horner plot of the buildup data. Extrapolation from the last two points to infinite time indicates a static formation pressure (p*) estimate of 983 psia. This estimate must be lower than the true static formation pressure because the data curve was continuing to steepen when the buildup was

44
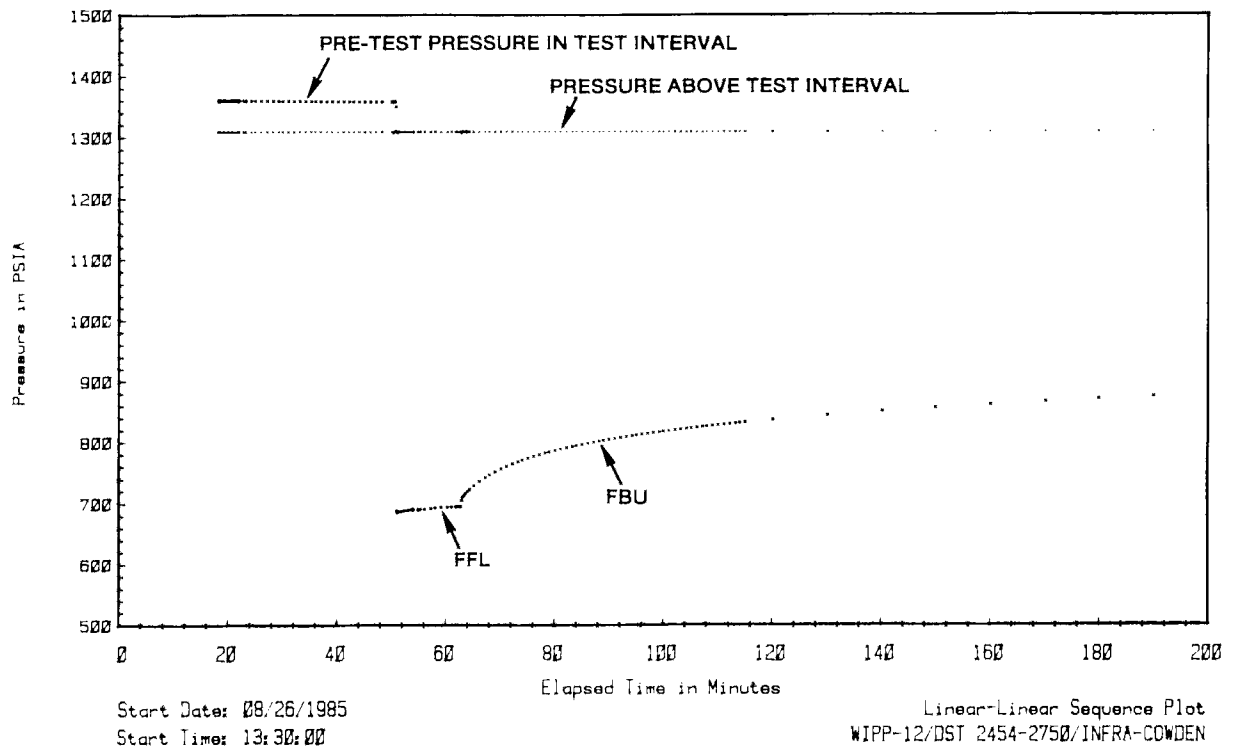
Figure 5-3. WIPP-12/Infra-Cowden Test Linear-Linear Sequence Plot
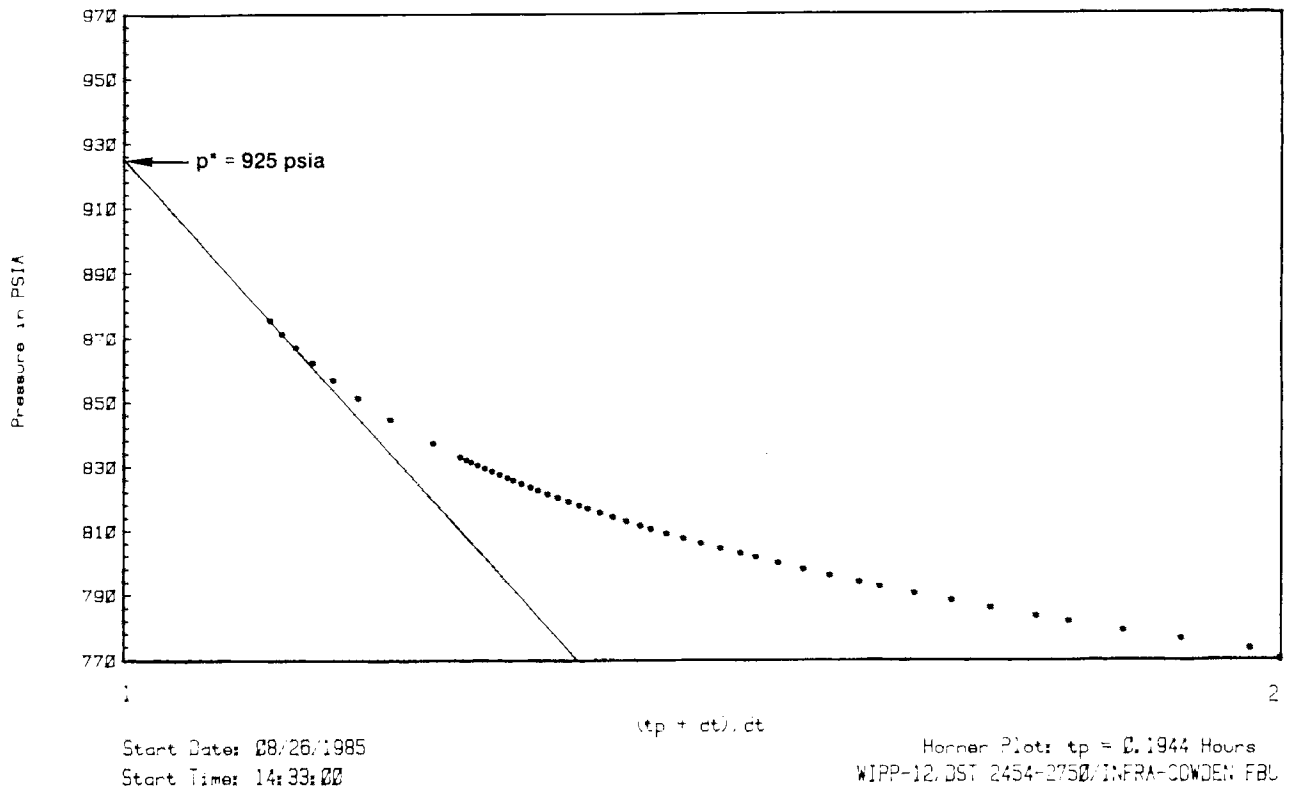
Figure 5-4. WIPP-12/Infra-Cowden First Buildup Horner Plot

Figure 5-5. WIPP-12/Salado Marker Bed 136 to Cowden Test Linear-Linear Sequence Plot
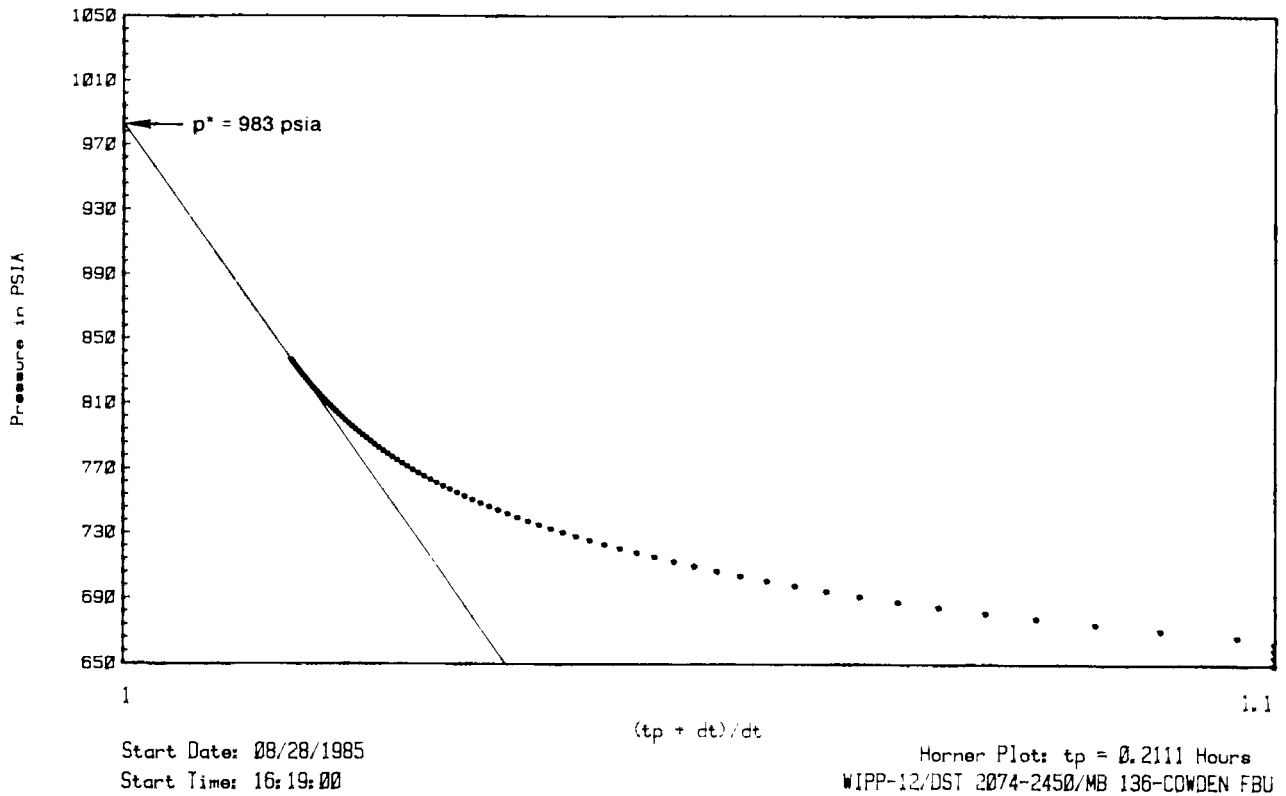
Figure 5-6. WIPP-12/Salado Marker Bed 136 to Cowden First Buildup Horner Plot

terminated. The curve would have to steepen considerably, however, to extrapolate to the approximately 1369 psia that, with the transducer at a depth of 2059.6 ft, would correspond to the 288 psig measured at the WIPP-12 wellhead. As was the case with the infra-Cowden test, the test of the interval between Marker Bed 136 and the Cowden gave no clear indication of that portion of the Salado being the source of the high pressures measured at the WIPP-12 wellhead.

5.1.3.3 Marker Bed 103 to Cowden Anhydrite.
The interval from just above Marker Bed 103 to the Cowden anhydrite, 1120 to 2450 ft deep, was tested on August 29 and 30, 1985. Testing consisted of a 16-minute flow period followed by a 13-hr buildup period (Figure 5-7). As was the case during the previous Salado tests, very little fluid entered the tubing during the flow period. The pressure recovery during the buildup period was slow, with a final rate of less than 5 psi/hr, and showed no clear signs of trending towards a positive surface pressure.

Figure 5-8 is a Horner plot of the buildup data. Extrapolation from the last two points to infinite time gives a static formation pressure (p*) estimate of 510 psia. Inasmuch as the data curve was continuing to steepen when the buildup was terminated, this estimate must be too low. Considerable steepening would be required, however, for the curve to extrapolate to the approximately 873 psia that, with the transducer at a depth of 1105.7 ft, would correspond to the 288 psig measured at the WIPP-12 wellhead. As was the case with the previous Salado tests, the interval from Marker Bed 103 to the Cowden gave no clear indication of containing the source of the high pressures measured at the WIPP-12 wellhead.
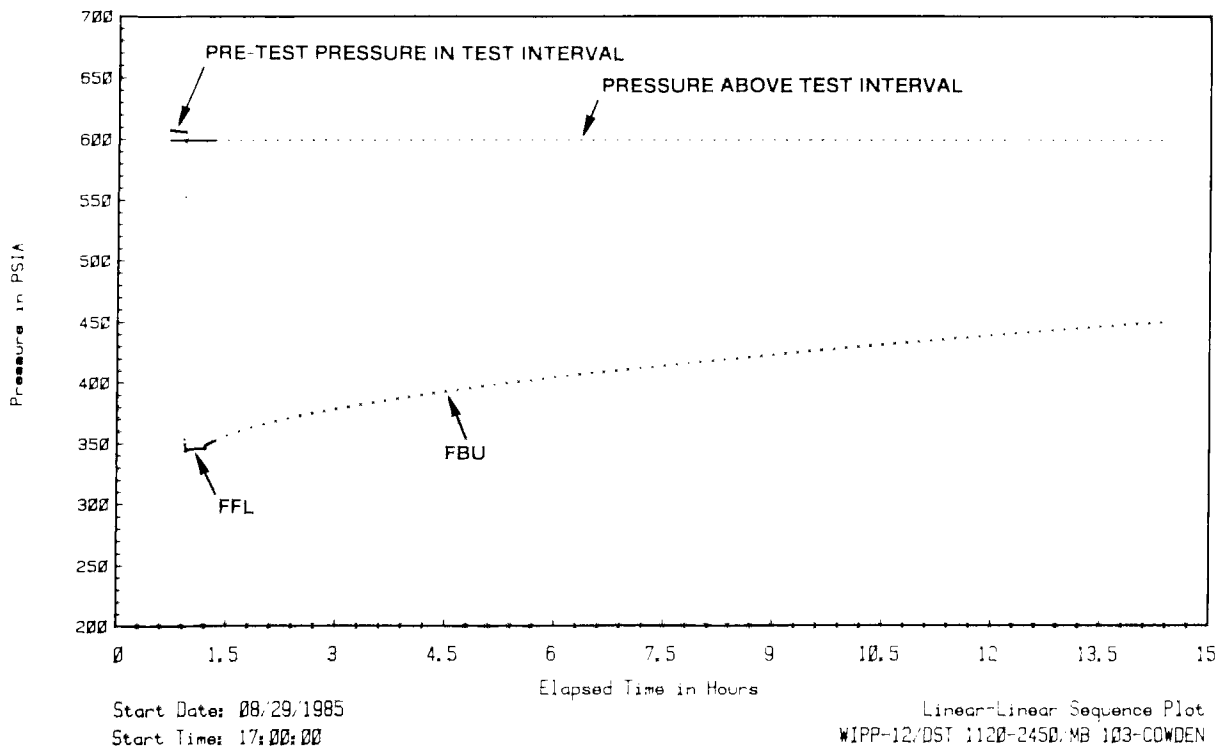
Figure 5-7. WIPP-12/Salado Marker Bed 103 to Cowden Test Linear-Linear Sequence Plot
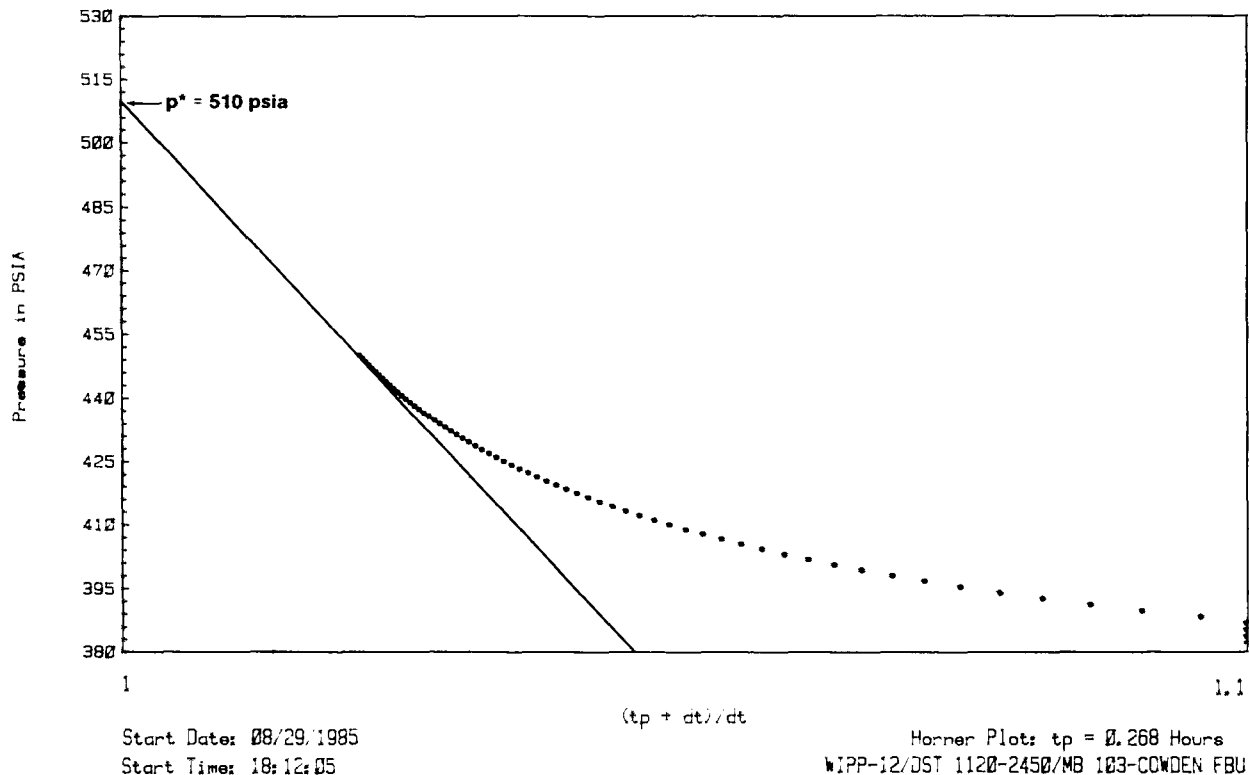
Figure 5-8. WIPP-12/Salado Marker Bed 103 to Cowden First Buildup Horner Plot

5.1.3.4 Well Casing to Cowden Anhydrite. The final test of the Salado at WIPP-12 was performed on an interval extending from the base of the well casing to the Cowden anhydrite, 1004.5 to 2450 ft deep. The test was performed on August 30, 1985, and consisted of a 30-minute flow period followed by a buildup period lasting about 139 minutes (Figure 5-9). As was the case with the other Salado tests, very little fluid entered the tubing during the flow period. The pressure buildup was slow, with a final rate of about 10 psi/hr, and showed no indication of trending towards a positive surface pressure.

Figure 5-10 is a Horner plot of the buildup data. The static formation pressure (p*) estimated by extrapolating from the last two points to infinite time is 333 psia. This estimate must be too low because the data curve was continuing to steepen when the buildup was terminated. The curve would have to steepen considerably, however, to extrapolate to the approximately 813 psia that, with the transducer at a depth of 990.7 ft, would correspond to the 288 psig

measured at the WIPP-12 wellhead. As was the case with all the other Salado tests, the test of the interval from the well casing to the Cowden anhydrite gave no clear indication of that portion of the Salado containing the source of the high pressures measured at the WIPP-12 wellhead.

5.1.4 Conclusions From Castile and Salado Tests. The tests of the brine-reservoir plug and the Castile Formation showed a constant-pressure response apparently governed by the brine reservoir in the lower part of the Anhydrite III unit of the Castile. This constant pressure, however, is lower than the pressures measured at the WIPP-12 wellhead, and therefore cannot be their source. None of the tests of the Salado provided any indication of the source of the high pressures. All of the zones tested exhibited pressure buildups, but none of the buildups clearly extrapolated to positive surface pressures. In fact, given the 6.5+ years of high pressures to which the entire borehole was subject preceding these tests, we cannot say with certainty which, if any, of the observed pressure
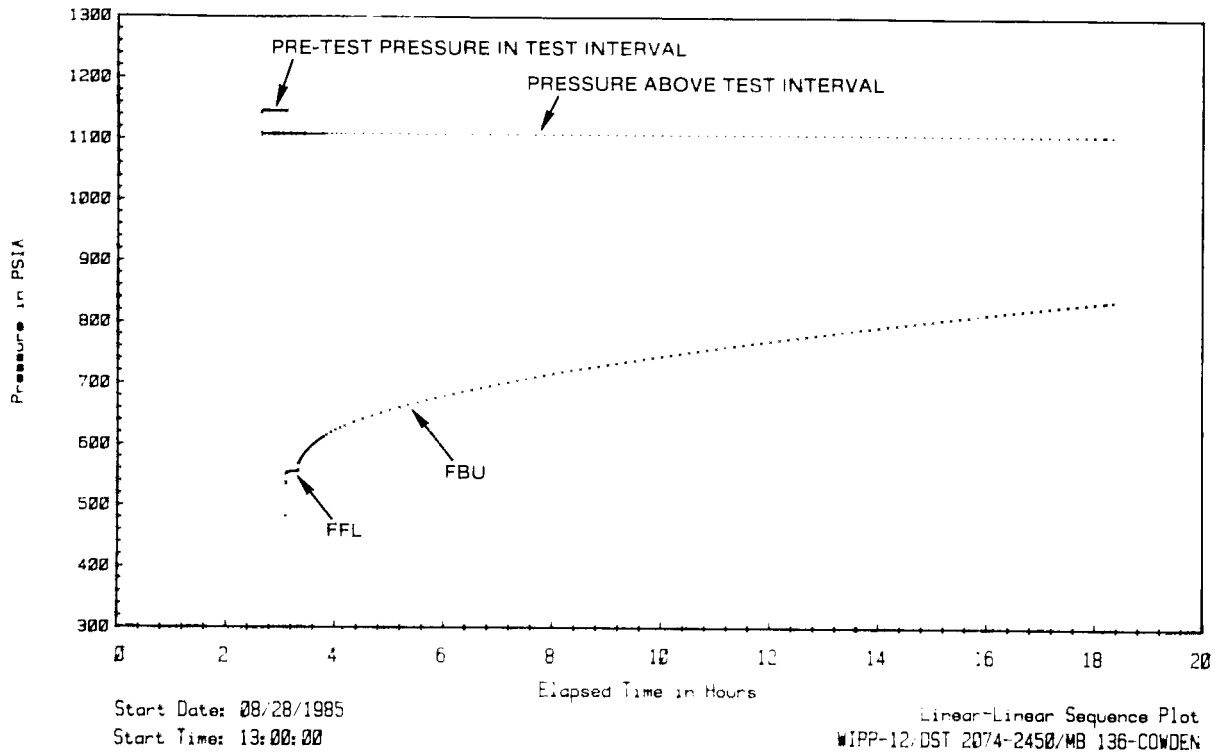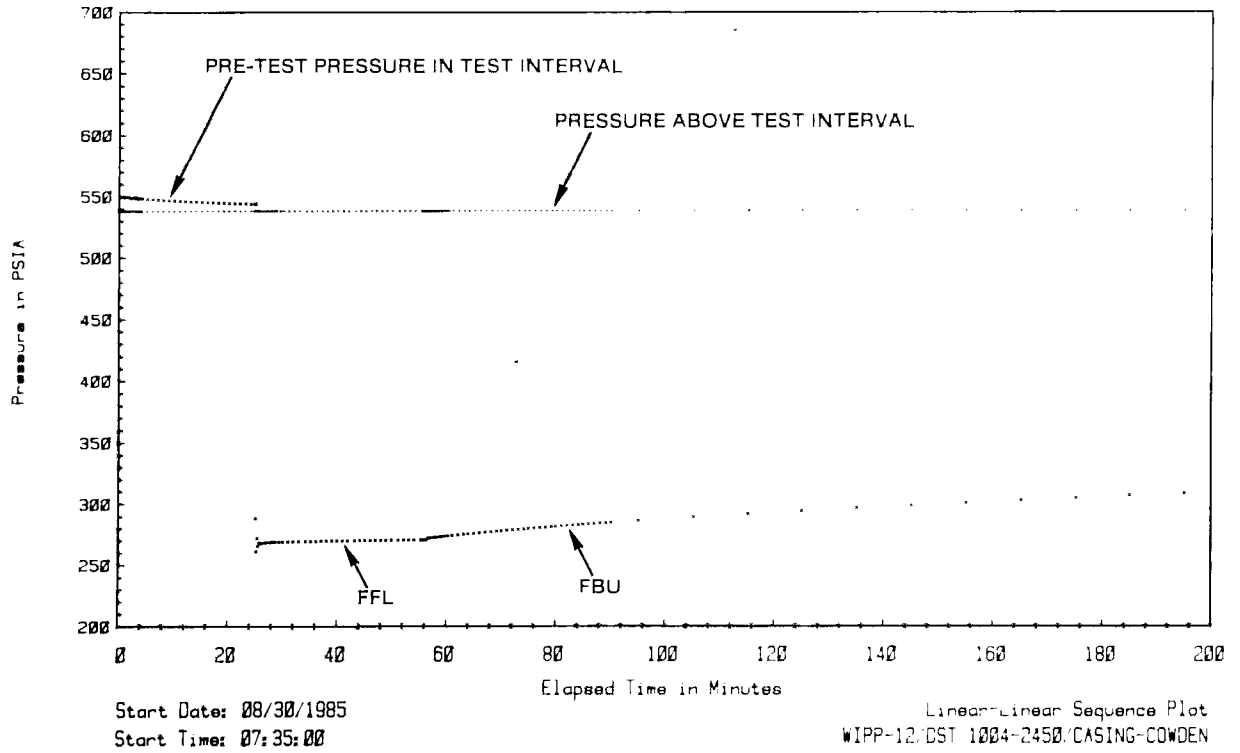
Figure 5-9. WIPP-12/Salado Casing to Cowden Test Linear-Linear Sequence Plot
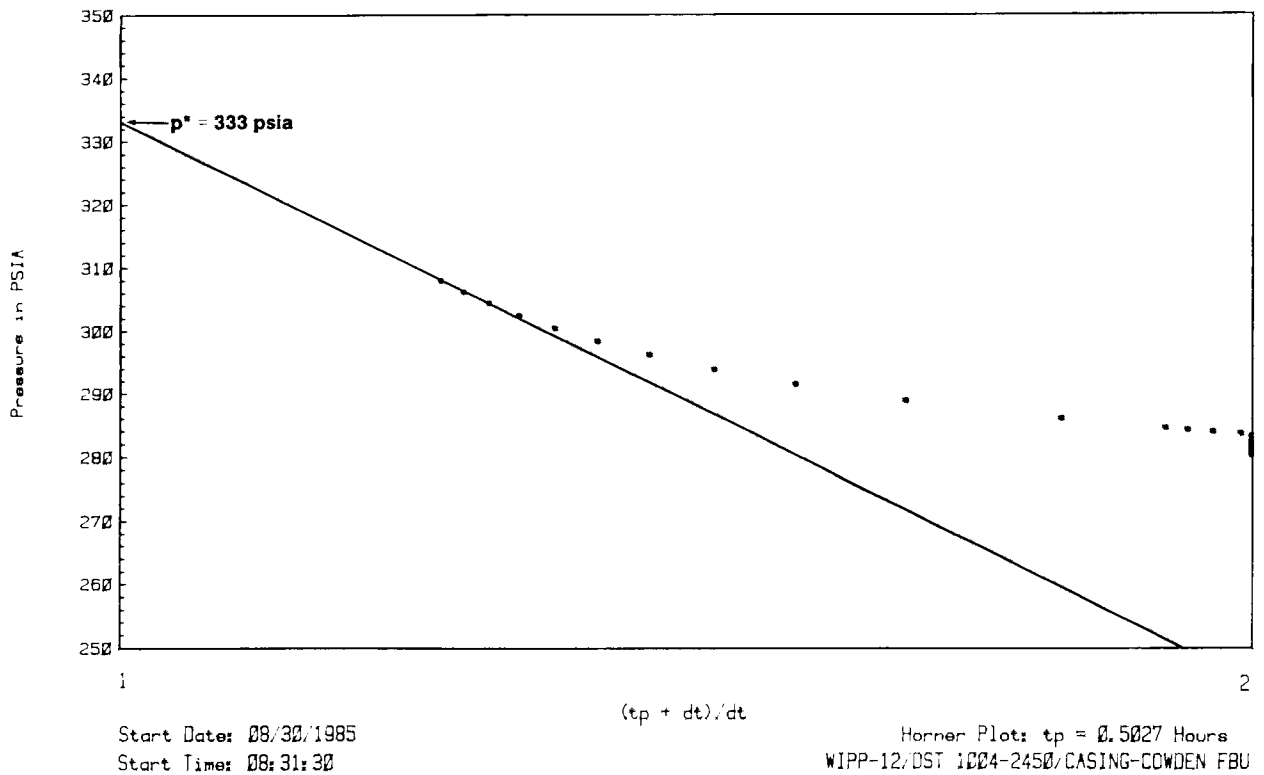
Figure 5-10. WIPP-12/Salado Casing to Cowden First Buildup Horner Plot

buildups were caused by the natural pressures in those parts of the Salado, and which were partially or completely caused by residual overpressurization of the entire wellbore.

The only conclusion that could be drawn from this testing was that the source(s) of the high pressures has a low flow capacity, and is rapidly depleted. Even in a shut-in situation, the source must take days to weeks to manifest itself; it was not apparent in tests lasting less than a day. This conclusion was borne out by observations made after testing was completed. On September 4, 1985, the WIPP-12 wellbore was filled with brine and the wellhead was resealed. By October 2, 1985, the pressure at the wellhead had built back up to 248 psig (Stensrud et al., 1987).

5.2 Rustler Formation

Hydraulic tests were attempted in all five members of the Rustler Formation. The unnamed lower member of the Rustler was tested only at well H-16. The Culebra dolomite was tested in wells H-1, H-4c, H-8b, H-12, H-14, H-15, H-16, H-17, H-18, WIPP-12, WIPP-18, WIPP-19, WIPP-21, WIPP-22, WIPP-30, P-15, P-17, P-18, ERDA-9, Cabin Baby-1, DOE-1, and Engle. The Tamarisk, Magenta, and Forty-niner Members were tested in H-14 and H-16.

5.2.1 Unnamed Lower Member. The unnamed lower member of the Rustler was tested only at H-16. This testing had two objectives: 1) to determine the transmissivity of the unit; and 2) to determine the hydraulic head of the unit. The transmissivity is a parameter needed to calculate potential leakage rates from the unnamed lower member into the WIPP shafts. The hydraulic head is also needed for leakage calculations, as well as to evaluate directions of potential vertical movement of groundwaters within the Rustler Formation.

At H-16, the unnamed lower member of the Rustler lies between 724.4 and 841.5 ft below ground surface (Figure 3-8). DST's were performed on the interval from 739.2 to 850.9 ft, which includes the upper 9.4 ft of the Salado Formation. The most permeable portion of the unnamed lower member is probably the siltstone unit (designated S-1 by

Lowenstein, 1987) that extends from 777.7 to 839.1 ft. The other lithologies included in the test interval were halite, polyhalite, gypsum/anhydrite, and halitic claystone, which are believed to have extremely low permeabilities and to have made negligible contributions to the test responses observed.

The DST's were performed from August 14 to 17, 1987, and consisted of two flow periods and two buildup periods (Figure 5-11). Descriptions of the test instrumentation and the test data are contained in Stensrud et al. (1988). For analysis purposes (see Section 4.1), the FFL was divided into two flow periods with rates of 0.035 and 0.024 gallons per minute (gpm), and the SFL was divided into two flow periods with rates of 0.026 and 0.015 gpm (Table 5-1).

The FFL lasted about 22 minutes, and was followed by a 23-hr FBU. Figure 5-12 shows a log-log plot of the FBU data along with a simulation generated by the INTERPRET well-test-interpretation code (see Appendix A). An unusual feature of this figure is that the pressure-derivative data plot above (i.e., have a greater magnitude than) the pressure data. In most instances, pressure-derivative data plot below pressure data (see Figure A-2 in Appendix A). However, when a very low transmissivity medium is tested and the flow-period duration is much shorter than would be required for infinite-acting radial flow to develop, the subsequent buildup shows the type of behavior seen in Figure 5-12.

The simulation in Figure 5-12 is of a single-porosity medium with a transmissivity of 2.7×10^{-4} ft^2/day (Table 5-2). Assuming a porosity of 30%, a total-system compressibility of 1.0×10^{-5} psi^{-1}, and a fluid viscosity of 1.0 cp, the skin factor for the well in this simulation is -0.4, indicating a very slightly stimulated well. The dimensionless Horner plot of the FBU (Figure 5-13) shows an excellent fit of the simulation to the data, and indicates that the static formation pressure is about 213 psia.

The SFL lasted about 29 minutes, and was followed by a 50-hr SBU. The log-log plot of the SBU data (Figure 5-14) shows behavior similar to that seen in the FBU plot (Figure 5-12). The single-porosity
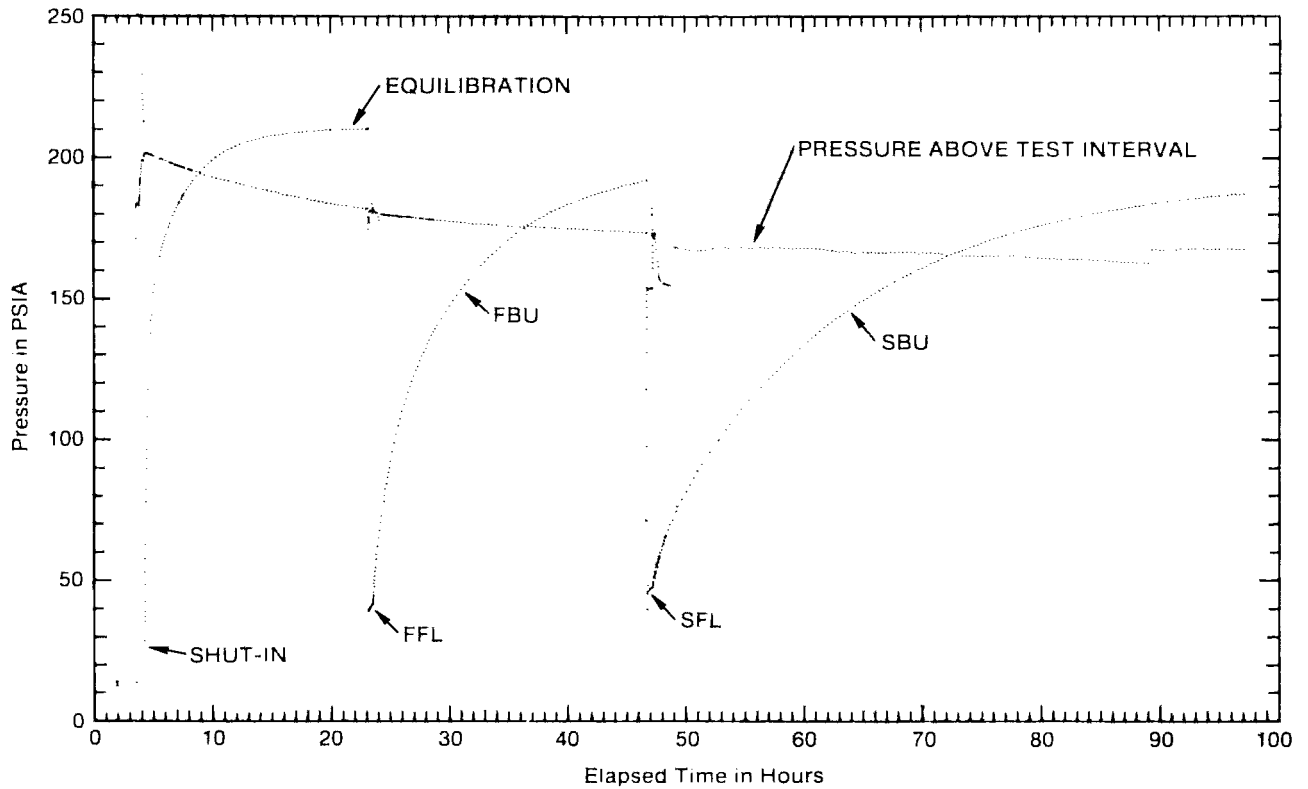
Figure 5-11. H-16/Unnamed Lower Member Siltstone Drillstem Test Linear-Linear Sequence Plot
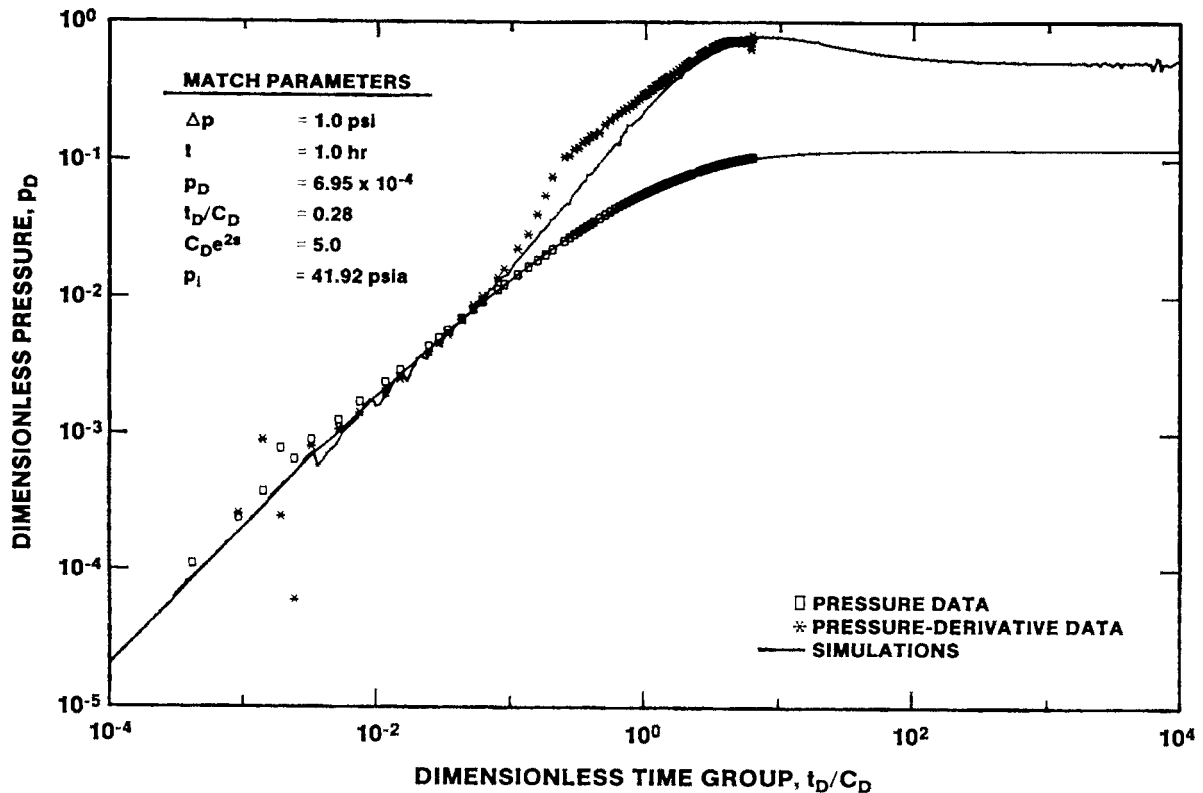
Figure 5-12.   H-16/Unnamed Lower Member Siltstone First Buildup Log-Log Plot
with INTERPRET Simulation

TABLE 5-1
EFFECTIVE DST FLOW RATES FOR BUILDUP ANALYSES

WELL	UNIT TESTED	FLOW PERIOD	DURATION (min)	RATE (gpm)
H-16	Unnamed lower member	First	15.13	0.035
			6.90	0.024
		Second	16.68	0.026
			12.54	0.015
H-14	Culebra	First	4.05	0.381
			10.25	0.260
		Second	7.27	0.271
			16.60	0.173
H-14	Upper Culebra	First	3.63	0.186
			8.05	0.132
			5.22	0.116
		Second	6.55	0.138
			20.78	0.097
H-15	Culebra	First	.55	0.147
			14.23	0.127
		Second	8.48	0.153
			17.25	0.124
			14.33	0.110
H-16	Culebra	First	6.72	0.731
			10.38	0.500
		Second	9.12	0.818
			15.06	0.512
H-17	Culebra	First	4.62	0.368
			11.58	0.259
		Second	6.48	0.443
			17.76	0.280

TABLE 5-1 (Continued)

WELL	UNIT TESTED	FLOW PERIOD	DURATION (min)	RATE (gpm)
H-18	Culebra	First	4.38	1.372
			6.54	1.083
		Second	6.06	1.200
			11.46	0.772
H-14	Magenta	First	1.62	0.049
			13.65	0.014
		Second	2.27	0.036
			27.95	0.010
		Third	13.35	0.014
			46.85	0.007
H-16	Magenta	First	12.30	0.062
			9.90	0.047
		Second	10.38	0.062
			20.64	0.045
H-14	Forty-niner claystone	First	4.52	0.028
			13.75	0.021
		Second	13.93	0.022
			18.20	0.017
H-16	Forty-niner clay	First	8.82	0.010
			12.54	0.005
		Second	6.66	0.016
			24.60	0.007

TABLE 5-2
SUMMARY OF NON-CULEBRA SINGLE-WELL TEST RESULTS

WELL	ZONE NAME	ZONE DEPTH INTERVAL (ft)	DEPTH INTERVAL TESTED (ft)*	TEST TYPE	TRANSMISSIVITY (ft²/day)	SKIN FACTOR
H-16	Unnamed lower member siltstone	778-842	739-851	DST/FBU DST/SBU	2.7×10^{-4} 2.2×10^{-4}	-0.4 0.2
H-14	Magenta	424-448	420-448	DST/FBU DST/SBU DST/TBU	5.6×10^{-3} 5.6×10^{-3} 5.3×10^{-3}	0.5 0.4 0.3
H-16	Magenta	590-616	589-621	DST/FBU DST/SBU slug	2.8×10^{-2} 2.8×10^{-2} 2.4×10^{-2}	-0.4 -0.8 —
H-14	Forty-niner claystone	390-405	381-409	DST/FBU DST/SBU slug	7.1×10^{-2} 6.9×10^{-2} 3.0×10^{-2}	3.2 3.3 —
H-16	Forty-niner clay	563-574	560-581	pulse DST/FBU DST/SBU slug	2.2×10^{-4} 5.3×10^{-3} 5.6×10^{-3} 5.0×10^{-3}	— 0.7 0.6 —
Carper	Cenozoic alluvium	263-386	263-386	pumping	55	—

*Actual intervals open to the wells.

54
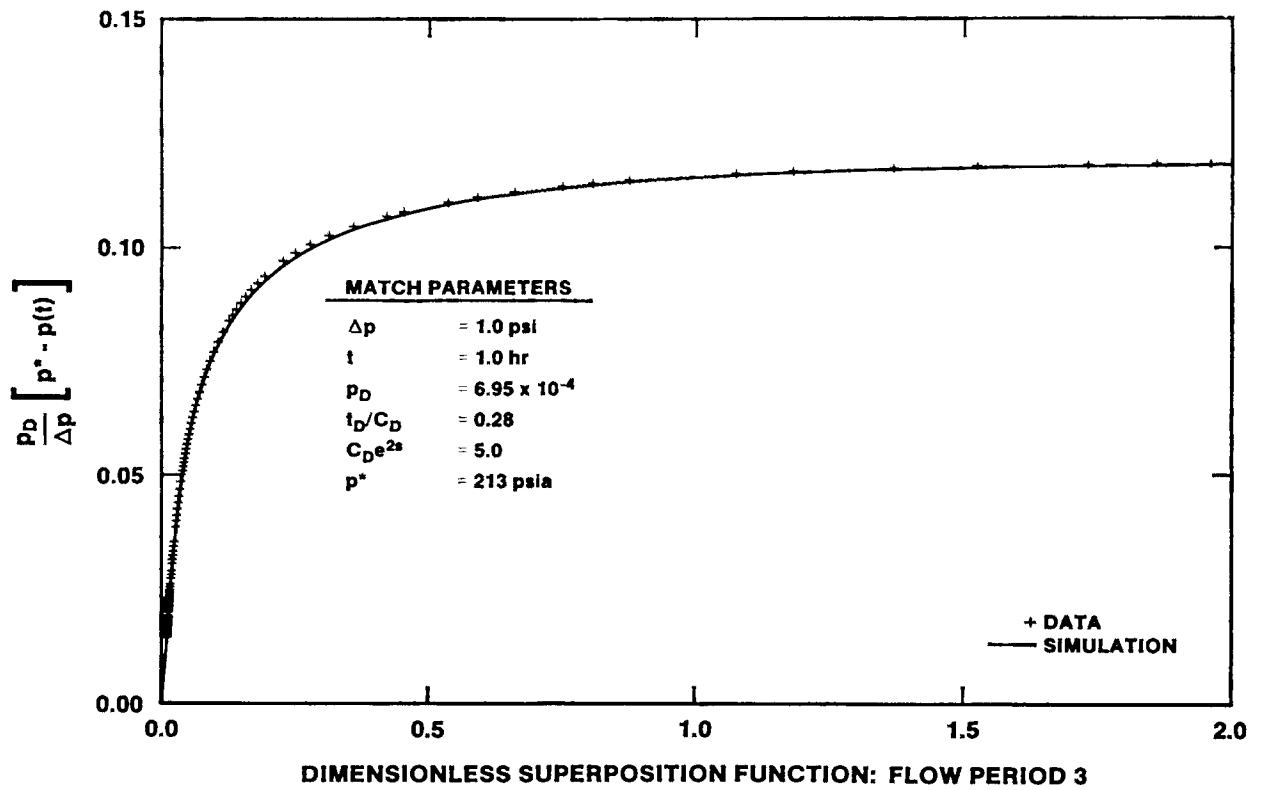
Figure 5-13.   H-16/Unnamed Lower Member Siltstone First Buildup Dimensionless
                 Horner Plot with INTERPRET Simulation
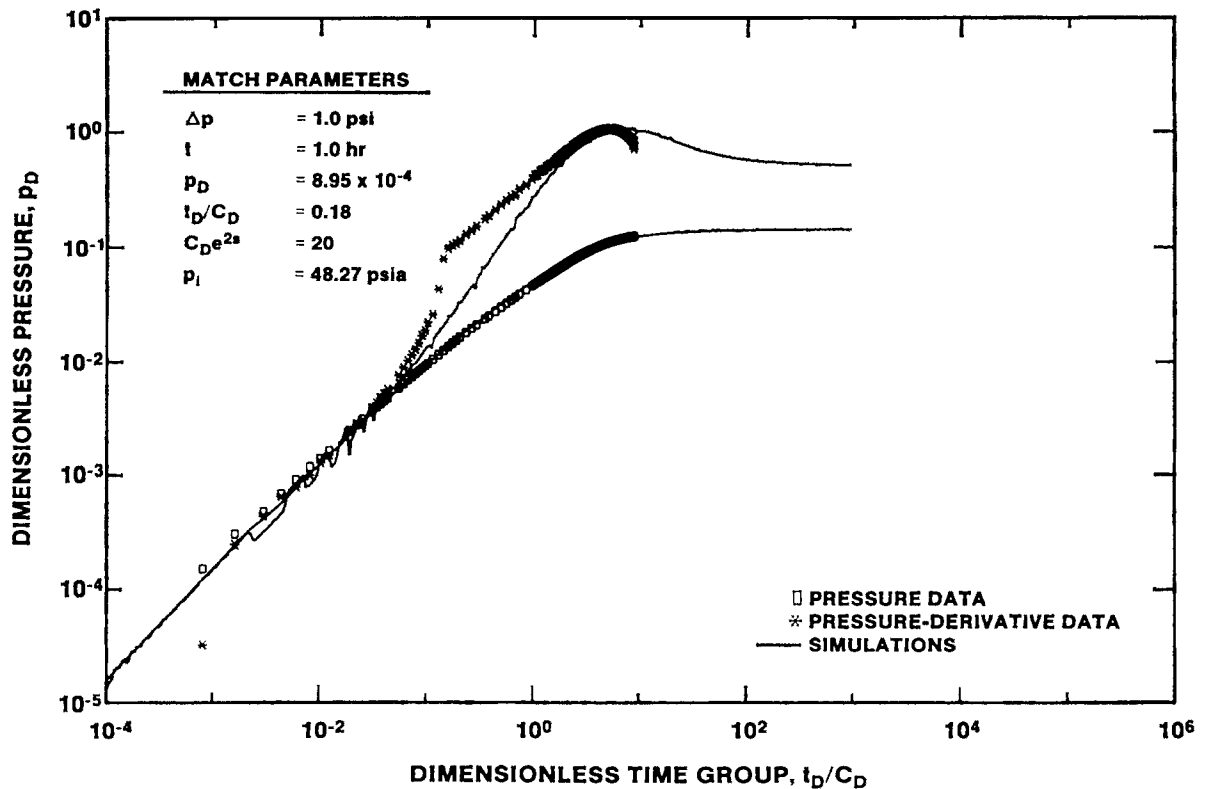
Figure 5-14.   H-16/Unnamed Lower Member Siltstone Second Buildup Log-Log Plot
                 with INTERPRET Simulation

simulation shown, however, uses a transmissivity of 2.2×10^{-4} ft²/day, and a skin factor of 0.2 (Table 5-2). These values imply a slightly less permeable formation and a slightly more damaged well than were indicated by the FBU analysis.

The sharp decline in the pressure derivative at late time in Figure 5-14 was probably caused by what Grisak et al. (1985) term a "pressure skin" on the formation. Pressure skins develop as wells are drilled and as they stand open before testing. As drilling fluid circulates during drilling, it exerts a fluid pressure on the exposed formations corresponding to the weight of the drilling-fluid column in the wellbore. In most formations, this pressure exceeds the ambient formation fluid pressure. As a result, an overpressurized zone (or overpressure skin) develops in the formations around the wellbore. Underpressure skins can also be created if the borehole history includes a period when the pressure exerted by the fluid in the hole is less than that of the adjacent formation(s).

The magnitudes and extents of these pressure skins depend on several factors, including the duration and magnitude of the induced pressure differential and the hydraulic properties of the affected formations. Once the formations are isolated from the overpressure or underpressure, the pressure skins begin to dissipate. When hydraulic tests are performed while a pressure skin still exists, however, the test data may be influenced by dissipation of the pressure skin. This is most commonly manifested, in the case of an overpressure skin, by a pressure recovery that appears to be trending towards some specific value representative of the pressure skin until, at late time, the pressure begins to deviate below this trend, often reaching a maximum at a lower value before beginning to decline towards the true formation pressure.

In the case of the testing of the unnamed lower member at H-16, the overpressure skin induced by the weight of the drilling fluid during coring and reaming on August 11 and 12, 1987 was dissipating during the DST's. One measure of the dissipation is provided by the different static formation pressures indicated by the FBU (Figure 5-13) and SBU (Figure 5-15) dimensionless Horner plots. The best-

fit simulation to the FBU data indicated that a static formation pressure of 213 psia was appropriate, whereas the SBU simulation used a value of 209 psia. The INTERPRET code has no way of correcting for the effects of pressure skins on test data. Inasmuch as the SBU data appear to have been more affected by pressure-skin dissipation than the FBU data, the FBU analysis, with the exception of the static formation pressure estimate, is probably more reliable than the SBU analysis.

Additional information on the true static formation pressure and overpressure skin of the unnamed lower member at H-16 is provided by the transducer installed at that horizon as part of the H-16 5-packer completion (Figure 3-8). From August 31, 1987, 4 days after the 5-packer installation was completed, until December 7, 1987, the pressure dropped from 203 to 197 psig, where it apparently stabilized. This transducer is located at a depth of 745.7 ft. In a hole containing brine with a specific gravity of 1.2, the corresponding pressure at the midpoint of the unnamed lower member siltstone 808 ft deep is about 229 psig. In contrast, the 209 psia indicated by the data from the DST transducer, which was set 721.3 ft deep, corresponds to a pressure of 254 psia at a depth of 808 ft. This value is reduced to 240 psig when the atmospheric pressure of 14 psia measured by the DST transducer is subtracted. Hence, an additional 11 psi of overpressure skin apparently dissipated between the end of the DST's and December 7, 1987.

The static formation pressure estimate of 229 psig discussed above, however, may not represent the pressure that would exist in the absence of the WIPP site. Considering the proximity of H-16 to the WIPP shafts, the pressure in the unnamed lower member (and in all other Rustler members) at H-16 may be artificially low and continually changing because of drainage from that member into the shafts.

5.2.2 Culebra Dolomite Member. The tests of the Culebra Dolomite Member of the Rustler Formation were primarily intended to provide additional transmissivity data on the most permeable water-bearing unit at the WIPP site. Inasmuch as all of the wells in which the Culebra was tested were ultimately left as permanent Culebra completions, obtaining

$$\frac{P_D}{\Delta p}\left[p^* - p(t)\right]$$

MATCH PARAMETERS

Δp	$= 1.0$ psi
t	$= 1.0$ hr
P_D	$= 8.95 \times 10^{-4}$
t_D/C_D	$= 0.18$
$C_D e^{2s}$	$= 20$
p^*	$= 209$ psia

+ DATA
—— SIMULATION

DIMENSIONLESS SUPERPOSITION FUNCTION: FLOW PERIOD 6
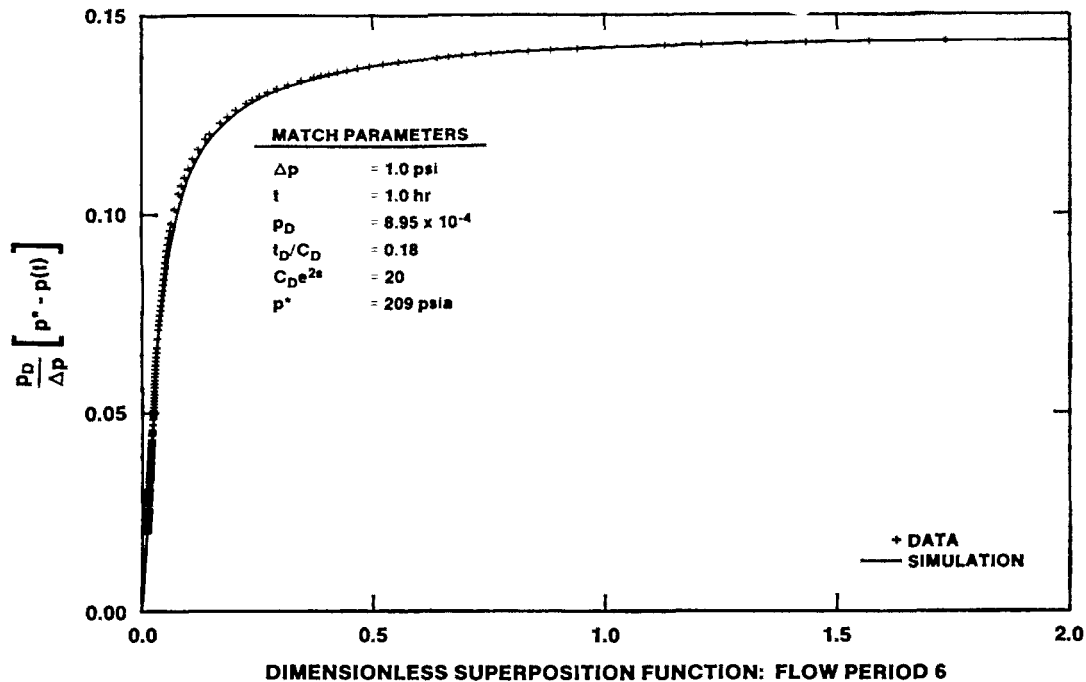
Figure 5-15.   H-16/Unnamed Lower Member Siltstone Second Buildup Dimensionless Horner Plot with INTERPRET Simulation

accurate static formation pressure estimates during testing was not of major concern. At wells H-1, H-4c, H-12, WIPP-12, WIPP-18, WIPP-19, WIPP-21, WIPP-22, WIPP-30, P-15, P-17, ERDA-9, and Cabin Baby-1, the Culebra was tested by performing falling-head slug tests. Rising-head slug tests were also performed at H-1 and P-18. Drillstem tests and rising-head slug tests were performed in the Culebra at wells H-14, H-15, H-16, H-17, and H-18. Pumping tests of the Culebra were performed at H-8b, DOE-1, and the Engle well.

5.2.2.1 H-1. Mercer (1983) reported a transmissivity value of 0.07 ft²/day for the Culebra at H-1, based on a bailing test performed shortly after the Culebra interval was perforated in 1977 (Mercer and Orr, 1979). Because this value was significantly lower than the transmissivities measured at other nearby wells such as H-2, H-3, and ERDA-9, H-1 was developed and retested to confirm or modify the published value.

Retesting consisted of four slug tests: one rising-head slug test initiated on September 21, 1987 and three falling-head slug tests initiated on September 23, 25, and 28, 1987. All data from these tests are

contained in Stensrud et al. (1988). Complete recovery from the induced pressure differential was obtained in each test. Semilog plots of the data from the slug tests, along with the type curves which best fit the data, are shown in Figures 5-16 through 5-19. The type curves used were derived by Cooper et al. (1967) for single-porosity media (see Appendix A). The rising-head slug test (Figure 5-16) provided the highest transmissivity estimate, 1.0 ft²/day (Table 5-3). All three falling-head slug tests provided transmissivity estimates of 0.83 ft²/day (Table 5-3).

These transmissivity values are in better agreement with those from nearby wells than is the value reported by Mercer (1983). Apparently, the well development before testing (Section 3.1) and more rigorous testing techniques combined to produce more representative results than were obtained from the earlier bailing test.

5.2.2.2 H-4c. Mercer et al. (1981) reported a transmissivity for the Culebra at H-4b as 0.9 ft²/day based on a slug test, while Gonzalez (1983) reported a value of 1.6 ft²/day based on pumping tests. Gonzalez (1983) also reported the possible presence of a recharge boundary affecting the H-4 test data.

MATCH PARAMETERS

p^*	=	79.08 psig
p_i	=	65.03 psig
α	=	10^{-6}
β	=	1
t	=	0.16 hr
r_c	=	0.0831 ft

□ DATA
— TYPE CURVE

t_0 = 264:09:00:48
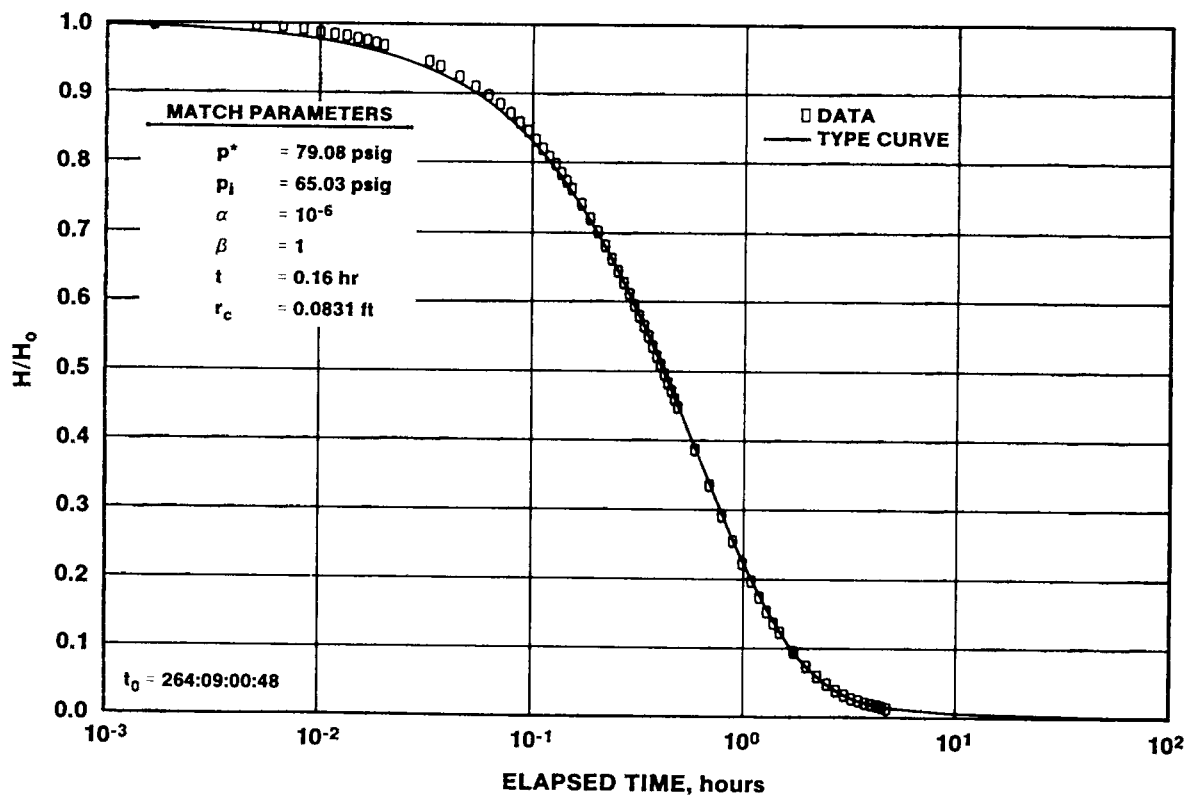
Figure 5-16. H-1/Culebra Slug-Test #1 Plot

MATCH PARAMETERS

p^*	=	79.70 psig
p_i	=	134.34 psig
α	=	10^{-7}
β	=	1
t	=	0.20 hr
r_c	=	0.0831 ft

□ DATA
— TYPE CURVE

t_0 = 266:13:00:24
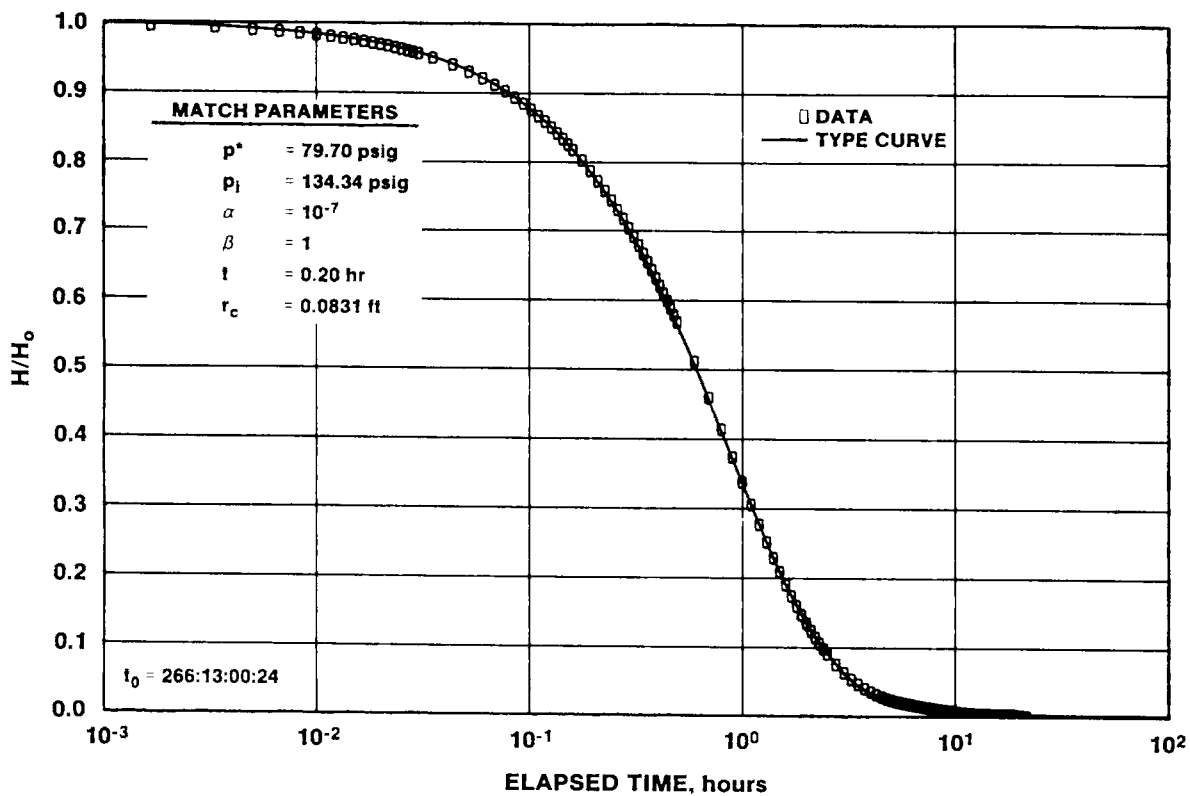
Figure 5-17. H-1/Culebra Slug-Test #2 Plot
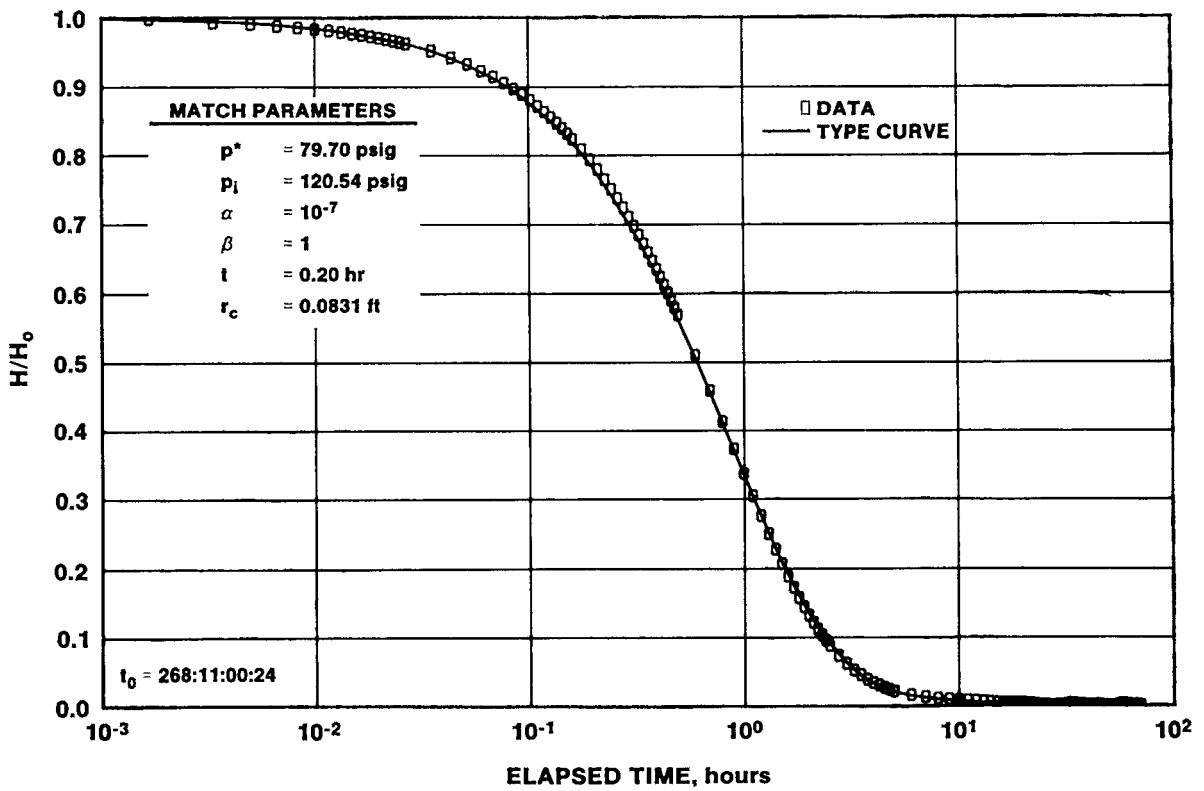
Figure 5-18. H-1/Culebra Slug-Test #3 Plot
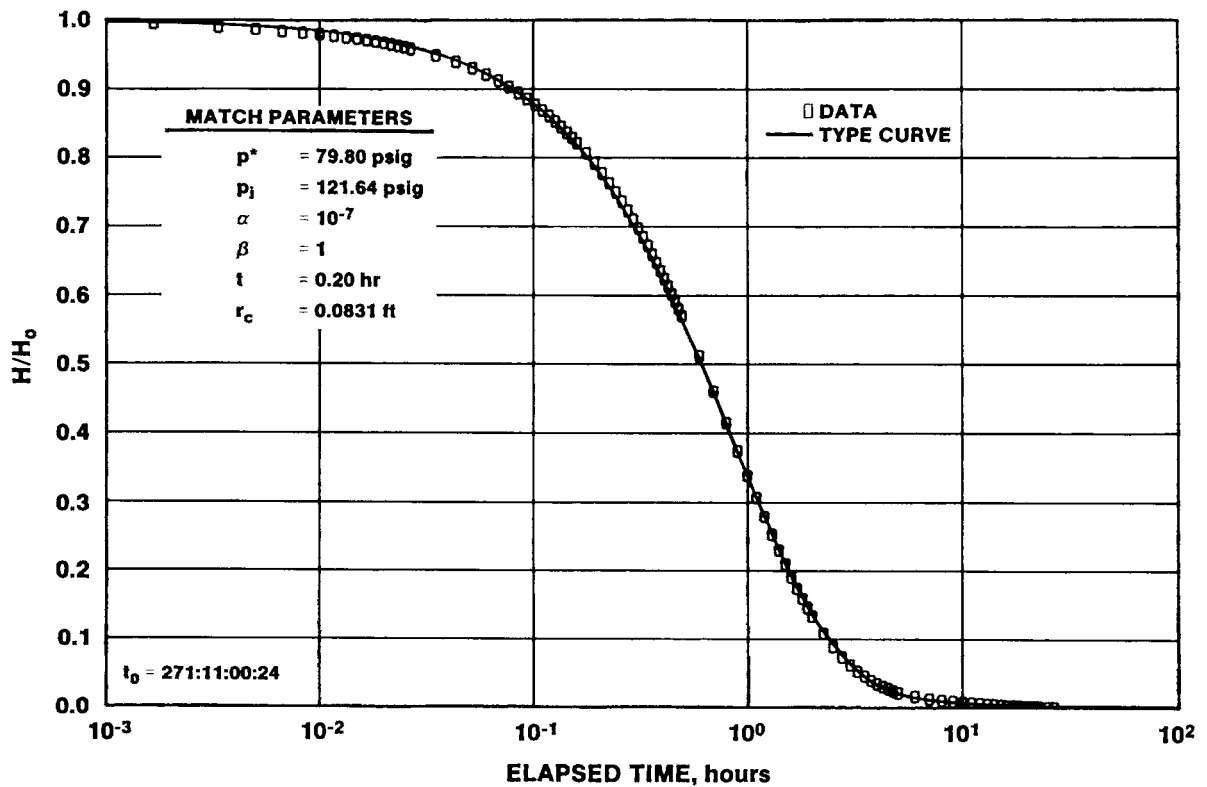
Figure 5-19. H-1/Culebra Slug-Test #4 Plot

TABLE 5-3
SUMMARY OF CULEBRA SINGLE-WELL TEST RESULTS

WELL	CULEBRA DEPTH INTERVAL (ft)	DEPTH INTERVAL TESTED (ft)*	TEST TYPE	TRANSMISSIVITY (ft^2/day)	SKIN FACTOR
H-1	676-699	675-703	slug #1	1.0	—
			slug #2	0.83	—
			slug #3	0.83	—
			slug #4	0.83	—
H-4c	490-516	494-520	slug	0.65	—
H-8b	588-614	574-624	pumping	8.2	-7.2
H-12	823-850	820-890	slug #1	0.18	—
			slug #2	0.18	—
H-14	545-571	533-551	DST/FBU	0.096	-0.8
			DST/SFL	0.10	—
			DST/SBU	0.10	-1.3
H-14	545-571	533-574	DST/FBU	0.30	-1.1
			DST/SBU	0.31	-1.8
			slug	0.30	—
H-15	861-883	853-890	DST/FBU	0.15	2.6
			DST/SBU	0.15	2.9
			slug	0.10	—
H-16	702-724	696-734	DST/FBU	0.85	0.0
			DST/SBU	0.85	-0.3
			slug	0.69	—
H-17	706-731	703-735	DST/FBU	0.21	-1.5
			DST/SBU	0.22	-1.2
			slug	0.22	—
H-18	689-713	685-714	DST/FBU	2.2	-0.2
			DST/SBU	2.2	-1.0
			slug	1.7	—
WIPP-12	810-835	815-840	slug #1	0.10	—
			slug #2	0.097	—

TABLE 5–3 (Continued)

WELL	CULEBRA DEPTH INTERVAL (ft)	DEPTH INTERVAL TESTED (ft)*	TEST TYPE	TRANSMISSIVITY (ft²/day)	SKIN FACTOR
WIPP-18	787-808	784-806	slug	0.30	--
WIPP-19	756-779	754-780	slug	0.60	--
WIPP-21	729-753	727-751	slug	0.25	--
WIPP-22	742-764	748-770	slug	0.37	--
WIPP-30	631-653	629-655	slug #1	0.18	--
			slug #2	0.17	--
P-15	413-435	410-438	slug #1	0.090	--
			slug #2	0.092	--
P-17	558-583	558-586	slug #1	1.0	--
			slug #2	1.0	--
P-18	909-938	909-940	slug	$4 \times 10^{-3}/7 \times 10^{-5}$	--
ERDA-9	704-727	705-728	slug #1	0.45	--
			slug #2	0.47	--
Cabin Baby-1	503-529	503-529	slug #1	0.28	--
			slug #2	0.28	--
DOE-1	821-843	820-843	pumping/ drawdown	28	-5.1
			recovery	11	6.0
Engle	659-681	648-683	pumping	43	4.2

*Actual intervals open to the wells.

Two factors raised questions about these data/interpretations. First, reported Culebra transmissivities are higher at holes northwest (P-14), southwest (H-7), northeast (H-3, DOE-1), and east (H-11) of H-4 than at H-4. Second, early tests of the Culebra at well DOE-2 appeared to indicate the presence of a recharge boundary, which was later shown to be simply poor hydraulic communication between the well and the formation. Good hydraulic communication was established by acidizing DOE-2, and subsequent tests revealed a transmissivity higher than previously estimated (Beauheim, 1986). Hence, concern arose as to whether the reported Culebra properties for H-4 were real, or were affected by poor communication between the H-4 wells and the formation.

To resolve this question, H-4c was acidized and a falling-head slug test was performed to evaluate whether or not the acidization had resulted in an increase in the apparent transmissivity of the Culebra. Well H-4c was selected as the test well because it is a cased hole with perforations providing access to the Culebra, similar to DOE-2. The well was acidized on July 16, 1986, by injecting nearly 200 gallons of a 20% hydrochloric acid solution at the Culebra level over a period of about 2 hr. After a waiting period of over an hour, the spent acid was swabbed from the well. The well was then developed over a 7-day period by repeatedly pumping most of the water from the well and allowing the water level to recover (Stensrud et al., 1987).

On July 31, 1986, a falling-head slug test was initiated in H-4c. The test continued for about 45 hr until August 2, 1986. The data from this test are reported in Stensrud et al. (1987). A plot of the test data and the best fit to a slug-test type curve are shown in Figure 5-20. The good fit between the data and the type curve indicates that on the scale of the test, the Culebra at H-4c behaves hydraulically as a single-porosity medium. No evidence of a recharge boundary is observed in the data.

MATCH PARAMETERS

p^* = 59.47 psig
p_i = 103.90 psig
α = 10^{-2}
β = 1.0
t = 1.2 hr
r_c^* = 0.181 ft

□ DATA
—— TYPE CURVE

t_0 = 212:13:32:18

ELAPSED TIME, hours
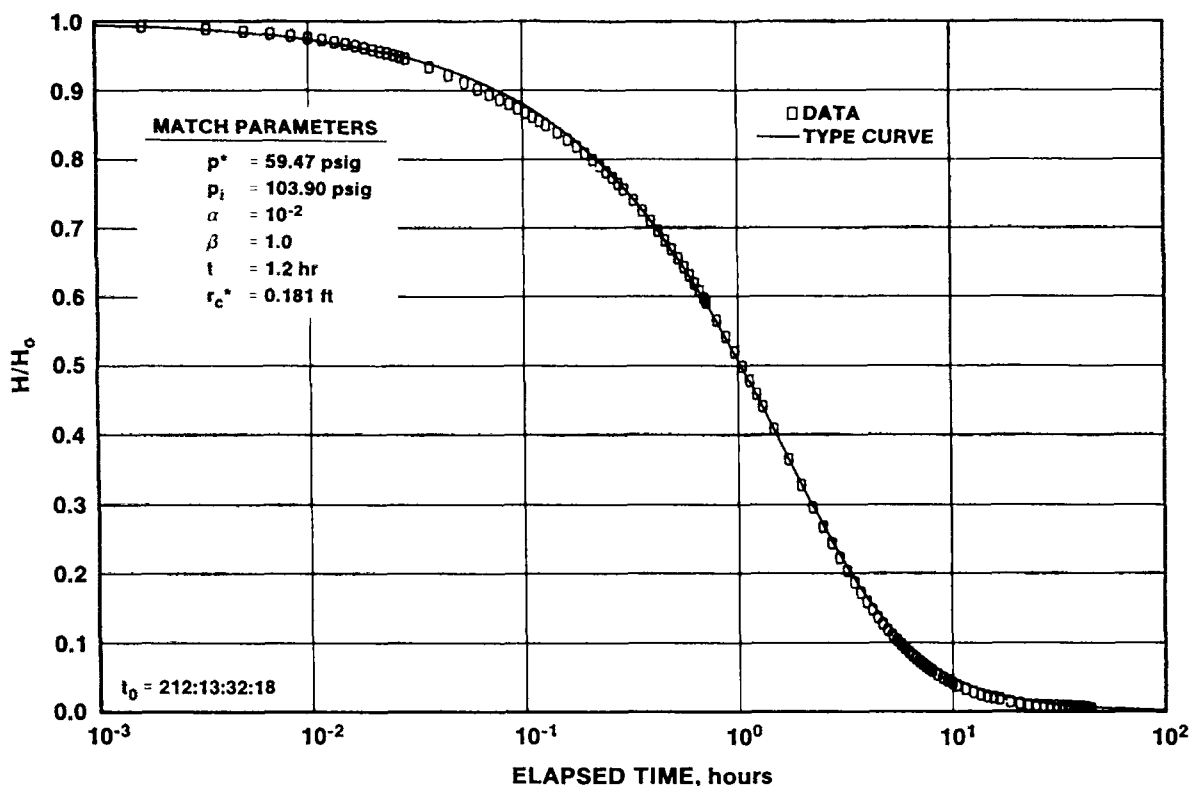
Figure 5-20. H-4c/Culebra Post-Acidization Slug-Test Plot

The test analysis produced a transmissivity value of 0.65 ft²/day (Table 5-3). Apparently, the acidization of the well did not result in a significantly better hydraulic connection between the well and the formation, indicating that an adequate connection already existed. Thus, a transmissivity on the order of 1 ft²/day, as reported by Mercer et al. (1981), Gonzalez (1983), and this study, is probably a representative value for the Culebra at H-4.

5.2.2.3 H-8b.

Mercer (1983) reported a transmissivity value for the Culebra at well H-8b of 16 ft²/day, based on 24 hr of recovery data following a 24-hr pumping test performed by the USGS in 1980 (Richey, 1986). A longer-term pumping test was planned to: 1) verify the transmissivity of the Culebra at H-8b; 2) determine whether the Culebra behaves hydraulically as a single- or double-porosity medium at H-8b; 3) attempt to obtain a storativity value by using the closest other Culebra well, the Poker Trap well located approximately 3000 ft southwest of H-8b, as an observation well; and 4) determine whether the Magenta or Rustler-Salado contact responded to Culebra pumping by monitoring water levels during the test in wells H-8a and H-8c, respectively.

Accordingly, a 72-hr pumping test of the Culebra dolomite at well H-8b was conducted from December 6 to 9, 1985. The well was pumped at an average rate of about 6.17 gpm. Following the pumping period, pressure recovery in the well was monitored for 9 days. A complete test description and data records are presented in INTERA Technologies (1986).

The observed fluid-pressure data were modified for analysis to eliminate initial pressure surges that occurred at the instants the pump was turned on and off. These pressure surges are related to turbulence in the wellbore caused by the pump, and not to the aquifer response. Thus, the initial pressure used for all pressure-drawdown calculations was the first pressure measured after the pump was turned on (44.87 psig) rather than the pressure measured just before the pump was turned on (48.08 psig). A corresponding initial pressure increase of 2.9 psig, observed at the instant the pump was turned off, was eliminated from the pressure-recovery calculations.

The H-8b pressure response during the pumping test appears to be that of a well completed in a double-porosity medium. Double-porosity media have two porosity sets which differ in terms of storage volume and permeability. Typically, the two porosity sets are a fracture network with higher permeability and lower storage, and the primary porosity of the rock matrix with lower permeability and higher storage. Double-porosity media are discussed more fully in Appendix A.

Figure 5-21 shows a log-log plot of the H-8b drawdown data along with a double-porosity simulation of those data generated with the INTERPRET well-test-analysis code. The simulation shown uses an unrestricted-interporosity-flow formulation, a transmissivity of 8.2 ft²/day (Table 5-3), and a no-flow, or decreased-transmissivity, boundary at a distance of about 780 ft from H-8b. The storativity ratio, w, is 0.01 for this simulation, which is an approximate measure of the percentage of water produced during the test coming from the fractures as opposed to from the matrix.

Assuming that the matrix porosity of the Culebra at H-8b is about 20% (Haug et al., 1987), that the fluid viscosity is about 1.0 cp, and that the total-system compressibility is about 1 x 10-5 psi-1, the skin factor (s) for the well is about -7.2. The highly negative skin factor derived from this analysis indicates that the wellbore is directly intersected by fractures (Gringarten et al., 1979). High-permeability fractures in direct connection with a wellbore may act as additional production surfaces to the well (in addition to the wellbore itself). Jenkins and Prentice (1982) term this type of wellbore-fracture system an "extended" well. Earlougher (1977) relates skin factor to an "effective" wellbore radius quantitatively by the following equation:

$$r_e = r_w e^{-s} \tag{5.1}$$

where: r_e = effective wellbore radius
        r_w = actual wellbore radius
        s   = skin factor.

This equation indicates that a well with a positive skin factor (wellbore damage) behaves hydraulically like a
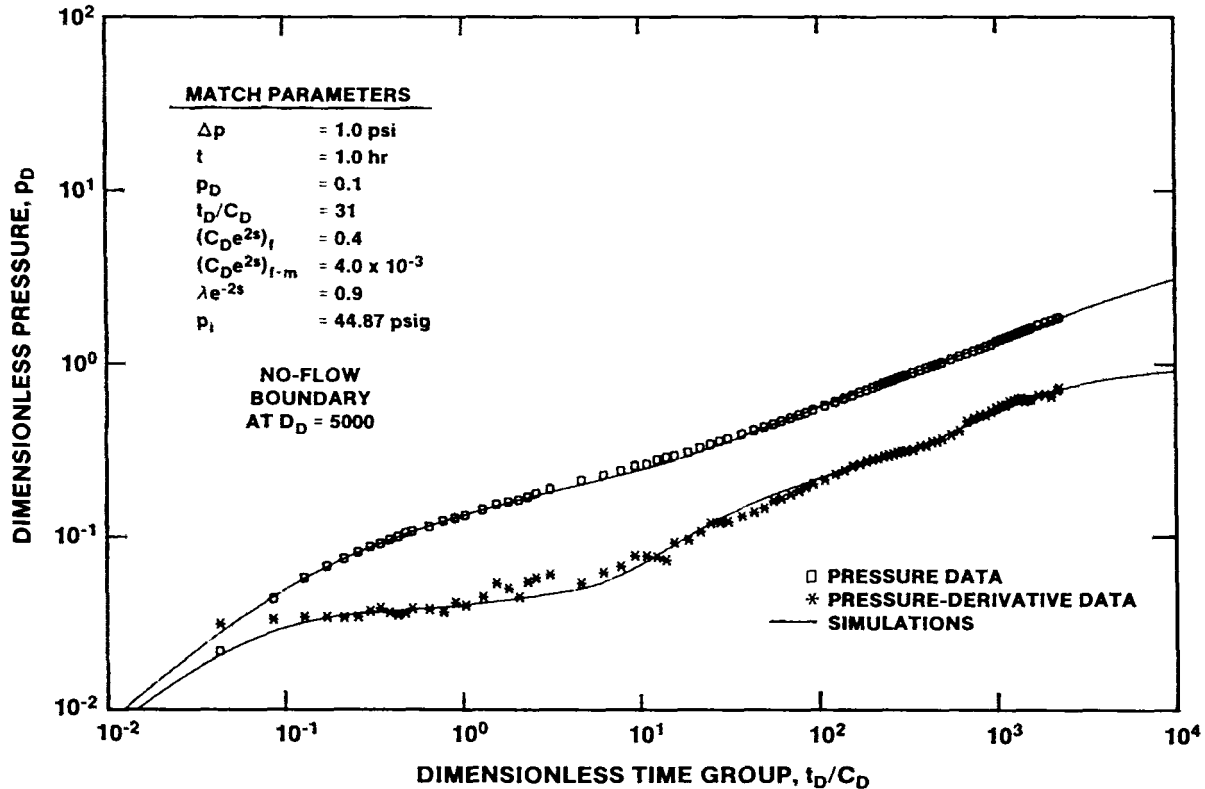
Figure 5-21. H-8b/Culebra Pumping Test Drawdown Log-Log Plot with INTERPRET Simulation

well with a smaller radius. Conversely, a well with a negative skin factor should behave like a well with a larger radius. H-8b, with a skin factor of -7.2 and an actual radius of 0.255 ft, behaves like a well with a radius of about 340 ft.

The reason for the two-fold discrepancy between the transmissivity reported by Mercer (1983) and that obtained from this test is not clear. The hydraulic boundary indicated by this test analysis was either not felt by the earlier, shorter test, or was not recognized. Without either data from multiple observation wells or independent geologic/geophysical information, the orientation of the boundary cannot be determined.

Figure 5-22 shows a log-log plot of the H-8b recovery data along with an INTERPRET simulation using exactly the same model as was used in the drawdown simulation (Figure 5-21). In an ideal system, this model should fit both the drawdown and recovery data identically. In general, the fit is excellent until extreme late time, at which point

apparent "over-recovery" on the order of 1 psi is observed (most clearly in the rise of the pressure derivative). This over-recovery may be related to residual recovery from some pre-test pumping activities associated with checking the pump and filling the discharge lines (INTERA Technologies, 1986). Figure 5-23, a linear-linear plot of both the drawdown (compensated for the initial 3.2-psi pump loss) and recovery data along with an INTERPRET-generated simulation, also shows the generally excellent fit between the data and the simulation, as well as the over-recovery beginning about 70 hr into the recovery period.

In general, the H-8b response was very similar to the responses observed at wells H-3b2, H-3b3, and WIPP-13 when those wells were pumped (Beauheim, 1987a and 1987b). At these locations, the Culebra exhibits unrestricted interporosity flow with rapid transition between flow from the fractures only and flow from both the fractures and the matrix. This type of response contrasts with the responses observed during pumping tests at wells DOE-1 (see Section
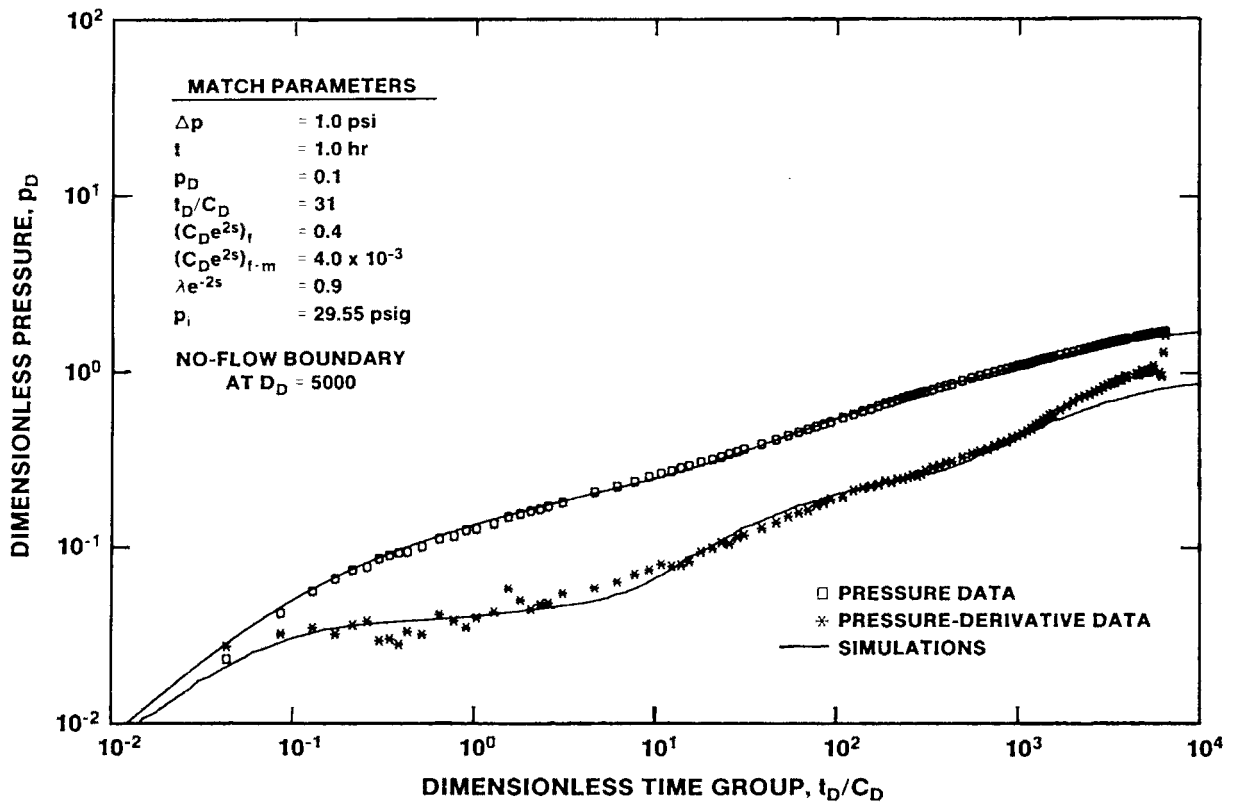
Figure 5-22. H-8b/Culebra Pumping Test Recovery Linear-Linear Sequence Plot with INTERPRET Simulation
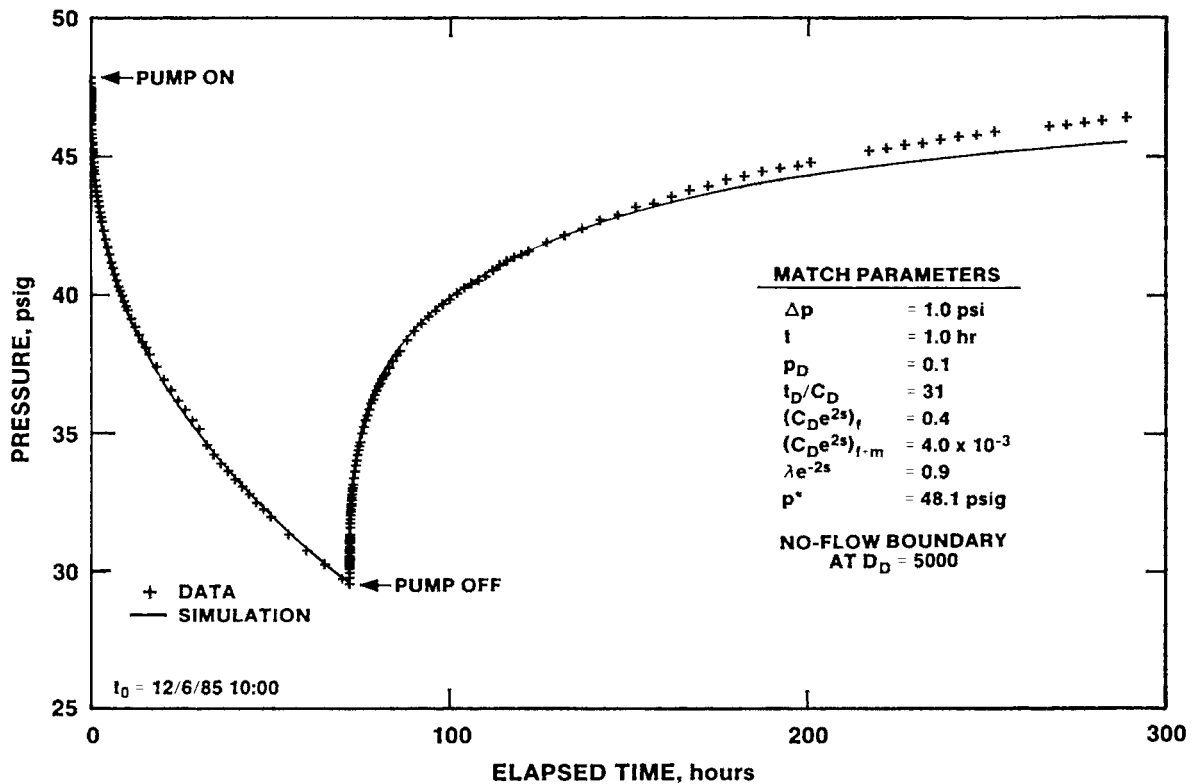
Figure 5-23. H-8b/Culebra Pumping Test Linear-Linear Sequence Plot with INTERPRET Simulation

5.2.2.21 below) and DOE-2 (Beauheim, 1986). Those wells exhibited restricted interporosity flow, with delayed transition between flow from the fractures only and flow from the fractures and matrix combined, and less negative skin factors (-6.0 and -4.7). The cause(s) of these differences in behavior is not understood at the present time.

Because the Poker Trap well did not respond to the pumping at H-8b (INTERA Technologies, 1986), no storativity value for the Culebra was obtainable from the test. The failure of either the Magenta in H-8a or the Rustler-Salado contact in H-8c to respond to the Culebra pumping at H-8b indicates that any existing communication between the Culebra and those units is of a degree too low to allow observable responses on the time scale of this test.

5.2.2.4 H–12. Although H-12 was completed in 1983, no well-controlled hydrologic testing of the

Culebra had ever been performed. Pressure data were collected during a water-quality sampling exercise in 1984 (INTERA and HydroGeoChem, 1985), but the data were inadequate for interpretation and provided only a qualitative indication of low transmissivity. Thus, two falling-head slug tests were performed in August and September 1987 to provide estimates of the Culebra transmissivity at H-12.

The first test was initiated on August 27, 1987, and the second test on September 1, 1987. The data from these tests are presented in Stensrud et al. (1988). Complete recovery from the induced pressure differential was obtained during each test. Figure 5-24 shows a semilog plot of the data from the first test, along with the best-fit type-curve match. This match provides a transmissivity estimate of 0.18 ft²/day (Table 5-3). The same type-curve match also fits the data from the second test quite well (Figure 5-25), resulting in an identical transmissivity estimate.

MATCH PARAMETERS

p^* = 12.95 psig
p_i = 90.53 psig
α = 10^{-5}
β = 1
t = 0.90 hr
r_c = 0.0831 ft

□ DATA
—— TYPE CURVE

t_0 = 239:09:00:30
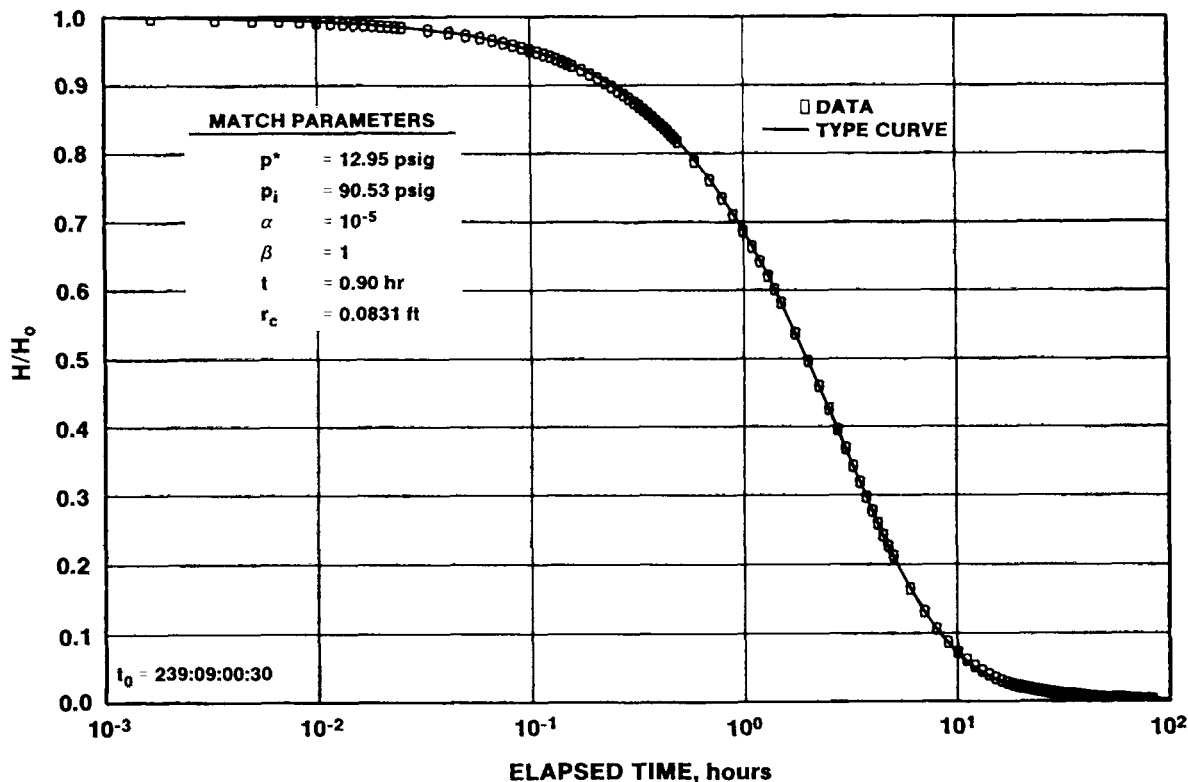
Figure 5-24. H-12/Culebra Slug-Test #1 Plot
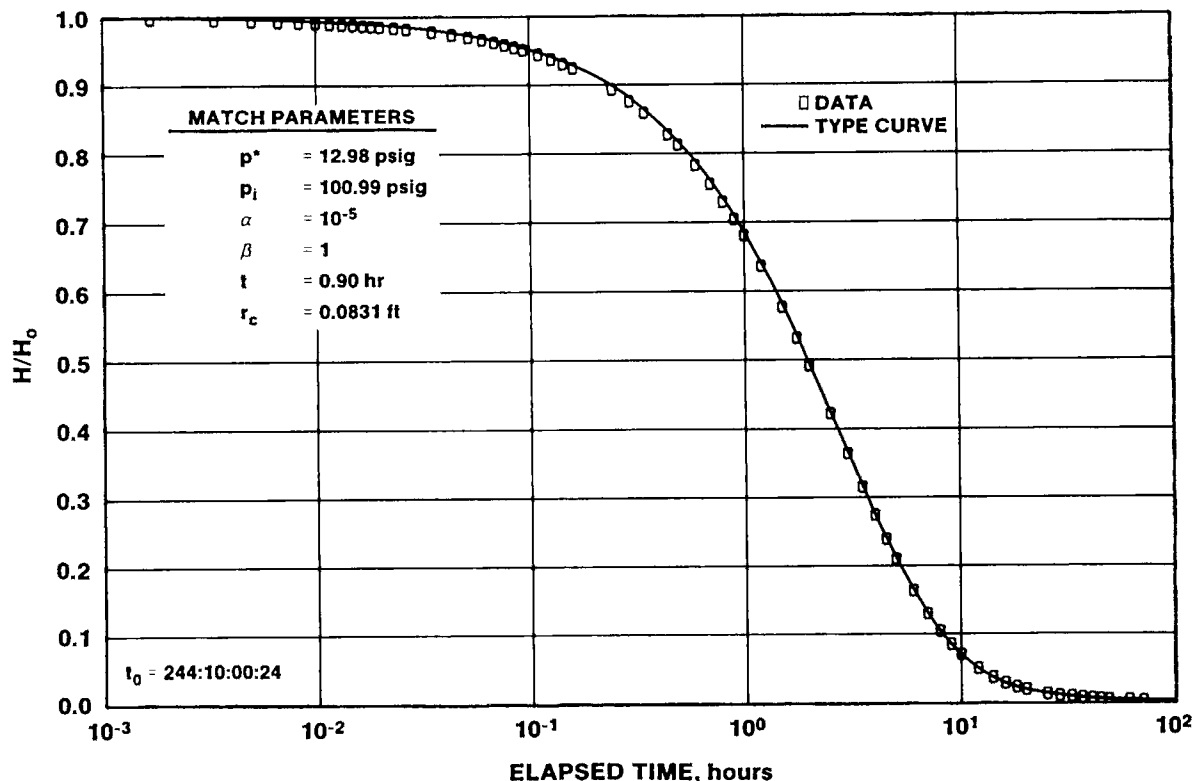
Figure 5-25. H-12/Culebra Slug-Test #2 Plot

5.2.2.5 H–14. Testing of the Culebra at H-14 was planned to try to reduce the uncertainty in the location of the transition zone between the higher transmissivity, fractured, double-porosity system observed at H-3 and the lower transmissivity, apparently unfractured, single-porosity system observed at H-4 (see Figure 1-1). An additional objective of the H-14 testing was to try to quantify the vertical heterogeneity of the Culebra by testing different portions of the Culebra as drilling progressed. The H-14 test data are presented in Stensrud et al. (1987).

At H-14, the Culebra lies from 544.9 to 571.4 ft deep (Figure 3-6). DST's and rising-head slug tests were performed in two stages in the Culebra as the hole was being drilled. The bit-penetration rate was monitored closely as the Culebra was cored. The penetration rate was rapid through the top 3 ft of Culebra, but then slowed significantly. At 5.8 ft (550.7 ft deep), coring was halted and DST's were performed. The DST's used a single-packer tool, with the packer set at the bottom of the well casing

between about 528 and 533 ft deep. The actual test interval included the lower 11.9 ft of Tamarisk anhydrite and the upper 5.8 ft of Culebra dolomite. The anhydrite was judged to have a permeability so much lower than that of the dolomite that the anhydrite section was not considered during test interpretation.

Following the upper Culebra DST's, coring continued through the remaining 20.7 ft of the Culebra and about 2.6 ft into the unnamed lower member of the Rustler to 574.0 ft. The DST tool was reset at the bottom of the well casing, and DST's and a rising-head slug test of the entire Culebra were performed.

Upper Culebra: The upper Culebra testing consisted of two flow periods and two buildup periods on October 21, 1986 (Figure 5-26). The first flow period (FFL) lasted about 17 minutes, followed by an 87-minute first buildup period (FBU). The second flow period (SFL) lasted about 27 minutes, and was followed by a second buildup period (SBU) lasting about 111 minutes. To analyze the buildup data, the
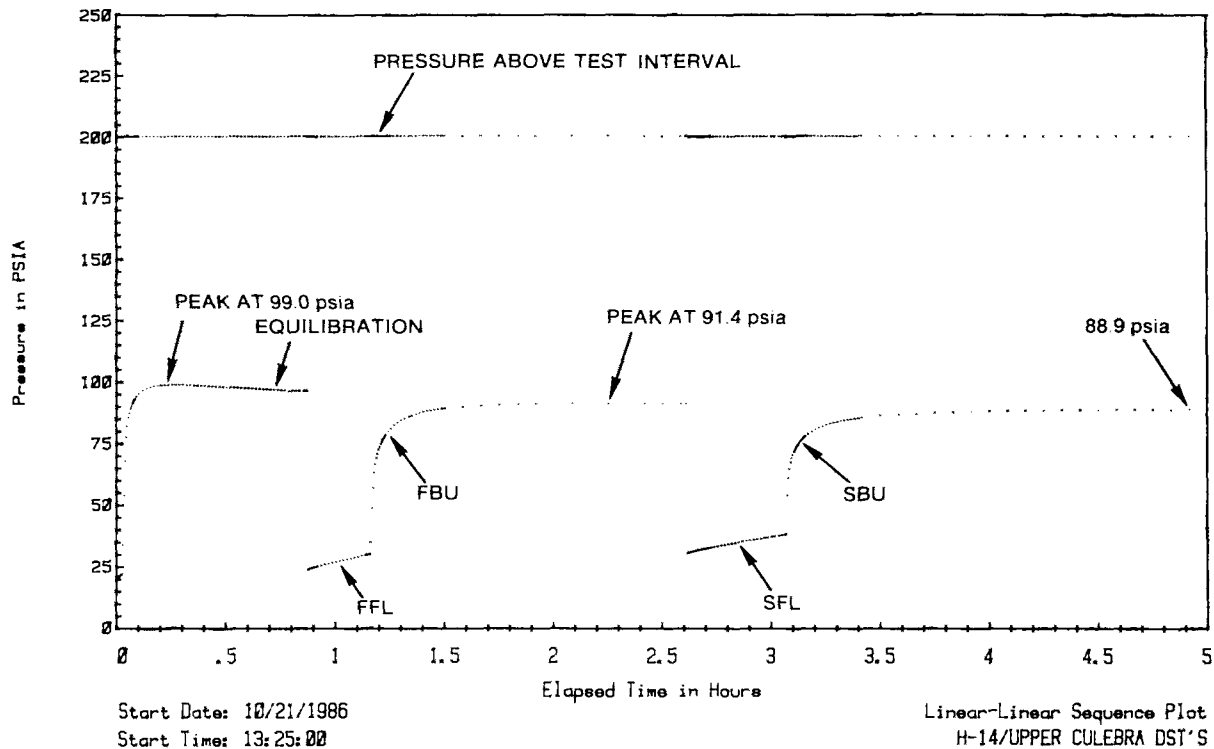
Figure 5-26. H-14/Upper Culebra Drillstem Test Linear-Linear Sequence Plot

FFL was divided into three flow periods with rates ranging from 0.186 to 0.116 gpm, and the SFL was divided into two flow periods with rates of 0.138 and 0.097 gpm (Table 5-1).

Figure 5-27 shows a log-log plot of the FBU data, along with an INTERPRET-generated simulation. The simulation is representative of a single-porosity medium with a transmissivity of 0.096 ft^2/day (Table 5-3). Assuming a Culebra porosity of 20%, a total-system compressibility of 1.0 x 10^{-5} psi^{-1}, and a fluid viscosity of 1.0 cp, the skin factor for this simulation is about -0.8, indicating a slightly stimulated well.

The sharp decline in the pressure derivative at late time in Figure 5-27 is an indication that the overpressure skin induced by the weight of the drilling fluid during coring of the upper Culebra was dissipating during the DST's. The effect of the overpressure skin is also seen in the dimensionless Horner plot for the FBU (Figure 5-28). The best simulation obtained shows that the pressure was

initially recovering towards 95.5 psia (the static pressure specified for that simulation), but then deviated towards a lower pressure at late time. This is also shown in Figure 5-26 by the pressure peak at 99.04 psia during the pre-test equilibration period, the subsequent peak during the FBU at 91.36 psia, and the near stabilization of the pressure at 88.94 psia at the end of the SBU.

Figure 5-29 shows a log-log plot of the SBU data, along with an INTERPRET-generated simulation. The simulation is representative of a single-porosity medium with a transmissivity of 0.10 ft^2/day (Table 5-3). Assuming a Culebra porosity of 20%, a total-system compressibility of 1.0 x 10^{-5} psi^{-1}, and a fluid viscosity of 1.0 cp, the skin factor for this simulation is about -1.3. These values are in excellent agreement with the FBU results, and indicate possible slight well development during the DST's. The decline in the pressure derivative in Figure 5-29 at late time shows the continuing influence of the overpressure skin on the data.
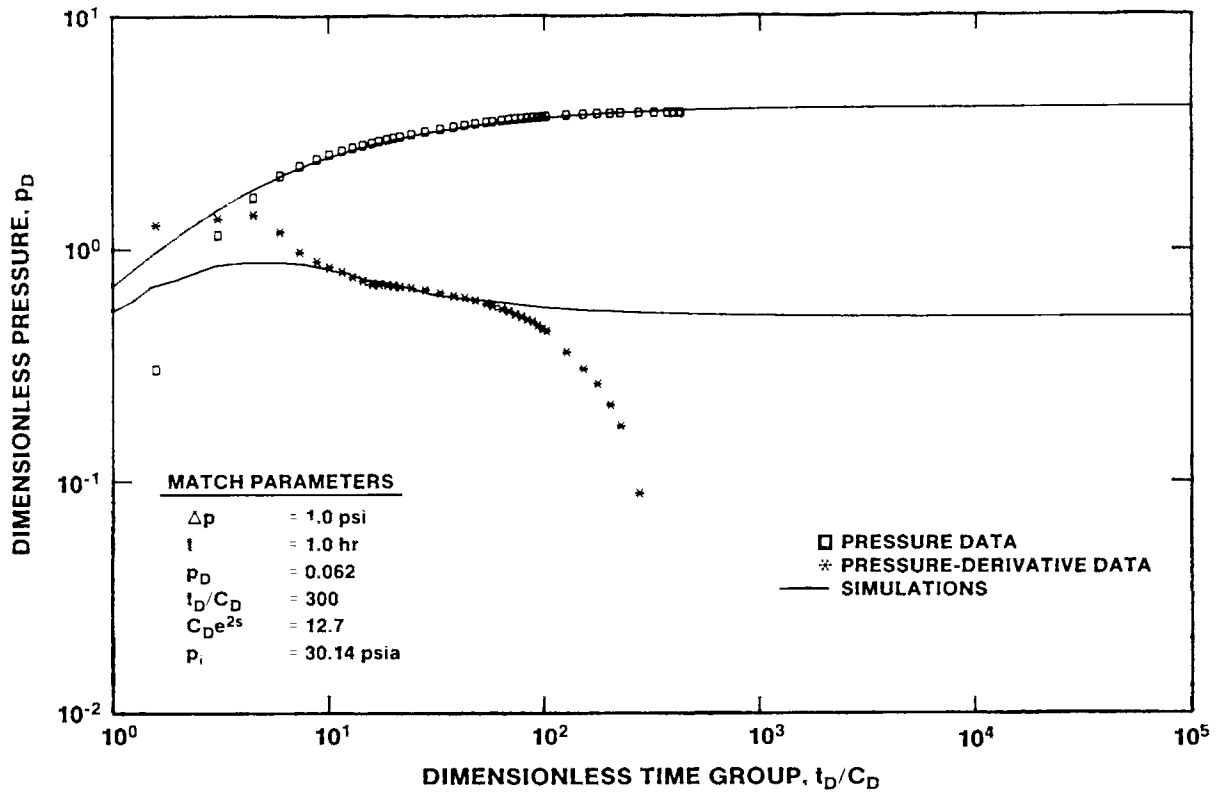
Figure 5-27. H-14/Upper Culebra First Buildup Log-Log Plot with INTREPRET Simulation
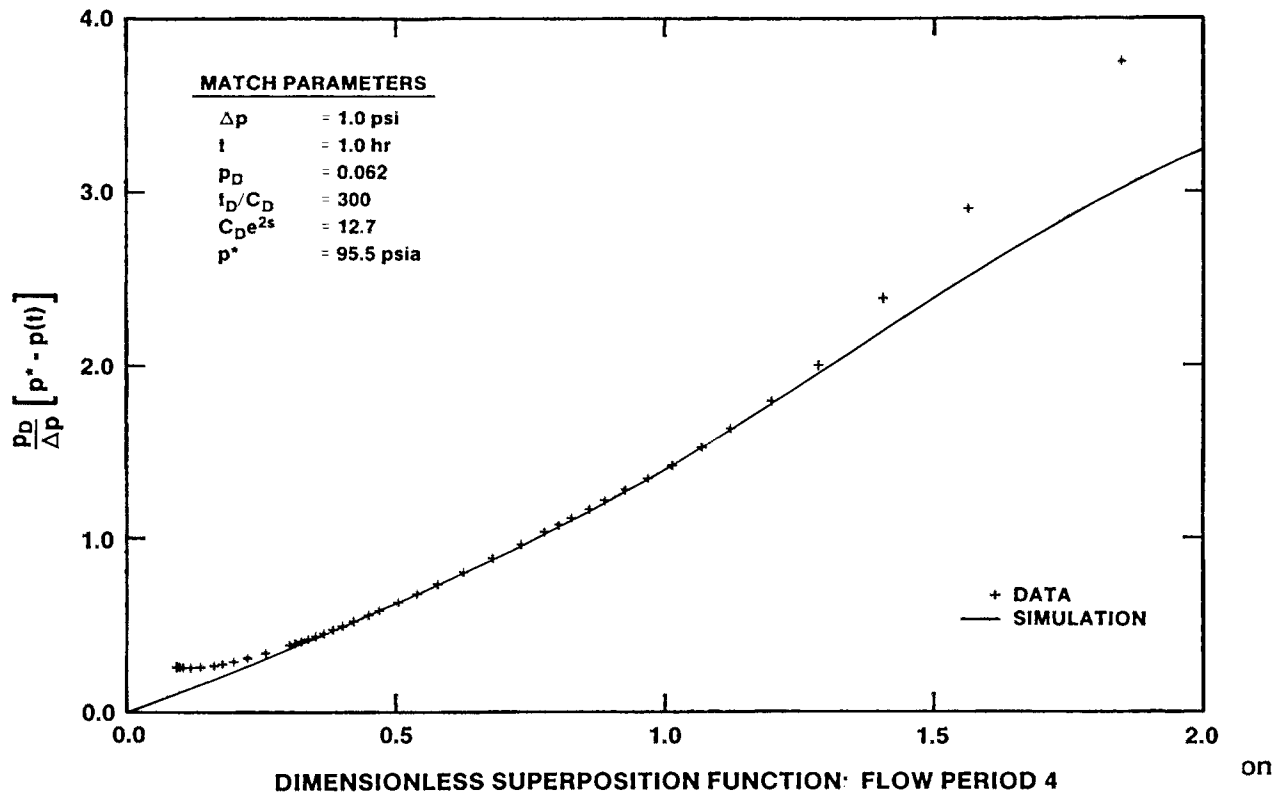
Figure 5-28. H-14/Upper Culebra First Buildup Dimensionless Horner Plot with INTERPRET Simulation
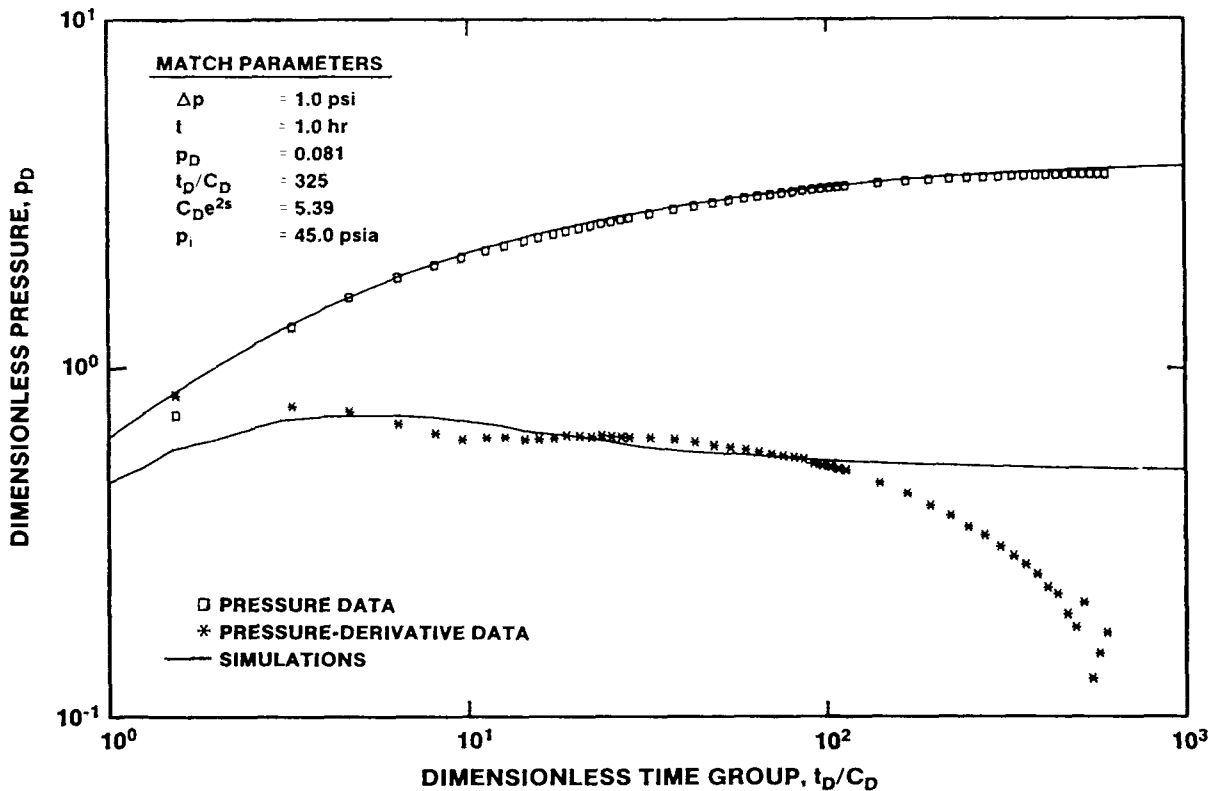
Figure 5-29. H-14/Upper Culebra Second Buildup Log-Log Plot with INTERPRET Simulation

For a final estimate of the upper Culebra transmissivity, the SFL data were analyzed as a slug test. Figure 5-30 shows a log-log early-time slug-test plot of the SFL data, along with the best-fit type curve. This fit provides a transmissivity estimate of 0.10 ft²/day (Table 5-3), which is in excellent agreement with the FBU and SBU results.

Complete Culebra: The testing of the complete Culebra consisted of two DST flow periods and two buildup periods, followed by a rising-head slug test, all on October 22, 1986 (Figure 5-31). The FFL lasted about 14 minutes, followed by a 77-minute FBU. The SFL lasted about 24 minutes, and was followed by a SBU lasting about 129 minutes. In order to obtain constant rates for the FBU and SBU analyses, the FFL and SFL were both divided into two flow periods. The rates for the FFL were 0.381 and 0.260 gpm, and those for the SFL were 0.271 and 0.173 gpm (Table 5-1). The slug test lasted about 204 minutes, by which time about 77% of the induced pressure differential had dissipated.

Figure 5-32 shows a log-log plot of the FBU data, along with an INTERPRET-generated simulation. The simulation is representative of a single-porosity medium with a transmissivity of 0.30 ft²/day (Table 5-3). Assuming a Culebra porosity of 20%, a total-system compressibility of 1.0×10^{-5} psi⁻¹, and a fluid viscosity of 1.0 cp, the skin factor for this simulation is about -1.1, indicating a moderately stimulated well.

As was the case for the upper Culebra tests, the pressure derivative in Figure 5-32 shows a sharp decline at late time related to overpressure skin. Effects of residual overpressure skin are also seen in Figure 5-31 by the pressure peak at 94.17 psia during the pre-test equilibration period, the subsequent stabilization of the pressure at the end of the FBU at 91.48 psia, and the pressure peak at 90.05 psia at the end of the SBU.

Figure 5-33 shows a log-log plot of the SBU data, along with an INTERPRET-generated simulation.

MATCH PARAMETERS

p^* = 92.5 psia
p_i = 30.32 psia
α = 10^{-4}
β = 1.0
t = 1.65 hr
r_c = 0.0831 ft

□ DATA
—— TYPE CURVE

t_0 = 294:16:01:47
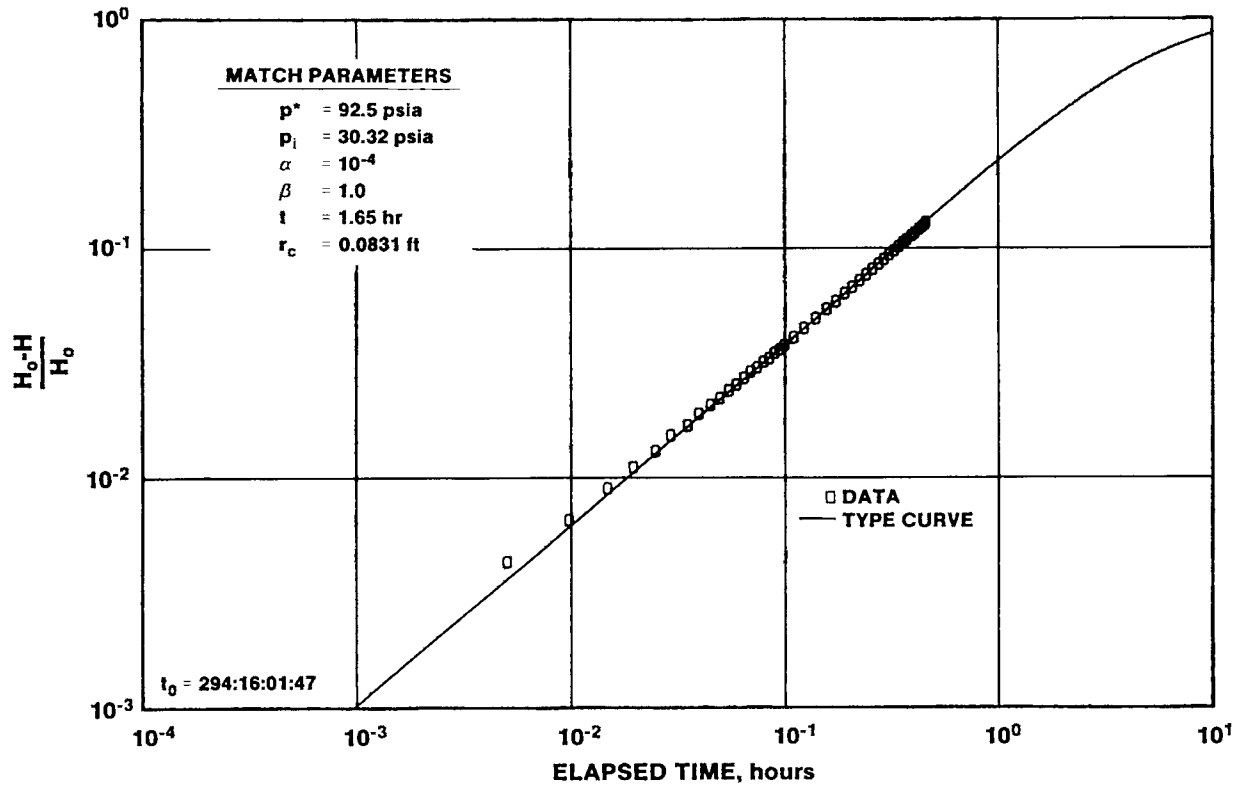
Figure 5-30. H-14/Upper Culebra Second Flow Period Early-Time Slug-Test Plot

Start Date: 10/22/1986
Start Time: 11:00:00

Linear-Linear Sequence Plot
H-14/COMPLETE CULEBRA TESTS
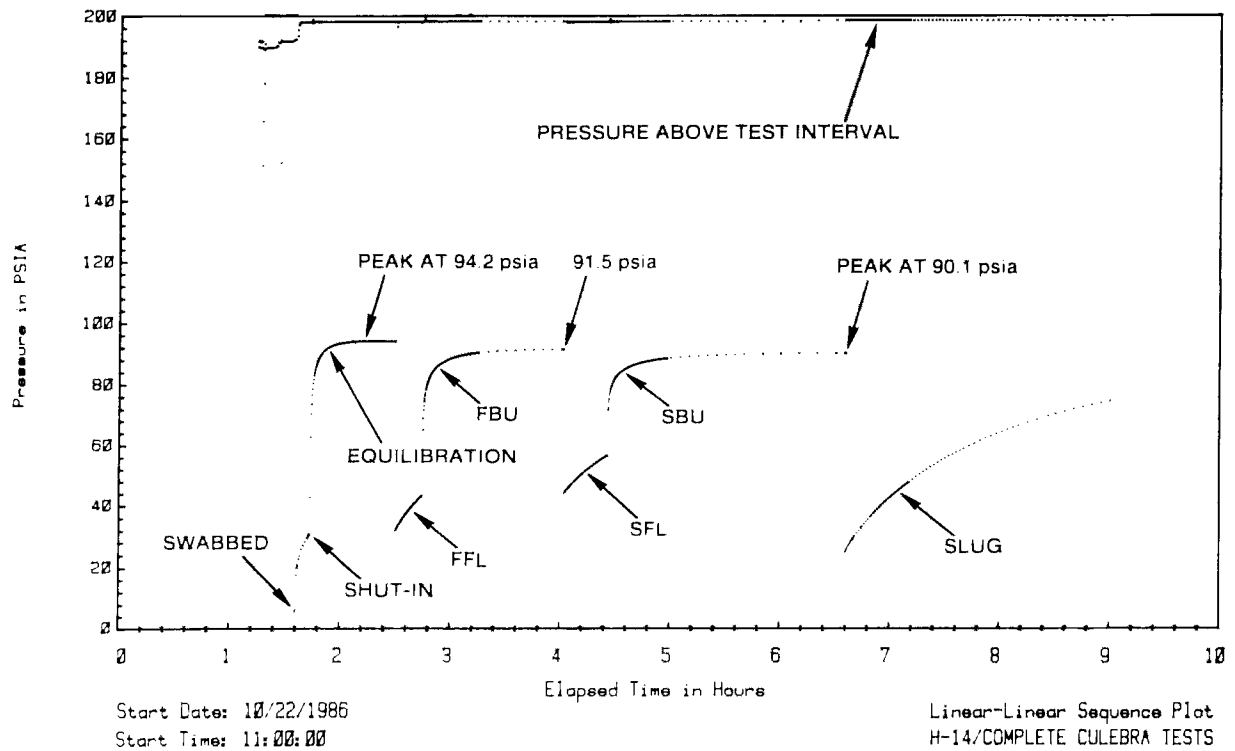
Figure 5-31. H-14/Complete Culebra Drillstem and Slug Testing Linear-Linear Sequence Plot
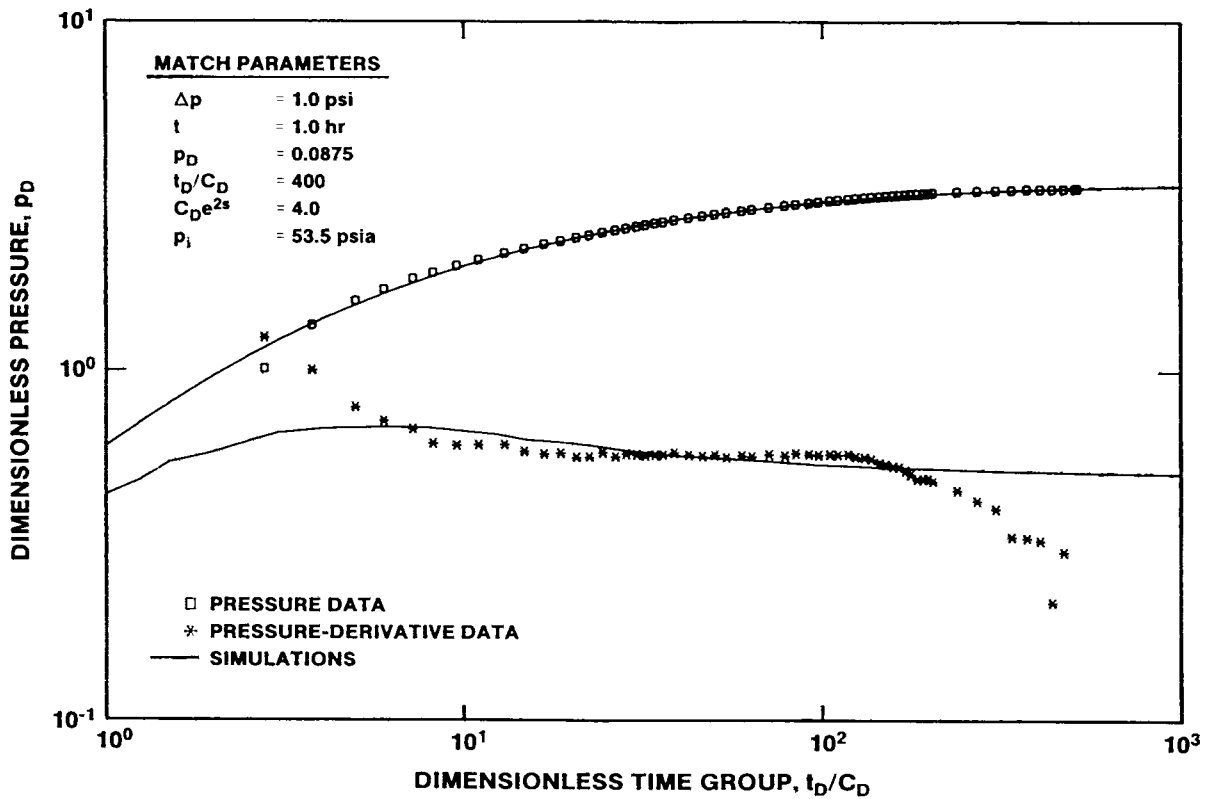
Figure 5-32. H-14/Culebra First Buildup Log-Log Plot with INTERPRET Simulation
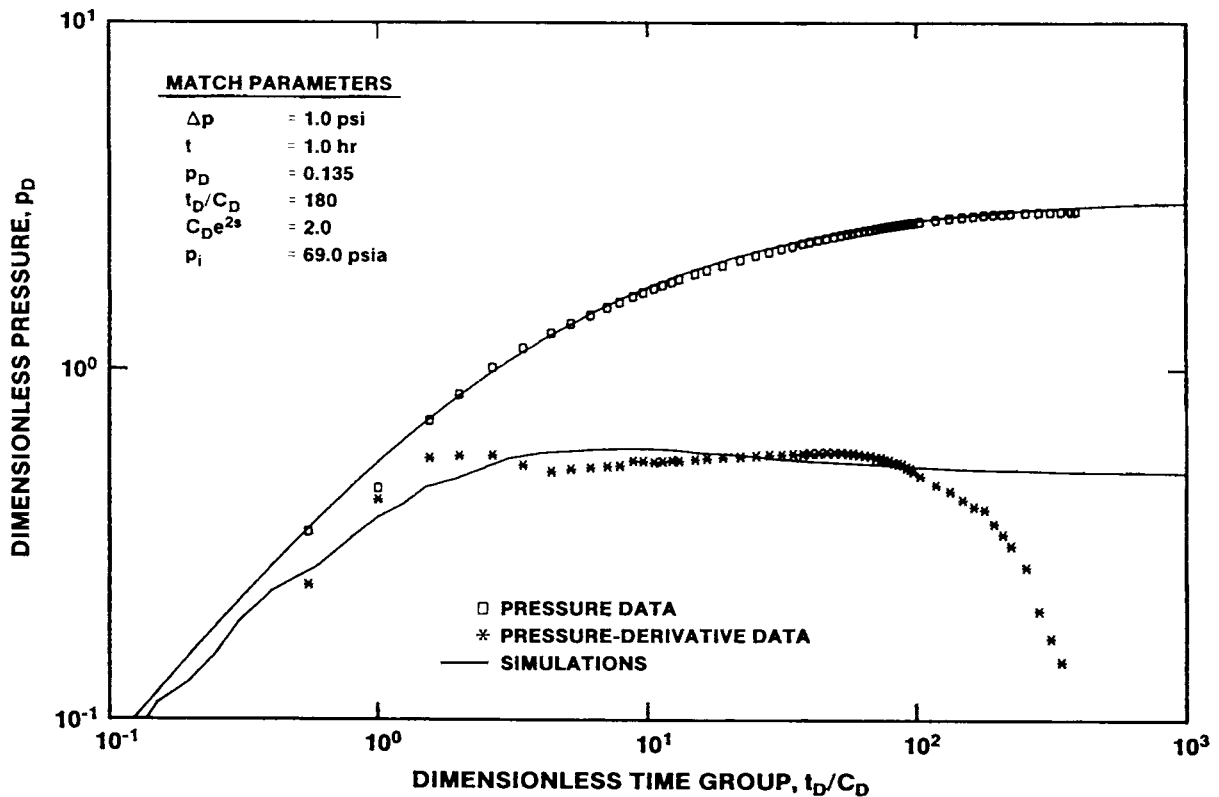
Figure 5-33. H-14/Culebra Second Buildup Log-Log Plot with INTERPRET Simulation

The simulation is representative of a single-porosity medium with a transmissivity of 0.31 ft²/day (Table 5-3). Assuming a Culebra porosity of 20%, a total-system compressibility of 1.0 x 10-5 psi-1, and a fluid viscosity of 1.0 cp, the skin factor for this simulation is about -1.8. These values are in excellent agreement with the FBU results, and indicate possible slight well development during the DST's. Again, the decline in the pressure derivative in Figure 5-33 at late time shows the continuing influence of the overpressure skin on the data.

Figure 5-34 shows a semilog plot of the rising-head slug-test data, along with the best-fit type curve. This fit provides a transmissivity estimate of 0.30 ft²/day (Table 5-3), which is in excellent agreement with the FBU and SBU results. This fit was achieved using a static formation pressure estimate of 90.0 psia, slightly below the pressure measured at the end of the SBU. The transducer used for the DST's and

slug test was set at a depth of 514.7 ft. The fluid in the hole during the testing had a specific gravity of 1.003, and the transducer measured an atmospheric pressure of 12.3 psia before testing began. Hence, 90.0 psia at the transducer depth corresponds to a static formation pressure of about 96.5 psig at the midpoint of the Culebra about 558 ft deep.

Conclusions: The Culebra is 26.5 ft thick at H-14. The transmissivity of the upper 5.8 ft is 0.10 ft²/day, while that of the entire unit is 0.30 ft²/day. Hence, the average hydraulic conductivity of the upper 5.8 ft of the Culebra appears to be about 1.8 times greater than that of the lower 20.7 ft. This difference does not represent a great degree of heterogeneity. Left unresolved by this testing is the distribution of hydraulic conductivity within the Culebra on a finer scale, such as hydraulic-conductivity differences between those portions that are less competent and core quickly, and those that are more competent and core more slowly.
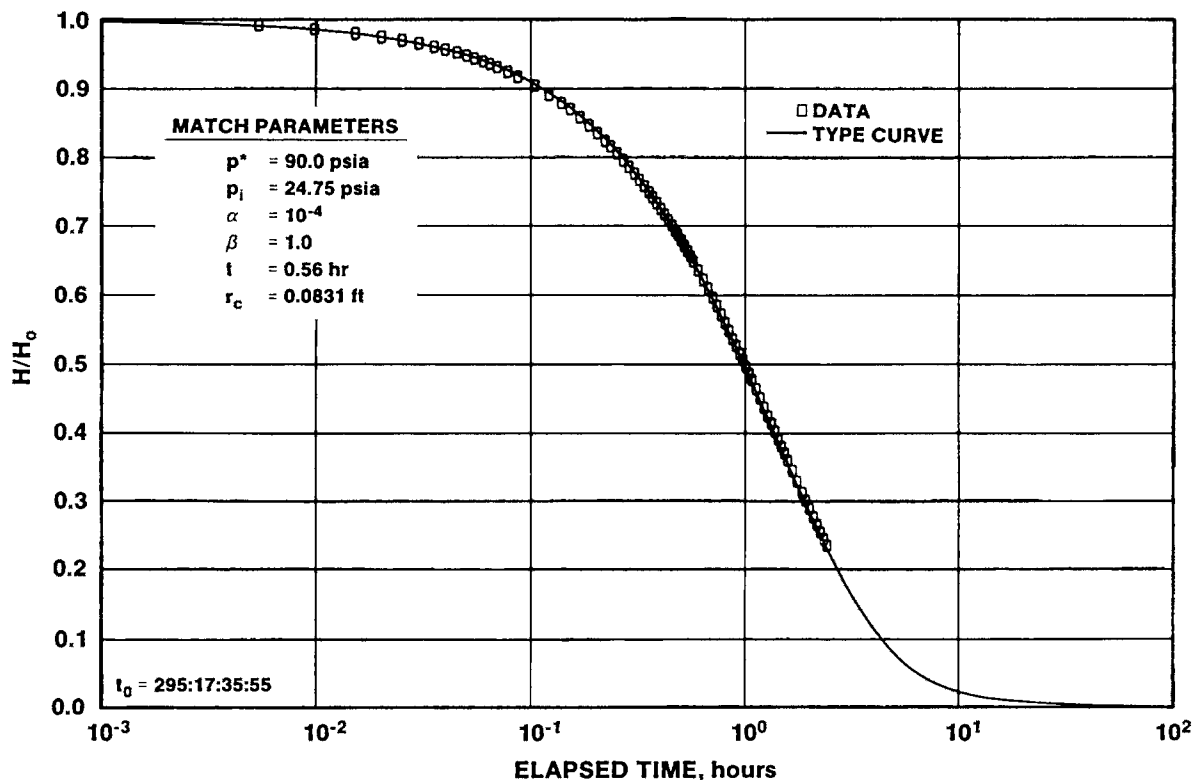
Figure 5-34. H-14/Culebra Slug-Test Plot

5.2.2.6 H-15. Drillstem testing of the Culebra at H-15 was planned to try to confirm the low transmissivity assumed for the eastern part of the WIPP site on the basis of measurements made at H-5 and P-18 (Mercer, 1983). The Culebra lies from 861 to 883 ft below land surface at H-15 (Figure 3-7). The actual interval tested extended from the bottom of the well casing at 853 ft to the then-bottom of the hole at 891 ft. Hence, the lower 8 ft of the Tamarisk Member and the upper 8 ft of the unnamed lower member of the Rustler were tested along with the Culebra. Because these portions of the members overlying and underlying the Culebra are composed of anhydrite and mudstone, they are not thought to have contributed significantly to the transmissivity measured during the Culebra testing and were, therefore, ignored in the analysis.

The Culebra testing at H-15 began on November 11, 1986, the day after the Culebra interval was cored, and continued until November 13, 1986. The testing consisted of two DST flow periods and two buildup periods, followed by a rising-head slug test

(Figure 5-35). The FFL lasted about 26 minutes, followed by an 865-minute FBU. The SFL lasted about 40 minutes, and was followed by a SBU lasting about 315 minutes. In order to obtain constant rates for the FBU and SBU analyses, the FFL was divided into two shorter flow periods, and the SFL was divided into three shorter flow periods. The rates for the FFL were 0.147 and 0.127 gpm, and those for the SFL were 0.153, 0.124, and 0.110 gpm (Table 5-1). The slug test lasted about 1029 minutes, by which time about 92% of the induced pressure differential had dissipated. The H-15 test data are presented in Stensrud et al. (1987).

Figure 5-36 shows a log-log plot of the FBU data, along with an INTERPRET-generated simulation. The simulation is representative of a single-porosity medium with a transmissivity of 0.15 ft²/day (Table 5-3). Assuming a Culebra porosity of 20%, a total-system compressibility of 1.0×10^{-5} psi^{-1}, and a fluid viscosity of 1.0 cp, the skin factor for this simulation is about 2.6, indicating a damaged well.

Figure 5-35. H-15/Culebra Drillstem and Slug Testing Linear-Linear Sequence Plot

MATCH PARAMETERS

Δp	= 1.0 psi
t	= 1.0 hr
p_D	= 0.082
t_D/C_D	= 500
$C_D e^{2s}$	= 3000
p_i	= 62.0 psia

□ PRESSURE DATA
✳ PRESSURE-DERIVATIVE DATA
— SIMULATIONS
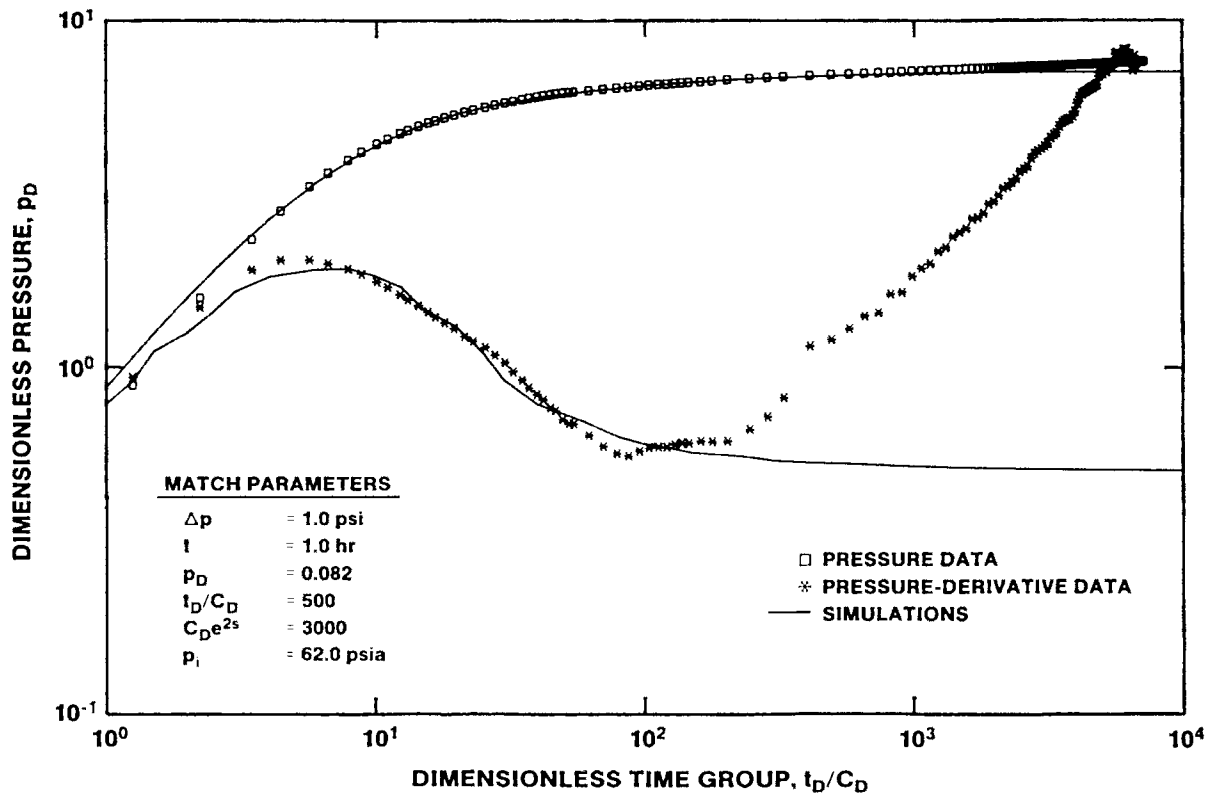
Figure 5-36. H-15/Culebra First Buildup Log-Log Plot with INTERPRET Simulation

Because of the problems encountered with overpressure skins during the H-14 testing, a different procedure was used in preparing H-15 for testing. After the Culebra was cored at H-15, most of the drilling fluid was evacuated from the borehole in an effort to counteract the overpressurization caused during drilling. The time elapsed from the first penetration of the Culebra by the core bit to the evacuation of the drilling fluid was about 19 hr. By the time the packer was set in preparation for testing the next day, the Culebra had been underpressurized for about 23 hr. The net result was that, when testing began, an underpressure skin was present near the wellbore.

This underpressure skin is manifested in Figure 5-36 by the sharp rise of the pressure-derivative data, and the more moderate rise of the pressure data, above the simulations. The underpressure skin is also seen in the dimensionless Horner plot of the FBU (Figure 5-37), which shows the pressure data recovering to the specified static pressure of

149.0 psia until very late time (time increases to the left), at which point the data deviate toward a higher pressure (downward on the plot).

The underpressure skin had less of an effect on the SBU data. The log-log plot of the SBU data (Figure 5-38) still shows some upward deviation of the pressure and pressure-derivative data, but not as much as during the FBU. The simulation shown is representative of a single-porosity medium with a transmissivity of 0.15 ft^2/day and a skin factor of 2.9 (Table 5-3), again indicating a damaged well.

The dimensionless Horner plot of the SBU (Figure 5-39) also shows underpressure skin effects at late time, but generally the data fit the simulation quite well. Note that, as would be expected with a dissipating underpressure skin, the specified static pressure (p*) of 153.2 psia for the SBU dimensionless Horner plot (Figure 5-39) is higher than the 149.0 psia specified for the FBU dimensionless Horner plot (Figure 5-37).
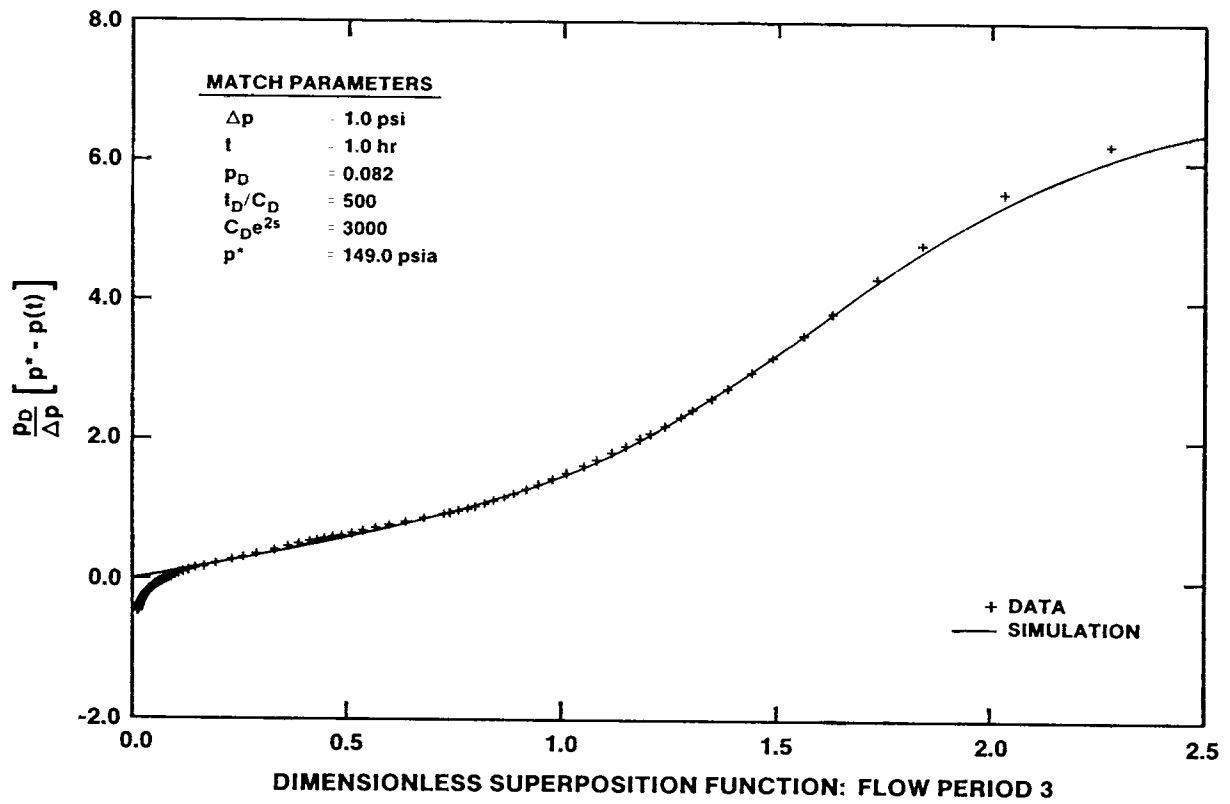
Figure 5-37. H-15/Culebra First Buildup Dimensionless Horner Plot with INTERPRET Simulation
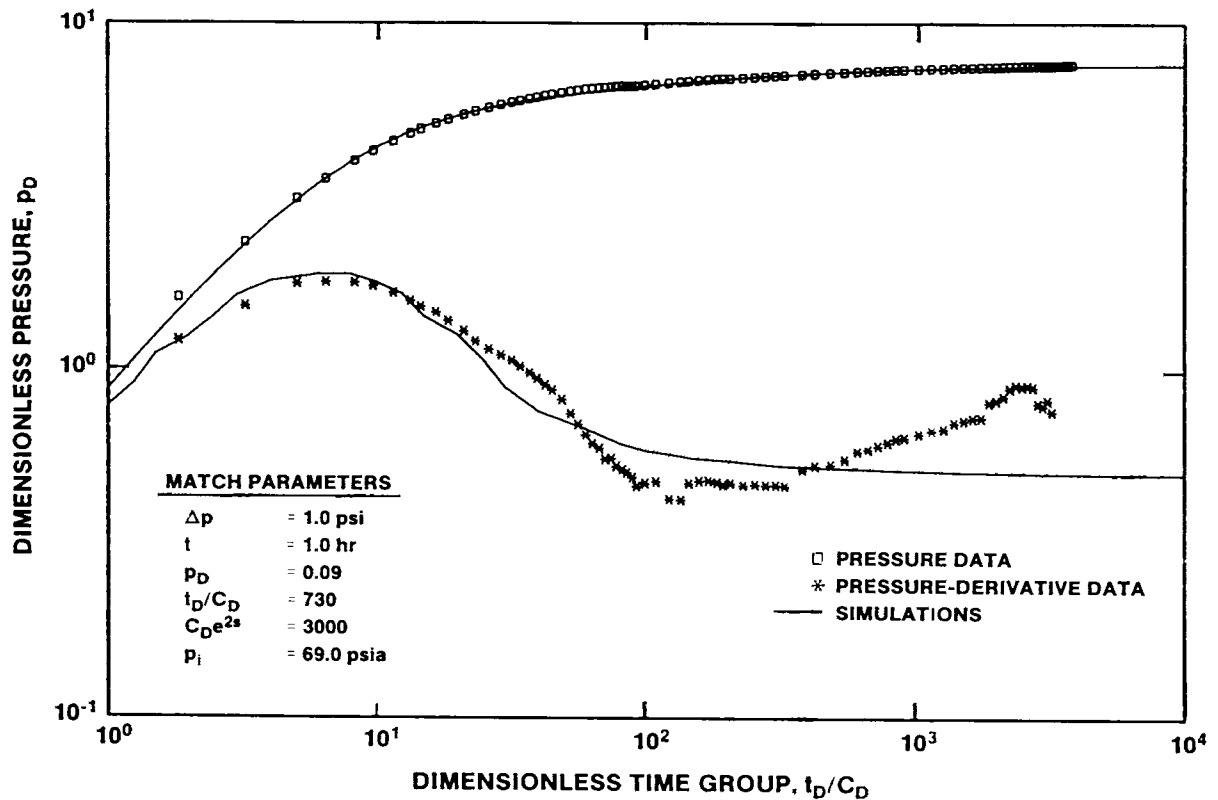
Figure 5-38. H-15/Culebra Second Buildup Log-Log Horner Plot with INTERPRET Simulation

Figure 5-39. H-15/Culebra Second Buildup Dimensionless Horner Plot with INTERPRET Simulation

Figure 5-40 shows a semilog plot of the rising-head slug-test data, along with the best-fit type curve. This fit provides a transmissivity estimate of 0.10 ft²/day (Table 5-3), which is in reasonable agreement with the FBU and SBU results. The best slug-test fit was obtained by assuming that the pressure was recovering to a static value of 160.0 psia, indicating the continuing influence of the underpressure skin after the SBU.

5.2.2.7 H-16. Testing of the Culebra at H-16 was planned to provide transmissivity data necessary to model the response of the Culebra to the construction of the Air-Intake Shaft at the WIPP. The Culebra lies from 702.5 to 724.4 ft deep at H-16 (Figure 3-8). The interval tested extended from 696.5 ft to the then-bottom of the hole at 733.9 ft. Thus, in addition to the Culebra, the lower 6 ft of the Tamarisk and the upper 9.5 ft of the unnamed lower member were tested. With the exception of the lower 2.9 ft of the Tamarisk, these overlying and underlying intervals are composed of gypsum and claystone, respectively, and were not considered to

have contributed significantly to the transmissivity measured during the Culebra testing. The lower 2.9 ft of the Tamarisk is composed of claystone, siltstone, and sandstone, and may have hydraulic properties similar to those of the underlying Culebra. Hydrologically, the Culebra and the lower Tamarisk probably behave as a single unit.

All of the Culebra testing was performed on August 7, 1987, the day after the Culebra was cored. The testing consisted of two DST flow periods, two buildup periods, and a rising-head slug test (Figure 5-41). The FFL lasted about 17 minutes, and was followed by a 161-minute FBU. The SFL lasted about 24 minutes, and was followed by a 208-minute SBU. For analyses of the buildup data, the FFL was divided into two flow periods with rates of 0.731 and 0.500 gpm, and the SFL was divided into two flow periods with rates of 0.818 and 0.512 gpm (Table 5-1). The slug test lasted 162 minutes, by which time 93% of the induced pressure differential had dissipated. The data from these tests are presented in Stensrud et al. (1988).

77

Figure 5-40. H-15/Culebra Slug-Test Plot

78   Figure 5-41. H-16/Culebra Drillstem and Slug Testing Linear-Linear Sequence Plot

Figure 5-42 shows a log-log plot of the FBU data along with an INTERPRET-generated simulation. The simulation shown is representative of a single-porosity medium with a transmissivity of 0.85 ft²/day (Table 5-3). Assuming a Culebra porosity of 20%, a total-system compressibility of 1.0×10^{-5} psi⁻¹, and a fluid viscosity of 1.0 cp, the sk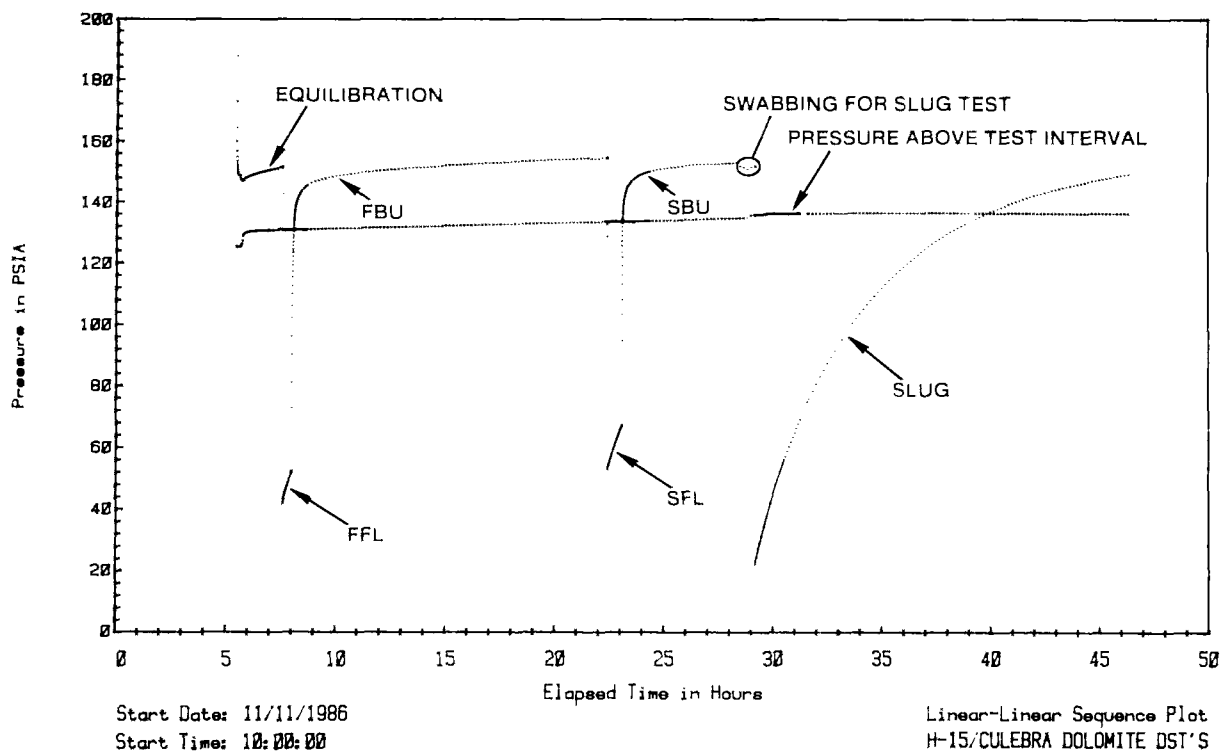in factor for this simulation is about 0.0, indicating no wellbore damage. The decline in the pressure derivative at late time is indicative of a residual overpressure skin created when the Culebra was cored and reamed on August 6, 1987. The dimensionless Horner plot of the FBU data (Figure 5-43) also shows the effects of the overpressure skin as the data trend slightly

upward at very late time (lower left corner of the plot) towards a pressure lower than the 136.2 psia specified as the static formation pressure for that simulation.

The log-log plot of the SBU data (Figure 5-44) shows no overpressure-skin effects. The simulation shown on the figure is representative of a single-porosity medium with a transmissivity of 0.85 ft²/day (Table 5-3), similar to the FBU simulation. The skin factor for this simulation is -0.3, indicating very slight stimulation of the wellbore. The SBU dimensionless Horner plot (Figure 5-45) shows the data recovering to a static formation pressure of 135.4 psia.

Figure 5-42. H-16/Culebra First Buildup Log-Log Plot with INTERPRET Simulation

MATCH PARAMETERS

Δp	= 1.0 psi
t	= 1.0 hr
p_D	= 0.126
t_D/C_D	= 2200
$C_D e^{2s}$	= 20
p^*	= 136.2 psia

+ DATA
—— SIMULATION

y-axis: $\dfrac{p_D}{\Delta p}\left[p^* - p(t)\right]$

x-axis: DIMENSIONLESS SUPERPOSITION FUNCTION: FLOW PERIOD 3
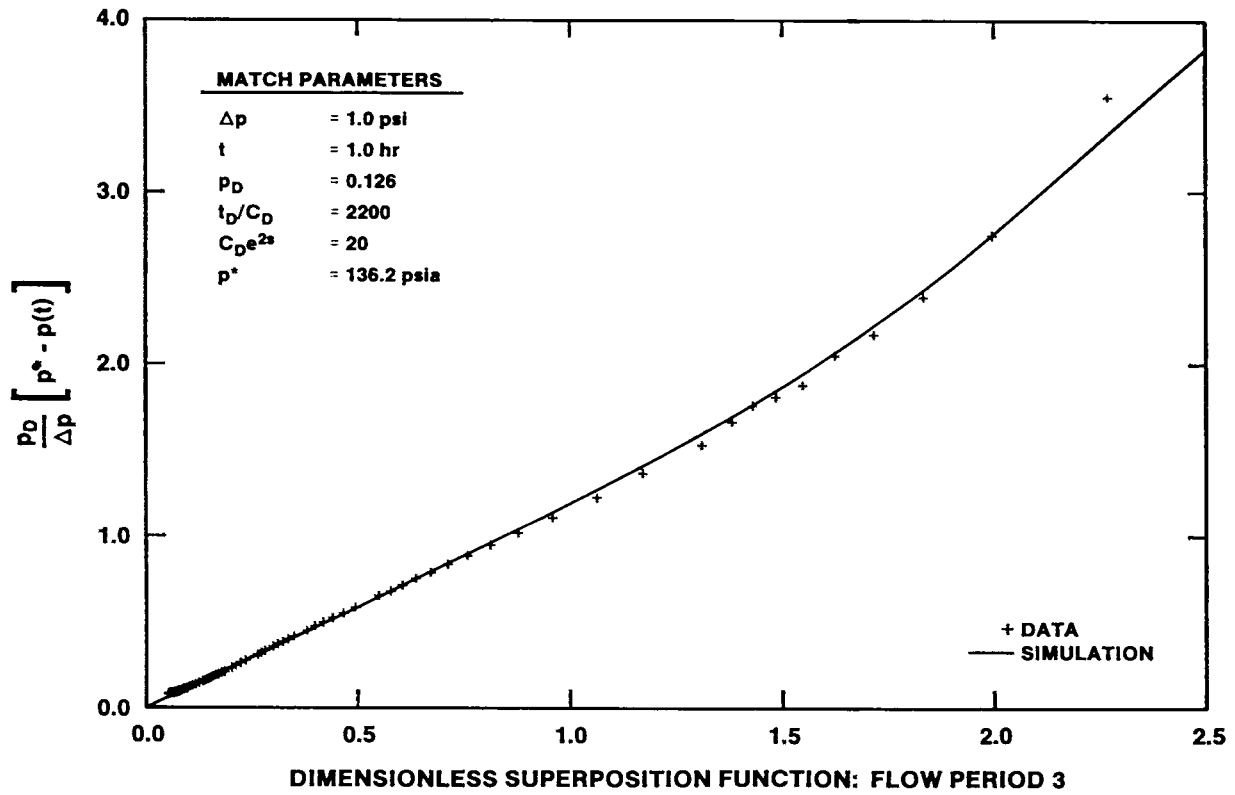
Figure 5-43. H-16/Culebra First Buildup Dimensionless Horner Plot with INTERPRET Simulation

MATCH PARAMETERS

Δp	= 1.0 psi
t	= 1.0 hr
p_D	= 0.123
t_D/C_D	= 2400
$C_D e^{2s}$	= 10
p_i	= 93.0 psia

□ PRESSURE DATA
✳ PRESSURE-DERIVATIVE DATA
—— SIMULATIONS

y-axis: DIMENSIONLESS PRESSURE, p_D

x-axis: DIMENSIONLESS TIME GROUP, t_D/C_D

Figure 5-44. H-16/Culebra Second Buildup Log-Log Plot with Interpret Simulation

MATCH PARAMETERS

Δp	$= 1.0$ psi
t	$= 1.0$ hr
p_D	$= 0.123$
t_D/C_D	$= 2400$
$C_D e^{2s}$	$= 10$
p^*	$= 135.4$ psia

+ DATA
—— SIMULATION

$p_D \left[\dfrac{p^* - p(t)}{\Delta p} \right]$

DIMENSIONLESS SUPERPOSITION FUNCTION: FLOW PERIOD 6
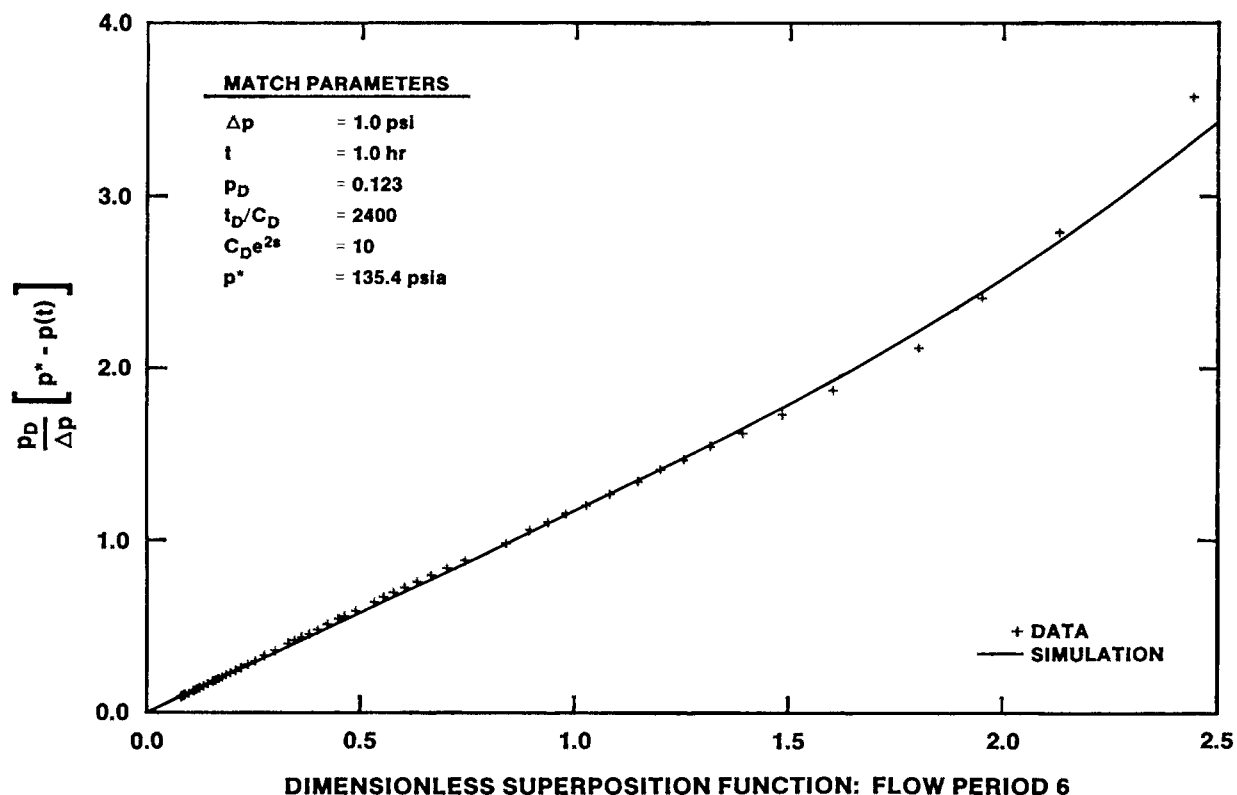
Figure 5-45. H-16/Culebra Second Buildup Dimensionless Horner Plot with INTERPRET Simulation
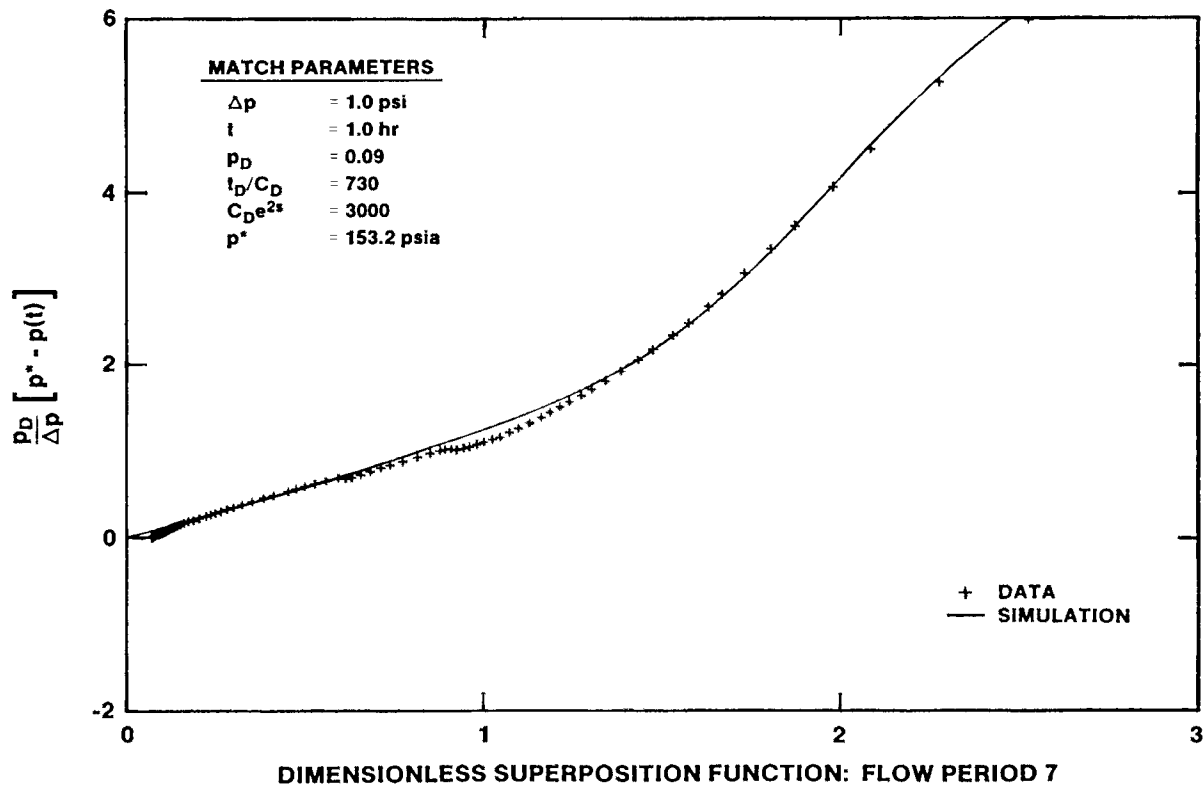
Figure 5-46 shows a semilog plot of the rising-head slug-test data, along with the best-fit type-curve match. The match shown provides a transmissivity estimate of 0.69 ft²/day (Table 5-3), slightly lower than the estimates from the DST analyses. The static formation pressure estimate of 134.8 psia used to achieve the fit in Figure 5-46 is also slightly lower than the values used in the DST analyses. This decrease probably indicates continued dissipation of an overpressure skin.

A comparison of the static formation pressure indicated by the slug test with the pressures measured by the transducer installed at the Culebra horizon as part of the H-16 5-packer completion (Figure 3-8) may also indicate the continued presence of an overpressure skin during the DST's and slug test. The transducer used for the DST's and slug test was set at a depth of 678.6 ft. H-16 contained water having a specific gravity of 1.02 at the time of the Culebra testing. The slug-test pressure of 134.8 psia reduces to 121.1 psig when the atmospheric pressure of 13.7 psia measured by that transducer is subtracted. The corresponding formation pressure at the midpoint of the Culebra 712 ft deep is about 136 psig. In contrast, the Culebra transducer of the 5-packer system, which is located at a depth of 702.6 ft, 24 ft deeper than the DST transducer, showed a pressure stabilization at 128 psig shortly after the 5-packer installation was completed (Stensrud et al., 1988). With the hole now containing brine having a specific gravity of 1.2, the corresponding formation pressure at the midpoint of the Culebra, 712 ft deep, is 133 psig. Hence, about 3 psi of additional pressure-skin dissipation may have occurred after the Culebra testing was completed. Alternatively, continued leakage of Culebra water into the WIPP shafts may have lowered the Culebra formation pressure at H-16.

5.2.2.8 H-17. Testing of the Culebra at H-17 was planned to determine whether or not the well had been successfully located in an area of high Culebra transmissivity. The Culebra lies from 705.8 to 731.4 ft deep at H-17 (Figure 3-9). The interval tested extended from 703.1 ft to the then-bottom of the hole
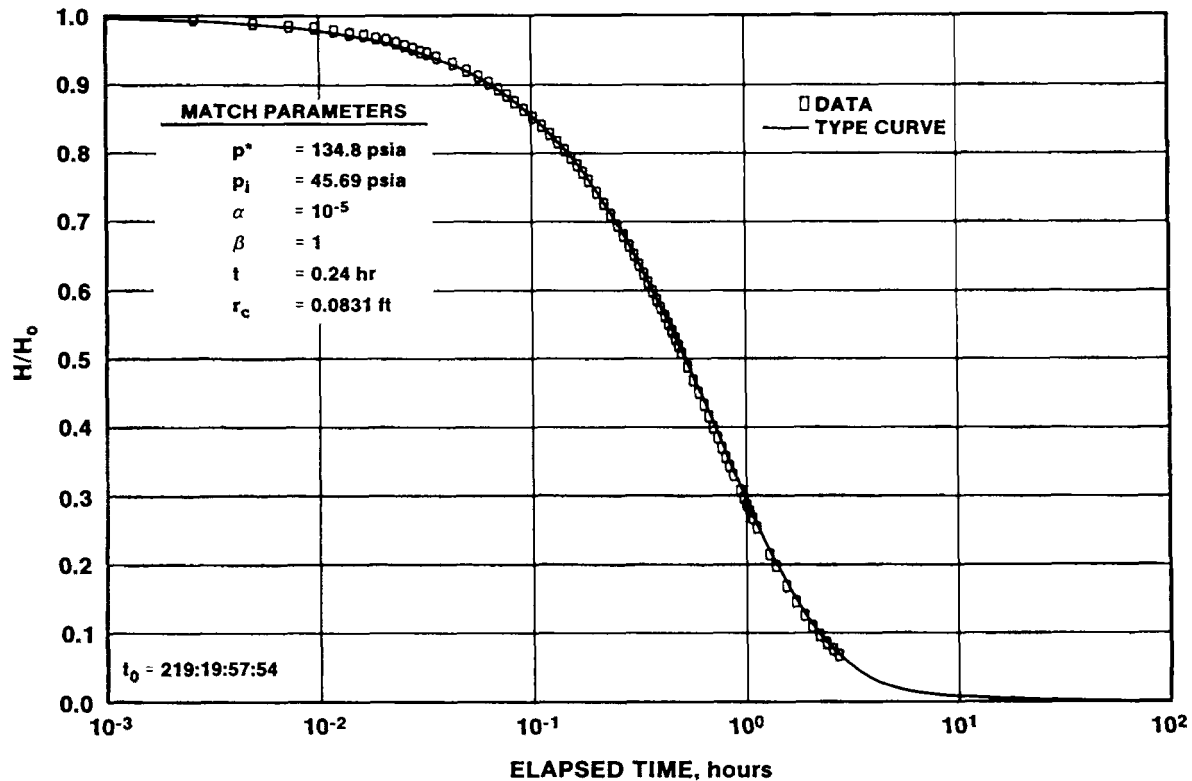
Figure 5-46. H-16/Culebra Slug-Test Plot

at 735.0 ft. Thus, the lower 2.7 ft of the Tamarisk and the upper 3.6 ft of the unnamed lower member were tested along with the Culebra. These overlying and underlying intervals are composed of anhydrite, gypsum, and/or clay, and were not considered to have contributed significantly to the transmissivity measured during the Culebra testing.

The H-17 Culebra testing was performed from October 9 to 12, 1987. The testing consisted of two DST flow periods, two buildup periods, and a rising-head slug test (Figure 5-47). The FFL lasted about 16 minutes, and was followed by a 449- minute FBU. The SFL lasted about 24 minutes, and was followed by a 939-minute SBU. To obtain constant flow rates for buildup analyses, the FFL was divided into two flow periods having rates of 0.368 and 0.259 gpm, and the SFL was divided into two flow periods having rates of 0.443 and 0.280 gpm (Table 5-1). The slug test lasted about 48 hr, by which time about 99% of the induced pressure differential had dissipated. The data from these tests are presented in Stensrud et al. (1988).
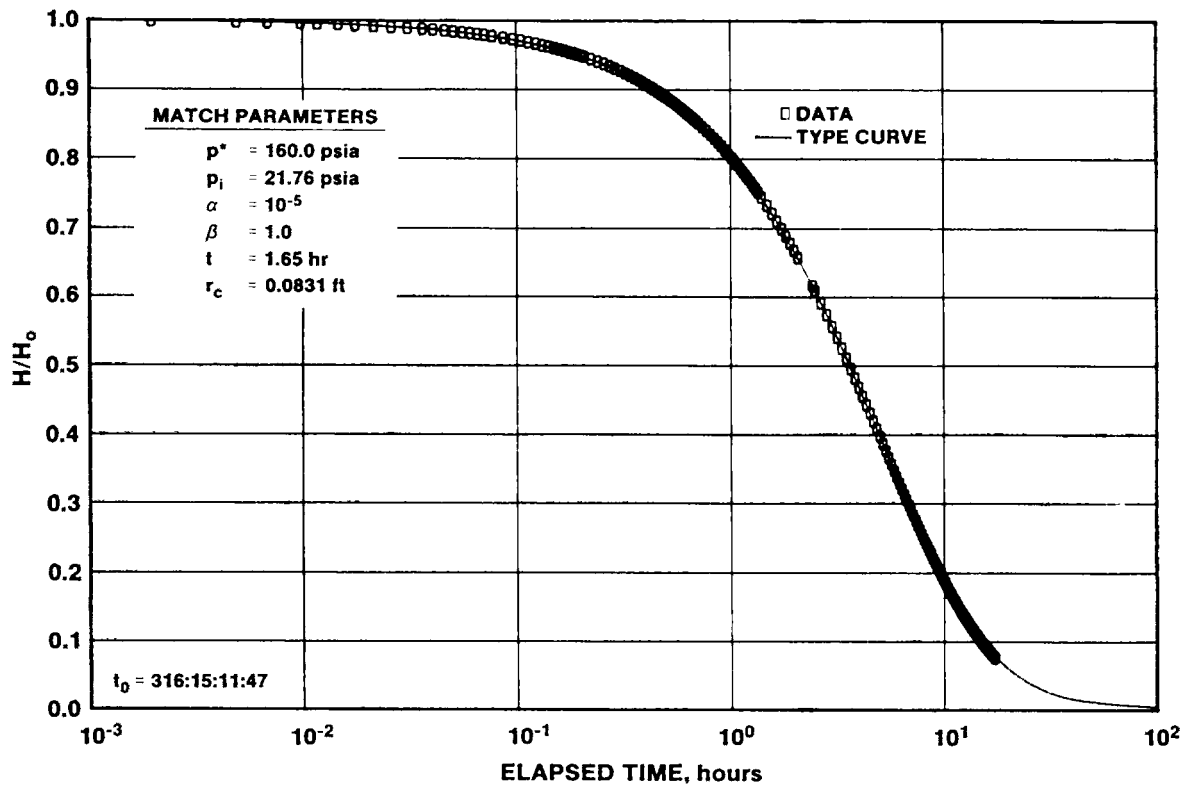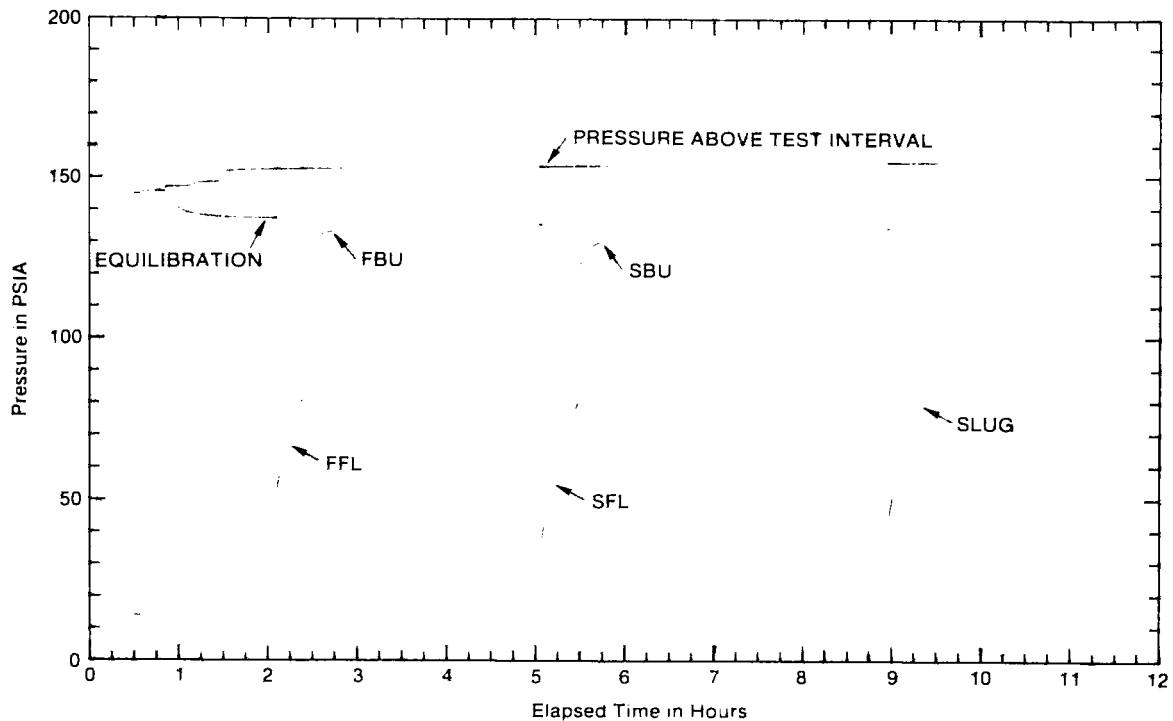
A log-log plot of the FBU data is presented in Figure 5-48, along with a simulation generated by INTERPRET. The simulation is representative of a single-porosity medium with a transmissivity of 0.21 ft²/day (Table 5-3). Assuming a Culebra porosity of 20%, a total-system compressibility of 1.0×10^{-5} psi^{-1}, and a fluid viscosity of 1.0 cp, the skin factor for this simulation is -1.5, indicating a moderately stimulated well. The decline in the pressure derivative at late time indicates the presence of an overpressure skin created during coring and reaming of the Culebra October 7 and 8, 1987. The dimensionless Horner plot of the FBU data (Figure 5-49) also shows the effects of the overpressure skin as the data trend slightly upward at very late time towards a pressure lower than the 145.5 psia specified as the static formation pressure for that simulation. In fact, the buildup pressure reached a maximum of 144.8 psia after 275 minutes of the FBU (Figure 5-47), and declined slightly thereafter. The data collected after the maximum pressure was reached are not included on the analysis plots.
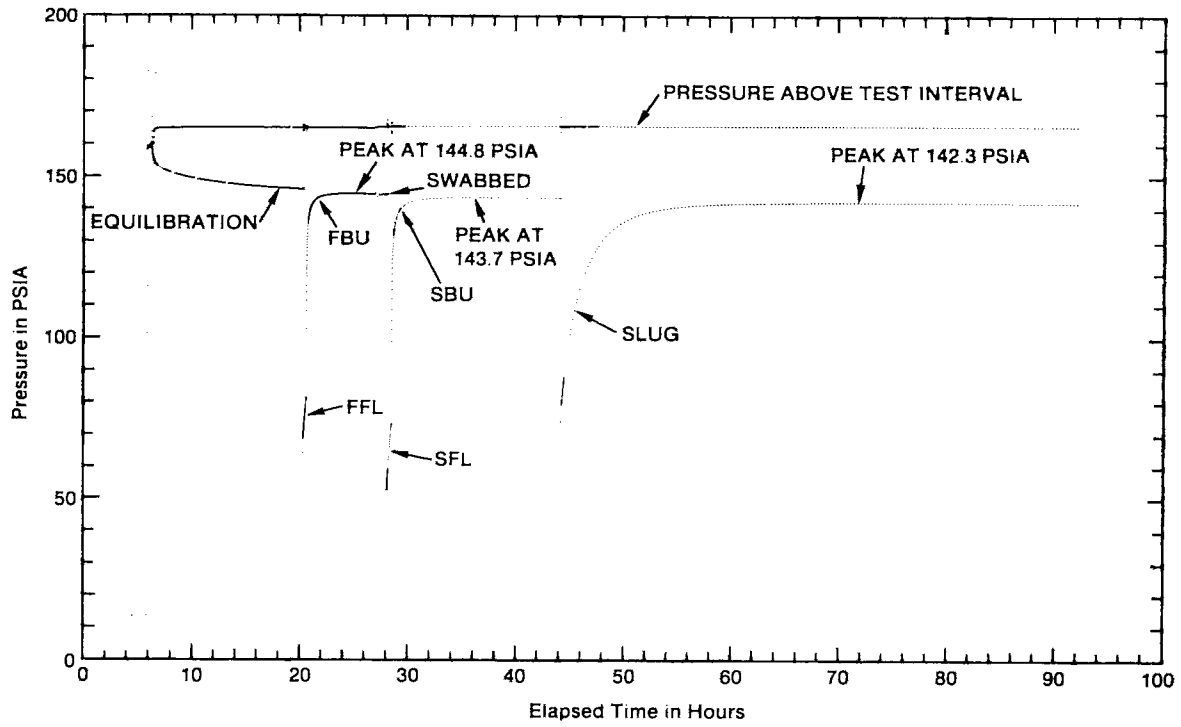
Start Date: 10/08/87
Start Time: 12:00:00

Linear-Linear Sequence Plot
H-17/DST 706-731/CULEBRA DOLOMITE

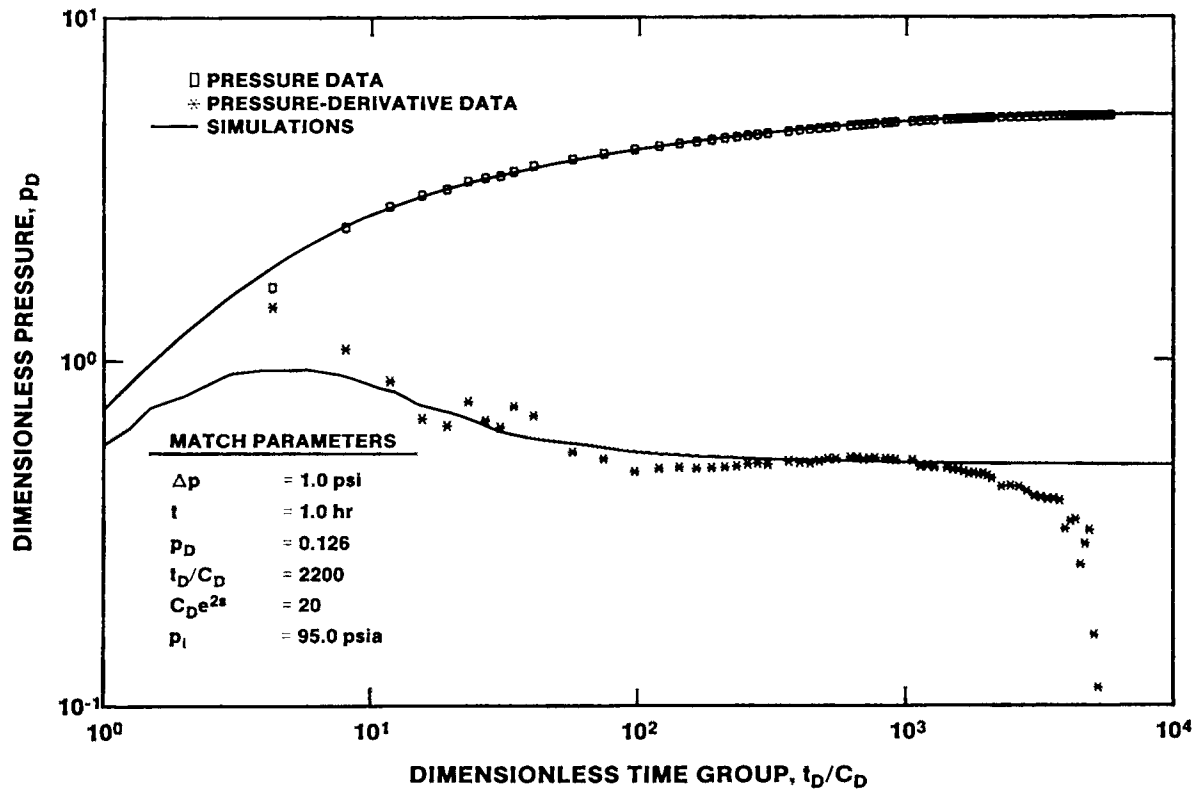Figure 5-47. H-17/Culebra Drillstem and Slug Testing Linear-Linear Sequence Plot
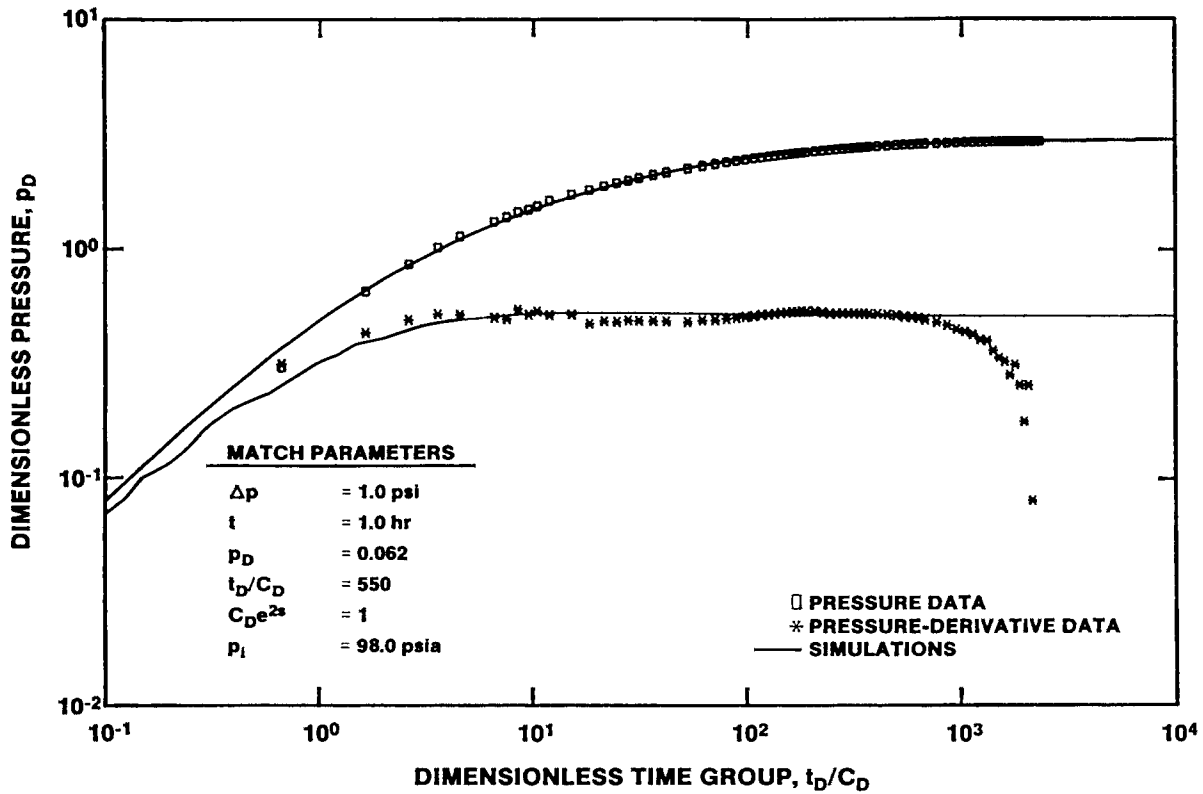
Figure 5-48. H-17/Culebra First Buildup Log-Log Plot with INTERPRET Simulation

Figure 5-49. H-17/Culebra First Buildup Dimensionless Horner Plot with INTERPRET Simulation
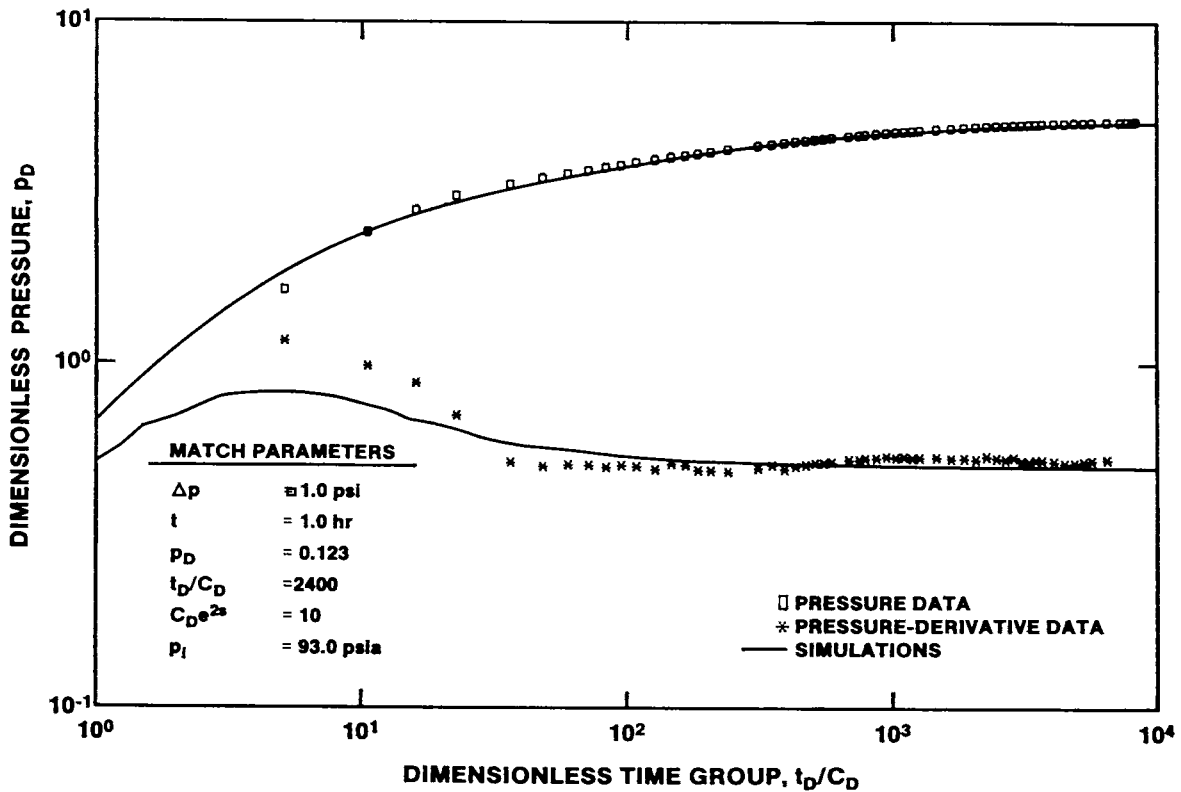
The SBU data log-log plot and simulation (Figure 5-50) are very similar to those of the FBU data (Figure 5-48). The SBU simulation is representative of a single-porosity medium with a transmissivity of 0.22 ft²/day (Table 5-3). The skin factor for this simulation is -1.2, again indicating a moderately stimulated well. Overpressure skin effects are evident in both the SBU log-log plot and the dimensionless Horner plot (Figure 5-51). On the former, the pressure derivative declines at late time, and on the latter, the late-time data trend toward a pressure lower than the static formation pressure of 144.6 psia specified for that simulation. In fact, the buildup pressure reached a maximum of 143.7 psia after about 7.5 hr of the SBU (Figure 5-47), and declined very slightly for the last 8 hr of the SBU. The data from these last 8 hr are not included on the analysis plots.

Figure 5-52 presents a semilog plot of the rising-head slug-test data, along with the best-fit type-curve match. This match provides a transmissivity estimate of 0.22 ft²/day (Table 5-3), which is in excellent

agreement with the DST results. The static formation pressure estimate used to fit the data in Figure 5-52 is 143.0 psia. In actuality, the fluid pressure peaked at 142.3 psia after 27 hr of the slug test, and declined slightly thereafter, indicating continued dissipation of an overpressure skin. The data collected after the pressure peaked are not included on this plot.

The analyses of the H-17 Culebra tests provide consistent transmissivity estimates of about 0.2 ft²/day. Thus, H-17 is not located in the high-transmissivity zone hypothesized by Haug et al. (1987) and Bartel (in preparation). This zone, if it exists, must lie farther to the west towards P-17 (Figure 1-1).

5.2.2.9 H-18. The objective of the Culebra testing at H-18 was to help determine where the transition occurs between the high-transmissivity region that includes WIPP-13 (69 ft²/day; Beauheim, 1987b) and the low-transmissivity region that includes H-2 (0.4 ft²/day; Mercer, 1983) (Figure 1-1). At H-18, the Culebra lies from 688.6 to 712.8 ft deep

Figure 5-50. H-17/Culebra Second Buildup Log-Log Plot with INTERPRET Simulation

Figure 5-51. H-17/Culebra Second Buildup Dimensionless Horner Plot with INTERPRET Simulation

MATCH PARAMETERS

$p^* = 143.0$ psia
$p_i = 74.52$ psia
$a = 10^{-4}$
$\beta = 1$
$t = 0.75$ hr
$r_c = 0.0831$ ft

□ DATA
—— TYPE CURVE

$t_0 = 283{:}08{:}07{:}20$

H/H₀ axis: H/H_o

ELAPSED TIME, hours

Figure 5-52. H-17/Culebra Slug-Test Plot

(Figure 3-10). The interval tested extended from 685.0 to 714.1 ft deep. Thus, the lower 3.6 ft of the Tamarisk and the upper 1.3 ft of the unnamed lower member were included in the test interval. Inasmuch as these overlying and underlying intervals are composed of anhydrite/gypsum and clay, respectively, they were not considered to have contributed significantly to the transmissivity measured during the Culebra testing.

The Culebra testing was performed on October 31, 1987, the day after the Culebra was cored. The testing consisted of two DST flow periods, two buildup periods, and a rising-head slug test (Figure 5-53). The FFL lasted about 11 minutes, and was followed by a 64-minute FBU. The SFL lasted about 18 minutes, and was followed by an 89-minute SBU. To obtain constant flow rates for buildup analyses, the FFL was divided into two flow periods having rates of 1.372 and 1.083 gpm, and the SFL was divided into two flow periods having rates of 1.200 and 0.772 gpm (Table 5-1). The slug test lasted about 90 minutes, allowing 92% of the

induced pressure differential to dissipate. The data from these tests are presented in Stensrud et al. (1988).

Figure 5-54 is a log-log plot of the FBU data, along with a simulation generated by INTERPRET. The simulation is representative of a single-porosity medium with a transmissivity of 2.2 ft²/day (Table 5-3). Assuming a Culebra porosity of 20%, a total-system compressibility of 1.0×10^{-5} psi⁻¹, and a fluid viscosity of 1.0 cp, the skin factor for this simulation is -0.2, indicating a minimally stimulated well. The decline in the pressure derivative at late time indicates the presence of an overpressure skin created during coring and reaming of the Culebra. This overpressure skin was strong enough to cause the pressure to peak at 157.3 psia after 42 minutes of the FBU (Figure 5-53). The dimensionless Horner plot of the FBU data (Figure 5-55) shows that the overpressure skin was driving the recovery toward a static formation pressure of 158.6 psia until late time, when the data began trending toward a lower pressure (upward on the plot) as the skin dissipated.

86

Figure 5-53. H-18/Culebra Drillstem and Slug Testing Linear-Linear Sequence Plot
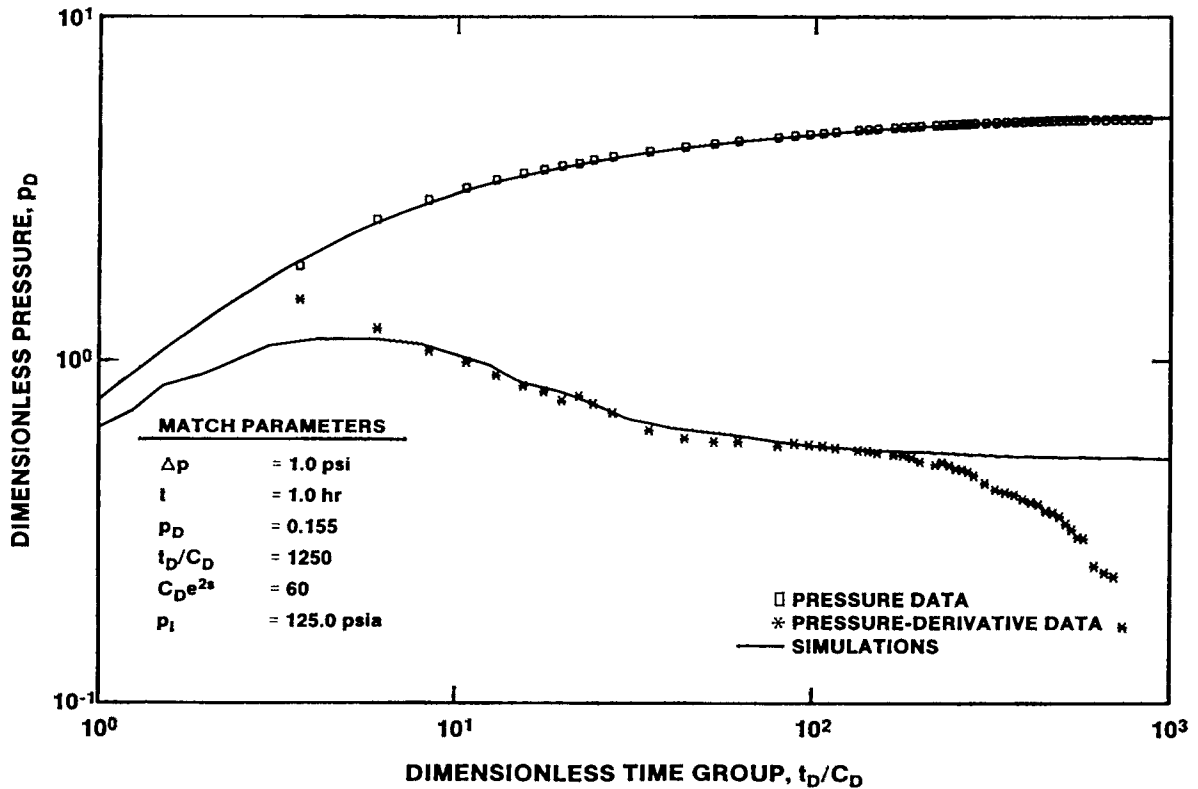
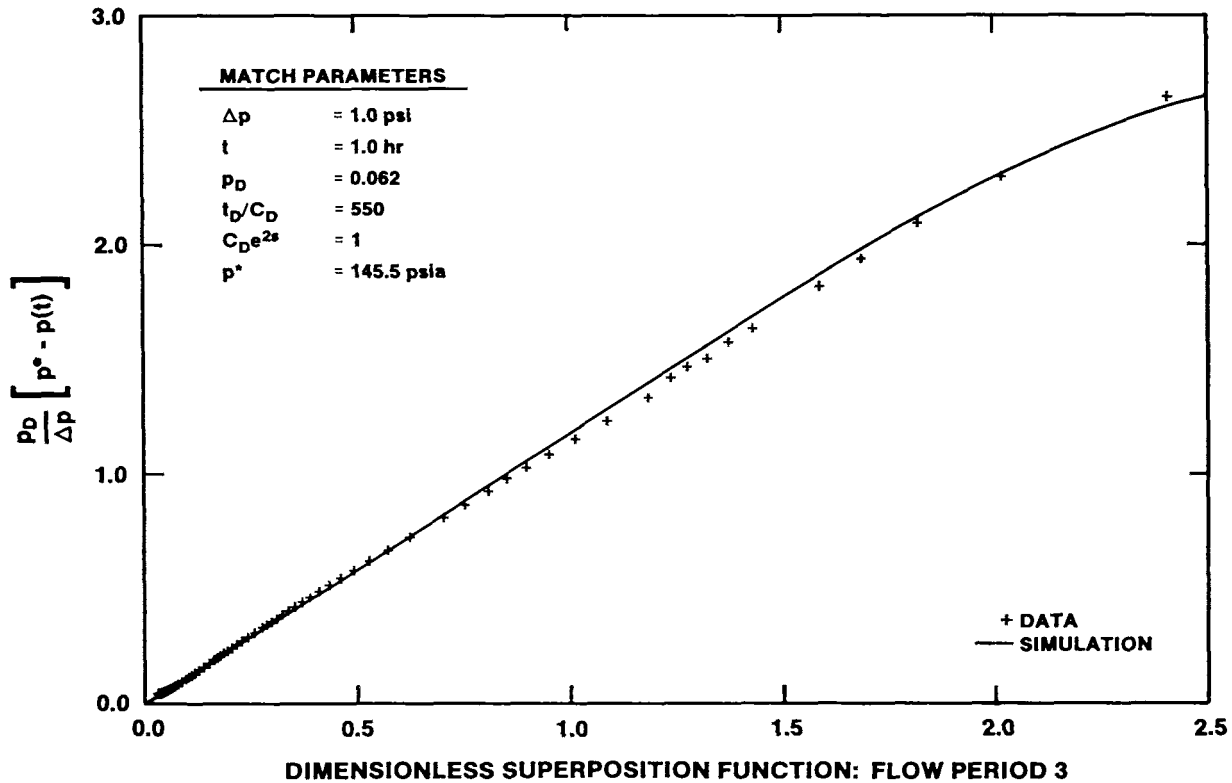Figure 5-54. H-18/Culebra First Buildup Log-Log Plot with INTERPRET Simulation
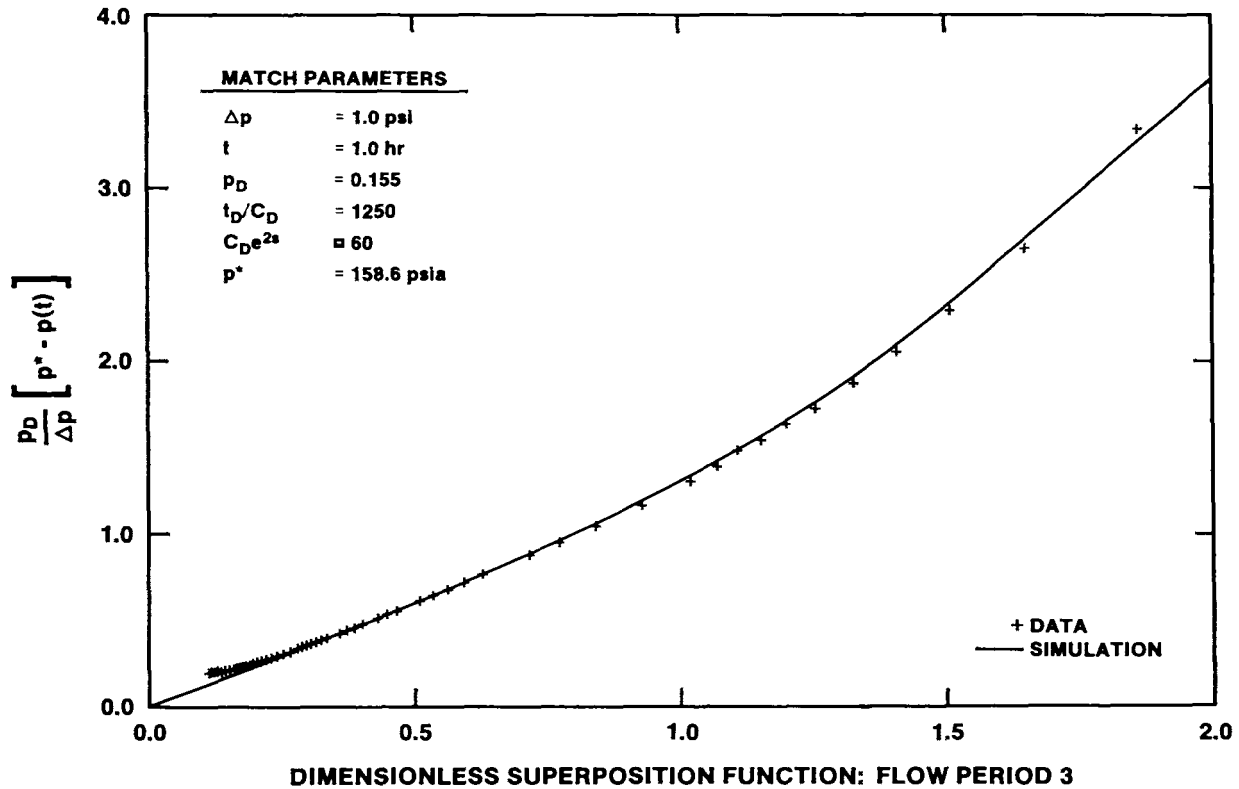
Figure 5-55. H-18/Culebra First Buildup Dimensionless Horner Plot with INTERPRET Simulation

The log-log plot of the SBU data (Figure 5-56) also shows overpressure skin effects as a decline in the derivative at late time. The simulation shown is similar to that developed for the FBU, and is representative of a single-porosity medium with a transmissivity of 2.2 ft²/day (Table 5-3). The skin factor for this simulation is -1.0, showing increased stimulation during the DST's. The overpressure skin caused the pressure to peak at 155.0 psia after 70 minutes of the SBU (Figure 5-53). The dimensionless Horner plot of the SBU data (Figure 5-57) shows that the overpressure skin was initially driving the recovery toward a static formation pressure of 156.1 psia, but that at late time the data deviated toward a lower pressure as the rates of pressure-skin dissipation and pressure recovery became more equivalent.

Figure 5-58 is a semilog plot of the rising-head slug-test data, along with the best-fit type-curve match. This match provides a transmissivity estimate of 1.7 ft²/day, slightly lower than those provided by the DST buildup analyses (Table 5-3). During the slug test, the pressure appeared to be recovering to a value of 154.5 psia, slightly lower than the final SBU value.

The transmissivity values provided by the DST's and slug test of about 2 ft²/day indicate that H-18 lies in a transitional region between the higher transmissivities to the north and the lower transmissivities to the south. Based on experience with similar transmissivities at H-3 (Beauheim, 1987a), the Culebra at H-18 might be expected to show double-porosity effects in its hydraulic responses. Fractures in the Culebra core from H-18 further indicate a potential for double-porosity behavior. No double-porosity behavior was observed, however, perhaps because the small spatial scale and the short test durations involved in DST's and slug tests allow for little interaction between fractures and matrix. A pumping test of several days' duration would provide a more definitive indication of whether or not the Culebra behaves hydraulically as a double-porosity system at H-18.
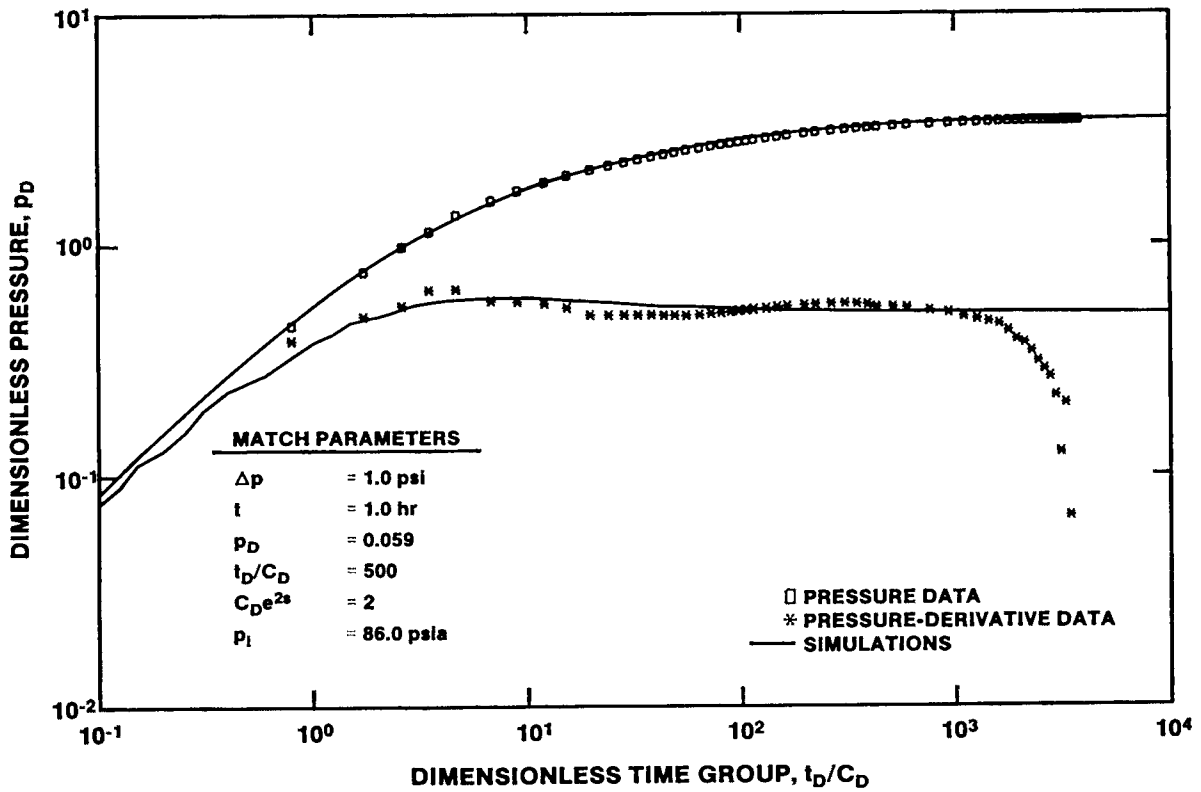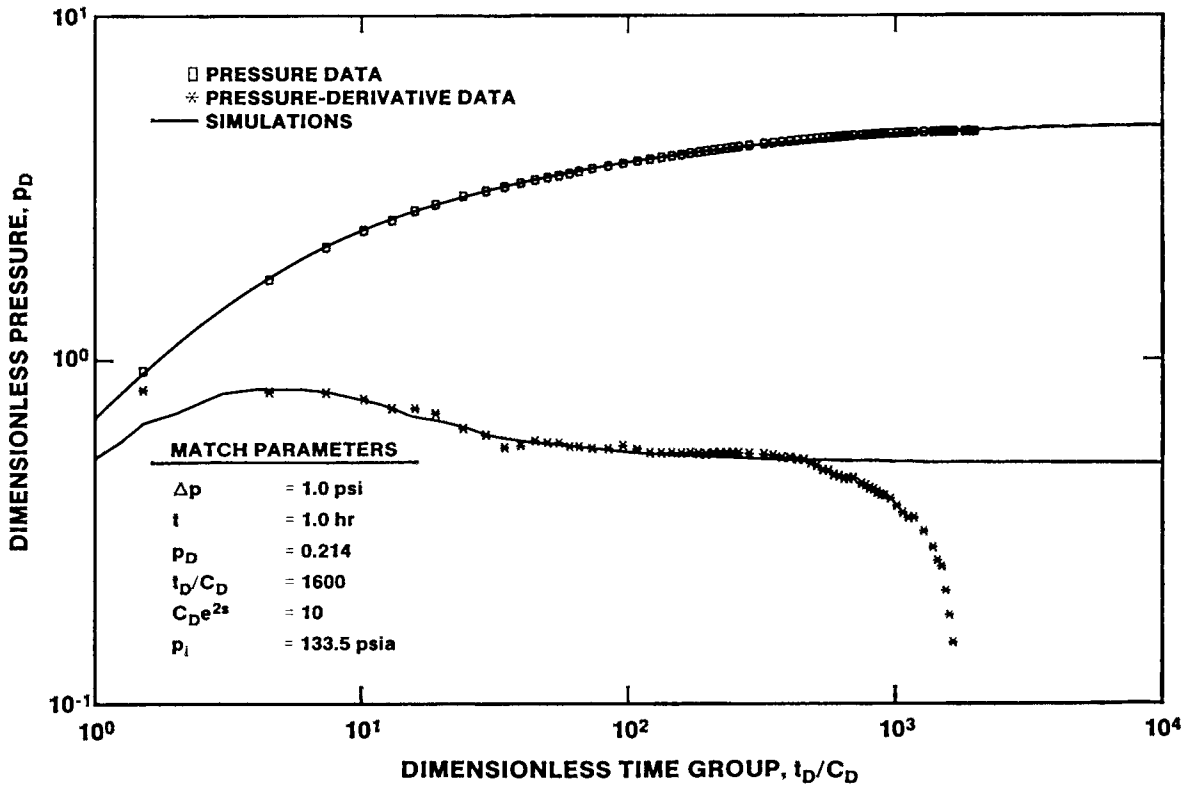
Figure 5-56. H-18/Culebra Second Buildup Log-Log Plot with INTERPRET Simulation
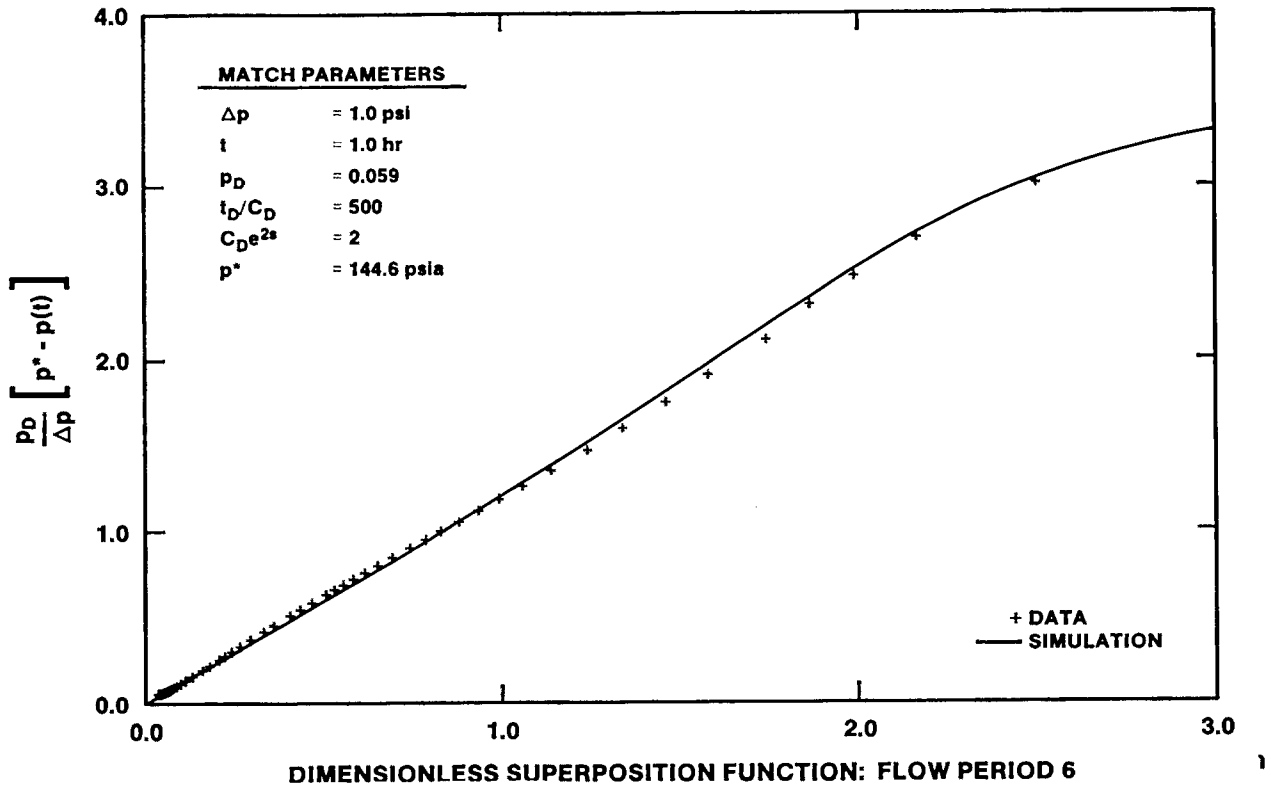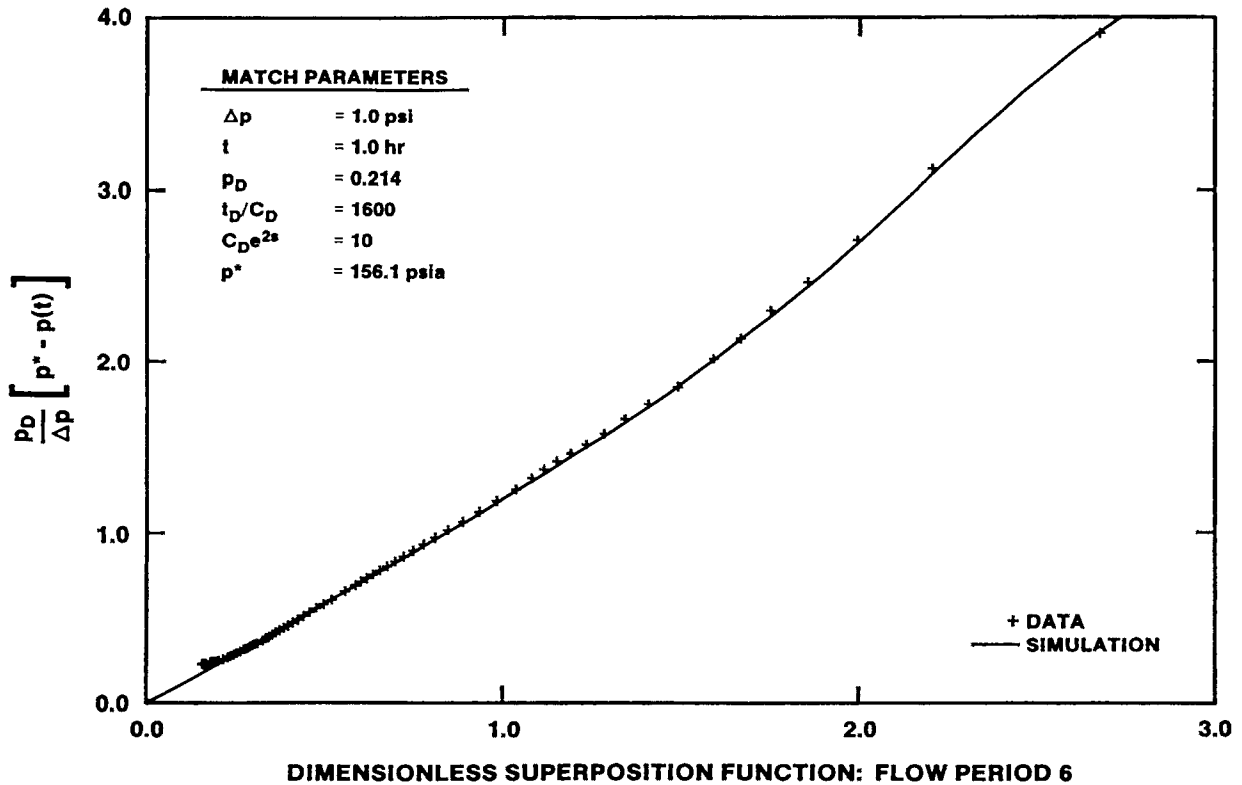

Figure 5-57. H-18/Culebra Second Buildup Dimensionless Horner Plot with INTERPRET Simulation
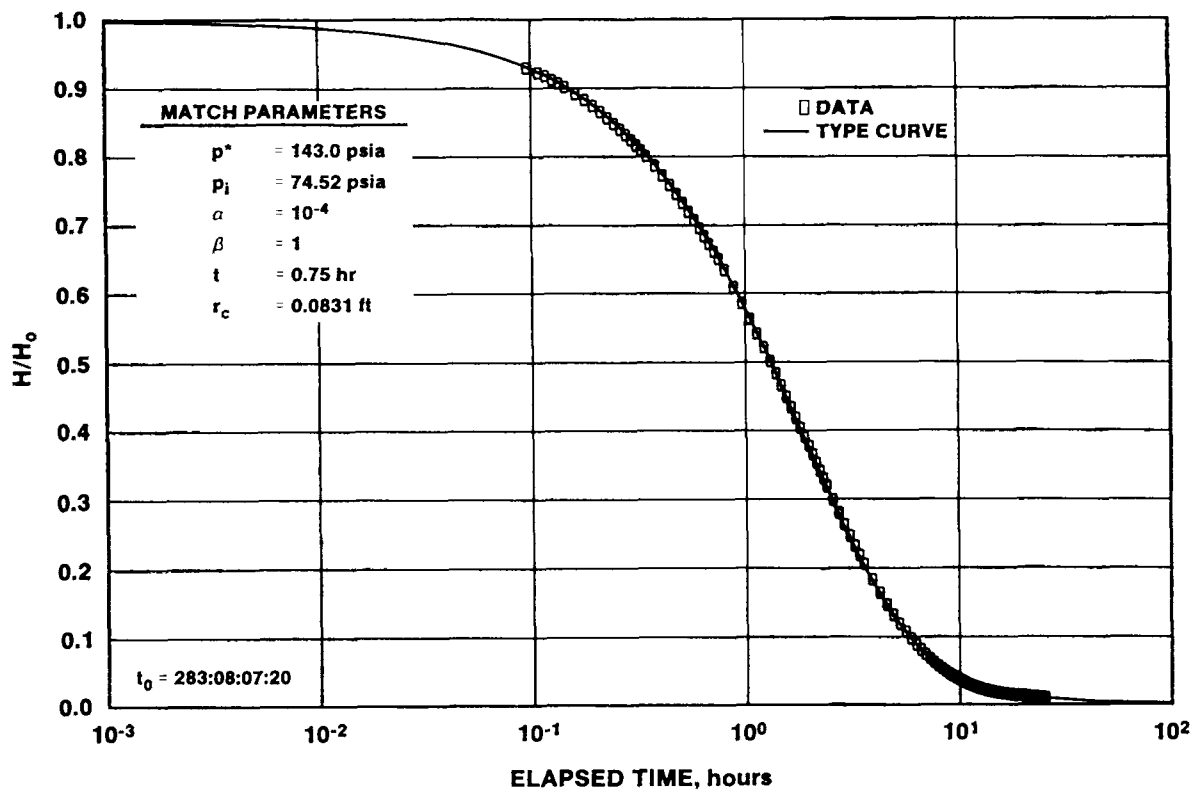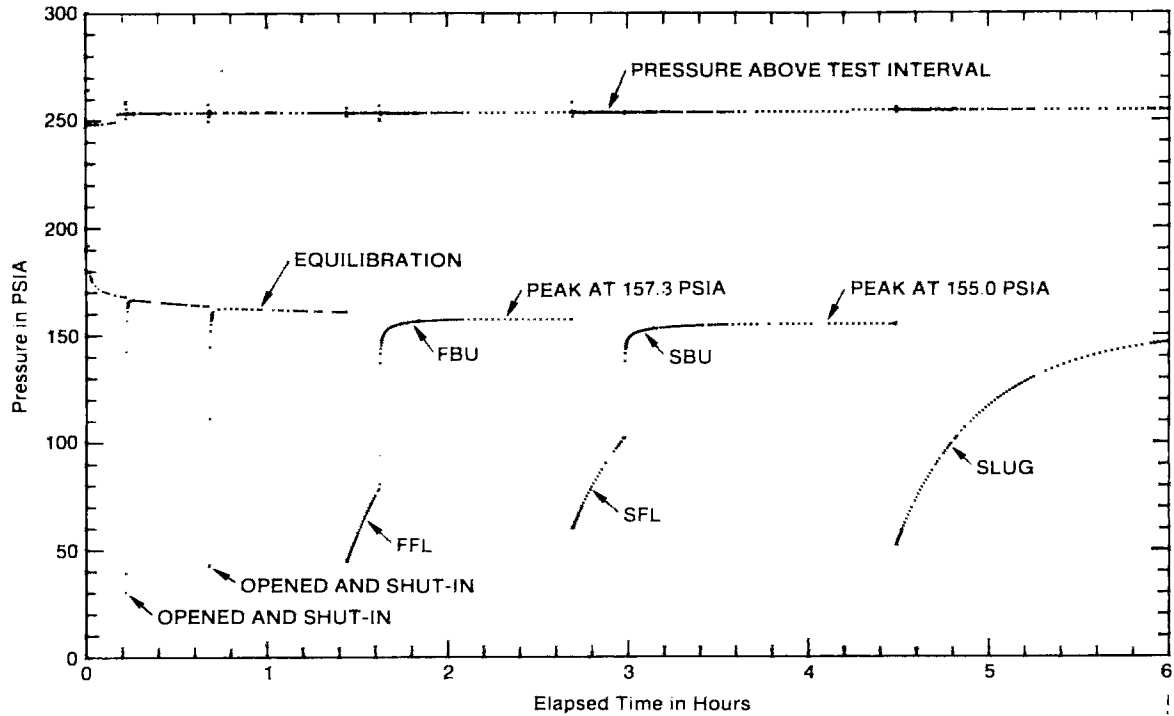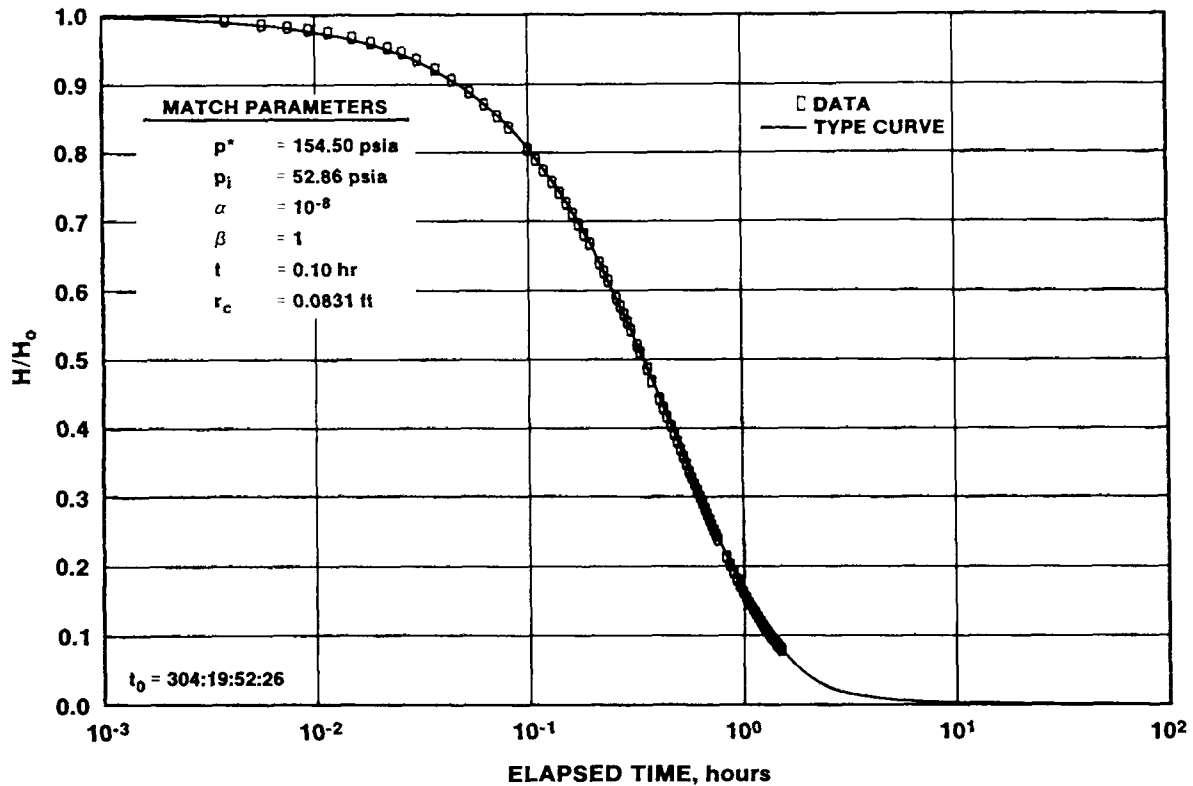
Figure 5-58. H-18/Culebra Slug-Test Plot

5.2.2.10 WIPP-12. Two falling-head slug tests of the Culebra were conducted at WIPP-12. The first test was initiated on December 22, 1987, and the second test was initiated on January 8, 1988. The fluid-pressure data from these tests will be reported in Stensrud et al. (in preparation). During each test, approximately 95% of the induced pressure differential was dissipated in 17 to 19 hr. The data from these periods fit the analytically derived type curves well. After 17 to 19 hr, however, the rates of recovery slowed for an unknown reason, causing deviation of the data from the type curves. Inasmuch as the test recoveries were nearly complete when these deviations occurred and the analyses of the data collected before these deviations provided consistent results for the two tests, the late-time (i.e., after 17 to 19 hr) data were ignored during analysis.

A semilog plot of the data from the first slug test, along with the best-fit type-curve match, are shown in Figure 5-59. This type-curve match provides a transmissivity estimate of 0.10 ft²/day for the Culebra at WIPP-12 (Table 5-3). The same type curve and a

similar match were used to fit the data from the second test (Figure 5-60). The transmissivity estimate provided by this match is 9.7 x 10-2 ft²/day (Table 5-3), similar to that from the first test.

5.2.2.11 WIPP-18. To evaluate the transmissivity of the Culebra at WIPP-18, a falling-head slug test lasting slightly over 46 hr was initiated on May 21, 1986. The fluid-pressure data from this test are reported in Saulnier et al. (1987). About 95% of the induced pressure differential was dissipated during the test. Figure 5-61 shows a semilog plot of the falling-head slug-test data, along with the best-fit type curve. This fit provides a transmissivity estimate of 0.30 ft²/day (Table 5-3).

5.2.2.12 WIPP-19. The transmissivity of the Culebra at WIPP-19 was evaluated by performing a falling-head slug test. The test was initiated on May 31, 1986, and lasted approximately 94 hr. The fluid-pressure data from this test are reported in Saulnier et al. (1987). About 98% of the induced pressure differential was dissipated during the test.

Figure 5-59. WIPP-12/Culebra Slug-Test #1 Plot
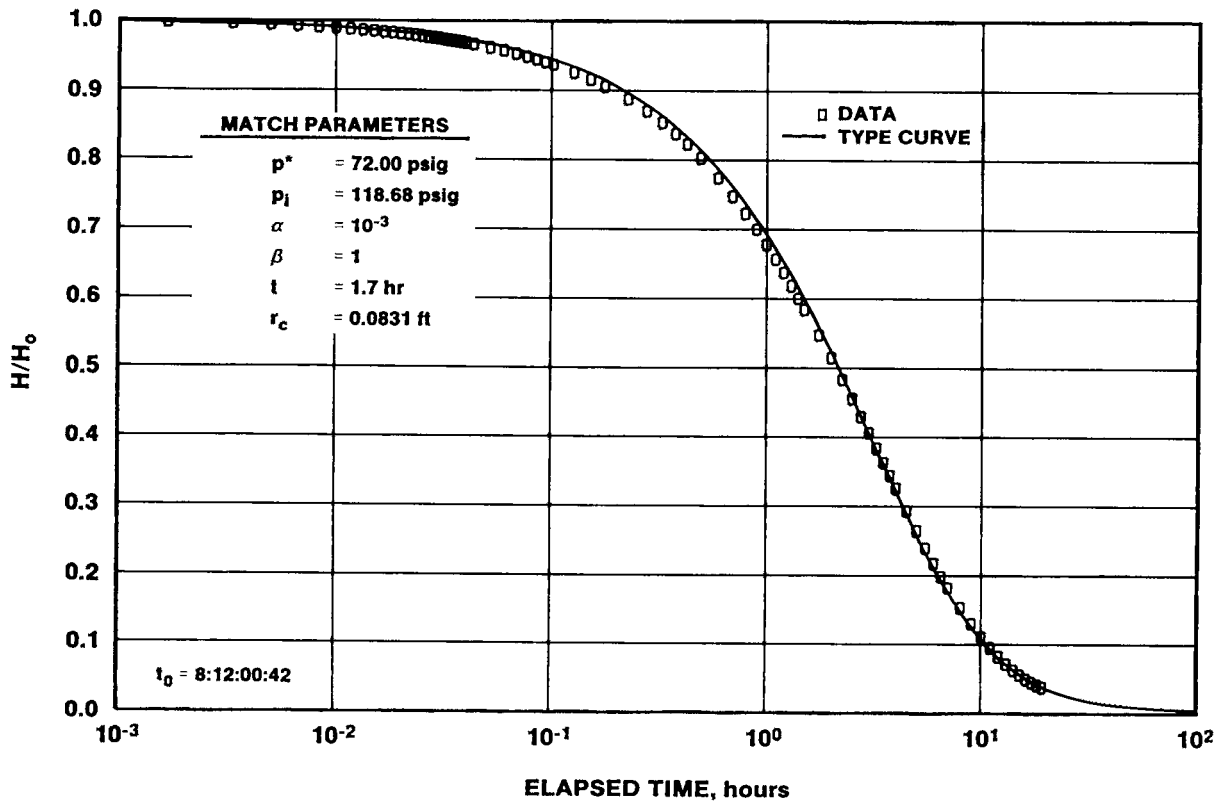
Figure 5-60. WIPP-12/Culebra Slug-Test #2 Plot

MATCH PARAMETERS

p^* = 154.10 psig
p_i = 194.76 psig
α = 10^{-7}
β = 1.0
t = 2.6 hr
r_c^* = 0.181 ft

t_0 = 141:10:05:00
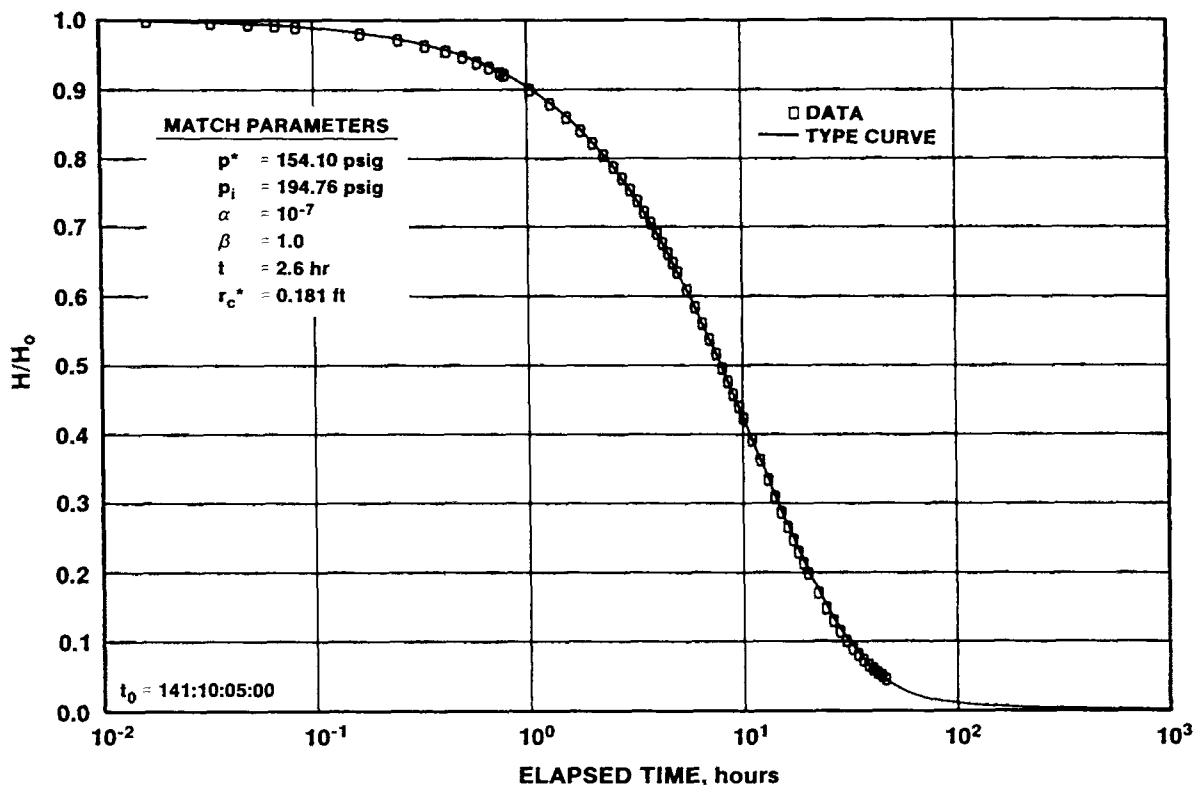
□ DATA
—— TYPE CURVE

Figure 5-61. WIPP-18/Culebra Slug-Test Plot

Figure 5-62 shows a semilog plot of the falling-head slug-test data, along with the best-fit type curve. This fit provides a transmissivity estimate of 0.60 ft²/day (Table 5-3).

5.2.2.13 WIPP-21. To evaluate the transmissivity of the Culebra at WIPP-21, a falling-head slug test lasting approximately 120 hr was initiated on July 11, 1986. The fluid-pressure data from this test are reported in Saulnier et al. (1987). About 99% of the induced pressure differential was dissipated during the test. Figure 5-63 shows a semilog plot of the falling-head slug-test data, along with the best-fit type curve. This fit provides a transmissivity estimate of 0.25 ft²/day (Table 5-3).

5.2.2.14 WIPP-22. The transmissivity of the Culebra at WIPP-22 was also evaluated by performing a falling-head slug test. The test was initiated on June 19, 1986, and lasted approximately 75 hr. The fluid-pressure data from this test are reported in Saulnier et al. (1987). About 98% of the

induced pressure differential was dissipated during the test. Figure 5-64 shows a semilog plot of the falling-head slug-test data, along with the best-fit type curve. This fit provides a transmissivity estimate of 0.37 ft²/day (Table 5-3).

5.2.2.15 WIPP-30. Mercer (1983) reported the transmissivity of the Culebra at WIPP-30 to be 0.3 ft²/day, based on a slug test performed by the USGS in 1980 (Richey, 1987). Verification of this value was considered warranted by two observations. First, WIPP-30 lies in an area where no halite is present beneath the Culebra in the unnamed lower member. At every other location where the Culebra has been tested and no halite is present in the unnamed member, the Culebra is fractured and has a transmissivity of at least 8 ft²/day (Mercer, 1983, and this report). Second, water-level responses observed in WIPP-30 to pumping at WIPP-13, 3.5 miles away, have led to an interpreted apparent transmissivity of 28 ft²/day for the Culebra between WIPP-30 and WIPP-13 (Beauheim, 1987b).
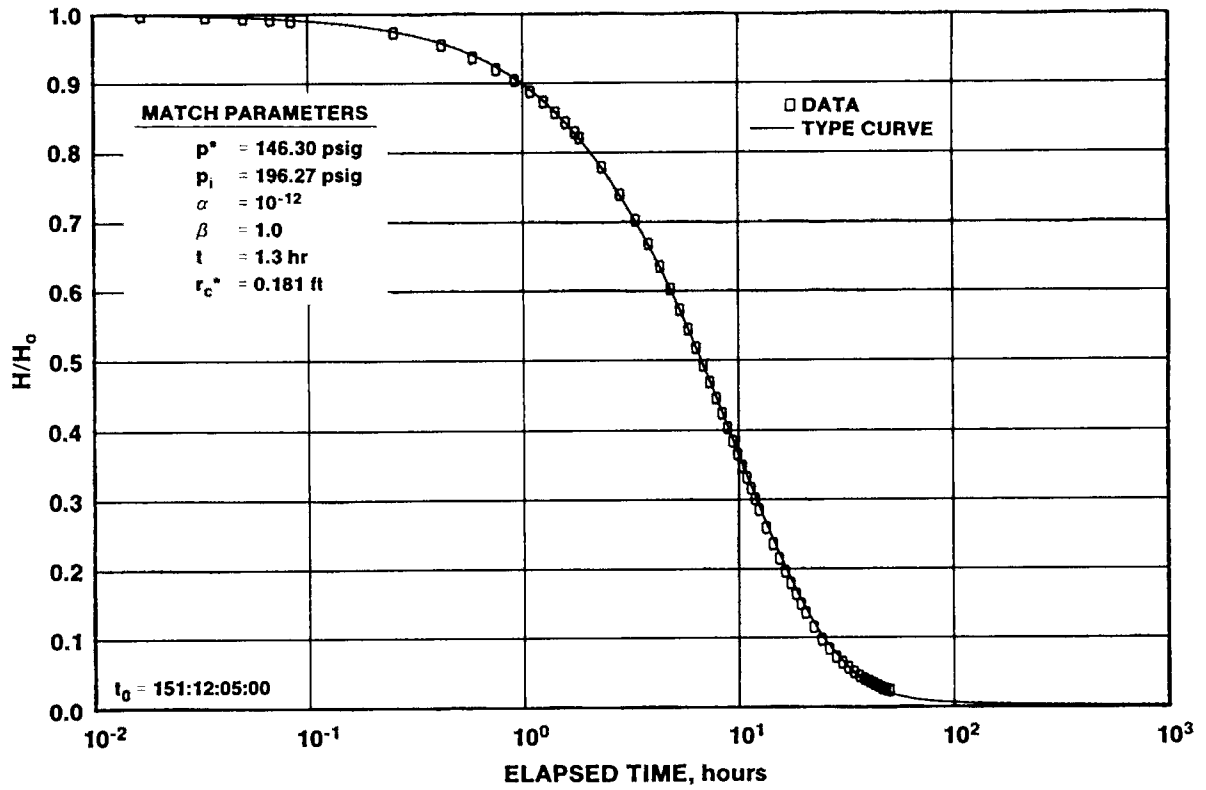
Figure 5-62. WIPP-19/Culebra Slug-Test Plot
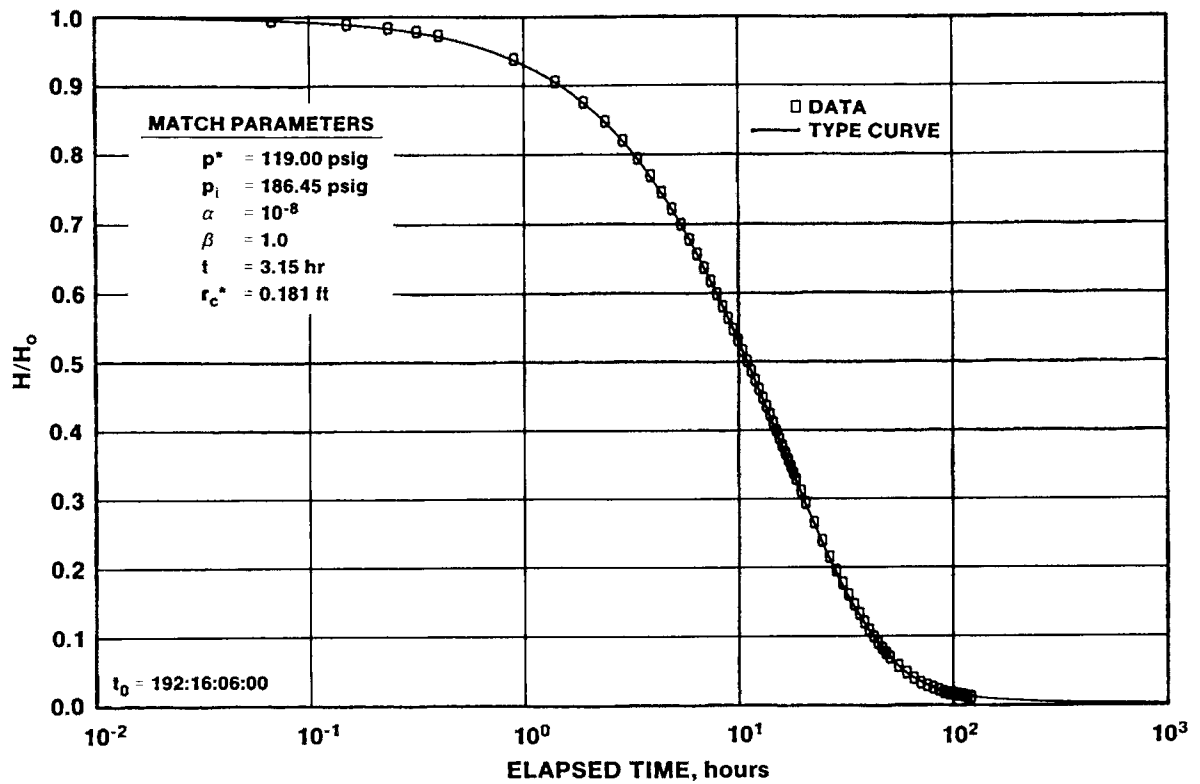
Figure 5-63. WIPP-21/Culebra Slug-Test Plot
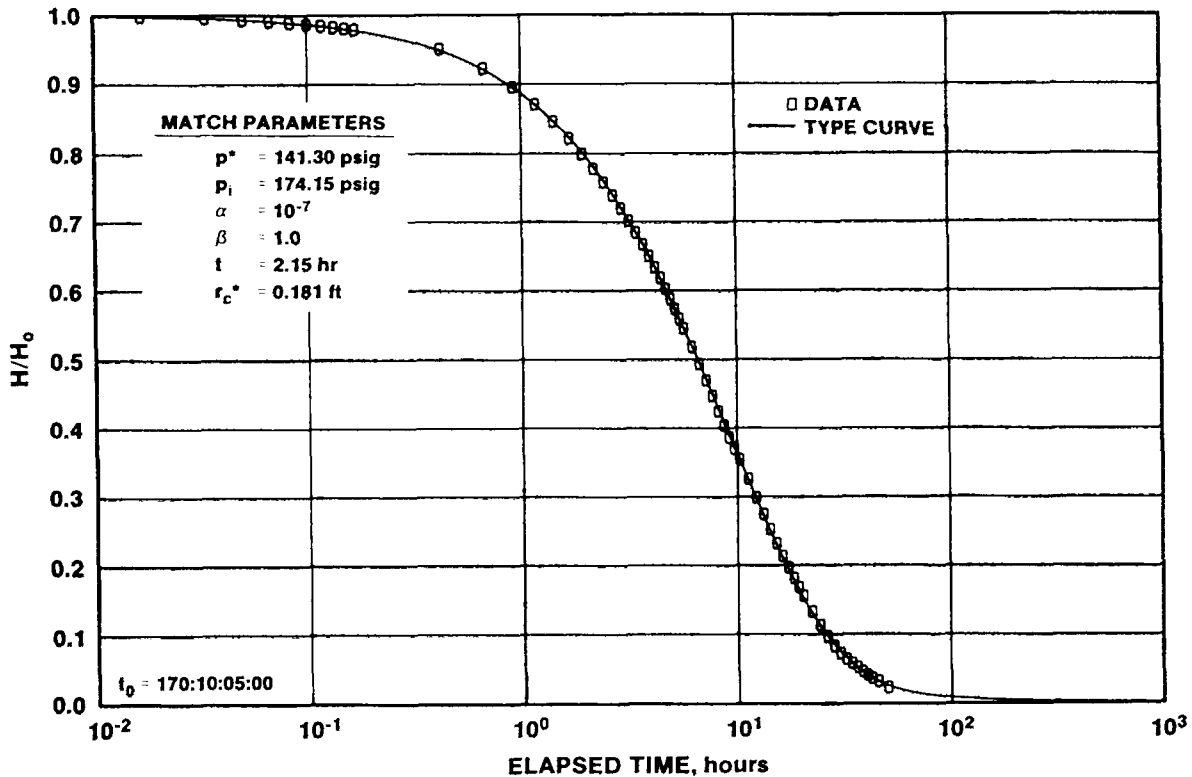
Figure 5-64. WIPP-22/Culebra Slug-Test Plot

Evaluation of the Culebra transmissivity at WIPP-30 was accomplished by performing two falling-head slug tests in December 1987. The fluid-pressure data collected during these tests will be presented in Stensrud et al. (in preparation). The first test was initiated on December 10, 1987, and lasted about 28 hr, by which time almost 99% of the induced pressure differential had dissipated. A semilog plot of the data from this test is shown in Figure 5-65, along with the best-fit type-curve match. This match provides a transmissivity estimate for the Culebra at WIPP-30 of 0.18 ft²/day (Table 5-3), 40% lower than the value reported by Mercer (1983).

The second test was initiated on December 15, 1987, and lasted about 52 hr, allowing >99% of the induced pressure differential to dissipate. Figure 5-66 shows a semilog plot of the data from this test, along with the best-fit type-curve match. This match is very similar to that obtained for the first test, and provides a transmissivity estimate of 0.17 ft²/day (Table 5-3).

The transmissivity values from both December 1987 tests are in fair agreement with the original value reported by Mercer (1983) and, most importantly, confirm the observation of low Culebra transmissivity at WIPP-30. Reconciliation of this low transmissivity with the absence of halite in the unnamed lower member at WIPP-30 is discussed in Section 6.1.

5.2.2.16 P-15. The transmissivity of the Culebra at P-15 was reported by Mercer (1983) to be 0.07 ft²/day based on a bailing test performed by the USGS in 1977 (Mercer and Orr, 1979). Because this value is significantly lower than the transmissivity of 0.9 ft²/day reported by Mercer (1983) for H-4b, the nearest other well, and because of limited well development before the bailing test, well development and retesting were performed in early 1987. Fluid-pressure data collected during the well development and testing are reported in Stensrud et al. (1988).
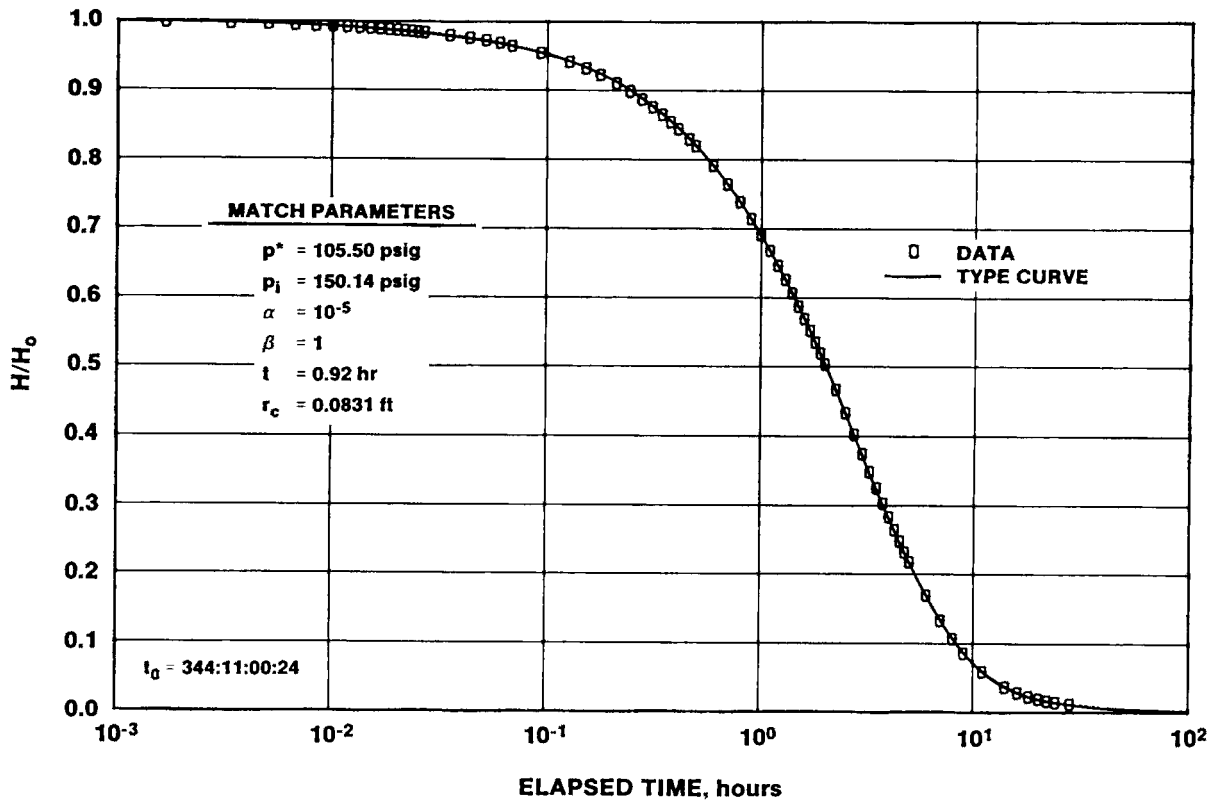
Figure 5-65. WIPP-30/Culebra Slug-Test #1 Plot

MATCH PARAMETERS

$p^* = 105.50$ psig
$p_i = 150.14$ psig
$\alpha = 10^{-5}$
$\beta = 1$
$t = 0.92$ hr
$r_c = 0.0831$ ft

$t_0 = 344:11:00:24$
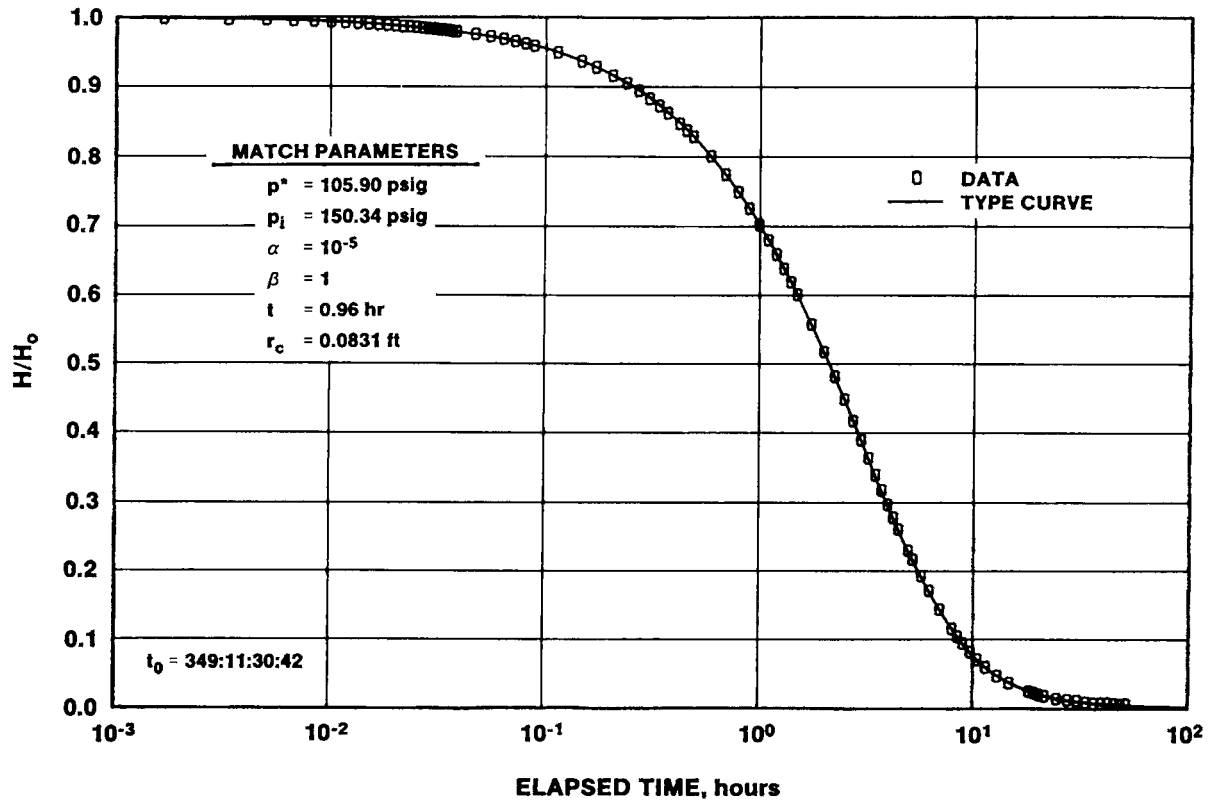
Figure 5-66. WIPP-30/Culebra Slug-Test #2 Plot

MATCH PARAMETERS

$p^* = 105.90$ psig
$p_i = 150.34$ psig
$\alpha = 10^{-5}$
$\beta = 1$
$t = 0.96$ hr
$r_c = 0.0831$ ft

$t_0 = 349:11:30:42$

P-15 was bailed on four occasions in March and April 1987 (Section 3.17) to develop the hydraulic connection between the perforated casing and the formation. In May 1987, two falling-head slug tests of the Culebra were performed. The first was initiated on May 16, and the second began on May 19. A semilog plot of the data from the first test is presented in Figure 5-67, along with the best-fit type-curve match. This match provides a transmissivity estimate of 0.090 ft²/day (Table 5-3). The semilog plot of the data from the second test (Figure 5-68) shows a fit to the same type curve, but with a slightly different time match. The transmissivity estimate from this match is 0.092 ft²/day (Table 5-3). These values are in excellent agreement, and are only slightly higher than the transmissivity value of 0.07 ft²/day reported by Mercer (1983) for the Culebra at P-15.

5.2.2.17 P–17. Mercer (1983) reported the transmissivity of the Culebra at P-17 to be 1.0 ft²/day, based on a slug test conducted by the USGS. P-17 was retested in November 1986 after the hydraulic head and fluid density of the Culebra at that location proved difficult to simulate with the existing data in an areal modeling exercise (Haug et al., 1987).

To verify the transmissivity of the Culebra at P-17, two falling-head slug tests were performed. The first test was initiated on November 20, 1986, and lasted nearly 22 hr, by which time 99% of the induced pressure differential had dissipated. Figure 5-69 shows a semilog plot of the falling-head slug-test data, along with the best-fit type curve. This fit provides a transmissivity estimate of 1.0 ft²/day (Table 5-3), which is the same value reported by Mercer (1983). The second test was begun on November 24, 1986, and lasted about 19 hr. A semilog plot of the data from the second test and the best-fit type-curve match are shown in Figure 5-70. The type-curve match for the second test is very similar to that used for the first test, and provides a second transmissivity estimate of 1.0 ft²/day (Table 5-3). The slight difference between the test data and the type curve at early time is probably due to the packer used in the test (Figure 3-19) continuing to deflate, and thus changing the wellbore volume, during the first few minutes of the test. The

fluid-pressure data collected during the P-17 slug tests are reported in Stensrud et al. (1987).

5.2.2.18 P–18. Mercer (1983) reported the transmissivity of the Culebra at P-18 to be 0.001 ft²/day based on a bailing test conducted by the USGS in 1977 (Mercer and Orr, 1979). This estimate of transmissivity was uncertain, however, because of the low degree of recovery obtained during the test. To evaluate the possibility that the low apparent transmissivity might be related to a poor hydraulic connection between the well and the formation, the Culebra interval in P-18 was reperforated (Section 3.18), a PIP was set in the well on 2.375-inch tubing to decrease the wellbore volume in communication with the Culebra, the tubing was bailed on two occasions to develop the well, and a rising-head slug test was performed.

The tubing was bailed for the last time on August 26, 1987, lowering the Culebra water level from about 543 ft to about 842 ft deep (Stensrud et al., 1988). On September 10, 1987, the water level had recovered to a depth of about 734 ft, and a minipacker with a feedthrough plug and attached pressure transducer was installed and inflated in the tubing at a depth of about 781 ft (Figure 3-20). The fluid-pressure buildup beneath the minipacker in response to the bailing was monitored with a transducer until November 6, 1987, by which time the pressure recovery had slowed to an erratic rate of about 0.1 psi/day. A rising-head slug test was initiated on November 6, 1987 by deflating the minipacker and removing it from the tubing, after which the rise in the P-18 water level was monitored for several months. The fluid-pressure and water-level data collected during the development and testing of P-18 will be reported in Stensrud et al. (in preparation).

The pretest stabilized formation pressure and the initial slug-test pressure at P-18 were measured by the transducer attached to the feedthrough plug in the minipacker in the tubing. These pressures were converted to water levels to allow interpretation of the water levels measured during the slug test. When the tubing was bailed on August 26, 1987, the fluid removed had a specific gravity of about 1.05.
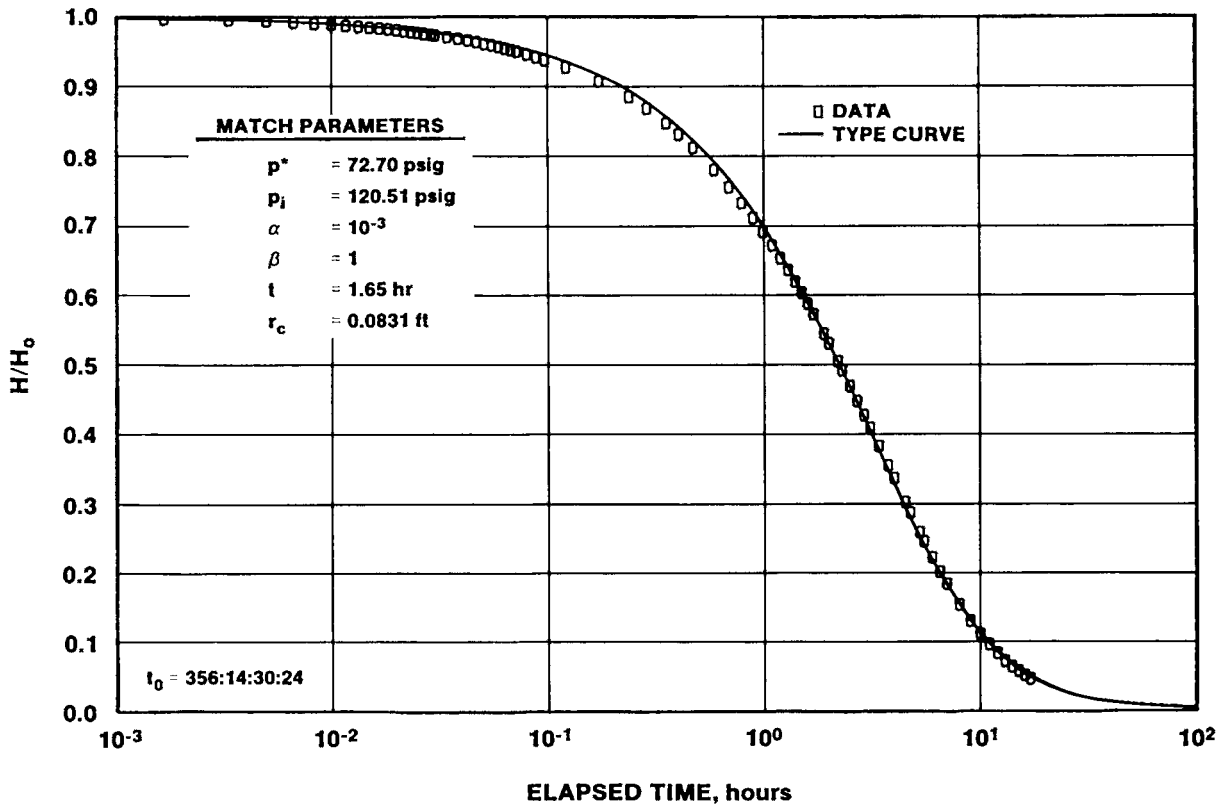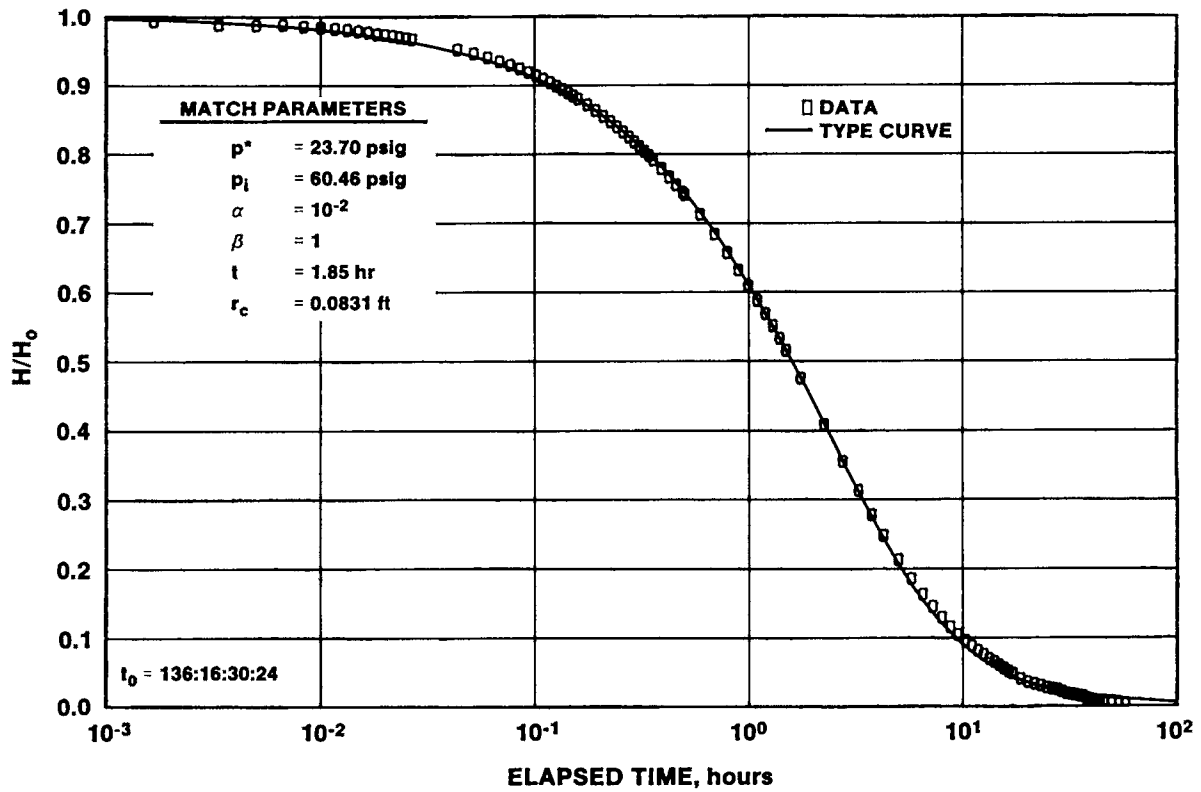
Figure 5-67. P-15/Culebra Slug-Test #1 Plot
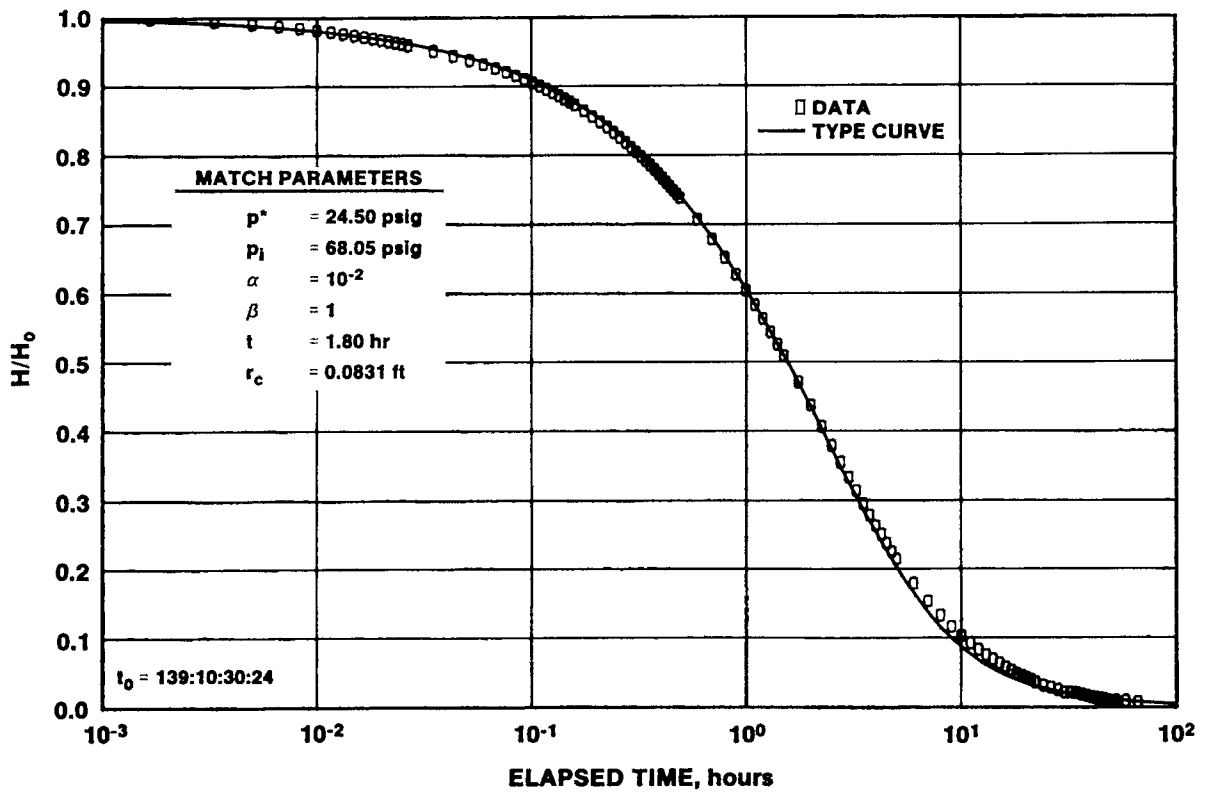
Figure 5-68. P-15/Culebra Slug-Test #2 Plot

97
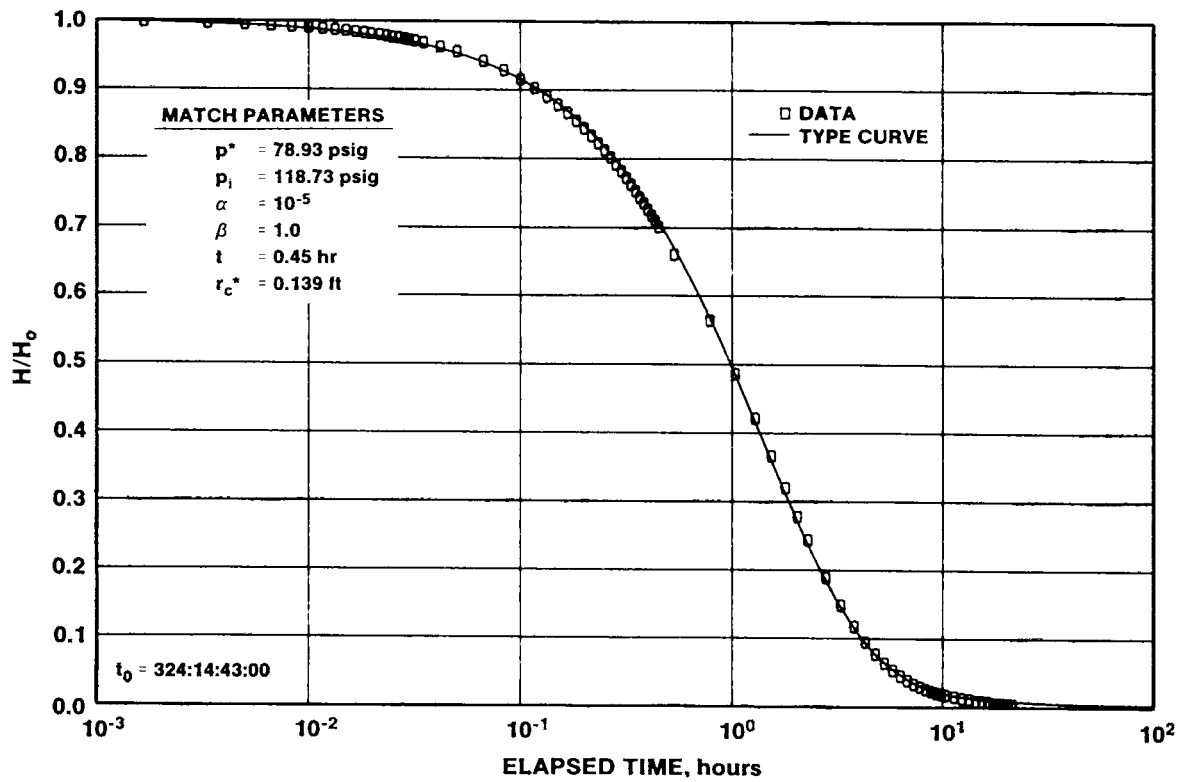
Figure 5-69. P-17/Culebra Slug-Test #1 Plot
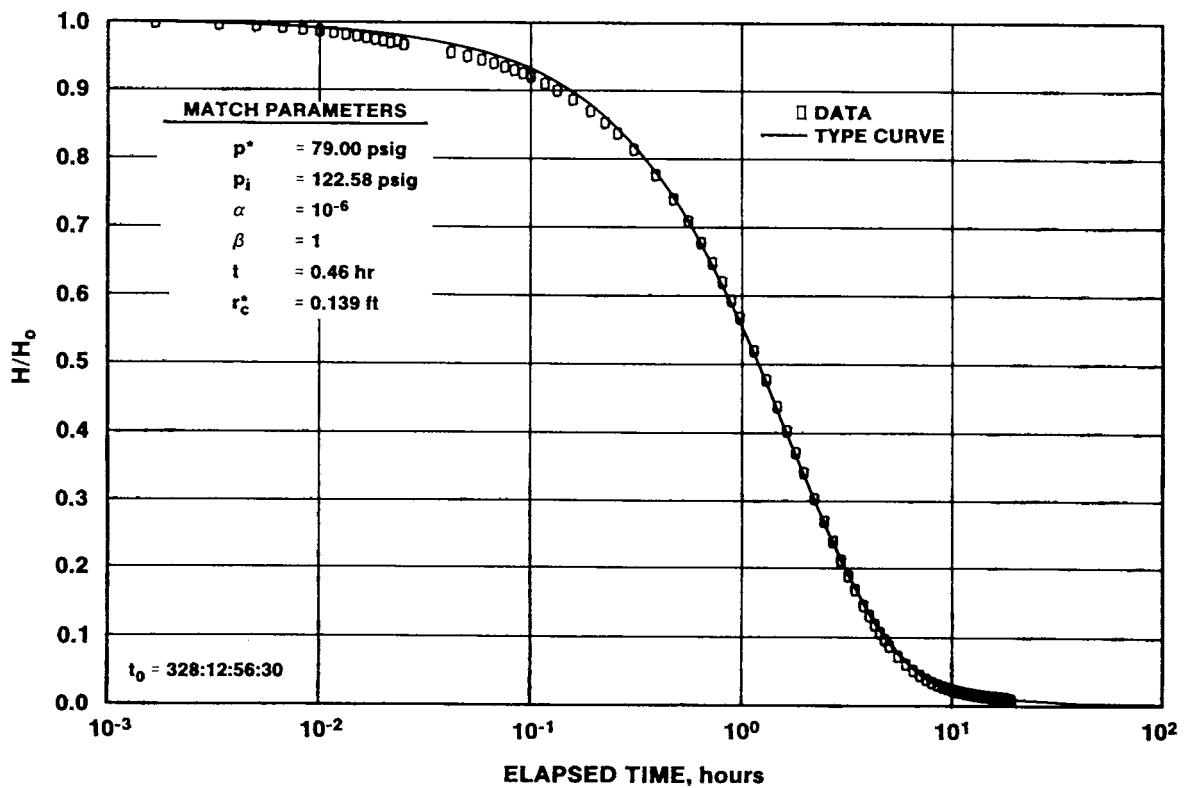
Figure 5-70. P-17/Culebra Slug-Test #2 Plot

Just before the minipacker was deflated on November 6, 1987, the transducer, located at a depth of 778.22 ft, measured a pressure of 110.9 psig. After the packer was deflated and just before it was removed from the tubing, the pressure was 43.15 psig. If the water above the transducer had a specific gravity of 1.05, a pressure of 43.15 psig would correspond to a water level about 683.4 ft deep. The first water-level measurement made after the minipacker was removed, however, showed a depth to water of 690.2 ft. Extrapolation of the first few water-level measurements back to the time when the minipacker was deflated indicate that the initial water level was probably about 690.9 ft deep. This extrapolation indicates that either the water in the tubing had a specific gravity of 1.14, or that the transducer was actually about 7.5 ft deeper than was thought. Because greater confidence was placed in the specific-gravity measurements made when the tubing was last bailed than in the transducer-depth measurement, the recorded transducer depth was assumed to be incorrect. With the transducer 7.5 ft

deeper, the pre-test "static" pressure of 110.9 psig would correspond to a depth to water of about 542.0 ft. Accordingly, an initial depth to water of (DTW_i) 690.9 ft and a static depth to water (DTW^*) of 542.0 ft were used in interpreting the P-18 slug test.

Figure 5-71 shows a semilog plot of the P-18 slug-test data. The most notable feature of the plot is a change in the slope of the data beginning about 600 hr after the test was initiated. Initially, the water level was rising relatively rapidly, as shown by the steep slope of the data in Figure 5-71. After 600 hr, however, recovery slowed and the slope of the data changed abruptly. The reason for the change in slope is unclear. This type of change would not occur if the Culebra were behaving hydraulically as an infinite, homogeneous medium on the scale of the test. The fact that the change did occur may indicate that the transmissivity of the Culebra near P-18 is not constant even over the small volume stressed by the slug test.
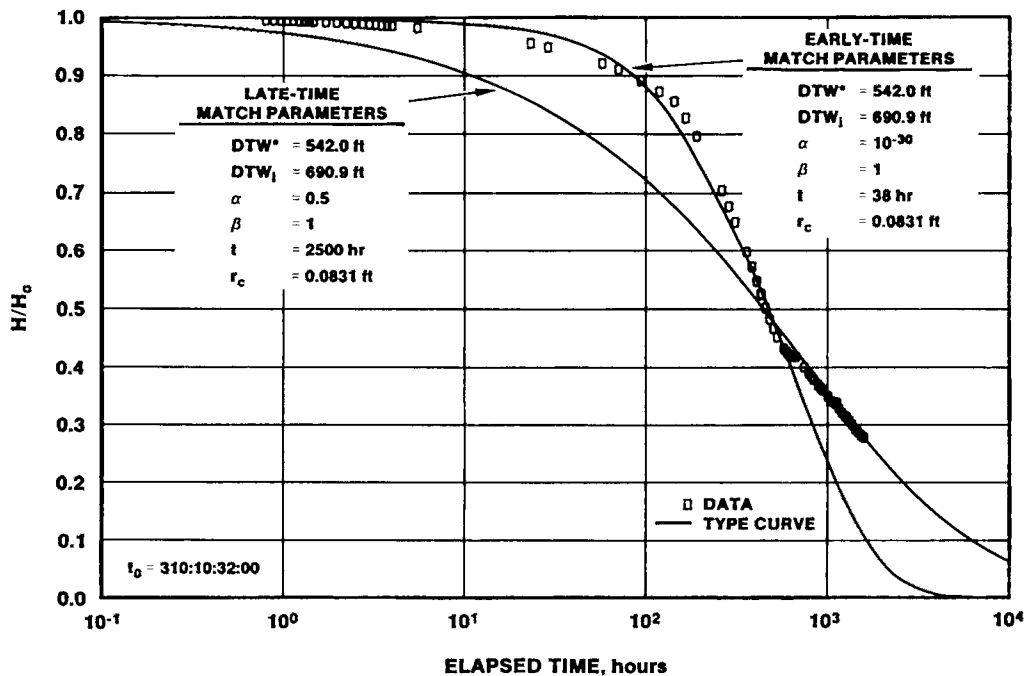
Figure 5-71. P-18/Culebra Slug-Test Plot

Two type-curve matches are shown with the test data on Figure 5-71. The early-time data were best fit by a type curve characteristic of damaged (i.e., having a positive skin) wells, whereas the late-time data were best fit by a type curve characteristic of undamaged (i.e., having a neutral or no skin) wells. The two type-curve matches also provide contrasting transmissivity estimates. The transmissivity derived from the early-time match is about 4 x 10-3 ft²/day, while that from the late-time match is about 7 x 10-5 ft²/day (Table 5-3). These observations indicate that the P-18 wellbore may be poorly connected hydraulically to a small portion of the Culebra having a higher transmissivity than more-distant portions. The contrast between the transmissivity of the Culebra and that of the well "skin" may decrease as the transmissivity of the Culebra decreases with distance from P-18, resulting in the neutral skin shown by the late-time data. The fact that the slope of the data on Figure 5-71 changes abruptly as opposed to smoothly appears to indicate that the change in transmissivity is discrete rather than gradational. Drilling of the borehole may have caused minor fracturing of the formation around the hole, which may have led to a slightly enhanced transmissivity in the immediate vicinity of the hole. Casing, cementing, and perforation may have resulted in a poor connection between the wellbore and the surrounding formation, resulting in the positive skin observed.

Given the peculiarities in the response to the P-18 slug test and the uncertainties as to their cause, the transmissivity of the Culebra at P-18 remains poorly defined. The estimate provided by the early-time type-curve match does not appear to be valid beyond the immediate vicinity (a few feet?) of the well. The transmissivity estimate provided by the late-time type-curve match may not be quantitatively reliable because the time match between the data and the type curve, which defines the transmissivity, would probably be greater, thus indicating a lower transmissivity, if the hydraulic response of the Culebra had been more consistent (i.e., homogeneous). In summary, the transmissivity estimate from the early-time data, 4 x 10-3 ft²/day, is probably unrealistically high, but is reliably a maximum value. The estimate from the late-time data, 7 x 10-5 ft²/day, is probably more representative of the Culebra in the vicinity of P-18, but cannot be interpreted as a minimum value.

5.2.2.19 ERDA-9. Two falling-head slug tests were performed in November 1986 to evaluate the transmissivity of the Culebra at ERDA-9. The first was initiated on November 20, 1986. The test lasted about 18 hr, by which time over 99% of the induced pressure differential had dissipated. Figure 5-72 is a semilog plot of the slug-test data, along with the best-fit type curve. This fit provides a transmissivity estimate of 0.45 ft²/day for the Culebra at ERDA-9 (Table 5-3). The second test began on November 24, 1986, and lasted about 16 hr. A semilog plot of the data from this test is presented in Figure 5-73, along with the best-fit type-curve match. This match is very similar to that used to fit the data from the first test, and provides a similar transmissivity estimate of 0.47 ft²/day (Table 5-3). The data from these tests are reported in Stensrud et al. (1987).

5.2.2.20 Cabin Baby-1. Two falling-head slug tests were performed at Cabin Baby-1 to evaluate the transmissivity of the Culebra at that location. The first test was initiated on March 10, 1987 and the second was initiated on March 12, 1987. Complete dissipation of the induced pressure differential was achieved during the first test, and about 99% dissipation during the second. The data from these tests are presented in Stensrud et al. (1987). Figure 5-74 is a semilog plot of the data from the first test, along with the best-fit type curve. This fit provides a transmissivity estimate of 0.28 ft²/day for the Culebra at Cabin Baby-1 (Table 5-3). The semilog plot of the data from the second test (Figure 5-75) shows an identical type-curve match with a slightly better overall fit, leading to a second transmissivity estimate of 0.28 ft²/day (Table 5-3).

5.2.2.21 DOE-1. After an 8-hr step-drawdown test of the Culebra conducted at DOE-1 on May 3, 1983 indicated that the productivity of the well was much higher than previously believed, a 440-hr pumping test was conducted beginning on May 6, 1983. The average pumping rate during the test was 9.93 gpm. After the pump was turned off, pressure recovery in the well was monitored for nearly 422 hr. The fluid-
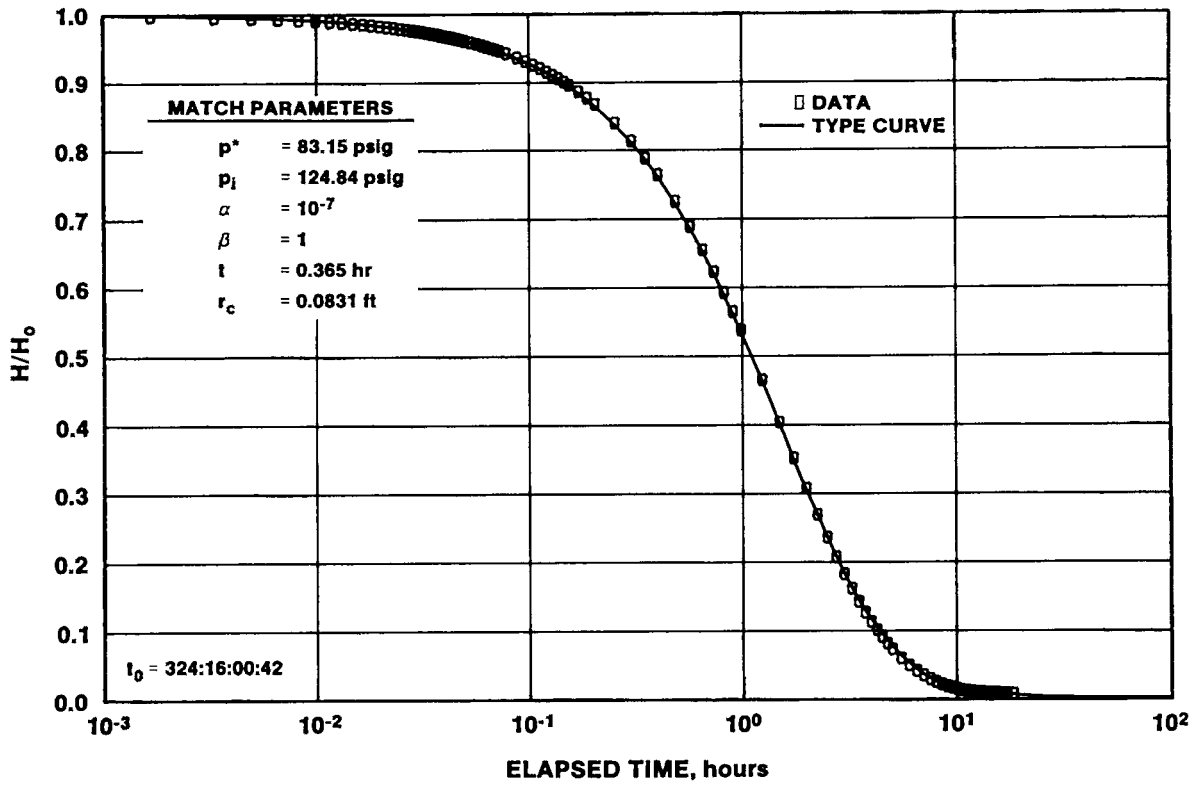
Figure 5-72. ERDA-9/Culebra Slug-Test #1 Plot
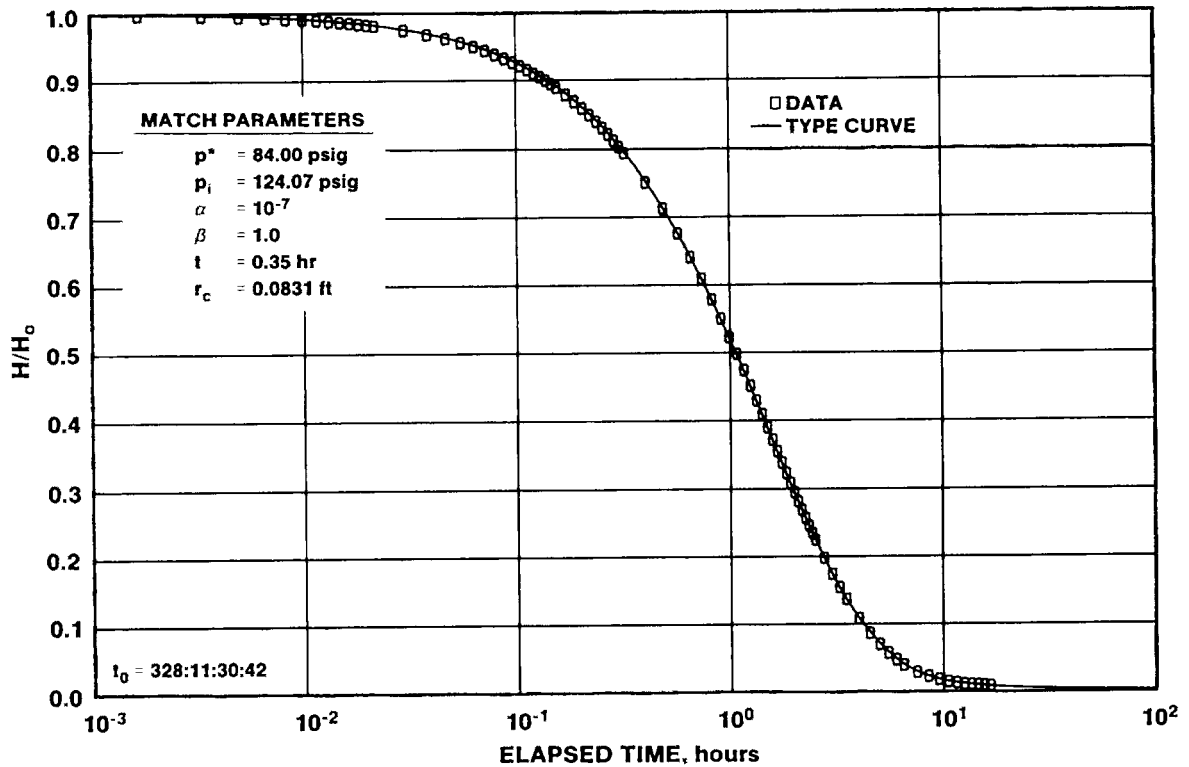
Figure 5-73. ERDA-9/Culebra Slug-Test #2 Plot

MATCH PARAMETERS

p^*	= 54.60 psig
p_i	= 87.08 psig
α	= 10^{-2}
β	= 1
t	= 0.60 hr
r_c	= 0.0831 ft

□ DATA
— TYPE CURVE

t_0 = 69:15:00:54
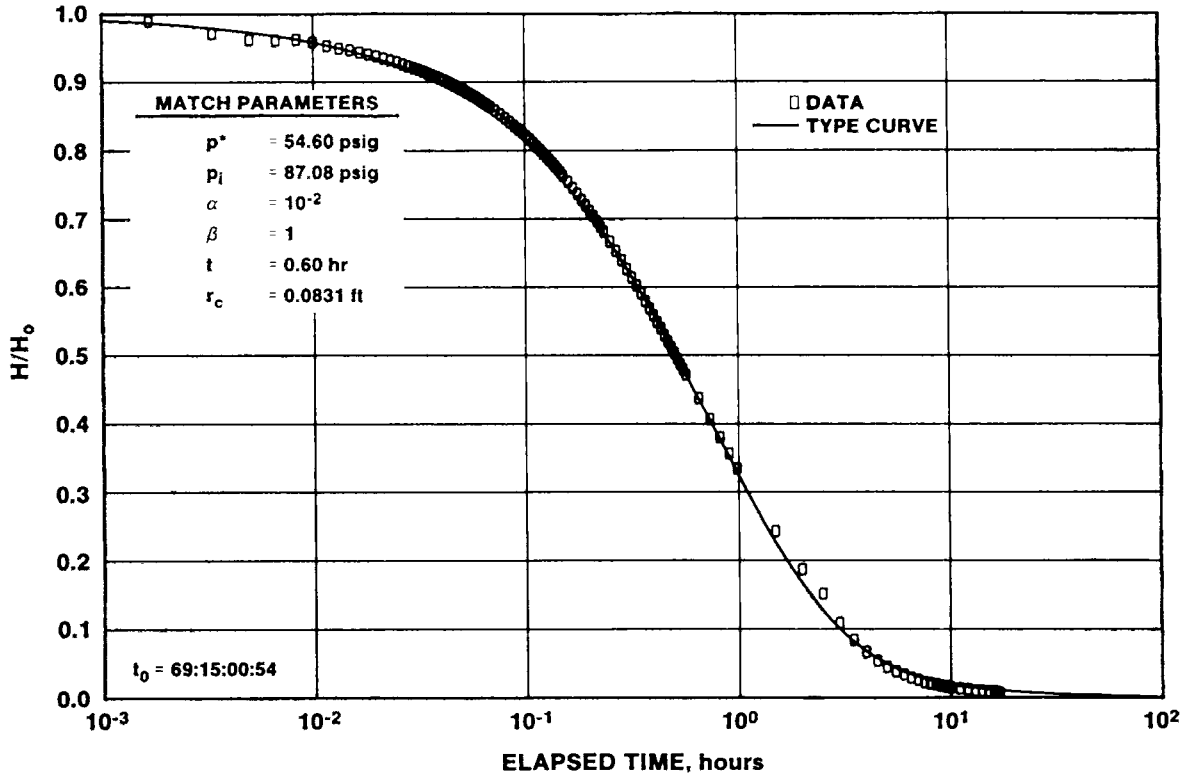
Figure 5-74. Cabin Baby-1/Culebra Slug-Test #1 Plot

MATCH PARAMETERS

p^*	= 54.30 psig
p_i	= 86.66 psig
α	= 10^{-2}
β	= 1.0
t	= 0.6 hr
r_c	= 0.0831 ft

□ DATA
— TYPE CURVE

t_0 = 71:09:00:48
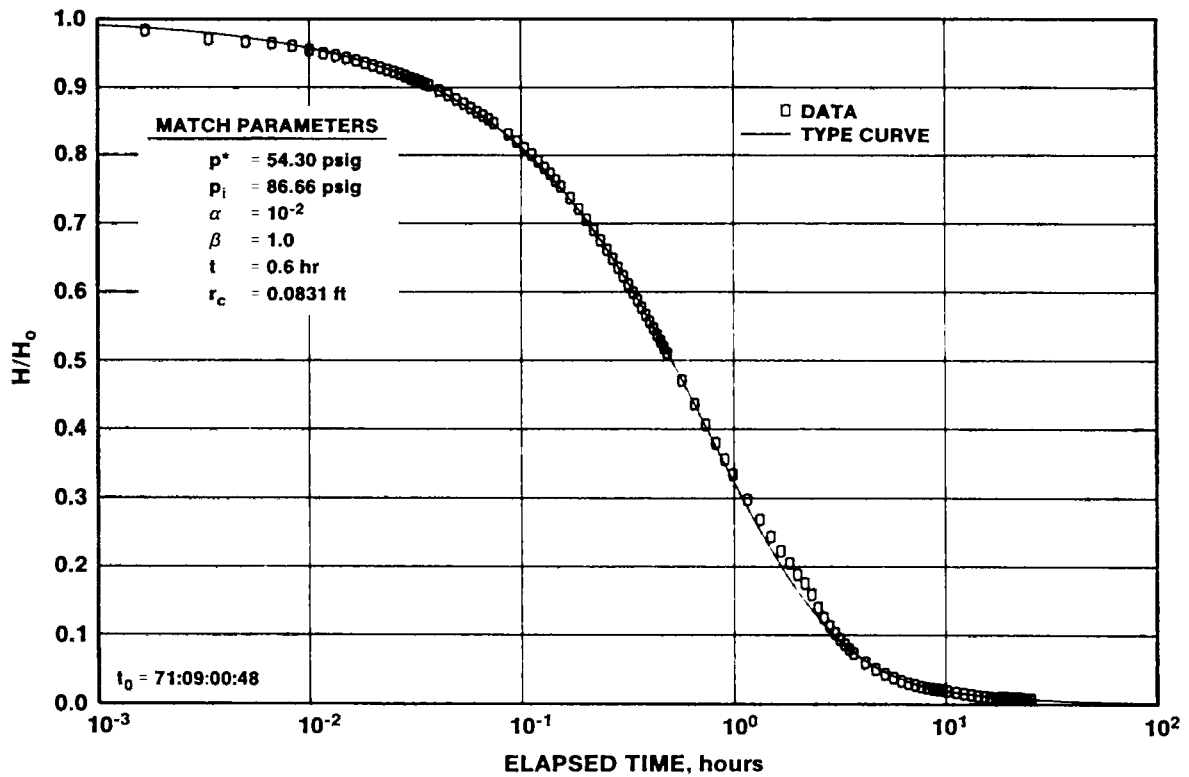
Figure 5-75. Cabin Baby-1/Culebra Slug-Test #2 Plot

pressure data recorded from downhole transducers during the pumping and recovery portions of this test are reported in HydroGeoChem (1985).

The fluid-pressure responses of DOE-1 during the drawdown and recovery periods were very different. The shape of the drawdown-data curve on a log-log plot (Figure 5-76) is indicative of a well intersecting a single, high-conductivity fracture, with multiple no-flow boundary effects evident at late time. The log-log plot of the recovery data (Figure 5-77), on the other hand, shows a clear double-porosity response with no indications of hydraulic boundaries.

The log-log drawdown plot (Figure 5-76) includes a simulation generated by INTERPRET for a well intersected by a single high-conductivity fracture. The transmissivity of the Culebra apart from the fracture is 28 ft²/day (Table 5-3) for this simulation. Assuming a porosity of 20%, a total-system compressibility of 1.0×10^{-5} psi^{-1}, and a fluid viscosity of 1.0 cp, the skin factor for this simulation is -5.1, a reasonable value for a well intersecting a fracture. The data match the simulation reasonably well for the first 13.5 hr, but then, starting with a discrete pressure drop caused by increasing the pumping rate from 9.1 to 10.3 gpm (HydroGeoChem, 1985), the data deviate above the simulation. This type of deviation is usually indicative of no-flow (or lower permeability) hydraulic boundaries. In this case, multiple boundaries are indicated by the amount of deviation from the simulation.

MATCH PARAMETERS

Δp = 1.0 psi
t = 1.0 hr
p_D = 0.21
t_D/C_D = 173
$C_D e^{2s}$ = 7.64 x 10^{-2}
p_i = 153.6 psig

□ PRESSURE DATA
* PRESSURE-DERIVATIVE DATA
—— SIMULATIONS
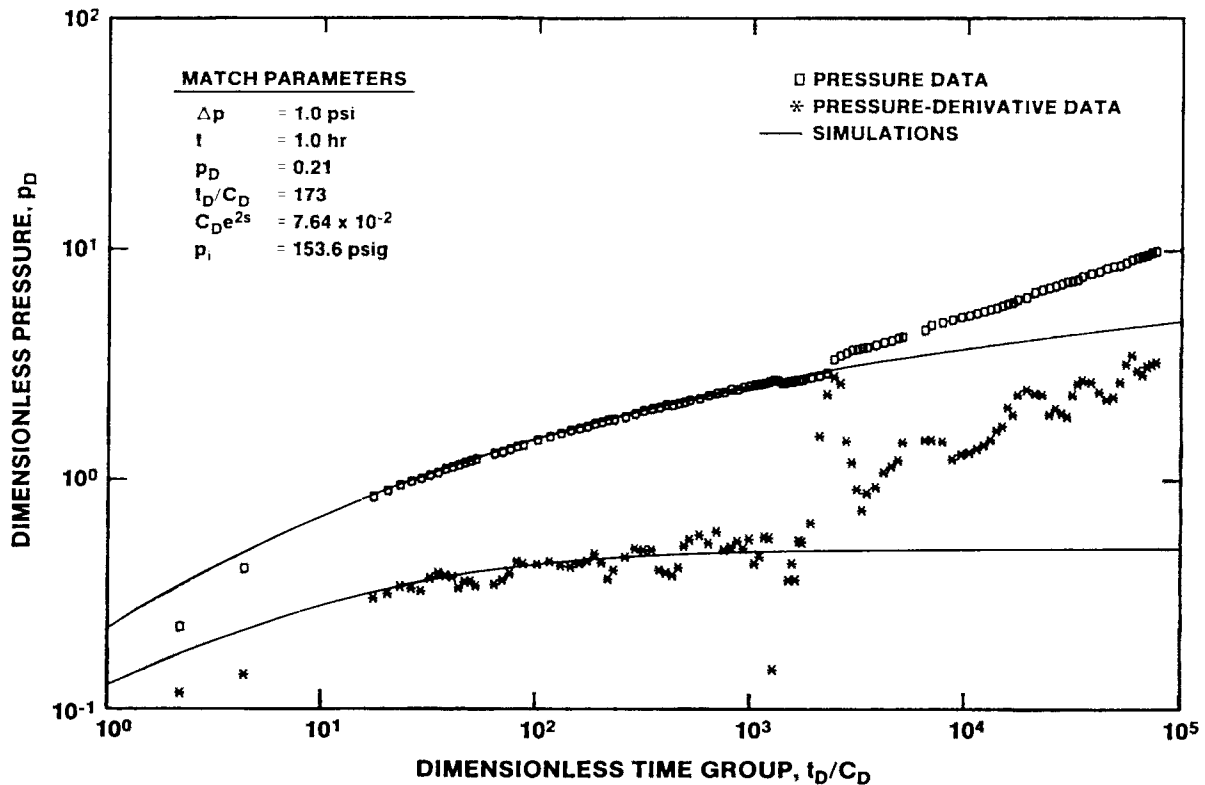
Figure 5-76. DOE-1/Culebra Pumping Test Drawdown Log-Log Plot with INTERPRET Simulation
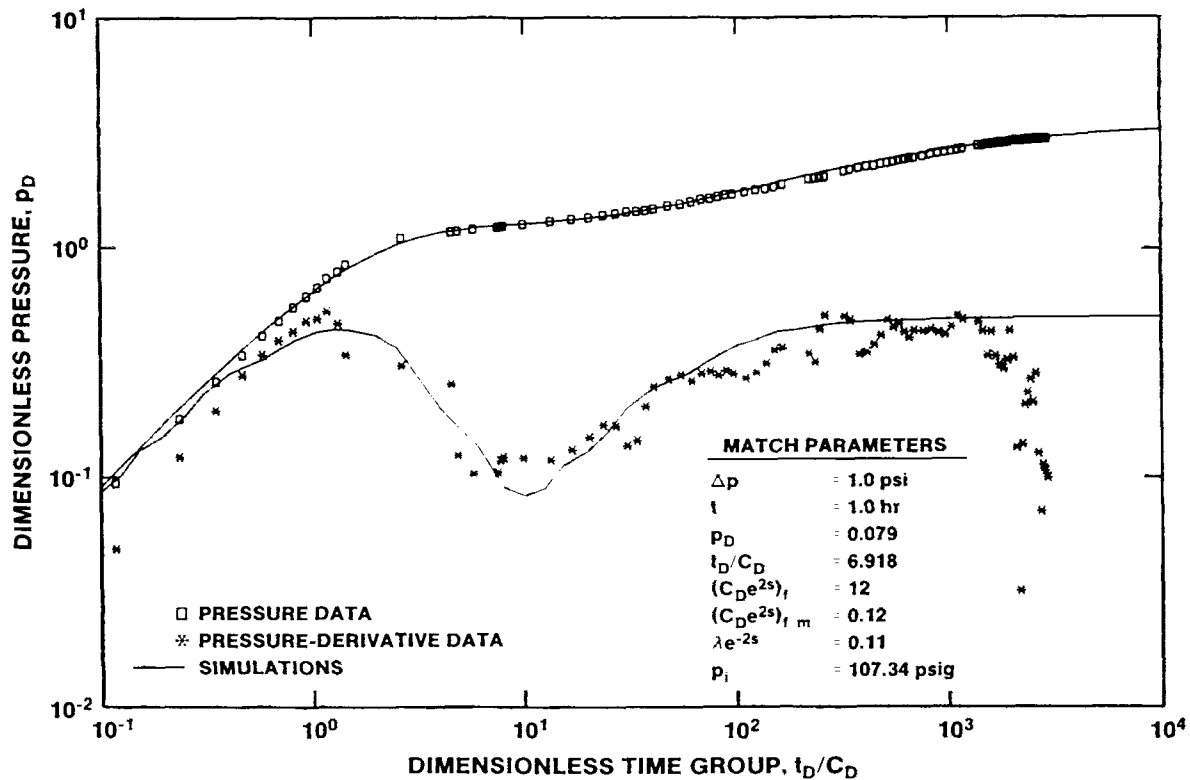
Figure 5-77. DOE-1/Culebra Pumping Test Recovery Log-Log Plot with INTERPRET Simulation

Several points are puzzling or inconsistent about this interpretation, however. First, the occurrence of a single fracture at this location seems inherently unlikely. Second, evidence from many tests in the Culebra (e.g., DOE-2, H-8b, H-11, WIPP-13) indicates that transmissivities greater than 1 or 2 ft²/day are related to extensive fracturing, and are not representative of intact Culebra. Third, the indications of hydraulic boundaries began at the same time that the flow rate was increased. Fourth, wellbore-storage effects in the pressure data (a unit slope on a log-log plot at early time) should be more evident than they are. A wellbore-storage coefficient of about 8.5 gal/psi can be calculated for DOE-1 based on the size of the casing and discharge line, and the specific gravity of the water being discharged. This high a wellbore-storage coefficient should cause observable effects. These effects are not seen, and the wellbore-storage coefficient obtained from the model used to generate the simulation is only 0.7 gal/psi. Finally, the recovery data show a completely different hydraulic behavior than the drawdown data.

The log-log recovery plot (Figure 5-77) includes a simulation generated by INTERPRET using a double-porosity model with restricted interporosity flow. The model uses a transmissivity of 11 ft²/day and a wellbore-storage coefficient of 6.8 gal/psi. The skin factor for this simulation, using the same parameter values used in the drawdown analysis presented above, is -6.0. The simulation fits the data very well, except for a sharp decline in the pressure-derivative data at extremely late time. This decline was caused by the rate of pressure recovery slowing significantly, as if an overpressure skin were present and dissipating. Why this decrease in the rate of recovery occurred is unknown, but it is the opposite of what would be expected if the no-flow boundaries indicated by the drawdown analysis were present.

Figure 5-78 shows a dimensionless Horner plot of the recovery data. The double-porosity simulation again matches the observed data very well. However, the static formation pressure (p*) specified for this simulation, 149.6 psig, is 4.0 psi lower than the pressure measured before the pump was turned

104

MATCH PARAMETERS

Δp	= 1.0 psi
t	= 1.0 hr
p_D	= 0.079
t_D/C_D	= 6.918
$(C_D e^{2s})_f$	= 12
$(C_D e^{2s})_{f-m}$	= 0.12
λe^{-2s}	= 0.11
p^*	= 149.6 psig

+ DATA
—— SIMULATION

$\frac{p_D}{\Delta p} \left[p^* - p(t) \right]$

DIMENSIONLESS SUPERPOSITION FUNCTION: FLOW PERIOD 2
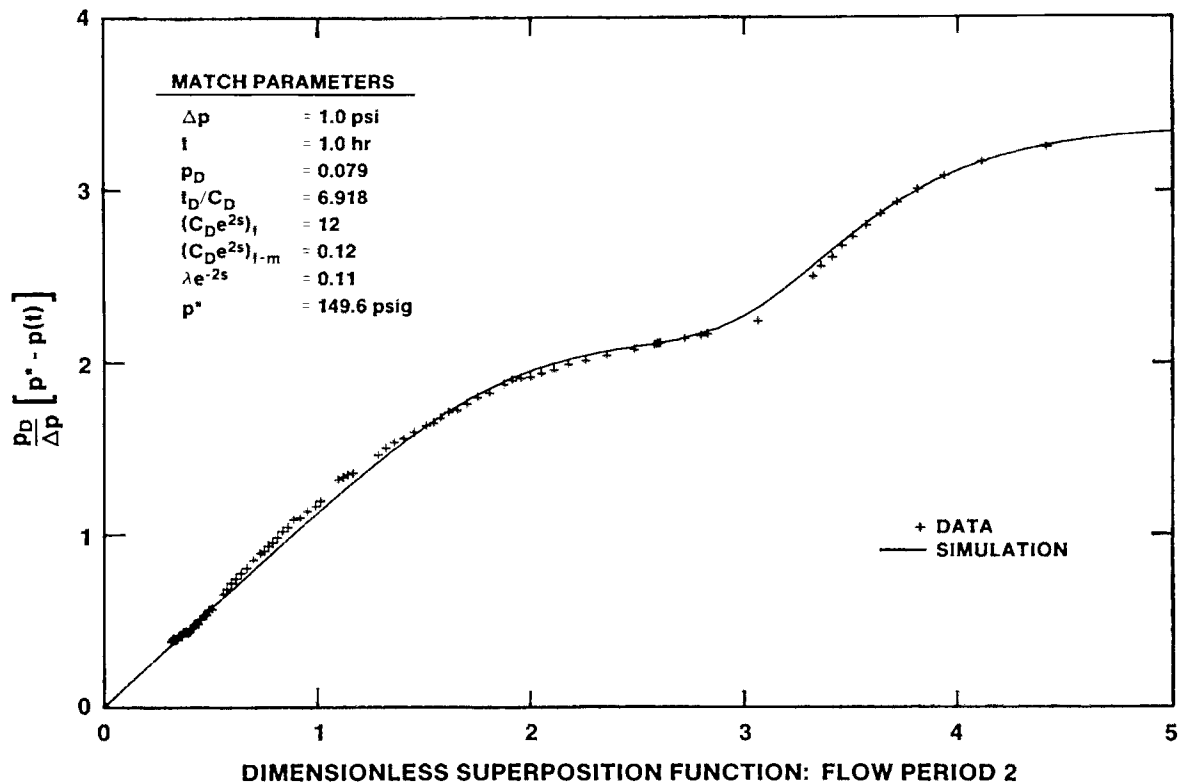
Figure 5-78. DOE-1/Culebra Pumping Test Recovery Dimensionless Horner Plot with INTERPRET Simulation

on. This difference between the observed and simulated static formation pressures may indicate that the Culebra pressure was not at equilibrium at the start of the test, and may be related to the observed late-time decline of the recovery pressure derivative.

Figure 5-79 shows a linear-linear plot of the entire DOE-1 testing sequence, along with a simulation of that sequence generated using the model derived from the recovery analysis. The shape of the simulation differs considerably from the drawdown data, but the simulation accurately predicts the total amount of drawdown (given that the simulation uses a starting pressure 4.0 psi lower than that measured). The simulation fits the recovery data quite well.

The overall hydraulic behavior of DOE-1 during the pumping test remains anomalous. One explanation for the discrepancy between the drawdown and recovery behavior is that the well may have been undergoing development during pumping, so that

the hydraulic properties governing the pressure response were changing as pumping progressed. The well-development activities performed during March and April 1983 preceded knowledge of the high Culebra transmissivity at DOE-1, and involved only bailing and low-volume pumping with a pump jack (see Section 3.21). The only high-volume pumping that occurred before the pumping test was an 8-hr step-drawdown test. These activities may have been inadequate to clean and develop the perforations in the well casing, and to clean the fractures in the Culebra that might have gotten plugged during drilling and cementing operations. The 440-hr pumping test should have done a much better job of well development. Once the pump was turned off, the hydraulic properties of the well and nearby aquifer probably stabilized, allowing the recovery data to show an unchanging double-porosity system. For this reason, the analysis of the recovery data is believed to provide the more representative understanding of the hydraulic behavior of the Culebra at DOE-1.

160

PUMP ON

MATCH PARAMETERS

Δp	1.0 psi
t	1.0 hr
p_D	0.079
$t_D C_D$	6.918
$(C_D e^{2s})_f$	12
$(C_D e^{2s})_{f,m}$	0.12
λe^{-2s}	0.11
p^*	149.6 psig

150

140

PRESSURE, psig

130

120

+ DATA
—— SIMULATION

110

PUMP OFF

t_0 = 5/6/83 10:00

100

0   200   400   600   800   1000

ELAPSED TIME, hours
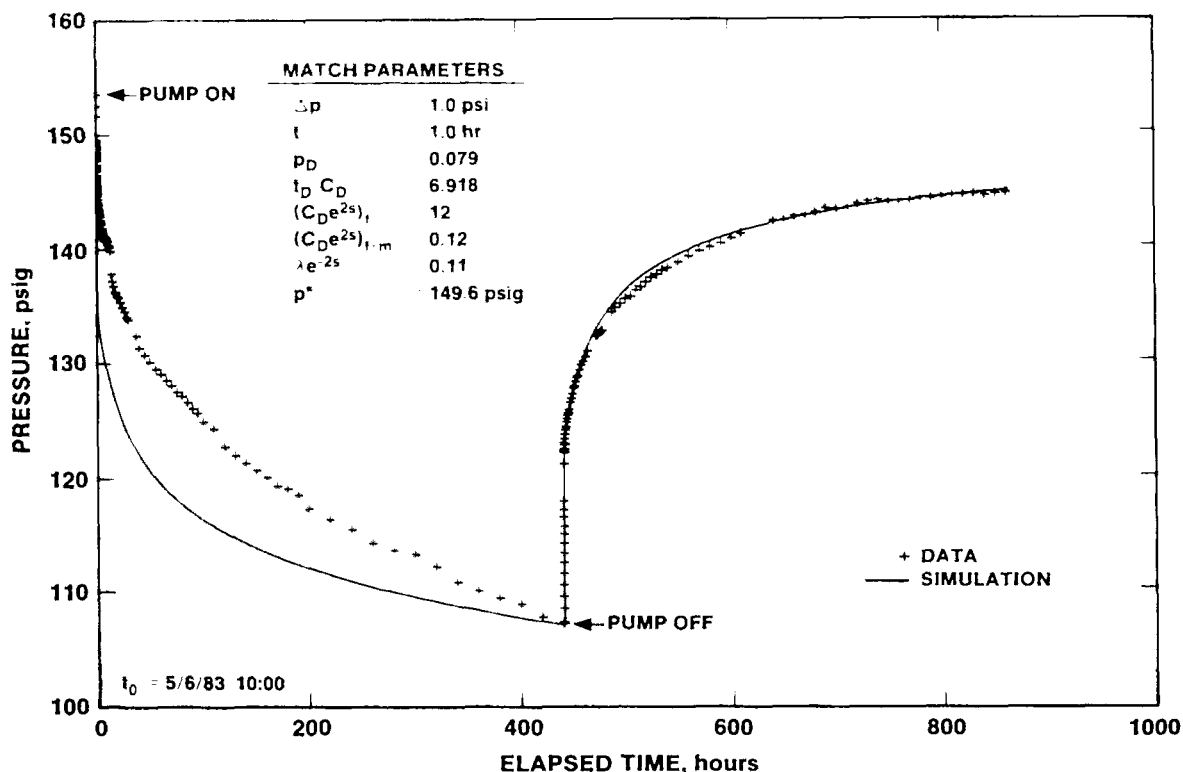
Figure 5-79. DOE-1/Culebra Pumping Test Linear-Linear Sequence Plot with INTERPRET Simulation

Drawdown responses probably related to the DOE-1 pumping were noted at wells H-3, H-1, P-17, and possibly H-4 during routine water-level monitoring. Because these responses were not anticipated, however, no pre-test baseline water-level monitoring had been performed at these wells. Consequently, the presence or absence of pre-existing water-level trends and water levels precisely at the beginning of DOE-1 pumping are not defined. In addition, well H-4c was being pumped for a tracer test during all phases of the DOE-1 pumping test, which may have influenced some of the water levels observed. Because of these uncertainties concerning the observed water-level data, the observation-well "responses" were not interpreted.

5.2.2.22 Engle. The Engle well was pumped for a period of 165.5 hr beginning November 4, 1983, to collect water-quality samples. The pumping rate was held at a nearly constant 9.8 gpm for approximately the first 97 hr of pumping. Pressure-drawdown data collected over this period are amenable to interpretation. Recovery data were collected for only

one hr after the pump was turned off, producing nothing useable for interpretation. A more complete description of this test and the test data are contained in Stensrud et al. (1987).

Figure 5-80 shows a log-log plot of the Engle drawdown data, along with simulations of the data generated by INTERPRET. Late-time scatter of the data, particularly of the pressure-derivative data, is probably related to pumping-rate fluctuations. The model used for the simulations is representative of a single-porosity medium with a transmissivity of 43 ft²/day (Table 5-3). Assuming a Culebra porosity of 20%, a total-system compressibility of 1.0 x 10-5 psi-1, and a fluid viscosity of 1.0 cp, the skin factor for this simulation is about 4.2. A dimensionless Horner plot of the drawdown data, along with a simulation generated using the same model, is shown in Figure 5-81. Again, the simulation matches the test data well until the data scatter at late time, indicating that an appropriate model was selected.

106
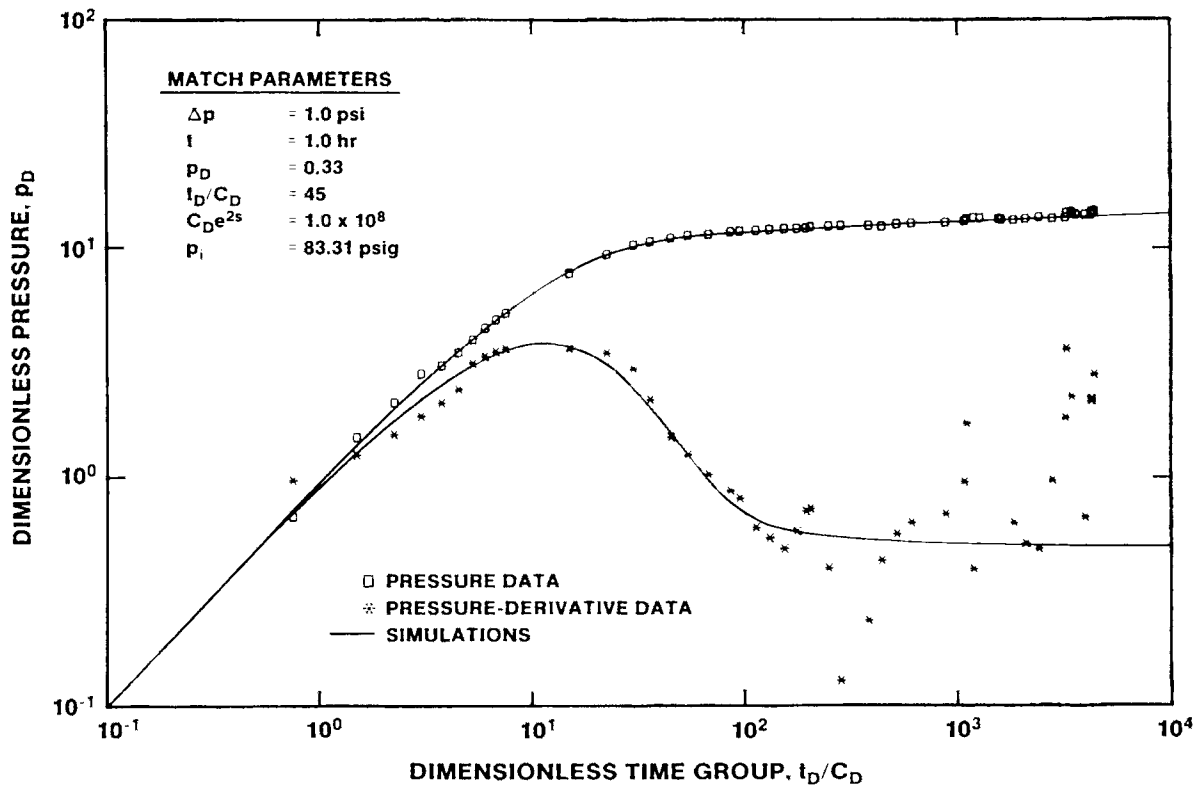
Figure 5-80. Engle/Culebra Pumping Test Drawdown Log-Log Plot with INTERPRET Simulation
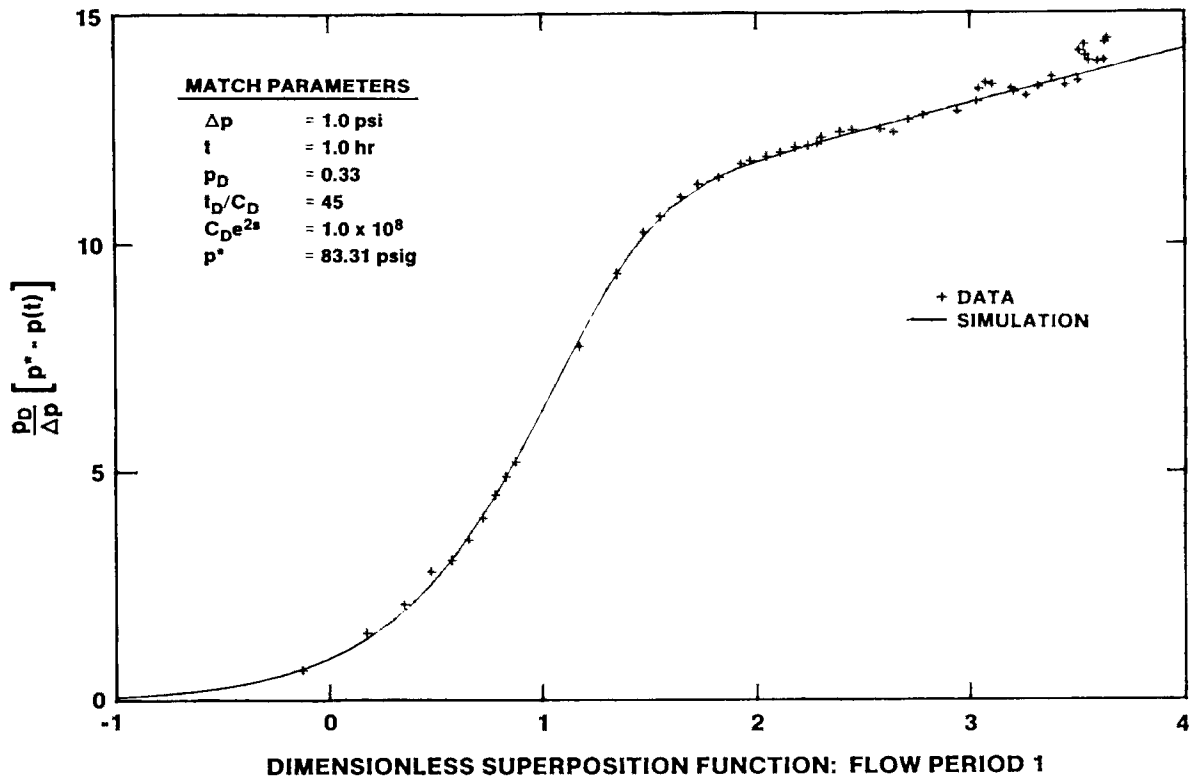
Figure 5-81. Engle/Culebra Pumping Test Drawdown Dimensionless Horner Plot with INTERPRET Simulation

Considering that all other pumping tests at wells where the Culebra has a transmissivity greater than about 1 ft²/day have shown double-porosity effects and negative skins caused by fracturing (e.g., DOE-1, DOE-2, H-3, H-8, H-11, WIPP-13), the relatively high transmissivity, positive skin, and single-porosity behavior indicated for the Engle well appear anomalous. One possible explanation for this apparent anomaly is that although the well has been pumped for years by a windmill, the low-volume windmill pump may never have stressed the aquifer enough to develop the well properly, i.e., to clean out the fractures. The positive skin factor obtained from this test provides an indication of wellbore damage consistent with this argument. DOE-2 provides an example, albeit extreme, of this phenomenon. Until it was acidized and developed, hydraulic responses to testing at DOE-2 showed only single-porosity behavior with a positive skin (Beauheim, 1986). While Engle does not display the extreme conditions shown by DOE-2 before acidization, its apparent single-porosity behavior and positive skin may, nevertheless, be related more to wellbore and near-wellbore conditions than to the true nature of the Culebra at this location.

5.2.3 Tamarisk Member. The Tamarisk Member of the Rustler Formation was tested in wells H-14 and H-16. The purposes of the Tamarisk testing were to: 1) define the hydraulic head of the unit; and 2) measure the transmissivity of the unit. Information on the hydraulic head of the Tamarisk is needed to evaluate potential directions of vertical movement of groundwater between the Rustler members. The transmissivity of the Tamarisk is a parameter needed for vertical cross-sectional or three-dimensional modeling of groundwater flow in the Rustler. The claystone/mudstone/siltstone portion of the Tamarisk (referred to hereafter simply as the claystone) is believed to be more permeable than the anhydrite/gypsum sections, and therefore easier to test. Consequently, tests were attempted only on the claystone portion of the Tamarisk at H-14 and H-16.

5.2.3.1 H–14. At H-14, the Tamarisk claystone extends from about 517 to 525 ft deep (Figure 3-6). The initial test was performed over an interval from the base of a packer at a depth of 494.5 ft to the then-

bottom of the hole 533 ft deep. Thus, the test interval included the 8-ft thickness of claystone, and 30.5 ft of overlying and underlying anhydrite and gypsum. Descriptions of the test instrumentation and the test data are contained in Stensrud et al. (1987).

Testing began on October 7, 1986, by setting the packer, swabbing the tubing to decrease the pressure in the test interval, and closing the shut-in tool to isolate the test interval and allow the test-interval pressure to recover and equilibrate at the existing static formation pressure. The pressure response observed during the testing is shown in Figure 5-82. After being shut in for nearly 37 hr, the fluid pressure in the Tamarisk claystone test interval had still not stabilized, but was rising at an ever-decreasing rate. The pressure in the wellbore above the packer, in contrast, was dropping as fluid was apparently entering the exposed Magenta and Forty-niner Members. Because the Tamarisk pressure had not stabilized, and did not appear likely to stabilize for several days or weeks, no drillstem tests were performed.

To verify that the observed response during the shut-in period was representative of the Tamarisk claystone and not caused by a tool malfunction, the packer was deflated and the DST tool was reset 8 ft deeper in the hole on October 9, 1986. After swabbing and shutting in the new test interval, a pressure buildup similar to that observed at the previous depth was measured for 4.5 hr (Figure 5-82). At this point, we concluded that the permeability of the Tamarisk at H-14 is too low to allow testing on the time scale of a few days, and abandoned the effort.

No conclusions about the static formation pressure of the Tamarisk can be drawn from the observed pressure buildups, because we have no way of evaluating the role played by the overpressure skin that was probably created during drilling. Subsequent testing of the Magenta and Forty-niner Members, discussed below, revealed fluid-pressure buildups to be significantly affected by overpressure skins.

5.2.3.2 H–16. At H-16, the Tamarisk claystone extends from 677.5 to 690.1 ft deep (Figure 3-8). The
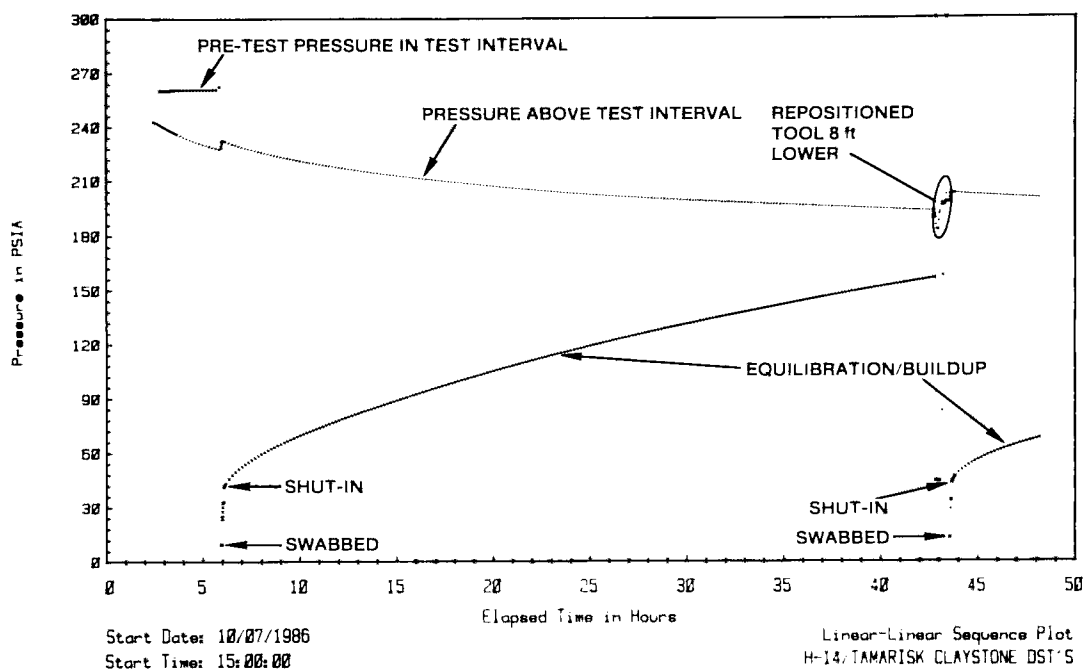
Figure 5-82. H-14/Tamarisk Claystone Shut-In Test Linear-Linear Sequence Plot

interval tested extended from 674.5 to 697.9 ft, the bottom of the hole at that time, thus including 10.8 ft of overlying and underlying gypsum. Descriptions of the test instrumentation and the test data are presented in Stensrud et al. (1988).

Testing was performed on August 5, 1987. After the packer was set, the tubing was swabbed and the shut-in tool was opened to relieve the pressure that had been exerted on the formation by the column of drilling fluid in the well. The test interval was then shut in to allow the wellbore and formation pressures to equilibrate. Figure 5-83 shows the slow pressure rise that resulted over the next 10 hr. This pressure recovery was very similar to that observed for the Tamarisk claystone at H-14 (Figure 5-82). Based on the similarity to the H-14 response and the conclusion that the Tamarisk could not be tested on the time scale of a few days at H-14, the testing effort at H-16 was abandoned.

This decision was borne out by subsequent pressure measurements made by the transducer installed at the Tamarisk horizon as part of the 5-packer installation in H-16 (Figure 3-8). From August 31, 1987, 4 days after the 5-packer installation was completed, until December 15, 1987, the pressure in the Tamarisk interval declined from 204 psig to 169 psig (Stensrud et al., 1988 and in preparation), with complete stabilization apparently several months in the future. The Tamarisk transducer in the 5-packer system is mounted at a depth of 647.1 ft. In a borehole containing brine with a specific gravity of 1.2, the pressure at the midpoint of the Tamarisk claystone 684 ft deep is about 19 psi higher than that measured by the transducer. Hence, the most that can be said at present is that the static formation pressure of the Tamarisk is less than 188 psig. The very slow pressure stabilization of the Tamarisk claystone likely indicates that its transmissivity is one or more orders of magnitude lower than that of the
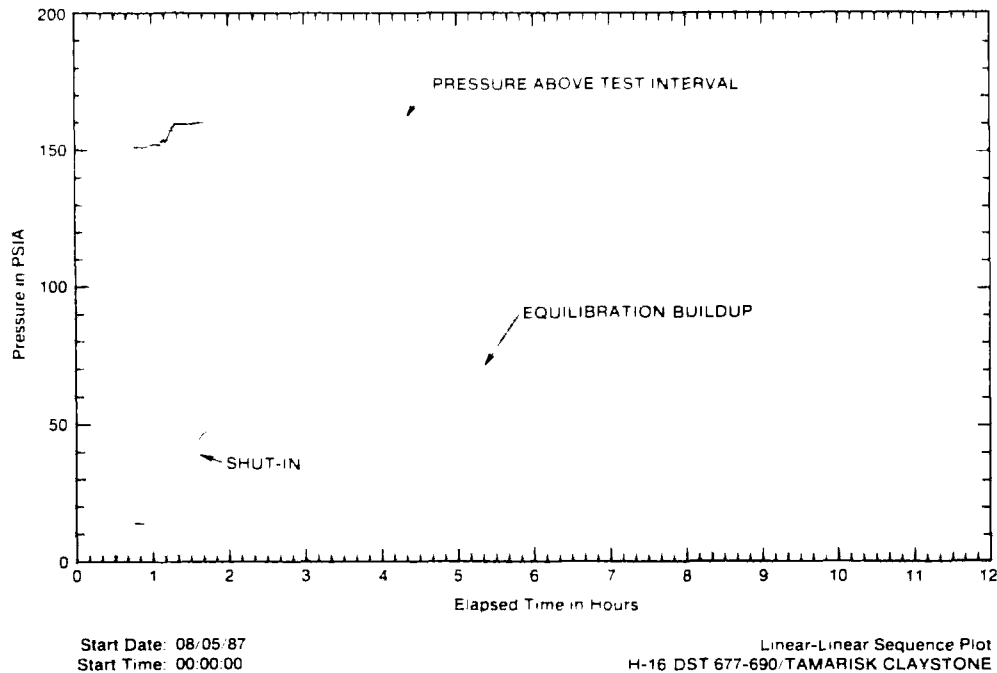
Figure 5-83. H-16/Tamarisk Claystone Shut-In Test Linear-Linear Sequence Plot

least-transmissive unit successfully tested in H-16, the unnamed lower member siltstone (2 x 10-4 ft²/day; Table 5-2).

5.2.4 Magenta Dolomite Member.
The Magenta dolomite was tested in wells H-14 and H-16. The objectives of the Magenta testing were to obtain quantitative information on the hydraulic head and transmissivity of the unit.

5.2.4.1 H–14. At H-14, the Magenta lies from 423.8 to 447.5 ft deep (Figure 3-6). The Magenta was tested in a DST straddle interval from 420.0 to 448.5 ft deep, which included 4.8 ft of overlying and underlying gypsum. This gypsum is not thought to have contributed significantly to the responses observed during testing. The Magenta was tested from October 10 to 13, 1986. Drillstem testing consisted of three flow periods and three buildup periods (Figure 5-84). Descriptions of the test instrumentation and the test data are contained in Stensrud et al. (1987).

To obtain equivalent constant-rate flow periods, each of the three flow periods was subdivided into two shorter periods. The FFL, which lasted about 15 minutes, was divided into two periods with flow rates of 0.049 and 0.014 gpm (Table 5-1). The SFL, which lasted about 30 minutes, was divided into two periods with flow rates of 0.036 and 0.010 gpm. Finally, the TFL, which lasted about 60 minutes, was divided into shorter periods with flow rates of 0.014 and 0.007 gpm. The durations of the buildup periods were approximately 18.5, 23.5, and 21.1 hr for the FBU, SBU, and TBU, respectively.

As can be seen first on the linear-linear sequence plot of the Magenta DST's (Figure 5-84), the presence of an overpressure skin had a significant effect on the observed buildup responses. When the Magenta interval was initially shut in for an equilibration period following swabbing, the fluid pressure rose to a peak of 134.2 psia and then gradually declined. Six hours into the FBU, the pressure peaked at 123.2 psia, and then declined for
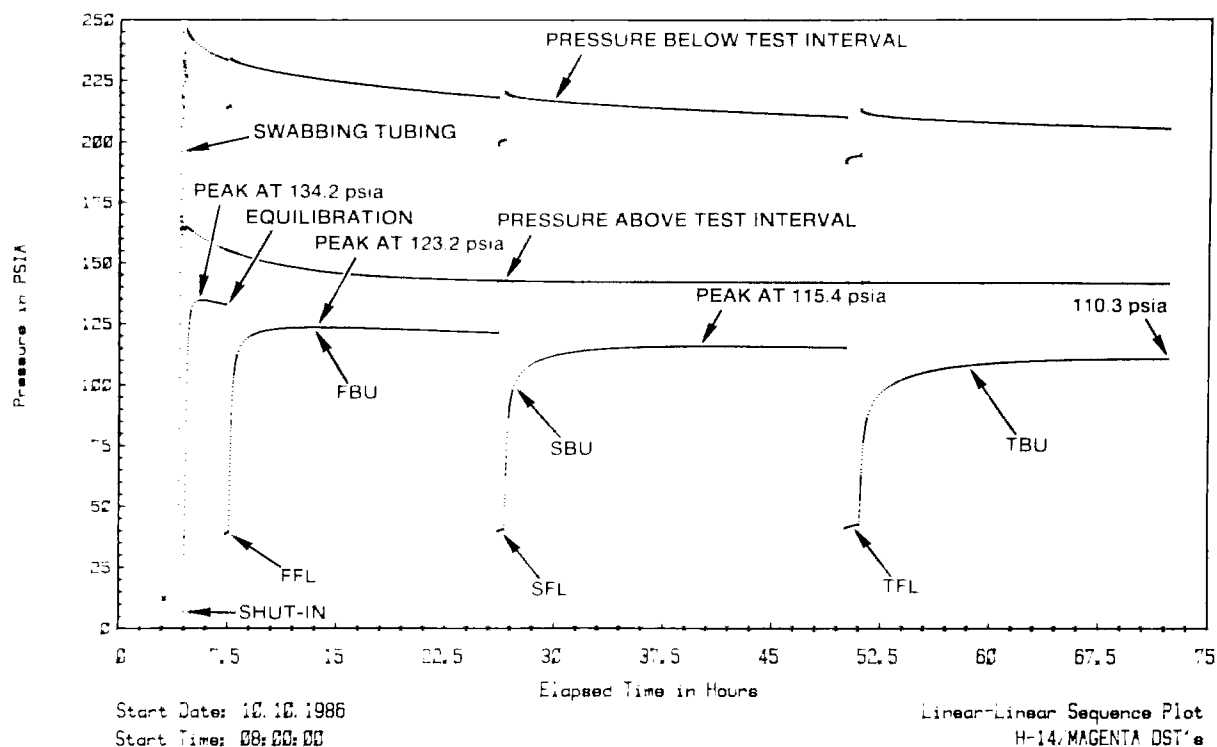
Figure 5-84. H-14/Tamarisk Claystone Shut-In Linear-Linear Sequence Plot

the remainder of the buildup period. After 13.5 hr of the SBU, the pressure peaked at 115.4 psia and then began to decline. At the end of the TBU, the pressure was essentially constant at 110.3 psia. This successive decrease in the magnitude of the pressure peaks provides a clear indication of the dissipation of an overpressure skin.

Figure 5-85 shows a log-log plot of the FBU data up to the time of the pressure peak, along with an INTERPRET-generated simulation. The simulation is representative of a single-porosity medium with a transmissivity of 5.6 x 10^{-3} ft²/day (Table 5-2). Assuming a porosity of 20%, a total-system compressibility of 1.0 x 10^{-5} psi^{-1}, and a fluid viscosity of 1.0 cp, the skin factor for this simulation is about 0.5, indicating a well with very little wellbore damage. The simulation does not fit the observed early-time data very well, but it does fit the middle- and late-time pressure data adequately. The sharp decline of the pressure derivative at late time clearly shows the effects of overpressure skin.

Figure 5-86 shows a log-log plot of the SBU data up to the time of the pressure peak, along with a simulation generated by INTERPRET. This simulation, like that of the FBU data (Figure 5-85), is representative of a single-porosity medium with a transmissivity of 5.6 x 10^{-3} ft²/day, but the skin factor is slightly lower at about 0.4 (Table 5-2). The expected sharp decline in the pressure derivative at late time due to the overpressure skin is evident on the plot, but an unexpected preceding rise in the derivative is also seen. The cause of this rise is not clearly understood. One possibility is that the pressure-derivative data show a superposition of pressure-skin effects resulting from episodes of significantly different hydraulic loading, such as the drilling of the Magenta and the later testing of the Tamarisk Member, with the residual effects of different episodes dominating at different times during the buildup.

The dimensionless Horner plot of the pre-peak SBU data also shows this superposition of pressure-skin

111
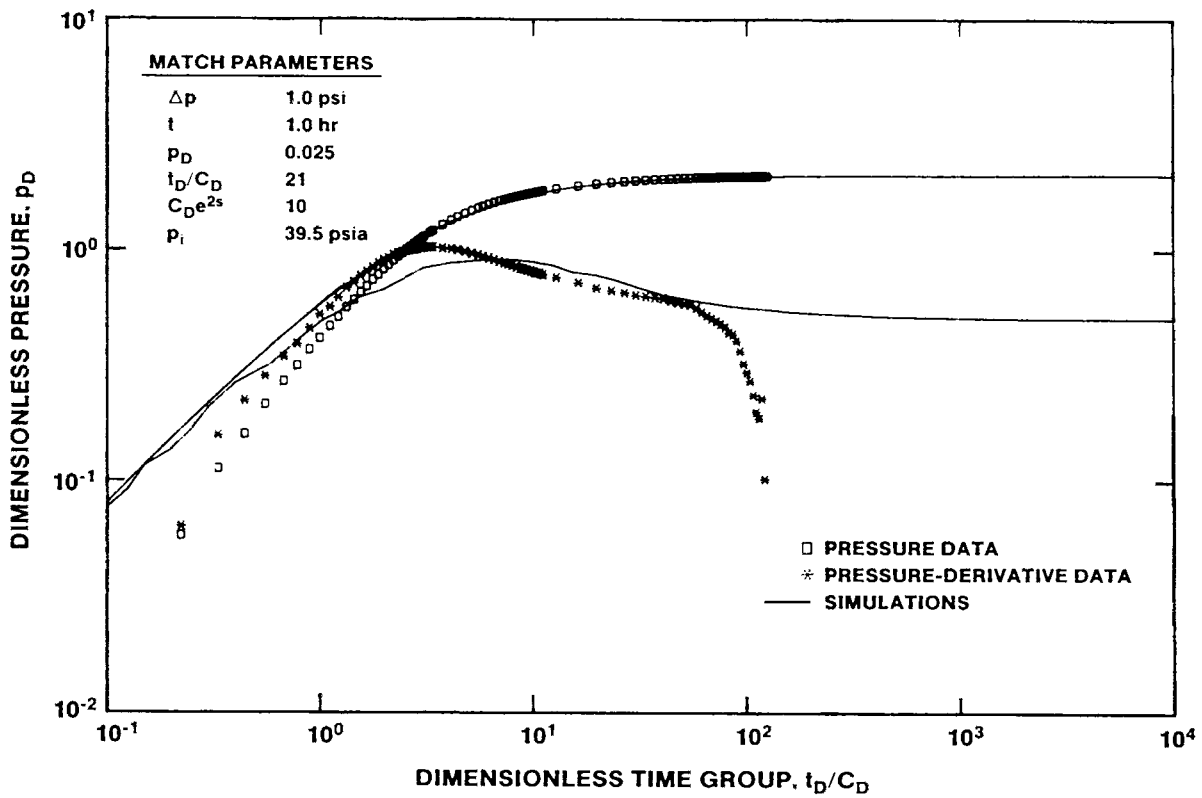
Figure 5-85. H-14/Magenta First Buildup Log-Log Plot with INTERPRET Simulation
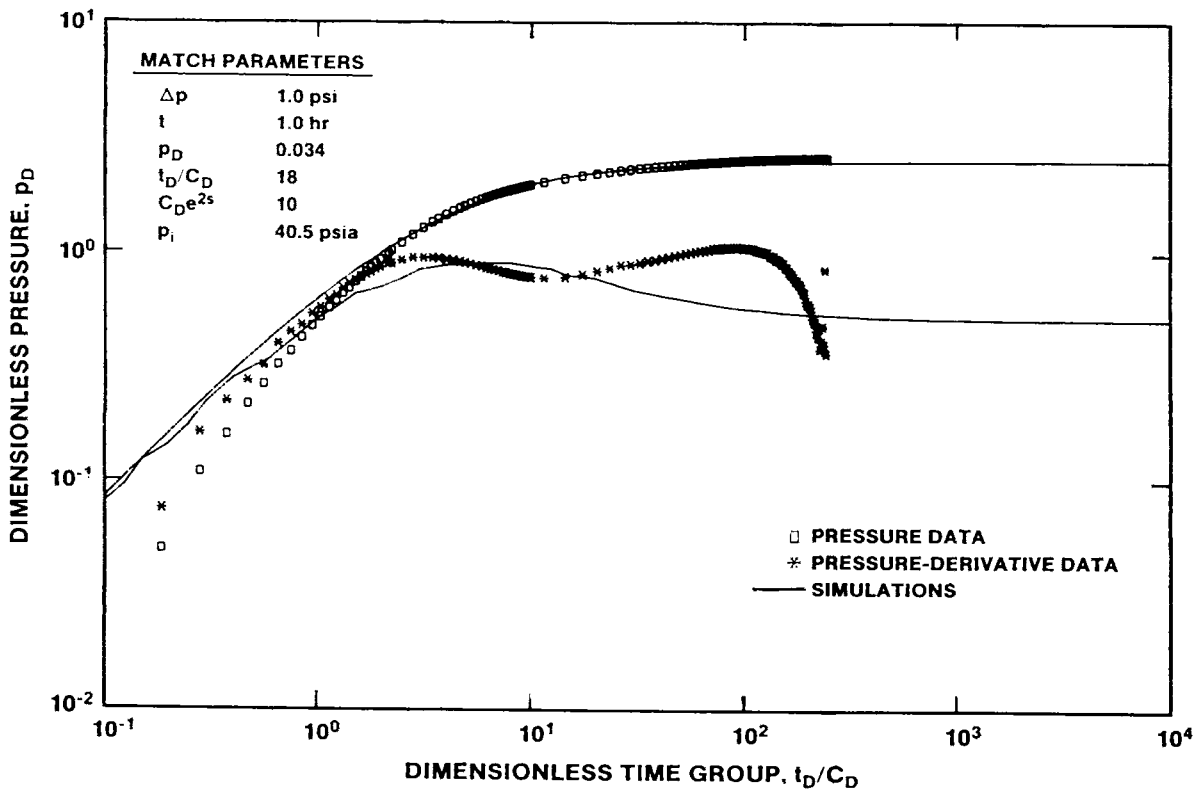
Figure 5-86. H-14/Magenta Second Buildup Log-Log Plot with INTERPRET Simulation

effects (Figure 5-87). The middle-time data (around 0.5 on the time axis) have a concave-upward curvature typical of ideal behavior. The simulation shown is the best fit obtained to those data using the model derived in conjunction with the log-log analysis, and shows that the buildup pressure is initially trending toward a static formation pressure (p^*) of about 113 psia. At late time, however, the data become concave-downward and appear to trend toward a higher formation pressure before reaching yet another inflection point and terminating with a concave-upward curvature. The pressure buildup appears to have been controlled by different formation pressures at different times.

The same responses to pressure-skin conditions are seen in the log-log plot of the TBU data (Figure 5-88). After beginning to stabilize, the pressure derivative rises, and then decreases sharply. The simulation shown in Figure 5-88 is similar to those of the FBU and SBU, but uses a transmissivity of 5.3 x 10^{-3} ft^2/day and a skin factor of 0.3 (Table 5-2). The dimensionless Horner plot of the TBU data (Figure 5-89) also shows the same curvatures as that of the SBU data (Figure 5-87). The middle-time TBU data, however, appear to be controlled by a formation pressure of about 106 psia, 7 psi lower than the value obtained for the SBU data.

MATCH PARAMETERS

Δp	= 1.0 psi
t	= 1.0 hr
P_D	= 0.034
t_D/C_D	= 18
$C_D e^{2s}$	= 10
p^*	= 113.0 psia

+ DATA
—— SIMULATION

DIMENSIONLESS SUPERPOSITION FUNCTION: FLOW PERIOD 6
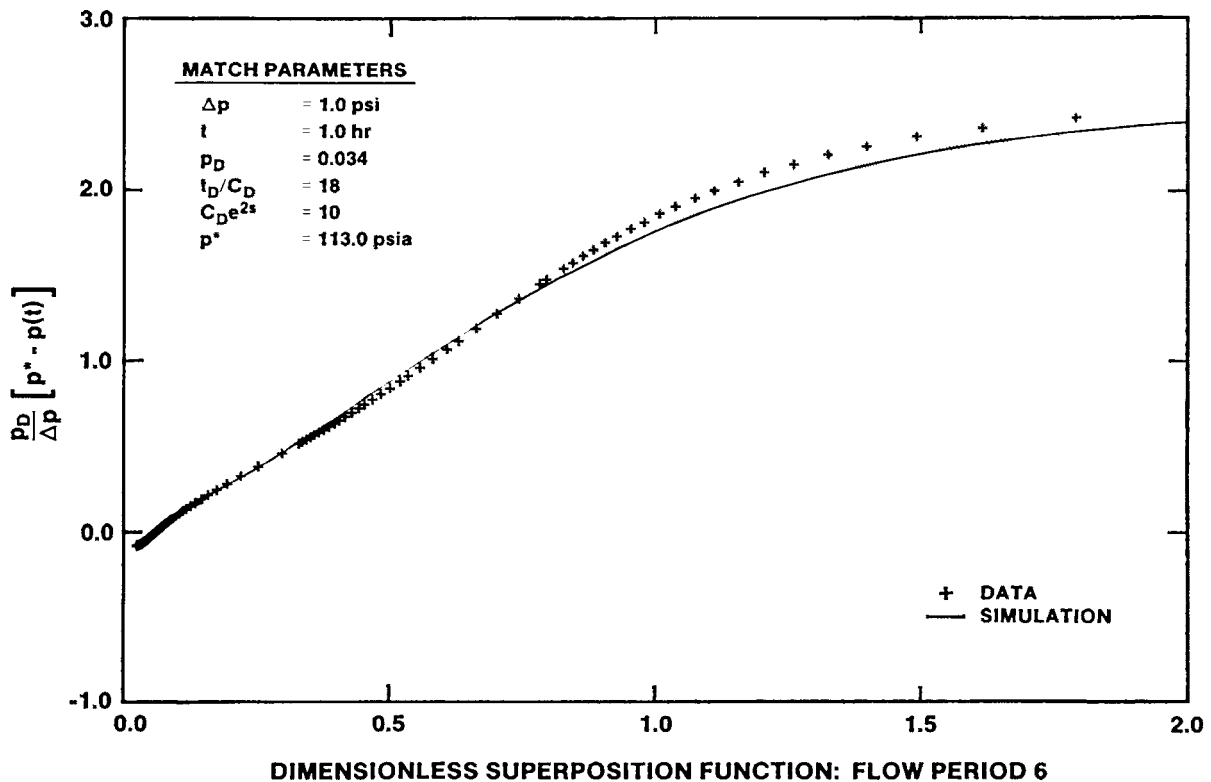
Figure 5-87. H-14/Magenta Second Buildup Dimensionless Horner Plot with INTERPRET Simulation
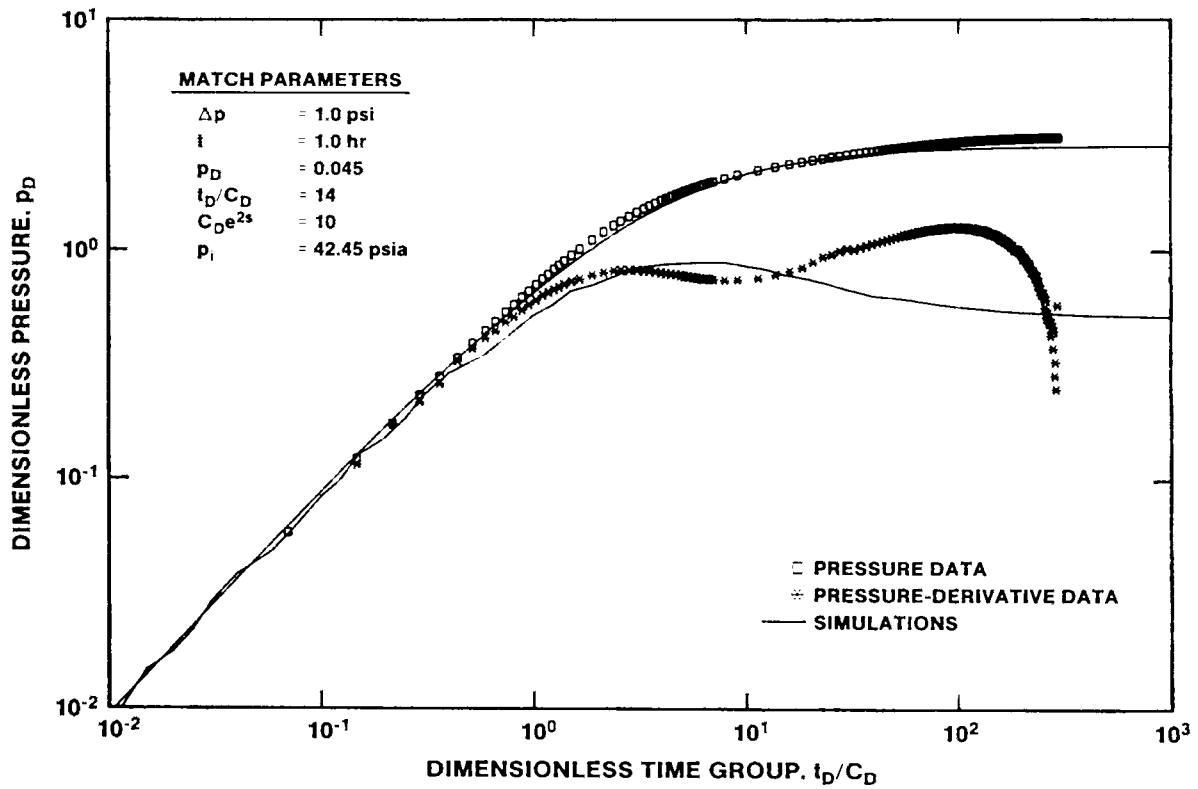
Figure 5-88. H-14/Magenta Third Buildup Log-Log Plot with INTERPRET Simulation
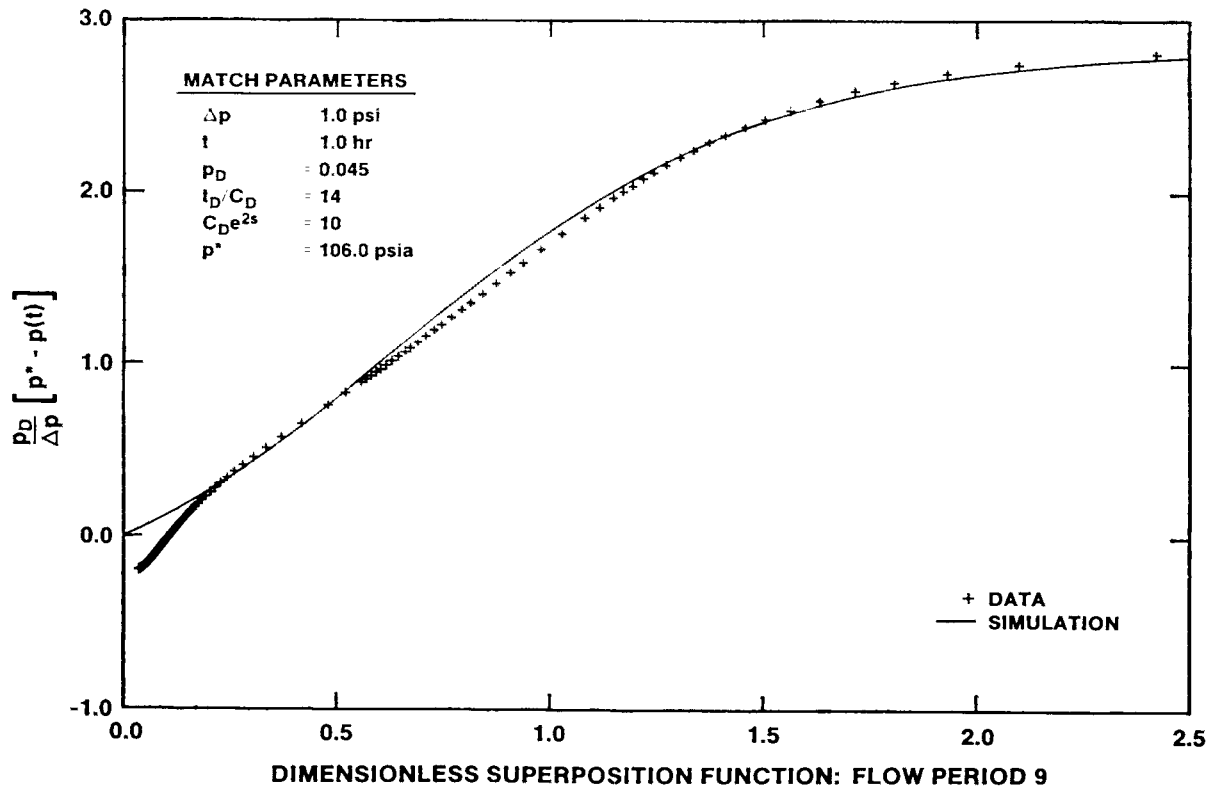
Figure 5-89. H-14/Magenta Third Buildup Dimensionless Horner Plot with INTERPRET Simulation

The complex pressure-skin effects seen during these tests make determination of a precise value for the hydraulic head of the Magenta at H-14 very difficult. Each buildup period indicated a lower static pressure than the preceding one. The shape of the TBU pressure derivative (Figure 5-88) indicates that the static pressure must be lower than the final pressure measured, 110.3 psia. The dimensionless Horner plot (Figure 5-89) indicates that 106 psia might be appropriate. Given that the fluid in the hole had a specific gravity of 1.2, that the transducer measured an atmospheric pressure of 12 psia, and that the transducer was at a depth of 401.9 ft, 106 psia corresponds to a pressure of about 112 psig at the midpoint of the Magenta about 436 ft deep. However, the Magenta response during the three buildup periods raises the question as to what static pressure a fourth buildup period might have shown. A rough interpolation from Magenta water levels at H-3b1 and H-4c in 1986 (Saulnier et al., 1987) indicates that the static pressure at H-14 may have been as low as about 102 psig.

In summary, no precise value can be assigned for the hydraulic head of the Magenta at H-14. The last measured pressure of 116 psig provides a probable maxiumum value, while estimates from H-3 and H-4 water-level data provide a lower estimate of about 102 psig. A permanent well completion in the Magenta at H-14 would be required to refine the value further.

5.2.4.2 H-16. At H-16, the Magenta lies from 590.2 to 615.6 ft deep (Figure 3-8). The Magenta was cored and reamed on July 28 and 29, 1987. Following reaming on July 29, 1987, the drilling fluid in the hole was partially unloaded by airlifting and the DST tool was set in the hole. The Magenta was tested in an interval that extended from 589.2 ft to the then-bottom of the hole 620.7 ft deep. Thus, the lower 1 ft of the Forty-niner and the upper 5.1 ft of the Tamarisk were included in the test interval. These intervals are composed of gypsum and anhydrite, however, and were judged to have permeabilities too low to have contributed significantly to the responses observed during testing.

Testing was performed on July 30 and 31, 1987, and consisted of two DST flow periods, two buildup

periods, and a rising-head slug test (Figure 5-90). The FFL lasted about 22 minutes and was followed by a 466-minute FBU. The SFL lasted about 31 minutes and was followed by a 927-minute SBU. To obtain constant flow rates for buildup analyses, the FFL was divided into two flow periods having flow rates of 0.062 and 0.047 gpm, and the SFL was divided into two flow periods having flow rates of 0.062 and 0.045 gpm (Table 5-1). The slug test lasted almost 8 hr, during which time about 45% of the induced pressure differential dissipated. Descriptions of the test instrumentation and the test data are contained in Stensrud et al. (1988).

Figure 5-91 shows a log-log plot of the FBU data, along with an INTERPRET-generated simulation. The simulation is representative of a single-porosity medium with a transmissivity of 2.8×10^{-2} ft^2/day (Table 5-2). Assuming a porosity of 20%, a total-system compressibility of 1.0×10^{-5} psi^{-1}, and a fluid viscosity of 1.0 cp, the skin factor for this simulation is -0.4, indicating a very slightly stimulated well. The pressure derivative shows oscillations similar, although with much lower amplitudes, to those observed in the H-14 Magenta SBU and TBU data (Figures 5-87 and 89). Again, these oscillations may be related to periods of different hydraulic loading on the Magenta during coring, reaming, and preparation for testing. The decline of the pressure derivative at late time clearly shows the effects of an overpressure skin.

The log-log plot of the SBU data (Figure 5-92) looks similar to that of the FBU data (Figure 5-91). The SBU simulation is representative of a single-porosity medium with a transmissivity of 2.8×10^{-2} ft^2/day and a skin factor of -0.8 (Table 5-2). The decline in the late-time pressure derivative indicates the continued presence of an overpressure skin.

Figure 5-93 is a linear-linear plot of the Magenta DST sequence with a simulation of the entire sequence generated by INTERPRET using the model derived in the FBU analysis. The static formation pressure specified for this simulation was 134.4 psia. Because of the continuing dissipation of the overpressure skin, the SBU data are generally slightly below the simulation. Otherwise, the match between the observed data and the simulation is excellent.
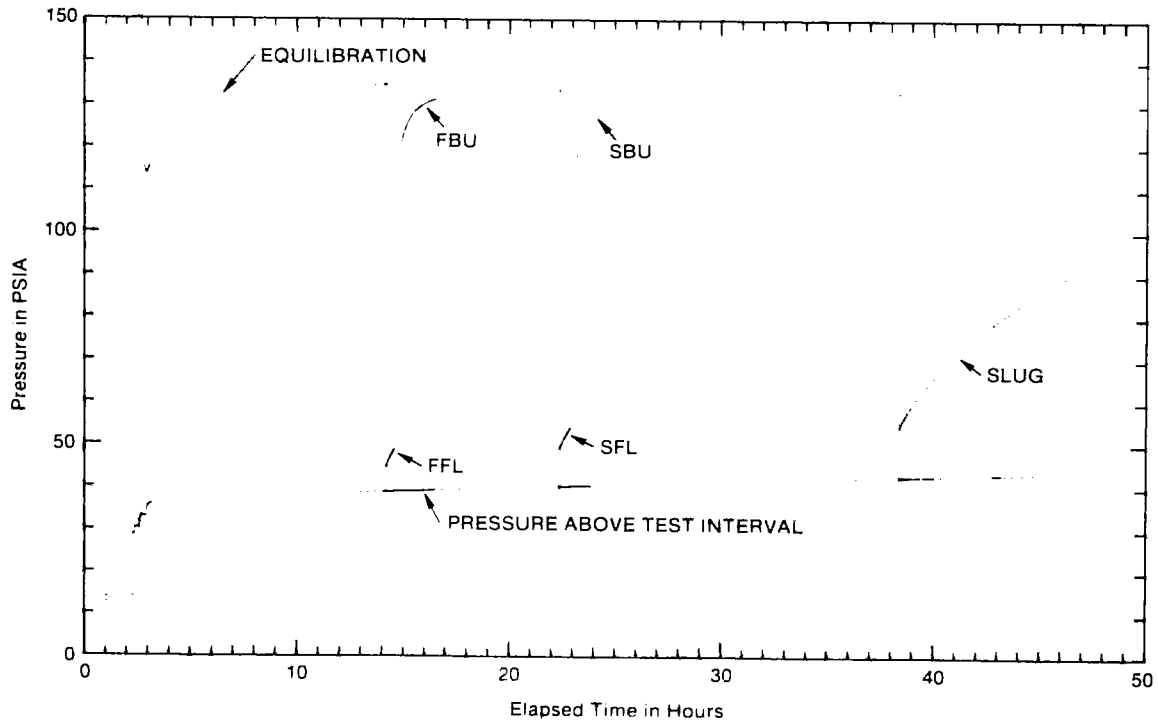
Figure 5-90. H-16/Magenta Drillstem and Slug Testing Linear-Linear Sequence Plot
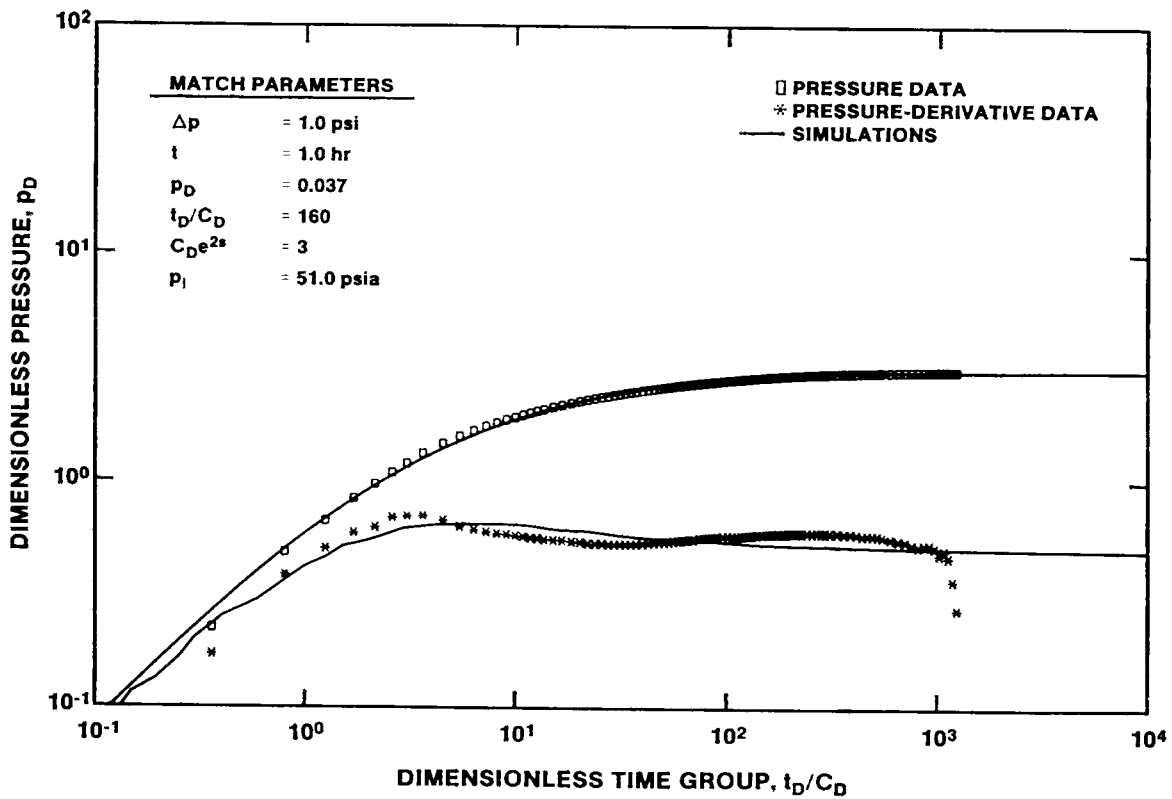
Figure 5-91. H-16/Magenta First Buildup Log-Log Plot with INTERPRET Simulation
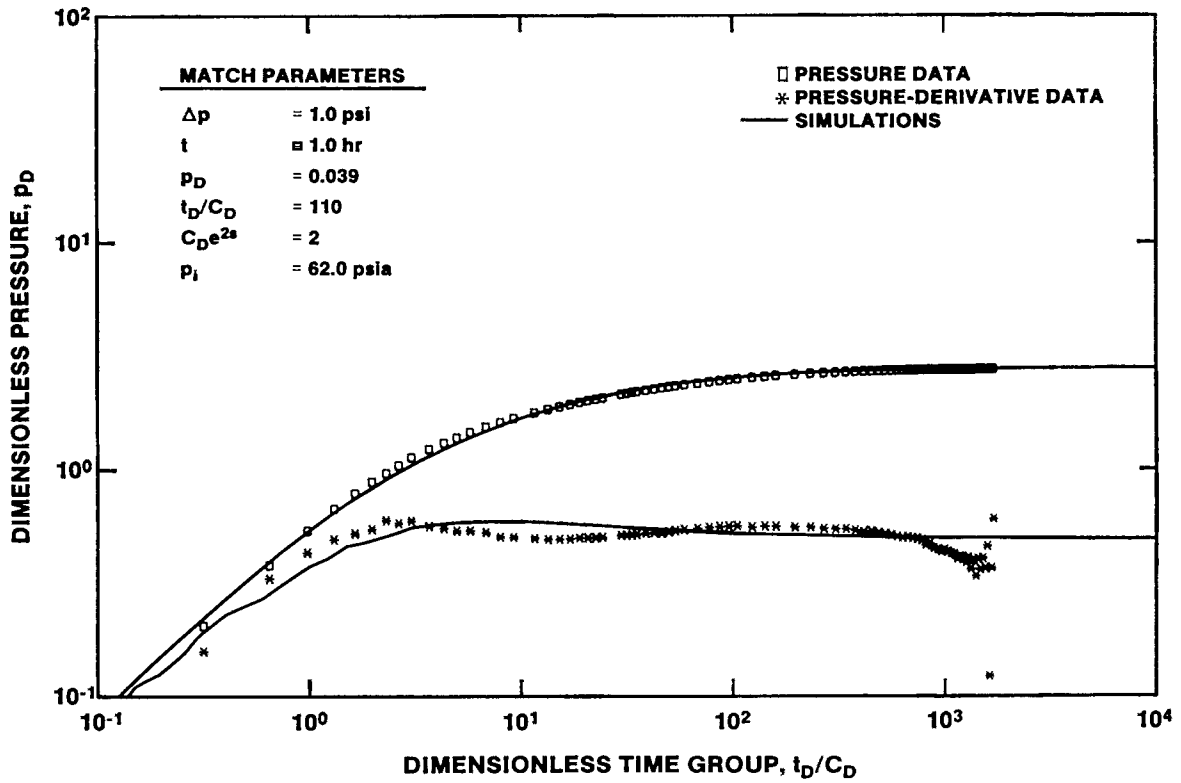
Figure 5-92. H-16/Magenta Second Buildup Log-Log Plot with INTERPRET Simulation
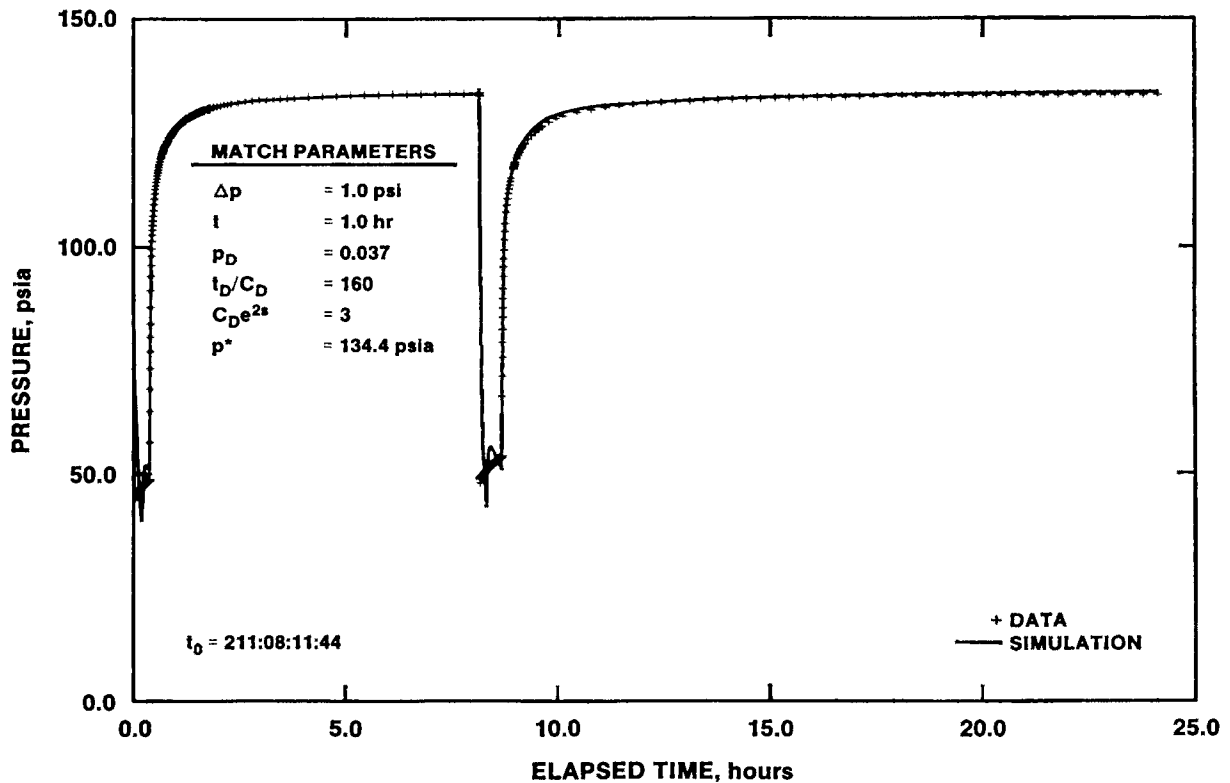
Figure 5-93. H-16/Magenta Drillstem Test Linear-Linear Plot with INTERPRET Simulation

Figure 5-94 is a log-log plot of the rising-head slug-test data, along with the best-fit type-curve match. The data were initially noisy before settling into a steady recovery. The match shown corresponds to a transmissivity estimate of 2.4×10^{-2} ft^2/day (Table 5-2), slightly lower than the values provided by the DST buildup analyses. The static formation pressure estimate used to obtain the fit in Figure 5-94 was 133.0 psia, slightly lower than the final SBU pressure.

The transducer was at a depth of 571.3 ft during the DST's and slug test. With the fluid in the borehole having a specific gravity of 1.2, a transducer reading of 133.0 psia corresponds to a pressure at the midpoint of the Magenta at 603 ft of about 149.5 psia. Subtracting the atmospheric pressure of 14 psia measured by the transducer before the test began leaves a static formation pressure of 135.5 psig. In comparison, the transducer installed at the Magenta horizon as part of the H-16 5-packer completion (Figure 3-8) provides a slightly lower estimate of the Magenta static formation pressure. This transducer indicates a stabilized pressure of 126 psig at a depth of 587.2 ft (Stensrud et al., 1988), corresponding to a pressure of about 134 psig at the midpoint of the Magenta. Continued pressure-skin dissipation since the completion of the slug test may account for the slight difference in static formation pressure estimates.
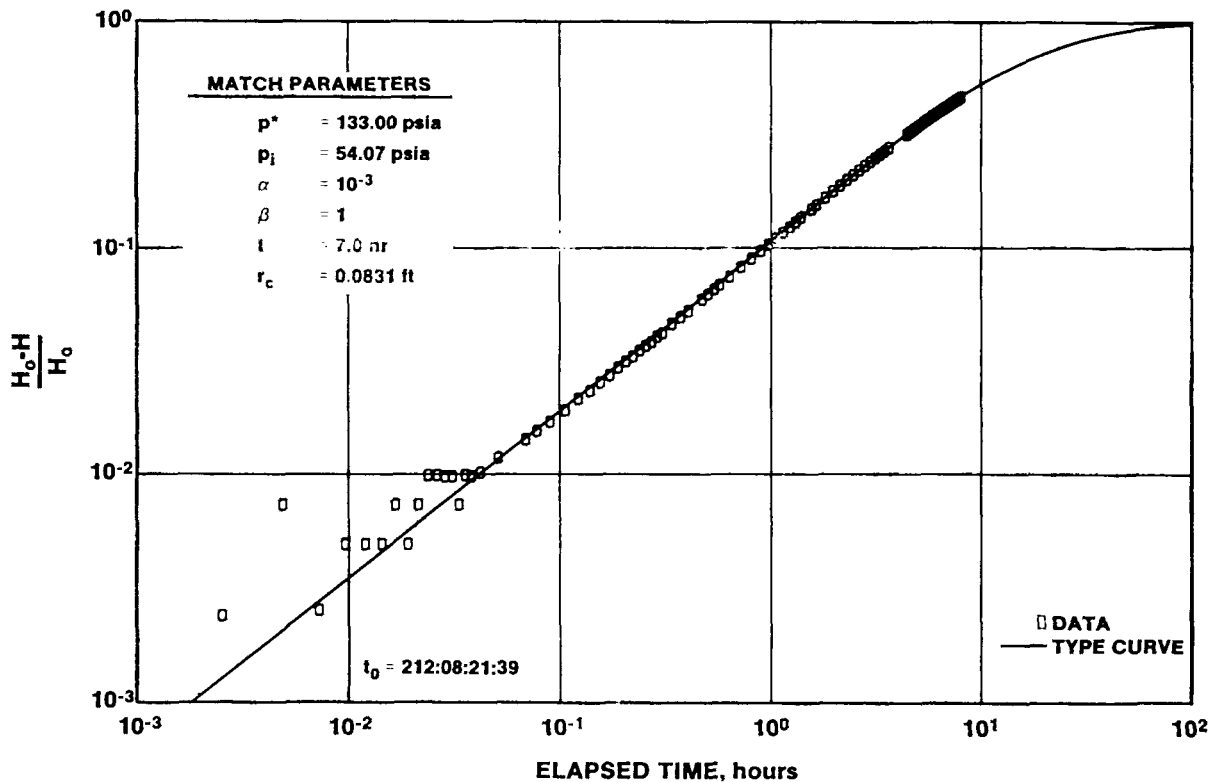
Figure 5-94. H-16/Magenta Early-Time Slug-Test Plot

5.2.5 Forty-niner Member.
The Forty-niner Member of the Rustler Formation was tested in wells H-14 and H-16. The objectives of the testing were to obtain hydraulic-head and transmissivity estimates. The hydraulic-head measurements are particularly important in helping to determine whether or not water from the Dewey Lake Red Beds, and by extension from the surface, can be recharging the Magenta and Culebra dolomites at the WIPP site. The transmissivity estimates allow an evaluation of the ability of the Forty-niner to provide water to the WIPP shafts, as well as providing data for cross-sectional or three-dimensional modeling of groundwater flow in the Rustler.

5.2.5.1 H-14. Two sets of Forty-niner tests were performed at H-14, tests of the medial claystone/mudstone/siltstone unit (hereafter referred to simply as claystone) and tests of the upper anhydrite unit. The claystone tests were to provide data on the hydraulic head and transmissivity of the most permeable section of the Forty-niner. The anhydrite tests were intended to verify the assumptions that the Rustler anhydrites are much less permeable than the claystones, and that they cannot be tested on the time scale of days.

Forty-niner Claystone: At H-14, the claystone portion of the Forty-niner lies between 390 and 405 ft deep (Figure 3-6). The claystone was tested in a DST straddle interval extending from 381.0 to 409.5 ft deep. Thus, about 13.5 ft of Forty-niner anhydrite and gypsum were included in the test interval. Descriptions of the test instrumentation and the test data are contained in Stensrud et al. (1987).

The Forty-niner claystone was tested on October 13 and 14, 1986. Testing consisted of two flow periods, two buildup periods, and a rising-head slug test (Figure 5-95). The FFL lasted about 18 minutes, and
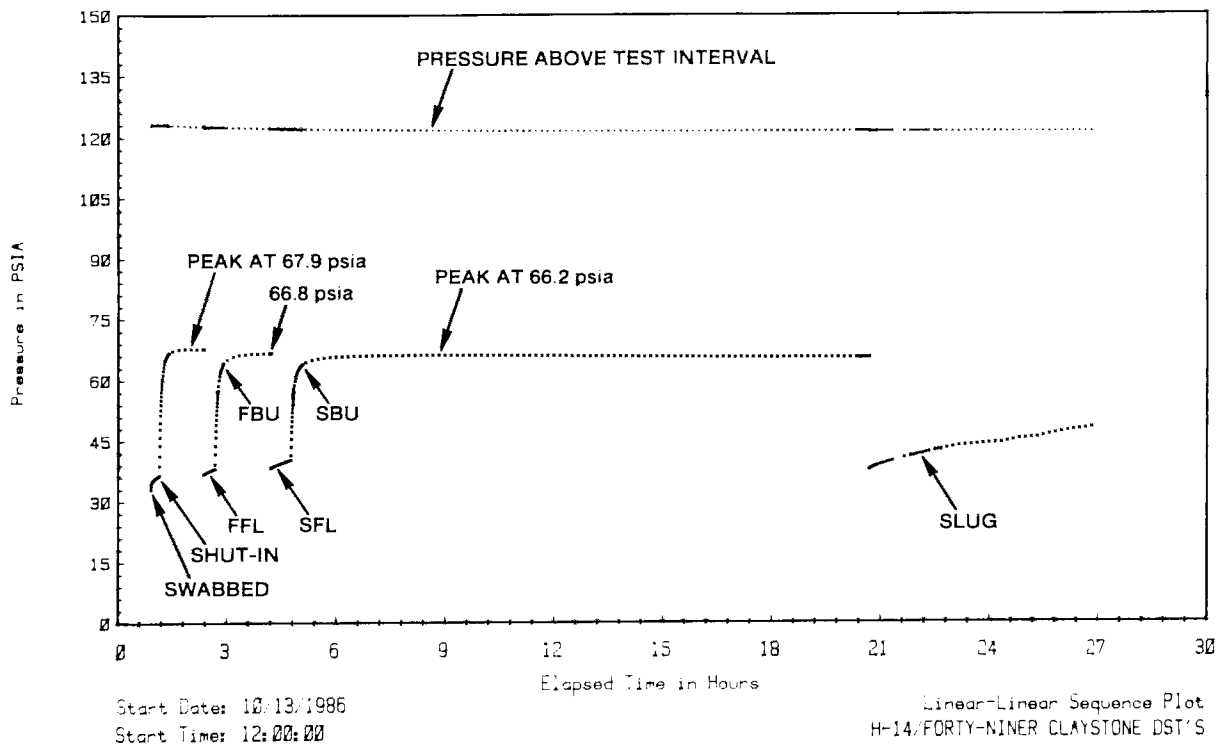
Figure 5-95. H-14/Forty-Niner Claystone Drillstem and Slug Testing Linear-Linear Sequence Plot

was followed by a 92-minute FBU. The SFL lasted about 32 minutes, and was followed by a SBU almost 16 hr long. To obtain equivalent constant-rate flow periods, each of the flow periods was divided into two shorter periods. The FFL was divided into two periods with flow rates of 0.028 and 0.021 gpm, and the SFL was divided into periods with flow rates of 0.022 and 0.017 gpm (Table 5-1). The slug test lasted slightly over 6 hr, by which time about 57% of the induced pressure differential had dissipated.

Overpressure-skin effects were apparent during the Forty-niner claystone testing, just as they were during all other testing at H-14. The fluid pressure reached a maximum of 67.9 psia during the initial equilibration period, was essentially constant at 66.8 psia at the end of the FBU, and peaked at 66.2 psia during the SBU (Figure 5-95). The superposition of pressure-skin effects manifested in the Magenta test data (see Section 5.2.4.1) was not apparent, however, in the Forty-niner claystone test data.

Figure 5-96 shows a log-log plot of the Forty-niner claystone FBU data with an INTERPRET-generated simulation. The late-time pressure derivative shows the decline indicative of overpressure skin. The simulation is representative of a single-porosity medium with a transmissivity of 7.1×10^{-2} ft^2/day (Table 5-2). Assuming a porosity of 30%, a total-system compressibility of 1.0×10^{-5} psi^{-1}, and a fluid viscosity of 1.0 cp, the skin factor for this simulation is about 3.2, indicating a damaged well.

The dimensionless Horner plot of the FBU data is shown in Figure 5-97. The simulation matches the observed data very well until late time, when the data deviate towards a static pressure lower than the 67.8 psia specified for the simulation. This discrepancy between the observed data and the
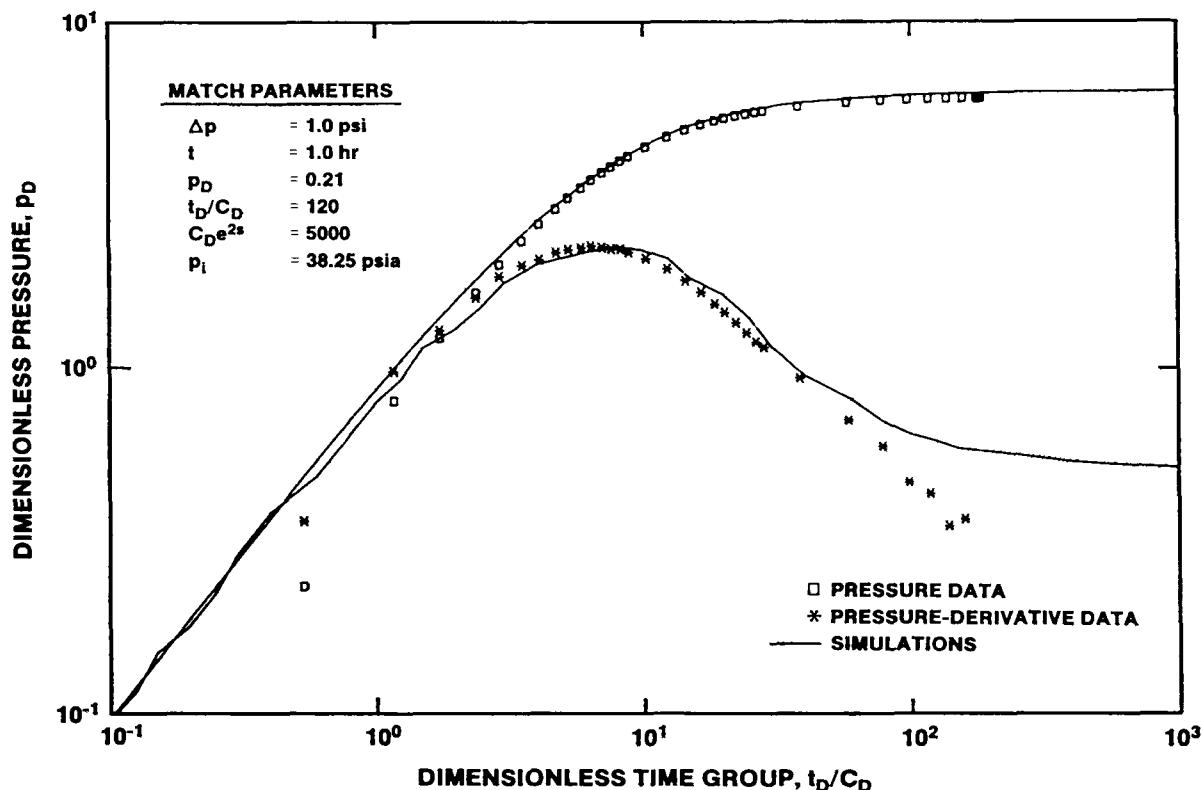
Figure 5-96. H-14/Forty-Niner Claystone First Buildup Log-Log Plot with INTERPRET Simulation
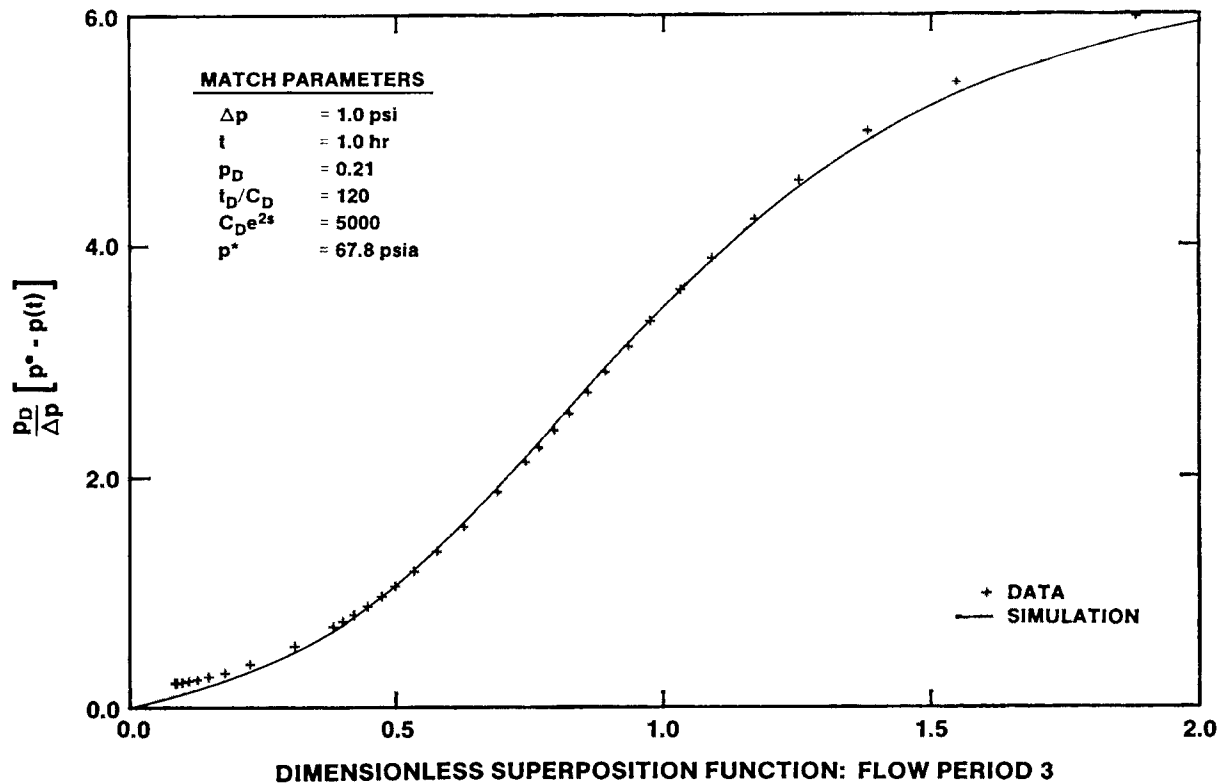
Figure 5-97. H-14/Forty-Niner Claystone First Buildup Dimensionless Horner Plot with INTERPRET Simulation

simulation is entirely consistent with the effects of an overpressure skin.

The log-log plot of the SBU data is shown in Figure 5-98. Overpressure-skin effects are once again evident in the late-time pressure derivative. The simulation shown was generated by INTERPRET using a single-porosity model and a transmissivity of 6.9×10^{-2} ft^2/day (Table 5-2). With the assumed parameter values listed above, the skin factor for this simulation is about 3.3, comparable to the value obtained from the FBU analysis.

A log-log early-time plot of the rising-head slug-test data is shown in Figure 5-99, along with the best-fit type curve. The fit is quite good until near the end, when the observed data oscillate for an unknown reason. The type-curve fit shown provides a transmissivity estimate of 3.0×10^{-2} ft^2/day (Table 5-2), which is slightly less than half of the values provided by the FBU and SBU analyses. A slightly different type-curve fit might have been

indicated had the late-time data been better behaved.

The static formation pressure for the Forty-niner claystone is difficult to estimate because of the overpressure-skin effects present during the buildup tests, and because of the nonideal behavior during the latter portion of the slug test. The static formation pressure must be less than the final pressure measured at the end of the SBU, 65.5 psia. The slug-test analysis relied on a static formation pressure estimate of 62 psia, although a reasonably good fit was also obtained using an estimate of 65 psia. Considering that the transducer during these tests was set 362.9 ft deep, that the transducer measured an atmospheric pressure of 12 psia before testing began, and that the borehole contained brine with a specific gravity of 1.2, 65 psia corresponds to a static formation pressure of 71 psig at the midpoint of the claystone 398 ft deep. This value is reliably a maximum.

Figure 5-98. H-14/Forty-Niner Claystone Second Buildup Log-Log Plot with INTERPRET Simulation

MATCH PARAMETERS

Δp	= 1.0 psi
t	= 1.0 hr
p_D	= 0.25
t_D/C_D	= 125
$C_D e^{2s}$	= 5000
p_i	= 40.36 psia

□ PRESSURE DATA
* PRESSURE-DERIVATIVE DATA
— SIMULATIONS

MATCH PARAMETERS

p^*	= 62.00 psia
p_i	= 37.75 psia
α	= 10^{-3}
β	= 1.0
t	= 5.6 hr
r_c	= 0.0831 ft

□ DATA
— TYPE CURVE

t_0 = 287:08:41:42
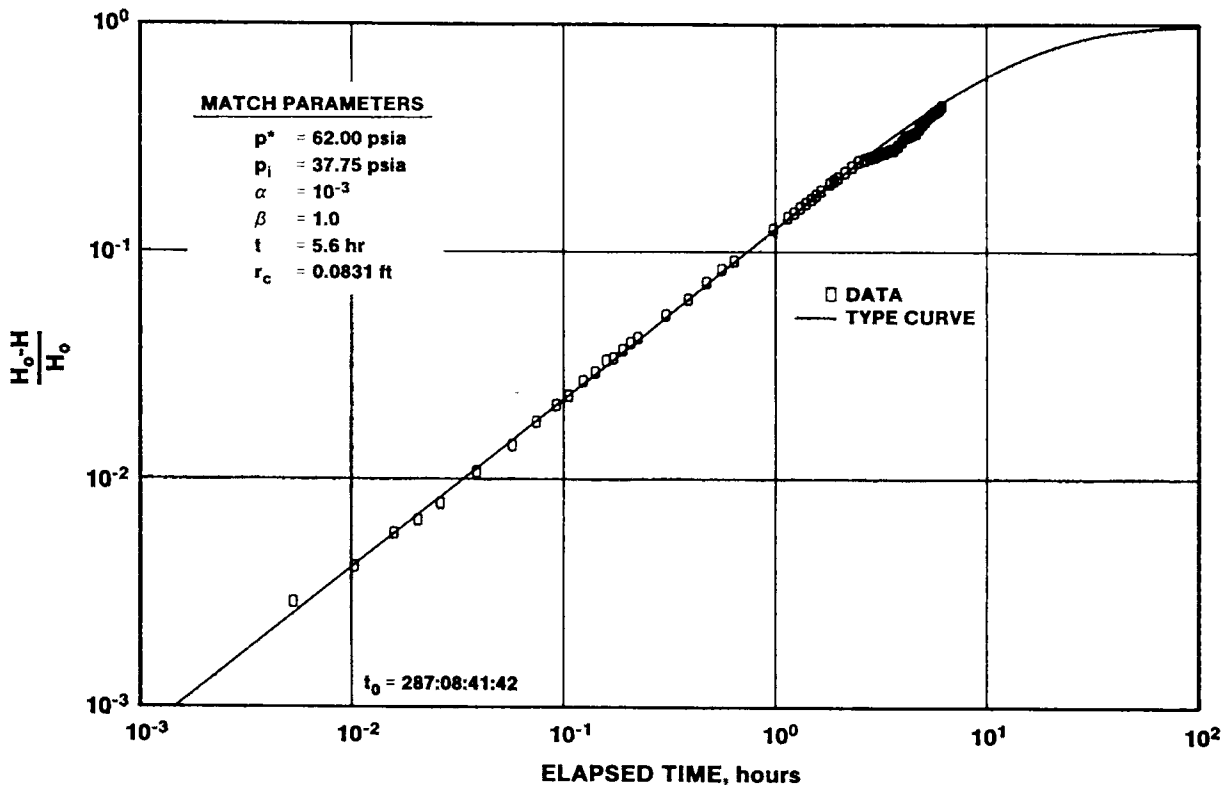
Figure 5-99. H-14/Forty-Niner Claystone Early-Time Slug-Test Plot

Forty-niner Anhydrite. The upper anhydrite and gypsum unit of the Forty-niner Member lies from 359.5 to 390 ft deep at H-14 (Figure 3-6). The unit is roughly 75% anhydrite and 25% gypsum, based on interpretation of a neutron log. The unit was tested in a DST straddle interval extending from 356.0 to 384.5 ft deep. Thus, the bottom 3.5 ft of the Dewey Lake Red Beds and the Dewey Lake/Rustler contact were included in the test interval. Descriptions of the test instrumentation and the test data are contained in Stensrud et al. (1987).

The Forty-niner anhydrite was tested from October 14 to 15, 1986. Because the anhydrite was expected to have too low a permeability to allow quantitative testing over the few days available for testing, no pressure-equilibration period preceded the testing. Instead, as soon as the packers were set, the tubing was swabbed with the shut-in tool open, and the test interval was left open to the tubing for about 16

minutes for a flow period (Figure 5-100). Very little fluid entered the tubing at this time. The test interval was then shut in for about 16.5 hr. The pressure increased by about 1 psi over the first 1.5 hr of the buildup, and by only another psi over the last 15 hr. At that time, the testing was terminated. The Forty-niner anhydrite was judged to have a permeability much lower than that of the claystone, and quantitative testing of the anhydrite appeared to require weeks to months of effort.

5.2.5.2 H-16. At H-16, only the medial clayey interbed of the Forty-niner was tested. At this location, this interbed is composed largely of clay, and is indurated to a claystone only in minor intervals. The clay lies from 562.6 to 573.8 ft deep (Figure 3-8), and was tested in an interval extending from 560.4 ft to the then-bottom of the hole at 580.7 ft. The portions of the test interval overlying and underlying the clay are composed of gypsum
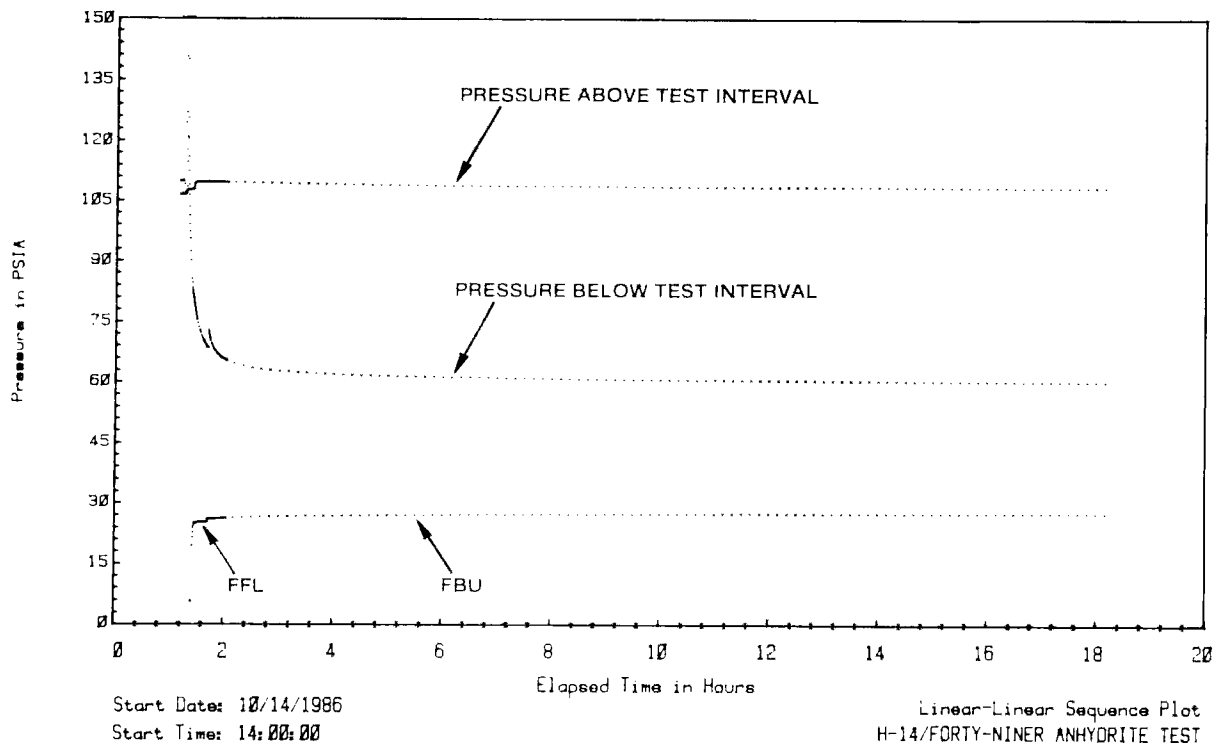
Figure 5-100. H-14/Forty-Niner Anhydrite Drillstem Test Linear-Linear Sequence Plot

123

and anhydrite, and were not considered to have contributed significantly to the fluid-pressure responses observed. Descriptions of the test instrumentation and the test data are presented in Stensrud et al. (1988).

Testing was performed on July 27 and 28, 1987, and consisted of a pulse-injection test followed by two DST flow periods, two buildup periods, and a rising-head slug test (Figure 5-101). The pulse test lasted about 249 minutes. The FFL lasted about 21 minutes, and was followed by a 429-minute FBU. The SFL lasted about 31 minutes, and was followed by a 594-minute SBU. To obtain constant flow rates for buildup analyses, the FFL was divided into two flow periods having flow rates of 0.010 and 0.005 gpm, and the SFL was divided into two flow periods having flow rates of 0.016 and 0.007 gpm (Table 5-1). The slug test lasted about 263 minutes, with only about 4.5% of the induced pressure differential dissipating during this time.

Figure 5-102 is a semilog plot of the Forty-niner pulse-test data, showing the best type-curve match achieved. The data and type curve match reasonably well, with the greatest discrepancy occurring at early time. The transmissivity calculated from this match is 2.2×10^{-4} ft²/day (Table 5-2).

Figure 5-103 is a log-log plot of the DST FBU data, along with a simulation generated by INTERPRET. The simulation fit the data very well, and is representative of a single-porosity medium with a transmissivity of 5.3×10^{-3} ft²/day (Table 5-2). Assuming a porosity of 30%, a total-system compressibility of 1.0×10^{-5} psi⁻¹, and a fluid viscosity of 1.0 cp, the skin factor for this simulation is 0.7, indicating a wellbore with little damage. The decline in the pressure derivative at late time reflects minor overpressure-skin effects. The dimensionless Horner plot of the FBU data (Figure 5-104) shows an excellent fit between the data and the simulation using a static formation pressure estimate of 117.2 psia.

Start Date: 07/24/87
Start Time: 19:00:00

Linear-Linear Sequence Plot
H-16/DST 563-574/FORTY-NINER CLAY
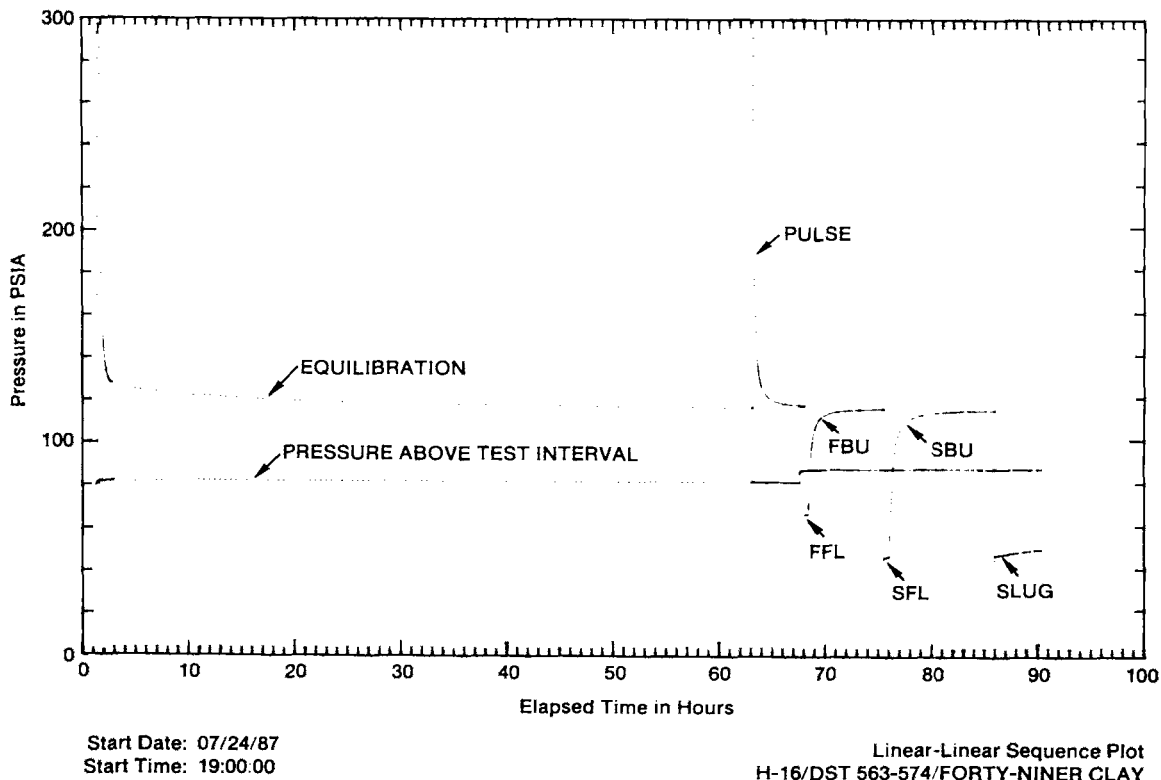
Figure 5-101. H-16/Forty-Niner Clay Pulse, Drillstem, and Slug Testing Linear-Linear Sequence Plot

MATCH PARAMETERS

p^*	$= 117.10$ psia
p_i	$= 298.63$ psia
α	$= 10^{-2}$
β	$= 1$
t	$= 0.09$ hr
$V_w C_w \rho_w g / \pi$	$= 8.25 \times 10^{-7}$ ft^2

□ DATA
— TYPE CURVE

$t_0 = 208{:}10{:}10{:}52$
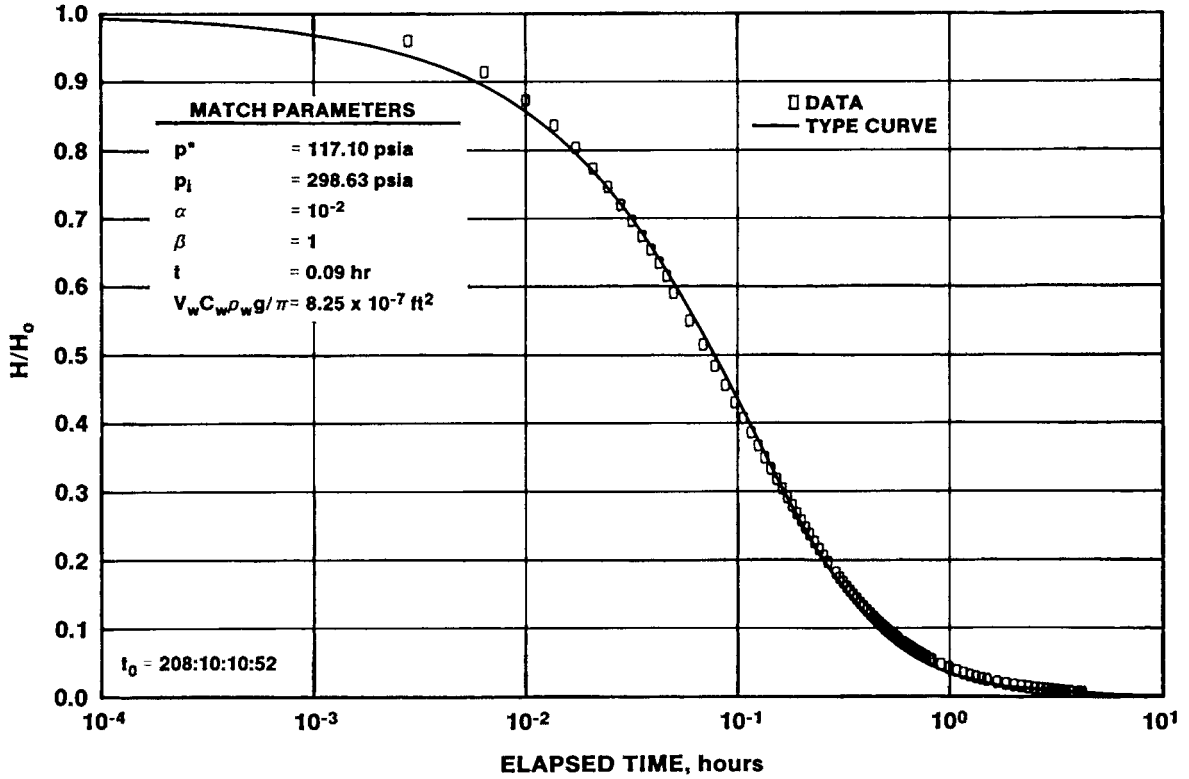
Figure 5-102. H-16/Forty-Niner Clay Pulse-Test Plot

MATCH PARAMETERS

Δp	$= 1.0$ psi
t	$= 1.0$ hr
p_D	$= 0.064$
t_D/C_D	$= 14$
$C_D e^{2s}$	$= 100$
p_i	$= 69.43$ psia

□ PRESSURE DATA
* PRESSURE-DERIVATIVE DATA
— SIMULATIONS

Figure 5-103. H-16/Forty-Niner Clay First Buildup Log-Log Plot with INTERPRET Simulation
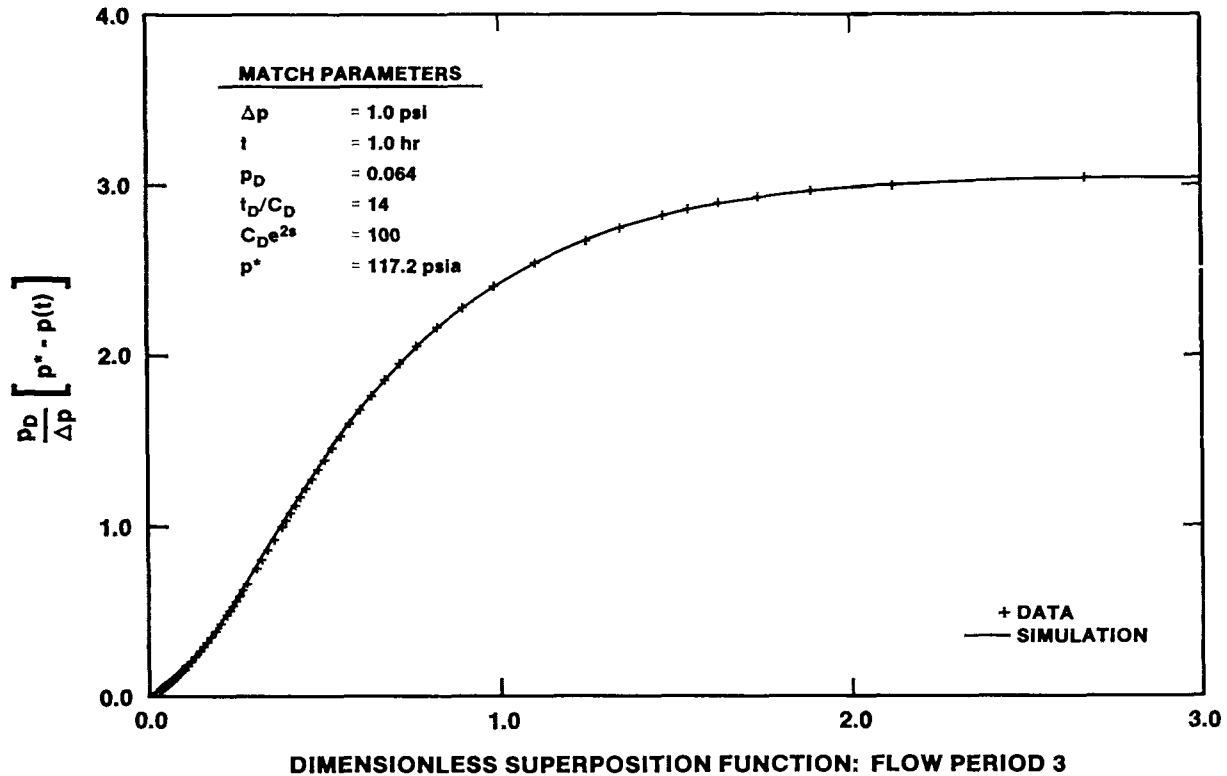
Figure 5-104. H-16/Forty-Niner Clay First Buildup Dimensionless Horner Plot with INTERPRET Simulation

The log-log plot of the SBU data (Figure 5-105) is very similar to that of the FBU data (Figure 5-103). The INTERPRET simulation is also similar, using a transmissivity of 5.6×10^{-3} ft²/day and a skin factor of 0.6 (Table 5-2). Again, overpressure-skin effects are evident in the late-time behavior of the pressure derivative.

Figure 5-106 is an early-time log-log plot of the Forty-niner slug-test data. Because of the low degree of pressure recovery during the slug test, the data are inadequate to provide definitive results on their own, but they do serve to confirm the DST results. The type-curve match shown provides a transmissivity estimate of 5.0×10^{-3} ft²/day (Table 5-2), and uses a static formation pressure estimate of 116.1 psia. Both of these values are in reasonable agreement with the DST interpretations.

In contrast, the transmissivity value provided by the pulse-test interpretation is over an order of magnitude lower than the transmissivity values estimated from the DST and slug-test analyses. This low apparent value of transmissivity may have been caused by two, perhaps interrelated, factors. First, pulse tests inherently test very small volumes of rock around a borehole, much smaller than do DST's and slug tests. The average transmissivity of the rock tested could easily change between the two scales of tests. Second, the pulse test was the first test performed and was an injection test, whereas the DST's and slug test were withdrawal tests. Any skin that may have been present on the borehole wall after drilling, such as a mud cake, could be loosened by a withdrawal test, but would be intensified by an injection test. Consequently, the pulse-injection test may have measured an average transmissivity of both the nearby rock and the wellbore skin. The subsequent DST's and slug test, which caused water to flow into the well, should have served to decrease any skin present, and this may be evidenced by the slight drop in skin values between the FBU and the SBU (Table 5-2). For these reasons, and because of the consistency of the DST and slug-test results, the most reliable value for the transmissivity of the Forty-niner clay at H-16 is probably about 5.3×10^{-3} ft²/day.

126
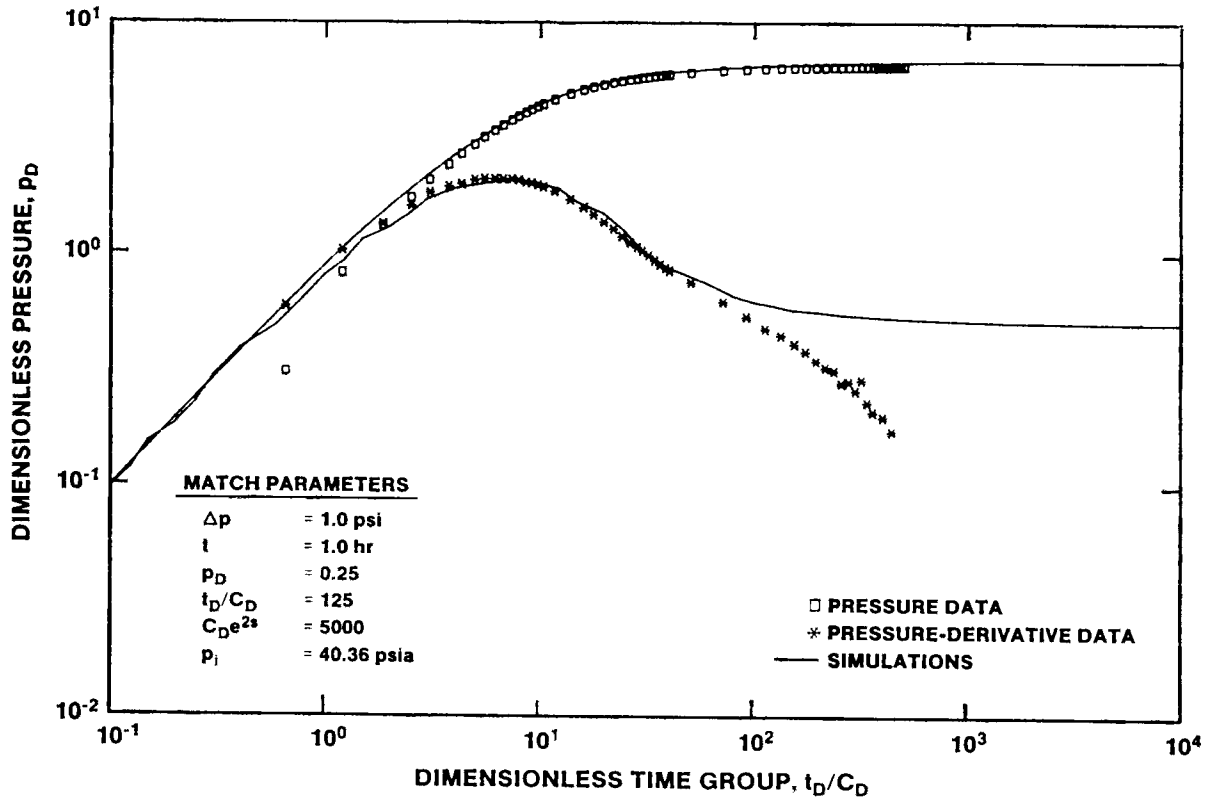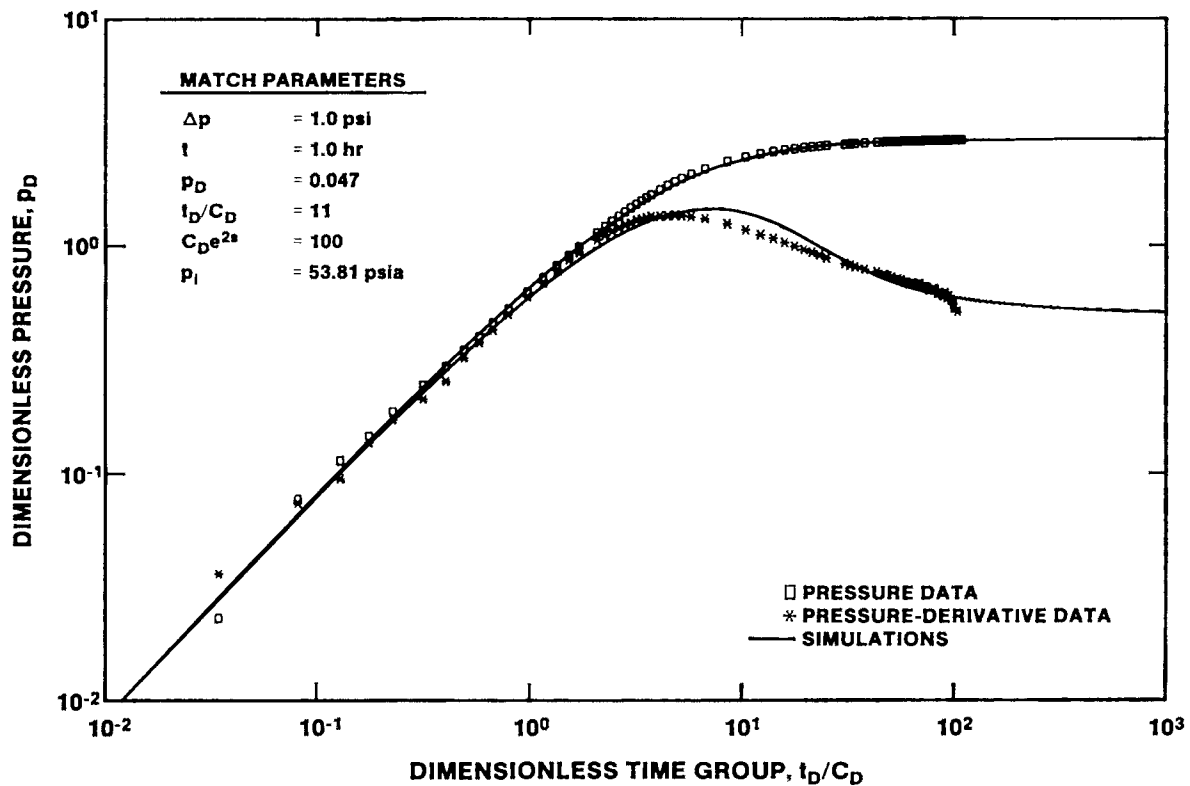
Figure 5-105. H-16/Forty-Niner Clay Second Buildup Log-Log Plot with INTERPRET Simulation
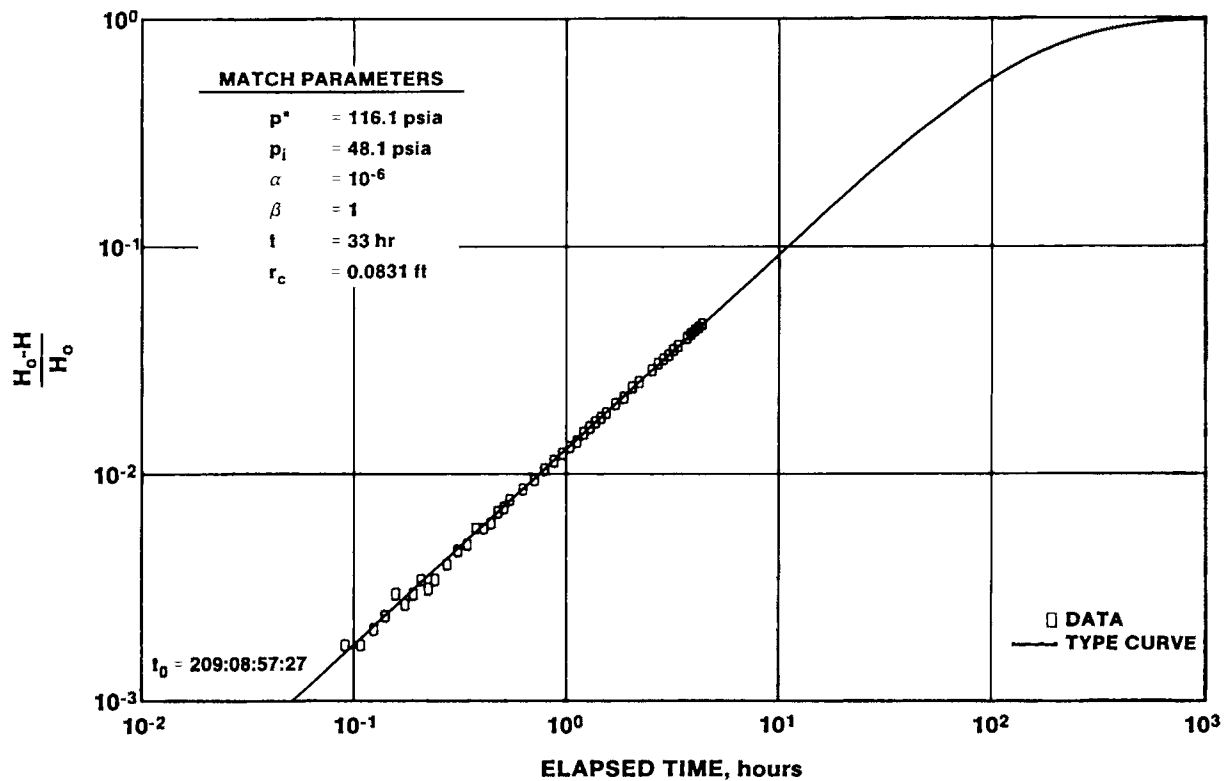
Figure 5-106. H-16/Forty-Niner Clay Early-Time Slug-Test Plot

Estimates of the static formation pressure of the Forty-niner clay at H-16 were obtained from the analyses of the DST and slug-test data, and from the transducer installed to measure the Forty-niner pressure as part of the H-16 5-packer system. The static formation pressure indicated by the slug-test analysis is 116.1 psia. This is 1 psi lower than the value indicated by the DST's, but is consistent with the dissipation of a slight overpressure skin. With the test transducer set at a depth of 542.5 ft in a hole containing fluid with a specific gravity of 1.2, and a measured atmospheric pressure of 14.3 psia, a pressure of 116.1 psia corresponds to a pressure of about 115 psig at the midpoint of the Forty-niner clay about 568 ft deep. In comparison, the Forty-niner transducer of the 5-packer system, which is set at a depth of 548.1 ft, showed a stabilized pressure of 105 psig within several weeks after installation (Stensrud et al., 1988). This also corresponds to a pressure of about 115 psig at the midpoint of the Forty-niner clay, indicating that the value is representative of the formation pressure existing in mid-1987. As noted with regard to the other Rustler members tested at H-16, however, the fluid pressure within the Forty-niner clay could be artificially low because of drainage of water from that unit into the WIPP shafts.

5.3 Dewey Lake Red Beds

Little testing of the Dewey Lake Red Beds near the WIPP site has ever been attempted, primarily because of a lack of evidence of continuous zones of saturation (Mercer, 1983). The Dewey Lake Red Beds are permeable, however, as evidenced by losses of circulation fluid during drilling of holes such as DOE-2 and H-3d, and therefore the unit remains of interest when considering groundwater-transport pathways in the event of a breach of the WIPP facility. Beauheim (1986) reported on unsuccessful attempts to test the lower Dewey Lake at DOE-2. The only other Dewey Lake testing attempted on behalf of the WIPP project was performed at well H-14. No information was obtained during the drilling of H-14 pertaining to the presence or absence of a water table in the Dewey Lake at that location. Nevertheless, limited testing of the lower portion of the Dewey Lake Red Beds was planned based on the supposition that either a water table did exist in the lower Dewey Lake, or sufficient water would have infiltrated into the Dewey Lake during drilling and Rustler testing to allow at least qualitative testing. Descriptions of the test instrumentation and the test data are reported in Stensrud et al. (1987).
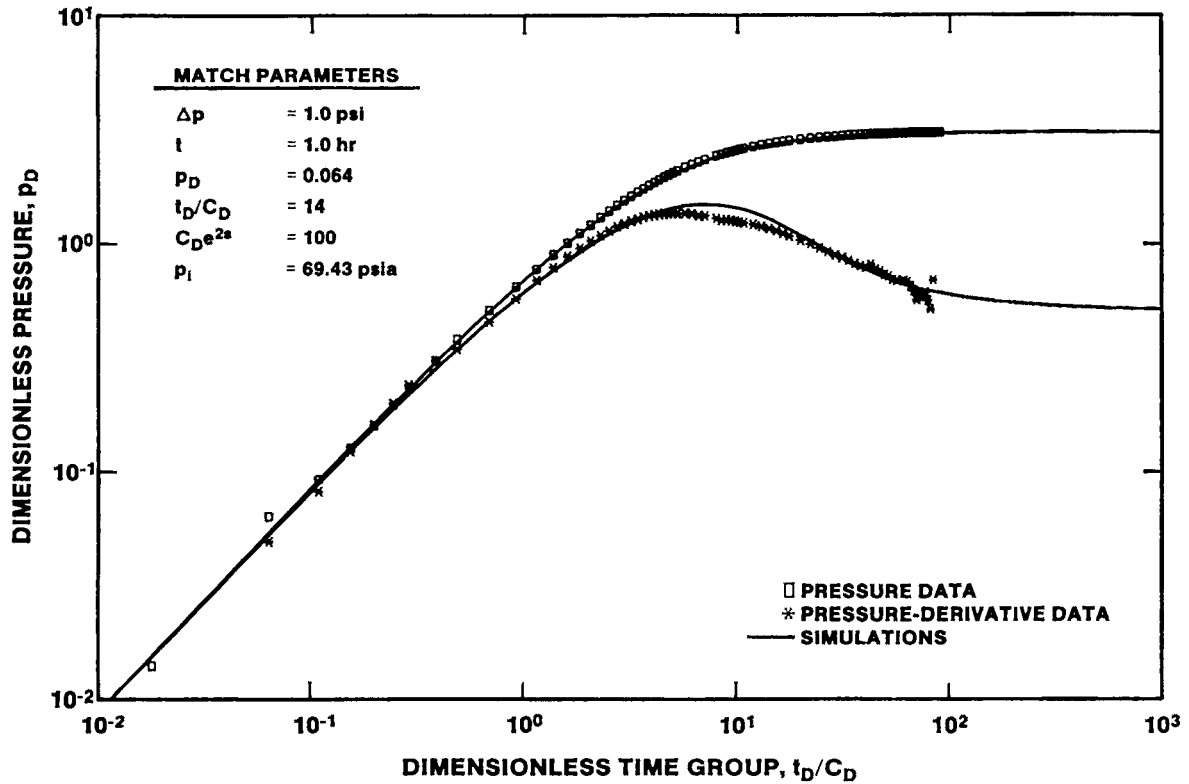
For the tests at H-14, an interval of the lower Dewey Lake from 327.5 to 356.0 ft deep was isolated with a DST straddle tool. The testing was performed on October 15 and 16, 1986 (Figure 5-107). Testing proceeded without a preliminary equilibration period because of assumed very low permeability. An initial 13-minute flow period resulted in very little fluid entering the tubing. The pressure rose about 3 psi during a subsequent 6-hr buildup period.

Start Date: 10/15/1986
Start Time: 08:00:00

Linear-Linear Sequence Plot
H-14/LOWER DEWEY LAKE TEST

Figure 5-107. H-14/Lower Dewey Lake Drillstem and Pulse Testing Linear-Linear Sequence Plot
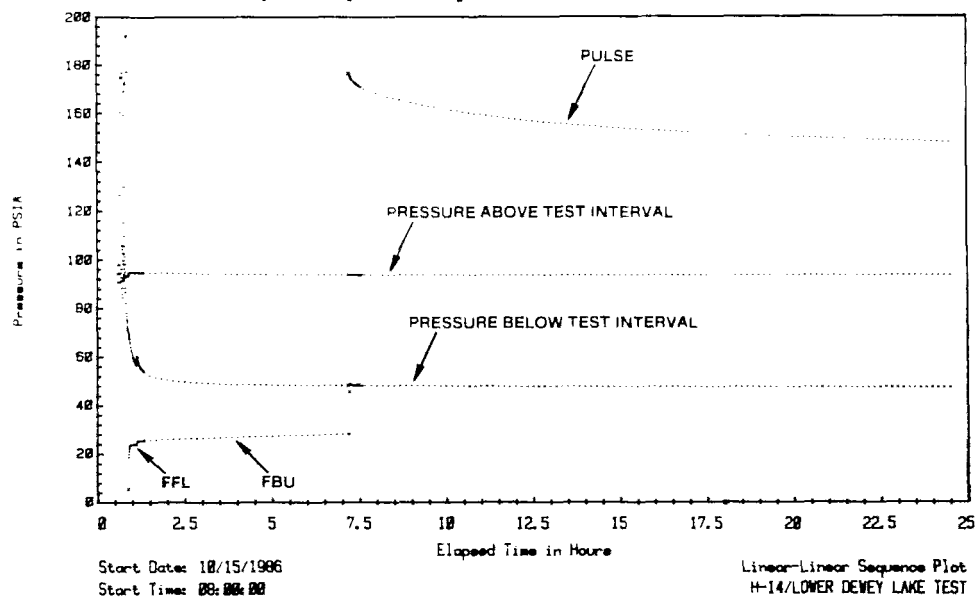
To evaluate the possibility that the pressure was not rising faster during the buildup period because it was already very near the static formation pressure, a pressure-pulse test was performed. The tubing was filled to the surface with brine, and the shut-in tool was opened briefly, transmitting a pressure pulse of about 148 psi to the test interval. The test interval was shut in, and the pressure pulse was allowed to decay for over 17 hr. At the end of that time, the pressure had decreased by only 29 psi, indicating that low permeability was responsible for the slow rate of pressure change during the buildup period.

If a water table exists in the lower Dewey Lake at H-14, then the buildup and pulse-test data in Figure 5-107 should be trending towards a common pressure corresponding to that surface. Given the decreasing slopes of both trends, the two would not intersect for a period measured in weeks, not days. No conclusion can be reached from these data as to the presence or absence of a water table. The transmissivity of the interval tested appears to be at least one, and possibly several, order(s) of magnitude lower than that of the unnamed lower member at H-16 (2×10^{-4} ft²/day), the lowest-transmissivity unit successfully tested.

5.4 Cenozoic Alluvium

The Carper well was the only well tested that is completed in Cenozoic alluvium. Carper was pumped to collect water-quality samples at an average rate of about 14.9 gpm for about 67.5 hr beginning February 14, 1984. Pressure-drawdown data collected during the first 47 hr of pumping are amenable to interpretation, subject to constraints imposed by our limited knowledge of the well completion and associated stratigraphy. No recovery data were collected after the pump was turned off. A more complete description of this test and the test data are contained in Stensrud et al. (1987).

Cooper and Glanzman (1971) reported that the Carper well is cased to 250 ft, and is plugged at 385.6 ft. Thus, the pre-test depth to water of 262.8 ft was below the bottom of the well casing in the open portion of the borehole. This may indicate that the

aquifer is under water-table (unconfined) conditions at this location. Richey et al. (1985) report that aquifers in the alluvium are "usually" under water-table conditions. A possibility also exists that the aquifer continues below the depth where the Carper well is plugged. In this case, the well would only partially penetrate the aquifer.

From a well-test interpretation standpoint, the possibilities mentioned above raise the following points. First, if the aquifer is unconfined and the amount of drawdown (s) is large compared to the total saturated thickness of the aquifer (b), then in the test analysis s should be replaced by s' (Kruseman and DeRidder, 1979), where:

$$s' = s - (s^2/2b). \tag{5.2}$$

Second, if the well does penetrate the aquifer only partially, a semilog plot of the drawdown data should show a decreasing slope with time (Hantush, 1961).

Figure 5-108 shows a log-log plot of the Carper drawdown data, modified using Eq 5.2 under the assumption that the approximately 120 ft of well beneath the static water level represents the entire saturated thickness of an unconfined aquifer. Simulations of these data generated by INTERPRET are also included in the figure. Oscillations induced by pumping-rate fluctuations are evident in both the pressure and pressure-derivative data. The model used for the simulations is representative of a single-porosity medium with a transmissivity of 55 ft²/day (Table 5-2). A dimensionless Horner plot of the modified drawdown data, along with a simulation generated using the same model, is shown in Figure 5-109. No decrease in the slope at late time indicative of partial-penetration effects is evident. The simulation fits the data reasonably well, indicating that an appropriate model has been selected. Hence, the transmissivity value presented above should be representative, at least for the thickness of Cenozoic alluvium tested. No skin factor is reported for this well because any value chosen for total-system compressibility would be purely speculative.
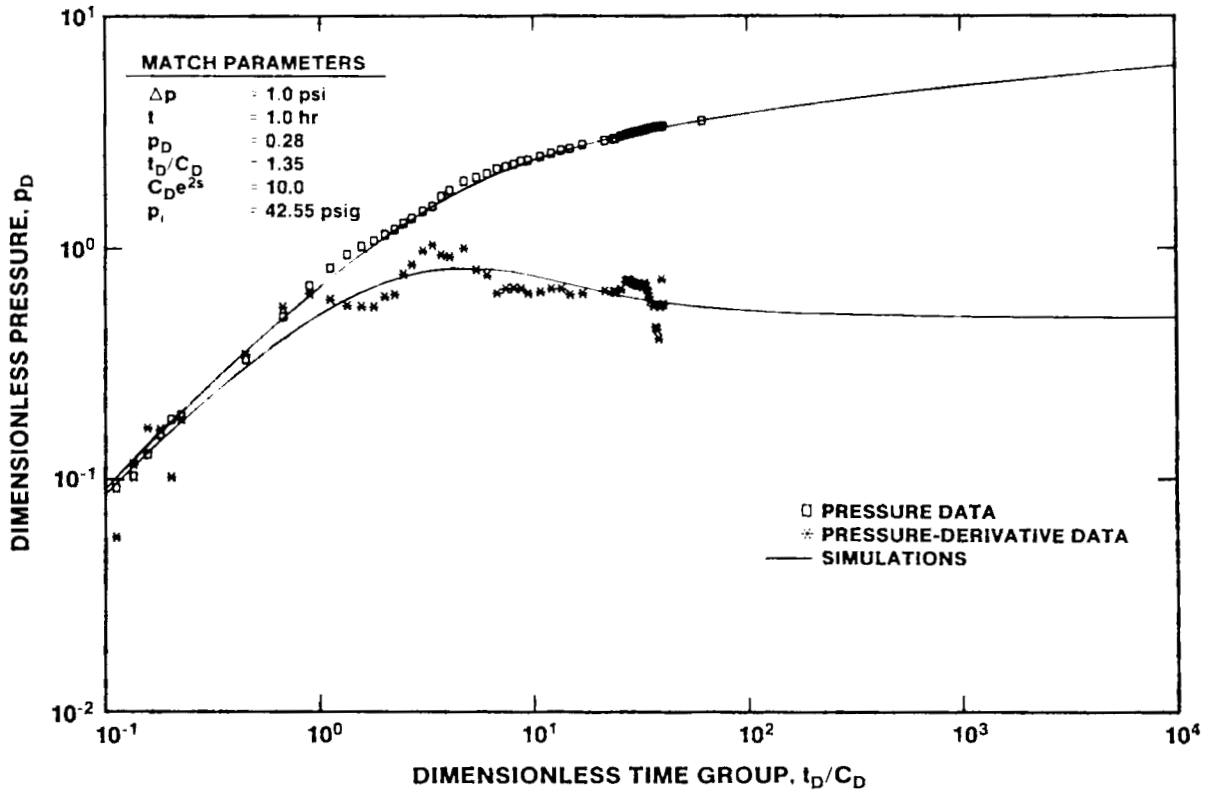
Figure 5-108. Carper/Cenozoic Alluvium Pumping Test Drawdown Log-Log Plot with INTERPRET Simulation
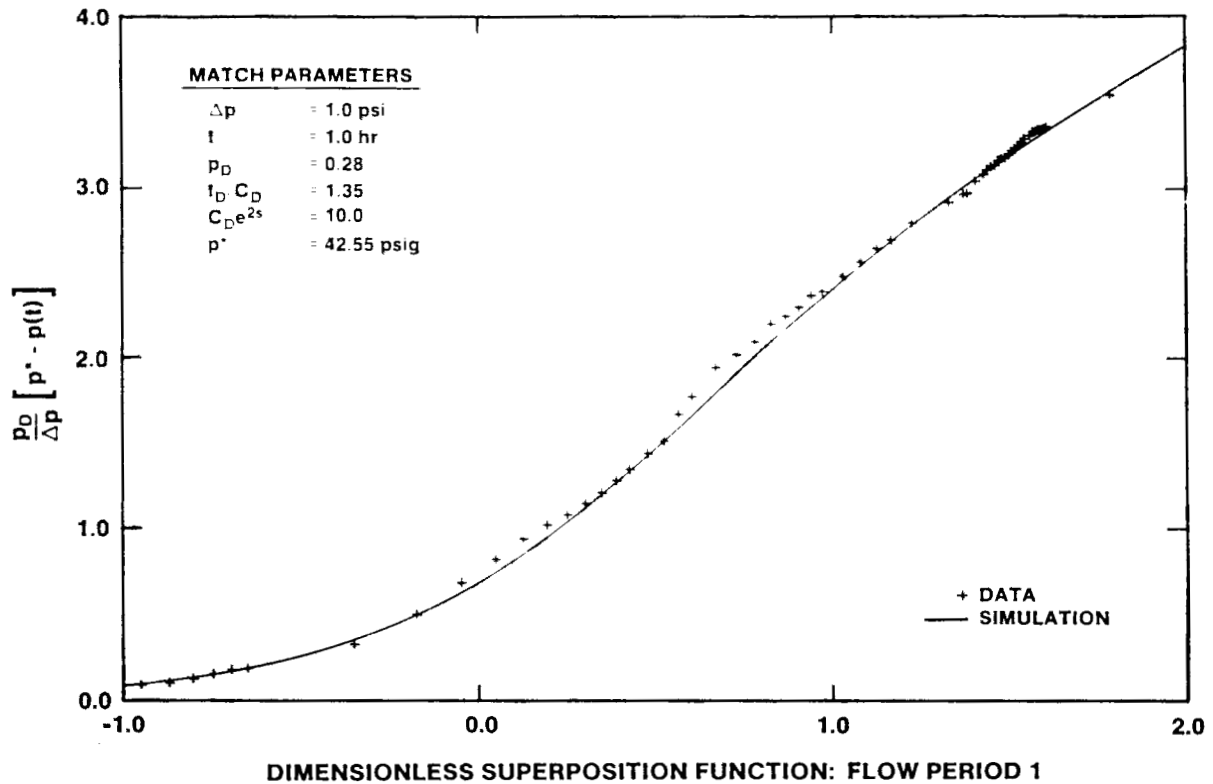
Figure 5-109.   Carper/Cenozoic Alluvium Pumping Test Drawdown Dimensionless Horner Plot
with INTERPRET Simulation

6. DISCUSSION OF RUSTLER FLOW SYSTEM

The single-well testing discussed in this report has provided significant information on the transmissivities and hydraulic-head relations of the five Rustler members. In particular, our knowledge of the distribution of transmissivity within the Culebra dolomite has increased considerably. Section 6.1 attempts to explain the distribution of Culebra transmissivity in the context of geologic models of halite deposition and dissolution within the Rustler Formation. Recent hydraulic-head measurements made at H-3d, H-14, H-16, and DOE-2 have helped to increase our understanding of the directions of potential vertical fluid movement within the Rustler. Section 6.2 discusses the hydraulic-head relations among the Rustler members, and their implications regarding recharge to the Rustler Formation.

6.1 Culebra Transmissivity

Mercer (1983) reported values for Culebra transmissivity at 20 locations. The testing described in this report has provided values for Culebra transmissivity at 15 new locations, and new estimates at 7 locations for which values had previously been reported. Combined with other recent work performed at DOE-2 (Beauheim, 1986), H-3 (Beauheim, 1987a), H-11 (Saulnier, 1987), and WIPP-13 (Beauheim, 1987b), the WIPP project has tested the Culebra at 38 locations. Figure 6-1 shows these 38 locations and the transmissivity values at each provided by this report or those referenced above.

Figure 6-2 shows the areas around the WIPP site where halite is present in the non-dolomite Rustler members, as indicated by Snyder (1985 and personal communication) and Powers (personal communication). According to Snyder, halite was originally deposited in the unnamed lower, Tamarisk, and Forty-niner Members of the Rustler over the entire area covered by Figure 6-2. The present-day absence of halite from these members reflects the eastward progression of a dissolution front. This dissolution front apparently affects the uppermost Rustler halite, that in the Forty-niner, first, and works progressively downsection to the upper Salado

Formation. Thus, the eastward extent of the Forty-niner dissolution front is greater than that of the Tamarisk dissolution front, which is in turn greater than the eastward extent of the dissolution front in the unnamed lower member (Figure 6-2). Dissolution of the upper Salado follows dissolution of halite from the unnamed lower member of the Rustler. Lagging behind the dissolution front in each member is a second front where anhydrite is being hydrated to gypsum. In Snyder's view, as halite is removed beneath the Rustler dolomites, the dolomites subside and fracture. Similar subsidence and fracturing may affect the anhydrites, allowing more groundwater flow through them which may effect their hydration to gypsum. Note that the areas shown on Figure 6-2 indicate only that some halite is present in the appropriate members, not that the full thicknesses originally deposited are present. For example, Snyder (1985) states that only about half of the halite originally present in the unnamed lower member at WIPP-21 is there today.

Alternatively, Holt and Powers (1988) believe that the different amounts of halite seen in the Rustler members at the WIPP site more likely represent original depositional differences and/or syndepositional dissolution than later progressive dissolution. They relate fracturing to stress relief caused by unloading of the Rustler, citing a preponderance of horizontal (as opposed to vertical) fractures within the Rustler as evidence. According to their hypothesis, fracturing would be expected to become less pronounced eastward as the depth of burial of the Rustler increases. Holt and Powers (1988) also do not believe that all of the gypsum present in the Rustler is related to the hydration of anhydrite, but that it is instead primary, pointing to the preservation of primary sedimentary structures as evidence. Holt and Powers do find evidence for late-stage dissolution of halite from the upper Salado in Nash Draw, however, and relate disruption of the overlying Rustler to this dissolution.

As can be seen on Figure 6-2, the highest values of Culebra transmissivity are found in areas in or close
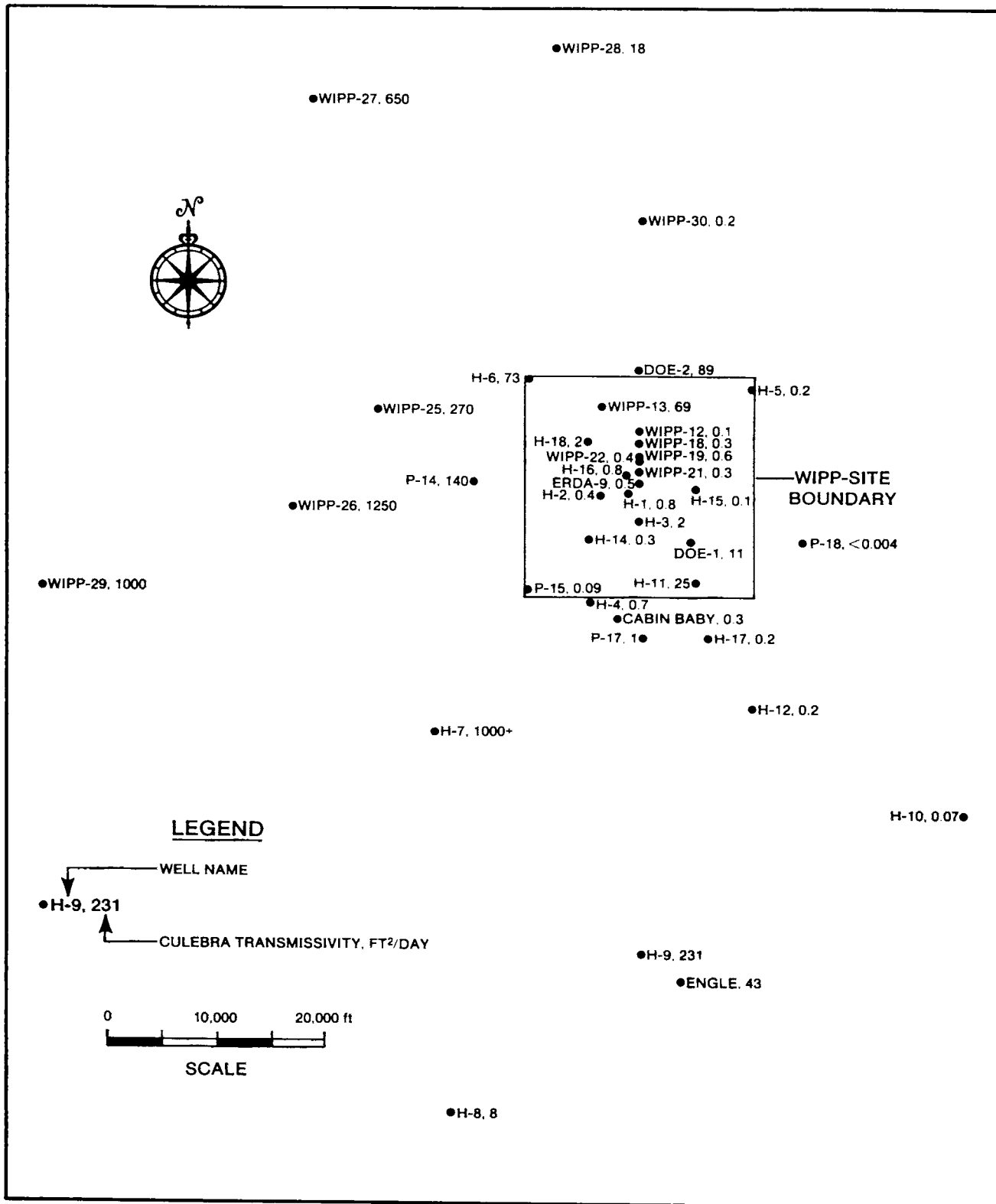
Figure 6-1. Culebra Wells Tested by the WIPP Project
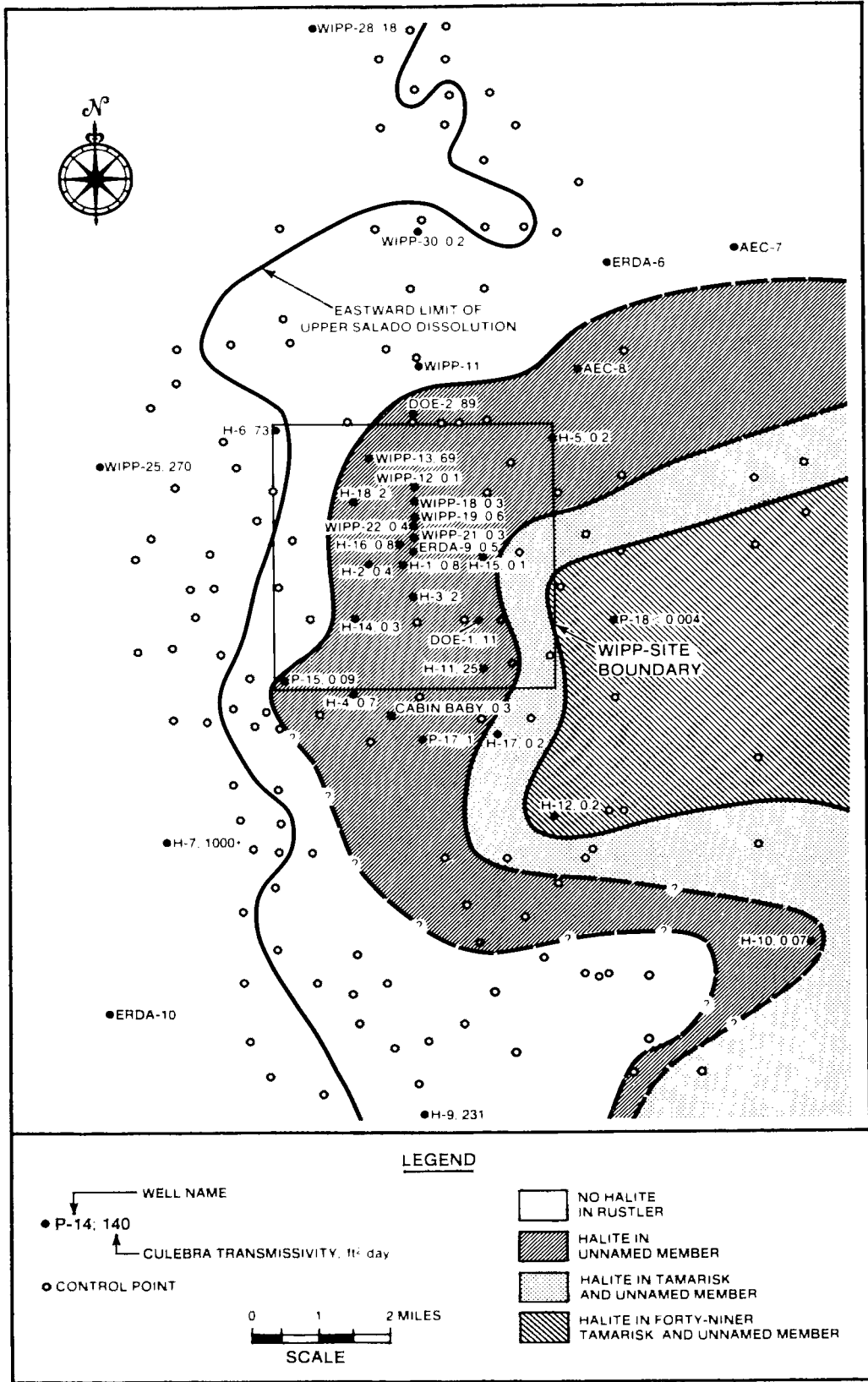
Figure 6-2. Distribution of Rustler Halite and Culebra Transmissivity Around the WIPP Site.

to Nash Draw where no halite is present in the Rustler. At DOE-2 and WIPP-13, which are very close to the boundary west of which no halite is present in the unnamed lower member, the transmissivity of the Culebra is also relatively high. Relatively high transmissivities are also found, however, at DOE-1 and H-11, where little or no halite is missing beneath the Culebra. WIPP-30, on the other hand, lies in an area of no Rustler halite, and yet the transmissivity of the Culebra is low at that location. Neither Snyder's (1985) nor Holt and Powers' (1988) model of halite deposition and dissolution can adequately explain the entire transmissivity distribution observed around the WIPP site.

If the absence of halite in the unnamed lower member is caused by dissolution and if this dissolution causes fracturing of the Culebra as Snyder (1985) suggests, then the high transmissivities shown in the area of no halite on Figure 6-2 would be expected. Further, the high transmissivities at DOE-2 and WIPP-13 could be explained as the result of partial dissolution of halite from the unnamed lower member. The lower transmissivity at H-18, farther east of the no-halite boundary, is also consistent with this hypothesis. The low transmissivity at WIPP-30, however, cannot be explained by this hypothesis, nor can the low transmissivities at H-14 and P-15, which are closer to the no-halite boundary than is H-18. The relatively high transmissivities at DOE-1 and H-11 also cannot be related to dissolution of underlying halite.

Holt and Powers' (1988) model could predict the high transmissivities in Nash Draw by relating them to dissolution of the upper Salado. Their model further states that no Rustler halite was deposited and no dissolution of the Salado has occurred at WIPP-30, thus explaining the low Culebra transmissivity at that location. If their argument that fracturing is related to unloading is correct, then a correlation between the present-day depth of burial of the Culebra and the transmissivity of the Culebra might be expected to exist. Preliminary evaluation by Holt (personal communication) indicates that some correlation between depth of burial and Culebra transmissivity is evident, but that the correlation is not perfect. For example, despite the fact that the Culebra is approximately 200 ft shallower at WIPP-30

than at DOE-2, the Culebra transmissivity is over two orders of magnitude lower at WIPP-30 than at DOE-2. Other, as yet undefined, factors may be as important as depth of burial in controlling the transmissivity of the Culebra. The Holt and Powers (1988) model also fails to explain the relatively high transmissivities at DOE-1 and H-11.

Clearly, neither of the geologic models cited above provides a complete understanding of the distribution of transmissivity within the Culebra. The two models need not be considered completely mutually exclusive, however, and as discussed above, elements of both models provide reasonable explanations of some features observed in the Culebra. Nondeposition (or syndepositional dissolution) of halite may have been more widespread than believed by Snyder (1985), and late-stage dissolution may have occurred more than is believed by Holt and Powers (1988). The most significant problem area is in the vicinity of DOE-1 and H-11, where relatively high transmissivities would not be expected based on either model.

One additional observation that can be made from consideration of Figure 6-2 is that all measurements of Culebra transmissivity greater than 1 ft^2/day coincide with areas having no halite in the Tamarisk. The simple dissolution of Tamarisk halite would not seem likely to affect the transmissivity of the Culebra. The lack of high Culebra transmissivity everywhere that halite has been removed from the Tamarisk further argues against a direct relationship between Culebra transmissivity and Tamarisk halite. Nevertheless, absence of Tamarisk halite appears to be a necessary, but not sufficient, condition for high Culebra transmissivity. Perhaps the removal of Tamarisk halite makes possible a second process that directly affects the transmissivity of the Culebra.

6.2 Hydraulic–Head Relations Among Rustler Members

Mercer (1983) published a set of potentiometric surface maps for the Rustler-Salado contact, Culebra, and Magenta showing the relative water levels of these units in the vicinity of the WIPP site expressed in terms of freshwater head. Although more qualitative than quantitative, the maps show that

freshwater heads in the unnamed lower member of the Rustler at the contact with the Salado Formation are generally higher than freshwater heads in the Culebra, except along the western side of the WIPP site and in Nash Draw. Freshwater heads in the Magenta are also higher than freshwater heads in the Culebra, although the differences between the two decrease to the west towards Nash Draw. These observations indicate that over most of the WIPP site potentials exist for flow upward from the unnamed lower member to the Culebra, and for flow downward from the Magenta to the Culebra. These observations neither support nor contradict the supposition that precipitation on the surface at the WIPP site could be recharging the Rustler, and more particularly, the Culebra.

More recent observations at H-3, H-14, H-16, DOE-2, and in the WIPP underground facility provide more detailed insight into potential directions of vertical fluid movement within the Rustler. Measurements made by the 5-packer tool in H-16 show that the static formation pressure of the unnamed lower member of the Rustler is about 229 psig at a depth of 808 ft (Section 5.2.1), and the static formation pressure of the Culebra is about 133 psig at a depth of 712 ft (Section 5.2.2.7). These values confirm Mercer's (1983) observation that the potential exists for flow vertically upwards from the unnamed lower member to the Culebra, regardless of any uncertainty in the relative specific gravities of the Culebra and unnamed member waters.

The highest specific gravity possible for the unnamed member water is about 1.2, the specific gravity of a brine saturated with respect to sodium chloride. With this specific gravity, the 96-ft elevation difference between the midpoints of the Culebra and the unnamed member siltstone could account for only about 50 psi of the observed 96-psi pressure difference between these two units at H-16. A lower value of specific gravity would lead to a larger residual pressure difference. Thus, the hydraulic gradient between the unnamed member and the Culebra at H-16 is definitely upwards.

The upward hydraulic gradient from the unnamed lower member to the Culebra may have a source below the Rustler in the Salado Formation. Peterson et al. (1987) report formation pressures of 1200 to 1500 psig for the Salado near the WIPP facility 2150 ft deep. The 1342-ft elevation difference between the facility and the midpoint of the unnamed lower member could account for a pressure difference between the two locations of about 700 psi, assuming a brine specific gravity of 1.2. Thus, the residual Salado fluid pressure at the elevation of the midpoint of the unnamed member would be 500 to 800 psig, considerably higher than the 229 psig measured in that member. Based on these data, the vertical hydraulic gradient between the Salado and the unnamed lower member of the Rustler should be upward. This discussion assumes, however, that the distribution of hydraulic properties throughout the Salado allows the pressures measured at the facility horizon to be transmitted upward (with some loss within the Salado) to the base of the Rustler, an assumption that has yet to be verified by hydraulic-head measurements at different depths within the Salado. Nevertheless, a potential for a vertical hydraulic gradient upward from the Salado to the unnamed lower member of the Rustler clearly exists.

Attempts at measuring the static formation pressure of the Tamarisk Member between the Magenta and Culebra failed at DOE-2, H-14, and H-16 because of low permeabilities and associated long pressure-stabilization times. Tamarisk pressures are expected, however, to be intermediate between those of the Magenta and Culebra.

Recent measurements of static formation pressures for the Magenta and Culebra at H-14, H-16, and DOE-2 show similar vertical hydraulic gradients. At H-14, the pressure at the midpoint of the Magenta is 6 to 16 psi higher than the pressure at the midpoint of the Culebra (Sections 5.2.4.1 and 5.2.2.5), while at H-16, the Magenta pressure is 1 psi higher than the Culebra pressure (Sections 5.2.4.2 and 5.2.2.7), and at DOE-2, the Magenta pressure is 3 psi lower than the Culebra pressure (Beauheim, 1986). Considering the elevation differences of 109 to 124 ft between the Magenta and Culebra at those locations, vertical hydraulic gradients must be downward from the Magenta towards the Culebra, regardless of the specific-gravity values used for Magenta and Culebra waters. Thus, these recent measurements of vertical hydraulic gradients agree with Mercer's (1983)

observations regarding the potential for vertical fluid movement downward from the Magenta to the Culebra.

Mercer (1983) had no data on the static formation pressure of the Forty-niner Member of the Rustler Formation. Data are now available from four locations at the WIPP site which show, with varying degrees of certainty, the relation between Forty-niner and Magenta hydraulic heads. The first, and most ambiguous, data were derived from testing at DOE-2 (Beauheim, 1986). The apparent static formation pressures for the Forty-niner claystone and the Magenta were (recalculated here for the midpoints of the units) 194 psig at a depth of 675 ft and 205 psig at a depth of 711 ft, respectively. Beauheim (1986) noted both as being upper bounds for uncertain values. Uhland et al. (1987) report the specific gravities of Magenta waters at H-5c and H-6c as 1.008 and 1.003, respectively. Inasmuch as DOE-2 is approximately midway between H-5c and H-6c, the specific gravity of Magenta water at DOE-2 may be assumed to be about 1.006. With this specific gravity, the fluid pressure from the Magenta would be about 16 psi lower at the midpoint of the Forty-niner claystone than at the midpoint of the Magenta, or about 189 psig. This value is 5 psi lower than the estimated static formation pressure of the Forty-niner, indicating a potential for downward flow from the Forty-niner to the Magenta at DOE-2. However, the uncertainties associated with both the Magenta and Forty-niner pressure estimates at DOE-2 are too great to allow any firm conclusions to be drawn.

Hydraulic-head data for the Magenta and Forty-niner from H-3, H-14, and H-16, however, allow unambiguous determination of vertical flow potentials between the two units. On the H-3 hydropad, well H-3b1 is completed in the Magenta and well H-3d, 32 ft away, is completed in the Forty-niner claystone. The static Magenta water level is about 249 ft below ground surface, and the static Forty-niner water level is about 311 ft below ground surface (Stensrud et al., 1988). The specific gravity of Magenta water at H-3b1 is about 1.006 (Uhland et al., 1987), and the midpoint of the Magenta is about 572 ft below ground surface at H-3b1 (Mercer and Orr, 1979). The static formation pressure of the Magenta is, therefore, about 141 psig at a depth of

572 ft at H-3b1. The specific gravity of the water in H-3d is unknown, but considering that the well was drilled with a brine saturated with respect to sodium chloride and has never been pumped, a specific gravity of 1.2 can be assumed. This assumption is conservative in the sense that it will maximize the calculated static formation pressure for the Forty-niner. With the midpoint of the Forty-niner claystone being about 539 ft deep, the static formation pressure of the Forty-niner is about 119 psig, 22 psi lower than the Magenta pressure. The 33-ft elevation difference between the midpoints of the Magenta and the Forty-niner claystone can account for 14 to 17 psi of this 22-psi difference, depending on whether a specific gravity of 1.006 or 1.2 is used in the calculations, but the Magenta pressure remains at least 5 psi higher than that of the Forty-niner. Furthermore, the possible sources of error in these calculations, notably the specific-gravity values used, all act to minimize the amount of pressure differential between the Forty-niner and the Magenta.

At H-14, the static formation pressure of the Magenta is estimated to be between 102 and 112 psig at a depth of 436 ft (Section 5.2.4.1), and the static formation pressure of the Forty-niner claystone is estimated to be ≤ 71 psig at a depth of 398 ft (Section 5.2.5.1). Thus, the minimum difference is 31 psi. Even using a specific gravity of 1.2, the 38-ft elevation difference between the two units could only account for a pressure difference of 20 psi. Consequently, the Magenta pressure is at least 11 psi higher than that of the Forty-niner claystone.

At H-16, data from the 5-packer tool provide static formation pressure estimates for the Magenta of 134 psig at a depth of 603 ft (Section 5.2.4.2) and for the Forty-niner clay of 115 psig at a depth of 568 ft (Section 5.2.5.2), a difference of 19 psi. Given that the waters in the Magenta and Forty-niner clay have specific gravities between 1.0 and 1.2, 15 to 18 psi of this difference can be accounted for by the elevation difference between the Magenta and the Forty-niner. Thus, the Magenta pressure appears to be slightly higher than that of the Forty-niner. However, conclusions about vertical hydraulic gradients at H-16 may be complicated by potential drawdown effects from fluid leakage from the Rustler members into the nearby WIPP shafts.

Thus, at three of the four locations where data have been collected on both Magenta and Forty-niner hydraulic heads, vertical hydraulic gradients are upward from the Magenta to the Forty-niner. Data from the fourth location, DOE-2, are too ambiguous to allow definition of the gradient. These observations imply that, at least at H-3, H-14, and H-16, precipitation cannot be infiltrating through the Dewey Lake Red Beds and other formations overlying the Rustler and recharging the Rustler below the Forty-niner. Furthermore, unless and until a water table is detected in the lower Dewey Lake and its hydraulic head is measured, the possibility of recharge from the surface reaching even the Forty-niner cannot be evaluated. Efforts are currently underway to determine whether or not a water table exists in the Dewey Lake at H-3 and H-16, but resolution of the question may take several years.

In summary, a more complete understanding of vertical hydraulic-head relations among the Rustler members is available today than existed in 1983.

Data from the WIPP underground facility (Peterson et al., 1987) and H-16 indicate a potential for an upward gradient from the Salado to the lower Rustler. Data from Mercer (1983) and from H-16 indicate that upward hydraulic gradients exist between the unnamed lower member of the Rustler and the Culebra over much of the WIPP site. Attempts to collect representative data on the formation pressure of the Tamarisk have failed to date, but recent data from DOE-2, H-14, and H-16 support Mercer's observation of downward hydraulic gradients from the Magenta to the Culebra at the WIPP site. Together these observations imply that the Culebra, the most transmissive member of the Rustler, acts as a drain on the overlying and underlying Rustler. The data from H-3, H-14, and probably H-16 indicate that the present hydraulic gradient between the Forty-niner and the Magenta is upward at those locations, effectively preventing modern precipitation at the surface from recharging the Magenta or deeper Rustler members. Figure 6-3 illustrates these relationships.
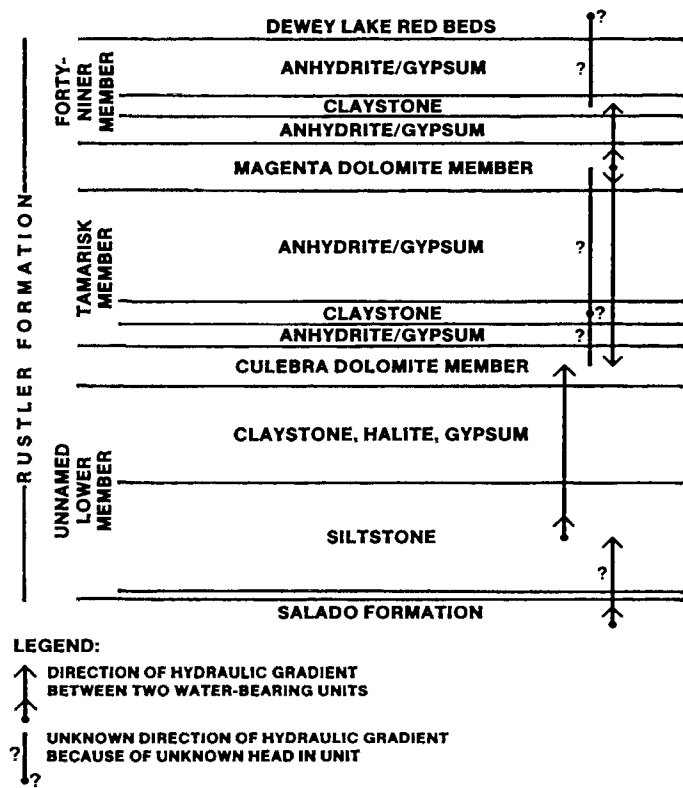

Figure 6-3. Vertical Hydraulic-Head Relations Among the Rustler Members at the WIPP Site

7. SUMMARY AND CONCLUSIONS

Single-well hydraulic tests have been performed at 23 wells at and near the WIPP site between 1983 and 1987. The stratigraphic horizons tested include the upper Castile Formation; the Salado Formation; the unnamed, Culebra, Tamarisk, Magenta, and Forty-niner Members of the Rustler Formation; the Dewey Lake Red Beds; and Cenozoic alluvium. Tests were also performed to assess the integrity of a borehole plug isolating a pressurized brine reservoir in the Anhydrite III unit of the Castile Formation. The types of tests performed included DST's, rising-head slug tests, falling-head slug tests, pulse tests, and pumping tests.

All Castile and Salado testing was performed at well WIPP-12. The purpose of this testing was to try to define the source of high pressures measured at the WIPP-12 wellhead between 1980 and 1985. The tests of the plug above the Castile brine reservoir indicated that the plug may transmit pressure, but that the apparent surface pressure from the underlying brine reservoir is significantly lower than the pressure measured at the wellhead. The remainder of the upper Castile showed no pressure response differentiable from that associated with the plug. After 17 attempts at testing the Salado using a straddle-packer DST tool failed because of an inability to locate good packer seats, 10 attempts were made using a single-packer DST tool and a bridge plug. Four of these attempts were successful. The lower Salado between the Cowden anhydrite and the Castile Formation was tested first, followed by successively larger portions of the Salado up from the Cowden to Marker Bed 136, Marker Bed 103, and finally the well casing. All zones tested showed pressure buildups, but none showed a clear trend to positive surface pressures. The results of the WIPP-12 testing indicate that the source of the high pressures observed at the WIPP-12 wellhead is probably in the Salado Formation rather than in the upper Castile, and that this source must have a very low flow capacity and can only create high pressures in a well shut in over a period of days to weeks.

The unnamed lower member of the Rustler Formation was tested only in well H-16, where DST's were performed on the lower siltstone portion of the unit. The transmissivity of the siltstone is about 2.4×10^{-4} ft^2/day (Table 5-2). The formation pressure of the siltstone is higher than that of the overlying Culebra at H-16 (compensated for the elevation difference), indicating the potential for vertical leakage upward into the Culebra.

The Culebra Dolomite Member of the Rustler Formation was tested in 23 wells. In 12 of these wells (H-4c, H-12, WIPP-12, WIPP-18, WIPP-19, WIPP-21, WIPP-22, WIPP-30, P-15, P-17, ERDA-9, and Cabin Baby-1), falling-head slug tests were the only tests performed. Both falling-head and rising-head slug tests were conducted in H-1, and only a rising-head slug test was conducted in P-18. DST's were performed in conjunction with rising-head slug tests in wells H-14, H-15, H-16, H-17, and H-18. At all of these wells except for H-18, the Culebra has a transmissivity of 1 ft^2/day or less (Table 5-3), and single-porosity models fit the data well. At H-18, the Culebra has a transmissivity of 2 ft^2/day, a value usually associated with double porosity. In this instance, only single-porosity behavior was evident, probably because of the small spatial scale of the tests. Pumping tests were performed in the other 3 Culebra wells: H-8b, DOE-1, and the Engle well. The Culebra appears to behave hydraulically like a double-porosity medium at wells H-8b and DOE-1, where transmissivites are 8.2 and 11 ft^2/day, respectively. The Culebra transmissivity is highest, 43 ft^2/day, at the Engle well. No double-porosity behavior was apparent in the Engle drawdown data, but the observed single-porosity behavior may be related more to wellbore and near-wellbore conditions than to the true nature of the Culebra at that location.

The claystone portion of the Tamarisk Member of the Rustler Formation was tested in wells H-14 and H-16. At H-14, the pressure in the claystone failed to

stabilize in three days of shut-in testing, leading to the conclusion that the transmissivity of the claystone is too low to measure in tests performed on the time scale of days. Similar behavior at H-16 led to the abandonment of testing at that location as well.

The Magenta Dolomite Member of the Rustler Formation was tested in wells H-14 and H-16. Examination of the pressure response during DST's revealed that the Magenta had taken on a significant overpressure skin during drilling and Tamarisk-testing activities. Overpressure-skin effects were less pronounced during the drillstem and rising-head slug tests performed on the Magenta at H-16. The transmissivity of the Magenta at H-14 is about 5.5 x 10^{-3} ft^2/day, while at H-16 it is about 2.7 x 10^{-2} ft^2/day (Table 5-2). The static formation pressures calculated for the Magenta at H-14 and H-16 are higher than those of the other Rustler members.

The Forty-niner Member of the Rustler Formation was also tested in wells H-14 and H-16. Two portions of the Forty-niner were tested in H-14: the medial claystone and the upper anhydrite. DST's and a rising-head slug test were performed on the claystone. The transmissivity of the claystone is about 7 x 10^{-2} ft^2/day (Table 5-2). A prolonged buildup test performed on the Forty-niner anhydrite revealed a transmissivity too low to measure on a time scale of days. A pulse test, DST's, and a rising-head slug test were performed on the Forty-niner clay at H-16, indicating the clay has a transmissivity of about 5.3 x 10^{-3} ft^2/day (Table 5-2). Formation pressures estimated for the Forty-niner at H-14 and H-16 are lower than those calculated for the Magenta (compensated for the elevation differences), indicating that water cannot be moving downwards from the Forty-niner to the Magenta at these locations.

The lower portion of the Dewey Lake Red Beds, tested only at well H-14, also has a transmissivity lower than could be measured in a few days' time.

No information was obtained at H-14 pertaining to the presence or absence of a water table in the Dewey Lake Red Beds.

The hydraulic properties of Cenozoic alluvium were investigated in a pumping test performed at the Carper well. The alluvium appears to be under water-table conditions at that location. An estimated 120 ft of alluvium were tested, with an estimated transmissivity of 55 ft^2/day (Table 5-2).

The database on the transmissivity of the Culebra dolomite has increased considerably since Mercer's (1983) summary report on WIPP hydrology. Mercer (1983) reported values of Culebra transmissivity from 20 locations. This report and other recent reports have added values from 18 new locations, and have significantly revised the estimated transmissivities reported for several of the original 20 locations. In general, the Culebra is fractured and exhibits double-porosity hydraulic behavior at locations where its transmissivity is greater than 1 ft^2/day. These locations usually, but not always, correlate with the absence of halite in the unnamed member beneath the Culebra, leading to a hypothesis that the dissolution of halite from the unnamed member causes subsidence and fracturing of the Culebra. This hypothesis is incomplete, however, because relatively high transmissivities have been measured at DOE-1 and H-11 where halite is still present beneath the Culebra, and low transmissivity has been measured at WIPP-30 where halite is absent beneath the Culebra.

Recent measurements of the hydraulic heads of the Rustler members confirm Mercer's (1983) observations that over most of the WIPP site, vertical hydraulic gradients within the Rustler are upward from the unnamed lower member to the Culebra, and downward from the Magenta to the Culebra. New data on hydraulic heads of the Forty-niner claystone show that hydraulic gradients are upward from the Magenta to the Forty-niner, effectively preventing precipitation at the surface at the WIPP site from recharging the Magenta or deeper Rustler members.

REFERENCES

Bachman, G.O. 1984. *Regional Geology of Ochoan Evaporites, Northern Part of Delaware Basin.* Circular 184 (Socorro, NM: New Mexico Bureau of Mines and Mineral Resources).

Bartel, L. C. in preparation. *Results From EM Surface Surveys to Characterize the Culebra Aquifer at the WIPP Site.* SAND87-1246 (Albuquerque, NM: Sandia National Laboratories).

Beauheim, R.L. 1986. *Hydraulic-Test Interpretations for Well DOE-2 at the Waste Isolation Pilot Plant (WIPP) Site,* SAND86-1364 (Albuquerque, NM: Sandia National Laboratories).

Beauheim, R.L. 1987a. *Analysis of Pumping Tests of the Culebra Dolomite Conducted at the H-3 Hydropad at the Waste Isolation Pilot Plant (WIPP) Site,* SAND86-2311 (Albuquerque, NM: Sandia National Laboratories).

Beauheim, R.L. 1987b. *Interpretation of the WIPP-13 Multipad Pumping Test of the Culebra Dolomite at the Waste Isolation Pilot Plant (WIPP) Site,* SAND87-2456 (Albuquerque, NM: Sandia National Laboratories).

Beauheim, R.L.; Hassinger, B.W.; and Klaiber, J.A. 1983. *Basic Data Report for Borehole Cabin Baby-1 Deepening and Hydrologic Testing.* WTSD-TME-020 (Albuquerque, NM: US DOE).

Black, S.R. 1982. *Basic Data Report for Borehole WIPP-12 Deepening.* TME 3148 (Albuquerque, NM: US DOE).

Borns, D.J., and Shaffer, S.E. 1985. *Regional Well-Log Correlation in the New Mexico Portion of the Delaware Basin,* SAND83-1798 (Albuquerque, NM: Sandia National Laboratories).

Bourdet, D., and Gringarten, A.C. 1980. *Determination of Fissure Volume and Block Size in Fractured Reservoirs by Type-Curve Analysis,* SPE 9293 (Richardson, TX: Soc Pet Eng).

Bourdet, D.; Ayoub, J.A.; and Pirard, Y.M. 1984. *Use of Pressure Derivative in Well Test Interpretation,* SPE 12777 (Richardson, TX: Soc Pet Eng).

Bredehoeft, J.D., and Papadopulos, S.S. 1980. "A Method for Determining the Hydraulic Properties of Tight Formations," *Water Resources Research* 16(1):233-38.

Cinco-Ley, H.; Samaniego-V., F.; and Kucuk, F. 1985. *The Pressure Transient Behavior for Naturally Fractured Reservoirs with Multiple Block Size,* SPE 14168 (Richardson, TX: Soc Pet Eng).

Cooper, H.H.; Bredehoeft, J.D.; and Papadopulos, I.S. 1967. "Response of a Finite-Diameter Well to an Instantaneous Charge of Water," *Water Resources Research* 3(1):263-69.

Cooper, J.B., and Glanzman, V.M. 1971. *Geohydrology of Project Gnome Site, Eddy County, New Mexico.* USGS Prof Paper 712-A (Washington, DC: US GPO), 24 pp.

D'Appolonia Consulting Engineers, Inc. 1983. *Data File Report, ERDA-6 & WIPP-12 Testing, Addendum 2,* Volume VI (Albuquerque, NM: US DOE).

de Swaan, A.O. 1976. "Analytical Solutions for Determining Naturally Fractured Reservoir Properties by Well Testing," *Soc Pet Eng J* (June 1976):117-22.

Earlougher, R.C., Jr. 1977. *Advances in Well Test Analysis.* Monograph Volume 5 (Dallas, TX: Soc Pet Eng of AIME), 264 pp.

Ehlig-Economides, C.A. 1979. *Well Test Analysis for Wells Produced at a Constant Pressure,* PhD Dissertation (Palo Alto, CA: Stanford Univ Dept of Pet Eng), 117 pp.

Ferris, J.G.; Knowles, D.B.; Brown, R.H.; and Stallman, R.W. 1962. *Theory of Aquifer Tests, Ground-Water Hydraulics.* USGS Water-Supply Paper 1536-E (Washington, DC: US GPO), 174 pp.

Freeland, M.H. 1982. *Basic Data Report for Borehole DOE-1.* TME 3159 (Albuquerque, NM: US DOE).

Freeze, R.A., and Cherry, J.A. 1979. *Groundwater* (Englewood Cliffs, NJ: Prentice-Hall, Inc), 604 pp.

Gonzalez, D.D. 1983. *Groundwater Flow in the Rustler Formation, Waste Isolation Pilot Plant (WIPP), Southeast New Mexico (SENM):* Interim Report, SAND82-1012 (Albuquerque, NM: Sandia National Laboratories).

Gringarten, A.C. 1984. "Interpretation of Tests in Fissured and Multilayered Reservoirs with Double-Porosity Behavior: Theory and Practice," *J Pet Tech* 36(4):549-64.

Gringarten, A.C. 1986. *Computer-Aided Well Test Analysis,* SPE 14099 (Richardson, TX: Soc Pet Eng).

Gringarten, A.C.; Ramey, H.J., Jr.; and Raghavan, R. 1974. "Unsteady-State Pressure Distributions Created by a Well with a Single Infinite-Conductivity Vertical Fracture," *Soc Pet Eng J* 14(4):347-60.

Gringarten, A.C.; Bourdet, D.P.; Landel, P.A.; and Kniazeff, V.J. 1979. *A Comparison Between Different Skin and Wellbore Storage Type-Curves for Early-Time Transient Analysis,* SPE 8205 (Richardson, TX: Soc Pet Eng).

Grisak, G.E.; Pickens, J.F.; Avis, J.D.; Belanger, D.W.; Thury, M.; and Schneider, A. 1985. "Principles of Hydrogeologic Investigations at Depth in Crystalline Rock," *Proc Int Assn of Hydrogeologists Memoires* 17(1):52-71 (Tucson, AZ, January 7-12, 1985).

Hantush, M.S. 1961. "Aquifer Tests on Partially Penetrating Wells," *J Hydraulics Division, Proc Am Soc Civil Eng* HY5:171-95.

Haug, A.; Kelley, V.A.; LaVenue, A.M.; and Pickens, J.F. 1987. *Modeling of Ground-Water Flow in the Culebra Dolomite at the Waste Isolation Pilot Plant (WIPP) Site:* Interim Report, SAND86-7167 (Albuquerque, NM: Sandia National Laboratories).

Holt, R.M., and Powers, D.W. 1988. *Facies Variability and Post-Depositional Alteration Within the Rustler Formation in the Vicinity of the Waste Isolation Pilot Plant, Southeastern New Mexico.* DOE/WIPP-88-004 (Carlsbad, NM: US DOE).

Horner, D.R. 1951. "Pressure Buildup in Wells," *Proc Third World Pet Cong* 2:503-23 (The Hague, Netherlands). Reprinted 1967. Pressure Analysis Methods, AIME Reprint Series 9:45-50 (Richardson, TX: Soc Pet Eng).

HydroGeoChem, Inc. 1985. *WIPP Hydrology Program, Waste Isolation Pilot Plant, SENM, Hydrologic Data Report #1,* SAND85-7206 (Albuquerque, NM: Sandia National Laboratories).

INTERA Technologies, Inc. 1986. *WIPP Hydrology Program, Waste Isolation Pilot Plant, Southeastern New Mexico, Hydrologic Data Report #3*, SAND86-7109 (Albuquerque, NM: Sandia National Laboratories).

Jenkins, D.N., and Prentice, J.K. 1982. "Theory for Aquifer Test Analysis in Fractured Rocks Under Linear (Nonradial) Flow Conditions," *Ground Water* 20(1):12-21.

Jones, C.L. 1978. *Test Drilling for Potash Resources: Waste Isolation Pilot Plant Site, Eddy County, New Mexico.* USGS Open-File Rpt 78-592, 2 volumes (Denver, CO).

Jones, C.L.; Bowles, C.G.; and Bell, K.G. 1960. *Experimental Drill Hole Logging in Potash Deposits of the Carlsbad District, New Mexico.* USGS Open-File Rpt 502 (Washington, DC: US GPO), 25 pp.

Kazemi, H. 1969. "Pressure Transient Analysis of Naturally Fractured Reservoirs with Uniform Fracture Distribution," *Soc Pet Eng J* (Dec 1969):451-62.

Kelley, V.A., and Pickens, J.F. 1986. *Interpretation of the Convergent-Flow Tracer Tests Conducted in the Culebra Dolomite at the H-3 and H-4 Hydropads, Waste Isolation Pilot Plant (WIPP)*, SAND86-7161 (Albuquerque, NM: Sandia National Laboratories).

Kruseman, G.P., and DeRidder, N.A. 1979. *Analysis and Evaluation of Pumping Test Data.* Bulletin 11 (Wageningen, the Netherlands: International Institute for Land Reclamation and Improvement), 200 pp.

Mavor, M.J., and Cinco-Ley, H. 1979. *Transient Pressure Behavior of Naturally Fractured Reservoirs*, SPE 7977 (Richardson, TX: Soc Pet Eng).

Mercer, J.W. 1983. *Geohydrology of the Proposed Waste Isolation Pilot Plant Site, Los Medanos Area, Southeastern New Mexico.* USGS Water-Resources Investigations Rpt 83-4016 (Albuquerque, NM), 113 pp.

Mercer, J.W. 1987. *Compilation of Hydrologic Data from Drilling the Salado and Castile Formations Near the Waste Isolation Pilot Plant (WIPP) Site in Southeastern New Mexico*, SAND86-0954 (Albuquerque, NM: Sandia National Laboratories).

Mercer, J.W.; Davis, P.; Dennehy, K.F.; and Goetz, C.L. 1981. *Results of Hydrologic Tests and Water-Chemistry Analyses, Wells H-4A, H-4B, and H-4C at the Proposed Waste Isolation Pilot Plant Site, Southeastern New Mexico.* USGS Water-Resources Investigations Rpt 81-36 (Albuquerque, NM), 92 pp.

Mercer, J.W., and Orr, B.R. 1979. *Interim Data Report on the Geohydrology of the Proposed Waste Isolation Pilot Plant Site, Southeast New Mexico.* USGS Water-Resources Investigations Rpt 79-98 (Albuquerque, NM), 178 pp.

Moench, A.F. 1984. "Double-Porosity Models for a Fissured Groundwater Reservoir with Fracture Skin," *Water Resources Research* 20(7):831-46.

Peterson, E.W.; Lagus, P.L.; and Lie, K. 1987. *WIPP Horizon Free Field Fluid Transport Characteristics*, SAND87-7164 (Albuquerque, NM: Sandia National Laboratories).

Popielak, R.S.; Beauheim, R.L.; Black, S.R.; Coons, W.E.; Ellingson, C.T.; and Olsen, R.L. 1983. *Brine Reservoirs in the Castile Formation, Southeastern New Mexico.* TME 3153 (Albuquerque, NM: US DOE).

Ramey, H.J., Jr.; Agarwal, R.G.; and Martin, I. 1975. "Analysis of 'Slug Test' or DST Flow Period Data," *J Can Pet Tech* 14(3):37-47.

Richey, S.F. 1986. *Hydrologic-Test Data from Wells at Hydrologic-Test Pads H-7, H-8, H-9, and H-10 Near the Proposed Waste Isolation Pilot Plant Site, Southeastern New Mexico.* USGS Open-File Rpt 86-413 (Albuquerque, NM), 126 pp.

Richey, S.F. 1987. *Preliminary Hydrologic Data for Wells Tested in Nash Draw, Near the Proposed Waste Isolation Pilot Plant Site, Southeastern New Mexico.* USGS Open-File Rpt 87-37 (Albuquerque, NM), 131 pp.

Richey, S.F.; Wells, J.G.; and Stephens, K.T. 1985. *Geohydrology of the Delaware Basin and Vicinity, Texas and New Mexico.* USGS Water-Resources Investigations Rpt 84-4077 (Albuquerque, NM), 99 pp.

Sandia Laboratories and U.S. Geological Survey. 1980a. *Basic Data Report for Drillhole WIPP 18 (Waste Isolation Pilot Plant - WIPP),* SAND79-0275 (Albuquerque, NM: Sandia National Laboratories).

Sandia Laboratories and U.S. Geological Survey. 1980b. *Basic Data Report for Drillhole WIPP 19 (Waste Isolation Pilot Plant - WIPP),* SAND79-0276 (Albuquerque, NM: Sandia National Laboratories).

Sandia Laboratories and U.S. Geological Survey. 1980c. *Basic Data Report for Drillhole WIPP 21 (Waste Isolation Pilot Plant - WIPP),* SAND79-0277 (Albuquerque, NM: Sandia National Laboratories).

Sandia Laboratories and U.S. Geological Survey. 1980d. *Basic Data Report for Drillhole WIPP 22 (Waste Isolation Pilot Plant - WIPP),* SAND79-0278 (Albuquerque, NM: Sandia National Laboratories).

Sandia National Laboratories and D'Appolonia Consulting Engineers. 1982. *Basic Data Report for Drillhole WIPP 12 (Waste Isolation Pilot Plant - WIPP),* SAND82-2336 (Albuquerque, NM: Sandia National Laboratories).

Sandia National Laboratories and U.S. Geological Survey. 1983. *Basic Data Report for Drillhole ERDA 9 (Waste Isolation Pilot Plant - WIPP),* SAND79-0270 (Albuquerque, NM: Sandia National Laboratories).

Saulnier, G.J., Jr. 1987. *Analysis of Pumping Tests of the Culebra Dolomite Conducted at the H-11 Hydropad at the Waste Isolation Pilot Plant (WIPP) Site,* SAND87-7124 (Albuquerque, NM: Sandia National Laboratories).

Saulnier, G.J., Jr.; Freeze, G.A.; and Stensrud, W.A. 1987. *WIPP Hydrology Program, Waste Isolation Pilot Plant, Southeastern New Mexico, Hydrologic Data Report #4,* SAND86-7166 (Albuquerque, NM: Sandia National Laboratories).

Snyder, R.P. 1985. *Dissolution of Halite and Gypsum, and Hydration of Anhydrite to Gypsum, Rustler Formation, in the Vicinity of the Waste Isolation Pilot Plant, Southeastern New Mexico.* USGS Open-File Rpt 85-229 (Washington, DC: US GPO), 11 pp.

Stensrud, W.A.; Bame, M.A.; Lantz, K.D.; LaVenue, A.M.; Palmer, J.B.; and Saulnier, G.J., Jr. 1987. *WIPP Hydrology Program, Waste Isolation Pilot Plant, Southeastern New Mexico, Hydrologic Data Report #5,* SAND87-7125 (Albuquerque, NM: Sandia National Laboratories).

Stensrud, W.A.; Bame, M.A.; Lantz, K.D.; Cauffman, T.L.; Palmer, J.B.; and Saulnier, G.J., Jr. 1988. *WIPP Hydrology Program, Waste Isolation Pilot Plant, Southeastern New Mexico, Hydrologic Data Report #6,* SAND87-7166 (Albuquerque, NM: Sandia National Laboratories).

Stensrud, W.A.; Bame, M.A.; Lantz, K.D.; Cauffman, T.L.; Palmer, J.B.; and Saulnier, G.J., Jr. in preparation. *WIPP Hydrology Program, Waste Isolation Pilot Plant, Southeastern New Mexico, Hydrologic Data Report #7*, SAND88-7014 (Albuquerque, NM: Sandia National Laboratories).

Theis, C.V. 1935. "The Relation Between the Lowering of the Piezometric Surface and the Rate and Duration of Discharge of a Well Using Ground-Water Storage," *Trans AGU* 2:519-24.

Warren, J.E., and Root, P.J. 1963. "The Behavior of Naturally Fractured Reservoirs," *Soc Pet Eng J* (Sept 1963):245-55.

Wells, J.G., and Drellack, S.L., Jr. 1982. *Geologic and Well-Construction Data for the H-8 Borehole Complex Near the Proposed Waste Isolation Pilot Plant Site, Southeastern New Mexico.* USGS Water-Resources Investigations Rpt 82-4118 (Albuquerque, NM), 42 pp.

APPENDIX A

TECHNIQUES FOR ANALYZING SINGLE-WELL HYDRAULIC-TEST DATA

The techniques used in this report to analyze data from single-well hydraulic tests may be divided by test type. The techniques used to interpret data from pumping tests and DST buildups are described in Section A.1. Section A.2 describes slug-test and DST flow-period data analysis. Pressure-pulse test analysis is discussed in Section A.3. The well-test interpretation code INTERPRET, used in the pumping-test and DST-buildup analyses, is described in Section A.4.

A.1 PUMPING-TEST AND DST-BUILDUP DATA ANALYSIS

Pumping-test data, both from the drawdown and recovery periods, may be analyzed with either single-porosity or double-porosity interpretation techniques, and with log-log and semilog plotting techniques. The same techniques can be applied to the interpretation of data from DST buildups. These techniques are described below. When interpreting pumping-test data, the drawdown and recovery analyses should provide nearly identical results. Consistency of results validates the conceptual model used in the analysis.

A.1.1 Single-Porosity Log-Log Analysis

Single-porosity log-log analysis of drawdown and buildup (recovery) data was performed using a method presented by Gringarten et al. (1979) and modified to include the pressure-derivative technique of Bourdet et al. (1984). This method applies to both the drawdown and buildup during or after a constant-rate flow period of a well that fully penetrates a homogeneous, isotropic, horizontal, confined porous medium. When used to interpret a test performed in a heterogeneous, anisotropic aquifer, the method provides volumetrically averaged results.

Gringarten et al. (1979) constructed a family of log-log type curves of dimensionless pressure, p_D, versus a dimensionless time group defined as dimensionless time, t_D, divided by dimensionless wellbore storage, C_D, where:

$$p_D = \frac{kh}{141.2qB\mu} \Delta p \tag{A-1}$$

$$t_D = \frac{0.000264 \, kt}{\phi\mu c_t r_w^2} \tag{A-2}$$

$$C_D = \frac{0.8936 \, C}{\phi c_t h r_w^2} \tag{A-3}$$

$$\frac{t_D}{C_D} = \frac{0.000295\ kht}{\mu C} \qquad\qquad\qquad (A\text{-}4)$$

and:

k = permeability, millidarcies (md)

h = test interval thickness, ft

Δp = change in pressure, psi

q = flow rate, barrels/day (BPD)

B = formation volume factor (B = 1.0 in single-phase water reservoir)

μ = fluid viscosity, centipoises (cp)

t = elapsed time, hr

ϕ = porosity

c_t = total-system compressibility, 1/psi

r_w = wellbore radius, ft

C = wellbore storage coefficient, barrels/psi.

Each type curve in the family of curves (Figure A-1) is characterized by a distinct value of the parameter $C_D e^{2s}$, where:

s = skin factor.
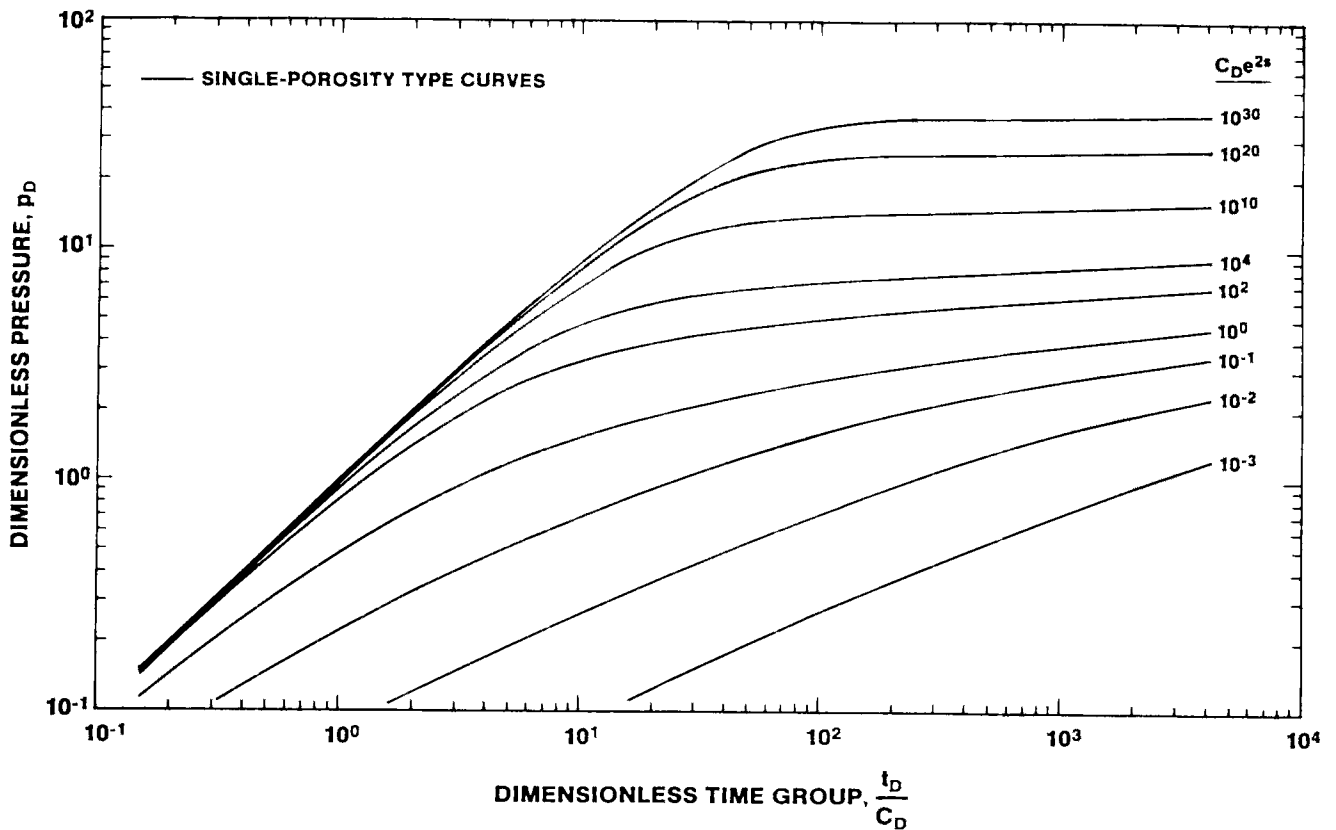
Figure A-1.   Single-Porosity Type Curves for Wells with Wellbore Storage and Skin

A positive value of s indicates wellbore damage, or a wellbore with a lower permeability than the formation as a whole as a result of drilling effects. Conversely, a negative value of s indicates a wellbore with enhanced permeability, usually caused by one or more fractures intersecting the wellbore.

The type curves begin with an initial segment having a unit slope, corresponding to early-time dominance of the pressure response by wellbore storage and skin effects. The duration of this unit slope segment is proportional to the amount of wellbore storage and skin that are present. At late time, the curves flatten as infinite-acting radial flow dominates.

Bourdet et al. (1984) added the pressure derivative to the analytical procedure by constructing a family of type curves of the semilog slope of the dimensionless pressure response versus the same dimensionless time group, t_D/C_D. The semilog slope of the dimensionless pressure response is defined as:

$$\frac{dp_D}{d\ln(t_D/C_D)} = \frac{t_D}{C_D}\frac{dp_D}{d(t_D/C_D)} = \frac{t_D\,p'_D}{C_D} \tag{A-5}$$

where: p'_D = dimensionless pressure derivative.

These curves are plotted on the same log-log graphs as the type curves of Gringarten et al. (1979), with the vertical axis now also labeled $(t_D/C_D)p'_D$ (Figure A-2). Again, each individual type curve is characterized by a

Figure A-2. Single-Porosity Type Curves and Pressure-Derivative Type Curves for Wells with Wellbore Storage and Skin

distinct value of $C_D e^{2s}$. Pressure-derivative type curves begin with an initial segment with unit slope corresponding to early-time wellbore storage and skin effects. This segment reaches a maximum that is proportional to the amount of wellbore storage and skin, and then the curve declines and stabilizes at a dimensionless pressure/semilog slope value of 0.5 corresponding to late-time, infinite-acting, radial flow.

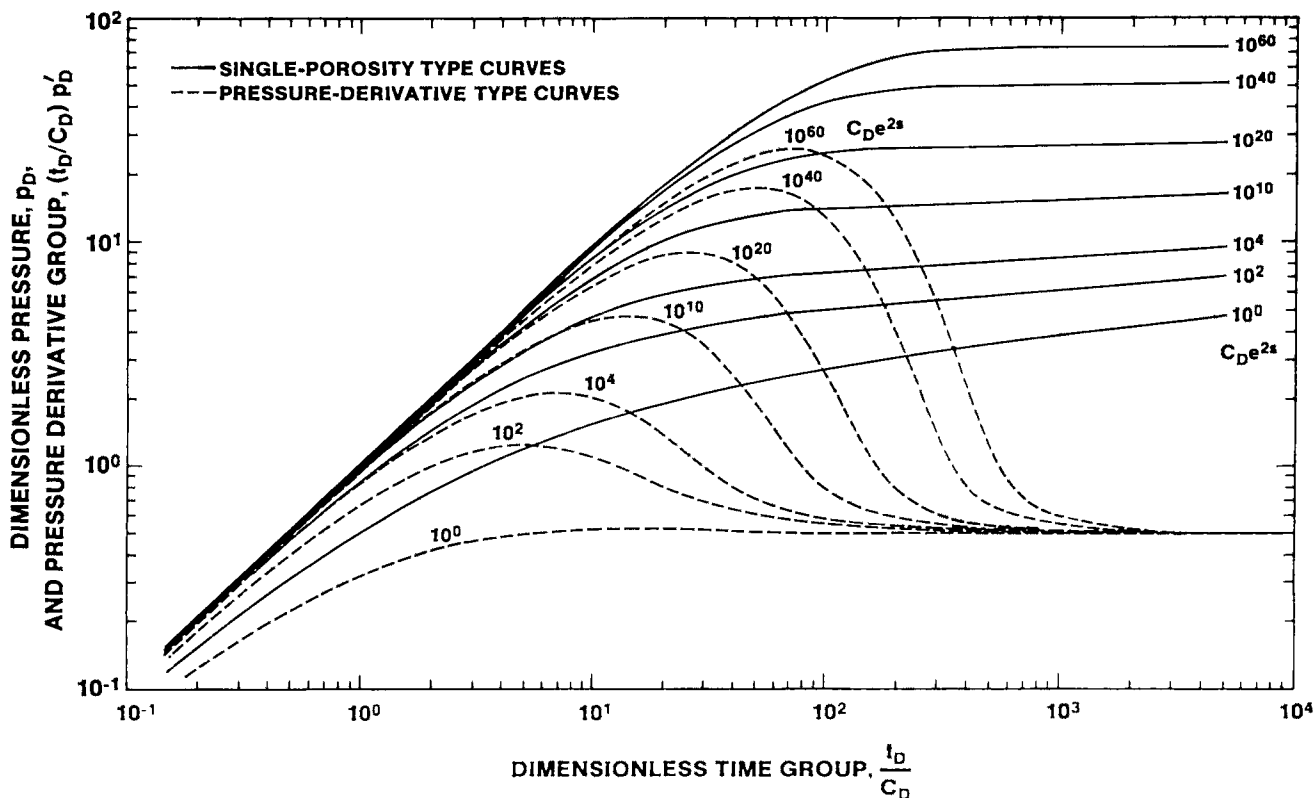Pressure-derivative data in combination with pressure data are much more sensitive indicators of double-porosity effects, boundary effects, nonstatic antecedent test conditions, and other phenomena than are pressure data alone. For this reason, pressure-derivative data are useful in choosing between conflicting conceptual models that often cannot be differentiated on the basis of pressure data alone. Pressure-derivative data are also useful in determining when infinite-acting, radial flow occurs during a test, because this condition causes the pressure derivative to stabilize at a constant value.

For any given point, the pressure derivative is calculated as the linear-regression slope of a semilog line fit through that point and any chosen number of neighboring points on either side. The equation for the derivative follows:

$$p' = \frac{n \sum_{i=1}^{n} x_i y_i - \sum_{i=1}^{n} x_i \sum_{i=1}^{n} y_i}{n \sum_{i=1}^{n} x_i^2 - \sum_{i=1}^{n} x_i^2} \qquad \text{(A-6)}$$

where, for a single constant-rate flow period:

n = number of points to be fitted

$x_i = \ln \Delta t_i$

$y_i = \Delta p_i$

Δt_i = elapsed test time at point i, hr

Δp_i = pressure change at Δt_i, psi.

For a multi-rate flow period or a buildup period, the time parameter is a superposition function calculated as:

$$x_i = \left\{ \sum_{i=1}^{n-1} (q_i - q_{i-1}) \log \left[\left(\sum_{j=1}^{n-1} \Delta t_j \right) + \Delta t \right] \right\} + (q_n - q_{n-1}) \log \Delta t \qquad \text{(A-7)}$$

where:

q = flow rate, BPD

Δt = elapsed time during a flow period, hr

with subscripts:

> i = individual flow period
> j = individual flow period
> n = number of flow periods considered.

In general, the fewer the number of points used in calculating the derivative, the more accurate it will be. Three-point derivatives, calculated using only the nearest neighbor on either side of a point, usually provide enough resolution to distinguish most important features. However, excessive noise in the data sometimes makes it necessary to use five- or seven-point derivatives, or various "windowing" procedures, to obtain a smooth curve. Unfortunately, these procedures may also smooth out some of the features of the curve needed for interpretation.

The type curves published by both Gringarten et al. (1979) and Bourdet et al. (1984) were derived for flow-period (drawdown) analysis. In general, the curves can also be used for buildup-period analysis, so long as it is recognized that, at late time, buildup data will fall below the drawdown type curves because of superposition effects.

If the test analysis is to be performed manually, the drawdown or buildup data are plotted as <u>pressure change</u> since drawdown or buildup began (Δp) versus <u>elapsed time</u> since drawdown or buildup began (t) on log-log paper of the same scale as the type curves. The derivative of the pressure change is also plotted using the same vertical axis as the Δp data. The data plot is then laid over the type curves and moved both laterally and vertically, so long as the axes remain parallel, until a match is achieved between the data and pressure and pressure-derivative curves with the same $C_D e^{2s}$ value. When the data fit the curves, an arbitrary match point is selected, and the coordinates of that point on both the data plot, t and Δp, and on the type-curve plot, p_D and t_D/C_D, are noted. The permeability-thickness product is then calculated from a rearrangement of Eq (A-1):

$$kh = 141.2qB\mu \ \frac{p_D}{\Delta p} \tag{A-8}$$

The groundwater-hydrology parameter transmissivity, T, is related to the permeability-thickness product by the following relationship, modified from Freeze and Cherry (1979):

$$T = kh\rho g/\mu \tag{A-9}$$

where:

> ρ = fluid density, M/L^3
> g = gravitational acceleration, L/T^2
> μ = fluid viscosity, M/LT

When T is given in ft^2/day, kh is given in millidarcy-feet, ρ is given in g/cm^3, g is set equal to 980.665 cm/s^2, and μ is given in centipoises, Eq (A-9) becomes:

$$T = 2.7435 \times 10^{-3} \ kh\rho/\mu \tag{A-10}$$

The wellbore storage coefficient is calculated from a rearrangement of Eq (A-4):

$$C = \frac{0.000295\ kht}{\mu t_D/C_D}$$

(A-11)

Finally, if estimates of porosity and total-system compressibility are available, the skin factor can be calculated from the value of the C_De^{2s} curve selected and Eq (A-3):

$$s = 0.5\ \ell n\ \left[\frac{C_De^{2s}}{0.8936C/\phi c_t\ hr_w{}^2} \right]$$

(A-12)

A.1.2 Double-Porosity Log-Log Analysis

Double-porosity media have two porosity sets that differ in terms of storage volume and permeability. Typically, the two porosity sets are (1) a fracture network with higher permeability and lower storage, and (2) the primary porosity of the rock matrix with lower permeability and higher storage (Gringarten, 1984). During a hydraulic test, these two porosity sets respond differently. With high-quality test data, the hydraulic parameters of both porosity sets can be quantified.

During a hydraulic test in a double-porosity medium, the fracture system responds first. Initially, most of the water pumped comes from the fractures, and the pressure in the fractures drops accordingly. With time, the matrix begins to supply water to the fractures, causing the fracture pressure to stabilize and the matrix pressure to decrease. As the pressures in the fractures and matrix equalize, both systems produce water to the well. The total-system response is then observed for the balance of the test.

The initial fracture response and the final total-system response both follow the single-porosity type curves described above. By simultaneously fitting the fracture response and the total-system response to two different C_De^{2s} curves, fracture-system and total-system properties can be derived. Information on the matrix, and additional information on the fracture system, can be obtained by interpretation of the data from the transition period when the matrix begins to produce to the fractures. Two different sets of type curves can be used to try to fit the transition-period data.

Transition-period data are affected by the nature, or degree, of interconnection between the matrix and the fractures. Warren and Root (1963) published the first line-source solution for well tests in double-porosity systems. They assumed that flow from the matrix to the fractures (interporosity flow) occurred under pseudosteady-state conditions; that is, that the flow between the matrix and the fractures was directly proportional to the average head difference between those two systems. Other authors, such as Kazemi (1969) and de Swaan (1976), derived solutions using the diffusivity equation to govern interporosity flow. These are known as transient interporosity flow solutions. Mavor and Cinco-Ley (1979) added wellbore storage and skin to the double-porosity solution, but still used pseudosteady-state interporosity flow. Bourdet and Gringarten (1980) modified Mavor and Cinco-Ley's (1979) theory to include transient interporosity flow, and generated type curves for double-porosity systems with both pseudosteady-state and transient interporosity flow.

Pseudosteady-state and transient interporosity flow represent two extremes; all intermediate behaviors are also possible. Gringarten (1984), however, states that the majority of tests he has seen exhibit pseudosteady-state interporosity flow behavior.

In recent years, Gringarten (1984, 1986) has suggested that the terms "restricted" and "unrestricted" interporosity flow replace the terms "pseudosteady-state" and "transient" interporosity flow. He believes that all interporosity flow is transient in the sense that it is governed by the diffusivity equation. But in the case where the fractures possess a positive skin (caused, for example, by secondary mineralization on the fracture surfaces) similar to a wellbore skin that restricts the flow from the matrix to the fractures, the observed behavior is similar to that described by the pseudosteady-state formulation (Moench, 1984; Cinco-Ley et al., 1985). "Transient" interporosity flow is observed when there are no such restrictions. Hence, the terms "restricted" and "unrestricted" more accurately describe conditions than do the terms "pseudosteady-state" and "transient." The recent terminology of Gringarten is followed in this report.

Restricted Interporosity Flow

Warren and Root (1963) defined two parameters to aid in characterizing double-porosity behavior. These are the storativity ratio, ω, and the interporosity flow coefficient λ. The storativity ratio is defined as:

$$\omega = \frac{(\phi V c_t)_f}{(\phi V c_t)_{f+m}} \qquad \text{(A-13)}$$

where:

ϕ = ratio of the pore volume in the system to the total-system volume

V = the ratio of the total volume of one system to the bulk volume

c_t = total compressibility of the system

with subscripts:

f = fracture system

m = matrix.

The interporosity flow coefficient is defined as:

$$\lambda = \alpha r_w^2 \frac{k_m}{k_f} \qquad \text{(A-14)}$$

where α is a shape factor characteristic of the geometry of the system and other terms are as defined above.

The shape factor, α, is defined as:

$$\alpha = \frac{4n(n+2)}{\ell^2} \qquad \text{(A-15)}$$

where:

n = number of normal sets of planes limiting the matrix

ℓ = characteristic dimension of a matrix block (ft).

Bourdet and Gringarten (1980) constructed a family of transition type curves for restricted interporosity flow on the same axes as the $C_D e^{2s}$ curves of Gringarten et al. (1979), with each transition curve characterized by a distinct value of the parameter λe^{-2s}. Together, the single-porosity type curves and the transition type curves make up the double-porosity type curves. (Figure A-3).

Figure A-3. Double-Porosity Type Curves for Wells with Wellbore Storage, Skin, and Restricted Interporosity Flow

In manual double-porosity type-curve matching, a log-log plot of the data is prepared as in single-porosity type-curve matching. The data plot is then laid over the double-porosity type curves and moved both laterally and vertically, keeping the axes parallel, until (1) the early-time (fracture-flow only) data fall on one $C_D e^{2s}$ curve, (2) the middle portion of the transition data falls on a λe^{-2s} curve, and (3) the late-time (total-system) data fall on a lower $C_D e^{2s}$ curve. In computer-aided analysis, pressure-derivative curves for double-porosity systems may also be prepared (Gringarten, 1986). The number of possible curve combinations, however, precludes preparation of generic pressure-derivative curves for manual double-porosity curve fitting.

When a match between the data plot and a type curve is achieved, an arbitrary match point is selected, and the coordinates of that point on both the data plot, t and Δp, and the type-curve plot, t_D/C_D and p_D, are noted. The values of $C_D e^{2s}$ and λe^{-2s} of the matched curves are also noted. The permeability-thickness product of the fracture system (and also of the total system because fracture permeability dominates) and the wellbore storage coefficient are calculated from Eqs (A-8) and (A-11). The storativity ratio, ω, is calculated from:

$$\omega = \frac{(C_D e^{2s})_{f+m}}{(C_D e^{2s})_f}$$

(A-16)

The dimensionless wellbore storage coefficient for the matrix is calculated as:

$$(C_D)_m = \frac{0.8936\, C}{(V\phi c_t)_m\, h r_w^2}$$

(A-17)

This leads to the dimensionless wellbore storage coefficient for the total system:

$$(C_D)_{f+m} = (C_D)_m \times (1-\omega)$$

(A-18)

Then the skin factor is calculated as:

$$s = 0.5\, \ell n \left[\frac{(C_D e^{2s})_{f+m}}{(C_D)_{f+m}} \right]$$

(A-19)

The interporosity flow coefficient is calculated from:

$$\lambda = \frac{\lambda e^{-2s}}{e^{-2s}}$$

(A-20)

If matrix permeability and geometry are known independently, Eqs (A-14) and (A-15) can be used to determine the effective dimensions of the matrix blocks.

Unrestricted Interporosity Flow

Matrix geometry is more important for unrestricted interporosity flow than for restricted interporosity flow, because the former is governed by the diffusivity equation. A different set of type curves is used, therefore, to match transition-period data when unrestricted interporosity flow conditions exist (Figure A-4). Bourdet and Gringarten (1980) characterize each curve with a different value of the parameter β, the exact definition of which is a function of the matrix geometry. For example, for slab-shaped matrix blocks, they give:
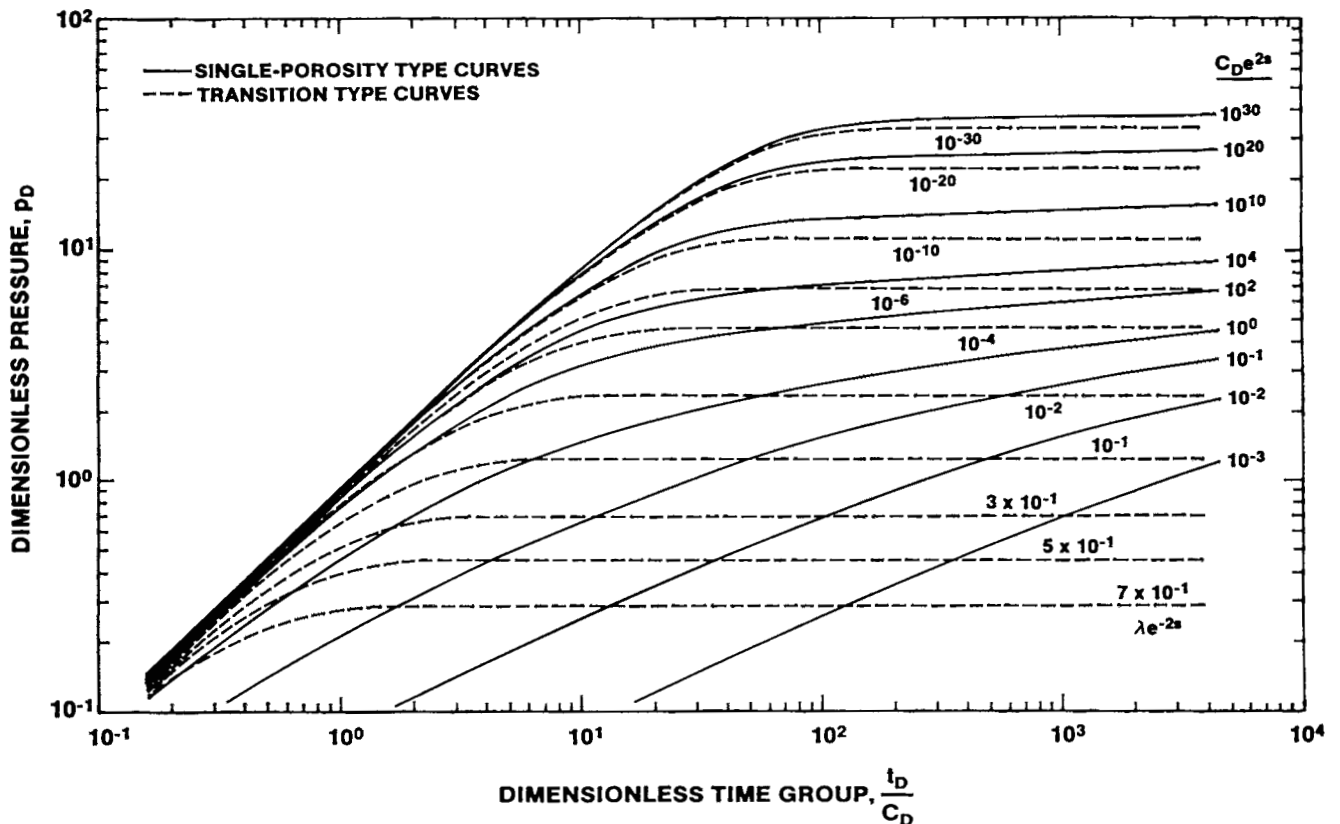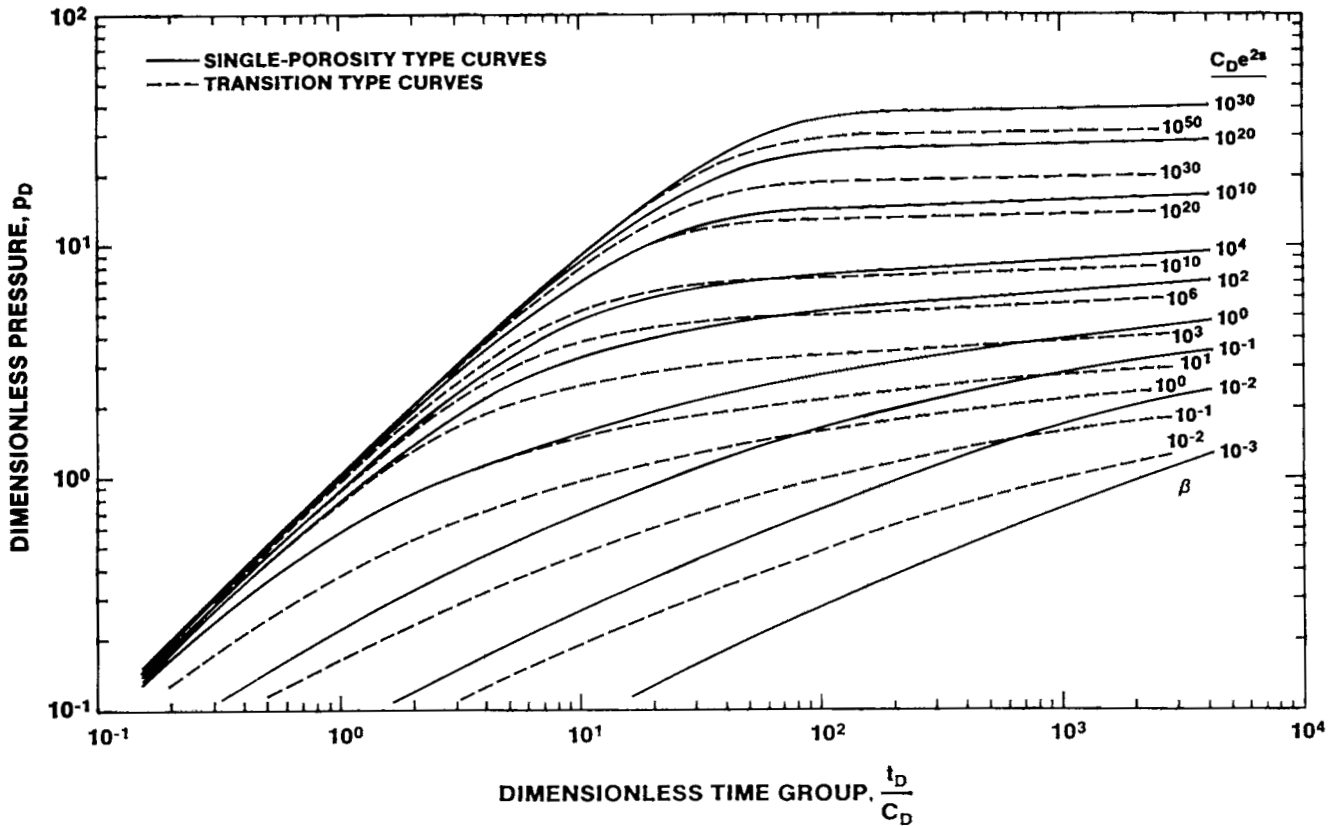
Figure A-4. Double-Porosity Type Curves for Wells with Wellbore Storage, Skin, and Unrestricted Interporosity Flow

$$\beta = \frac{6}{\gamma^2} \frac{(C_D e^{2s})_{f+m}}{\lambda e^{-2s}} \tag{A-21}$$

and for spherical blocks they give:

$$\beta = \frac{10}{3\gamma^2} \frac{(C_D e^{2s})_{f+m}}{\lambda e^{-2s}} \tag{A-22}$$

where: γ = exponential of Euler's constant (=1.781).

Moench (1984) provides an extensive discussion on the effects of matrix geometry on unrestricted interporosity flow.

Manual double-porosity type-curve matching with unrestricted-interporosity-flow transition curves is performed in exactly the same manner as with restricted-interporosity-flow transition curves, described above.

The same equations are used to derive the fracture and matrix parameters, except that the matrix geometry must now be known or assumed to obtain the interporosity flow coefficient, λ, from rearrangement of Eq (A-21) or (A-22).

A.1.3 Semilog Analysis

Two semilog plotting techniques were employed in this report to interpret pumping-test and DST-buildup data. These techniques produce a Horner plot and a dimensionless Horner plot.

Horner Plot

Horner (1951) provided a method of obtaining permeability and static formation pressure values independent of log-log type-curve matching, although the two methods are best used in conjunction. Horner's method applies to the buildup (recovery) of the pressure after a constant-rate flow period in a well that fully penetrates a homogeneous, isotropic, horizontal, infinite, confined reservoir. For a recovery after a single flow period, Horner's solution is:

$$p(t) = p^* - \frac{162.6qB\mu}{kh} \log \left[\frac{t_p + dt}{dt} \right] \tag{A-23}$$

where:

$p(t)$ = pressure at time t, psi
p^* = static formation pressure, psi
t_p = duration of previous flow period, hr
dt = time elapsed since end of flow period, hr

and other terms are as defined above under Eq (A-4). For a recovery after multiple flow periods, the time group in Eq (A-23) is replaced by the superposition function given in the right-hand side of Eq (A-7).

The permeability-thickness product (kh) is obtained by (1) plotting $p(t)$ versus log $[(t_p + dt)/dt]$ (or the superposition function), (2) drawing a straight line through the data determined from the log-log pressure-derivative plot to be representative of infinite-acting radial flow, and (3) measuring the change in $p(t)$ on this line over one log cycle of time (m). Equation (A-23) can then be rearranged and reduced to:

$$kh = 162.6 \, qB\mu/m. \tag{A-24}$$

Static formation pressure is estimated by extrapolating the radial-flow straight line to the pressure axis where log $[(t_p + dt)/dt] = 1$, representing infinite recovery time. In the absence of reservoir boundaries, the pressure intercept at that time should equal the static formation pressure.

Horner (1951) also suggested a modification of his method for the case where the flow rate was not held constant. This modification was later theoretically verified for the case of constant-pressure, variable-rate production by Ehlig-Economides (1979). The modification entails calculating a modified production time:

$$t_p^* = V/q_f \tag{A-25}$$

where:

V = total flow produced, bbl

q_f = final flow rate, bbl/hr.

The modified production time, t_p^*, is substituted for the actual production time, t_p, in Eq (A-23), and the analysis proceeds as before. The modified production time can also be used for calculation of buildup type curves for log-log analysis.

Dimensionless Horner Plot

The dimensionless Horner plot represents a second useful semilog approach to hydraulic-test interpretation. Once type-curve and match-point selections have been made through log-log analysis, this technique allows the single- or double-porosity $C_D e^{2s}$ type curves to be superimposed on a normalized semilog plot of the data. Logarithmic dimensionless times for the data are calculated using:

$$\frac{q_{n-1} - q_n}{|q_{n-1} - q_n|} \left[\sum_{i=1}^{n-1} \frac{q_i - q_{i-1}}{q_{n-1} - q_n} \; \log \left(\sum_{j=1}^{n-1} \Delta t_j + \Delta t \right) - \log \Delta t \right] \tag{A-26}$$

where all parameters are as defined above. The dimensionless times calculated using Eq (A-26) are plotted on a linear scale. Dimensionless pressures for the data are calculated using:

$$\frac{p_D}{\Delta p} [p^* - p(t)] \tag{A-27}$$

where p_D and Δp are the log-log match-point coordinates, and the other parameters are as defined above. Dimensionless pressures are also plotted on a linear scale.

The type curves are plotted on the same axes with dimensionless time defined as:

$$\frac{q_{n-1} - q_n}{|q_{n-1} - q_n|} \left[\sum_{i=1}^{n-1} \frac{q_i - q_{i-1}}{q_n - q_{n-1}} \; \log \left(\sum_{j=1}^{n-1} \Delta t_j + \Delta t \right) - \log \Delta t \right] \tag{A-28}$$

and dimensionless pressure defined as:

$$\frac{q_{n-1} - q_n}{|q_{n-1} - q_n|} \left[\sum_{i=1}^{n-1} \frac{q_i - q_{i-1}}{q_n - q_{n-1}} \; p_D \left(\sum_{j=1}^{n-1} \Delta t_j + \Delta t \right)_D - p_D (\Delta t)_D \right] \tag{A-29}$$

The dimensionless Horner plot is a very sensitive indicator of inaccuracies in type-curve, match-point, and static-formation-pressure selections (Gringarten, 1986). By iterating between dimensionless Horner and log-log plots, very accurate hydraulic parameters can be obtained.

A.2 SLUG-TEST AND DST FLOW-PERIOD DATA ANALYSIS

Slug-test and DST flow-period data were analyzed using a method first presented by Cooper et al. (1967) for slug tests, and adapted to DST's by Ramey et al. (1975). The method is used for calculating the transmissivity of a homogeneous, isotropic, confined porous medium of uniform thickness which is fully penetrated by a well. To initiate a slug test, a pressure differential is established between the wellbore and the surrounding formation by shutting in the test interval, swabbing the fluid from the tubing (in the case of a rising-head or slug-withdrawal test) or adding fluid to the tubing (in the case of a falling-head or slug-injection test), and then opening the test interval to the tubing. The problem is described mathematically in radial geometry by the diffusivity equation:

$$\frac{\partial^2 h}{\partial r^2} + \frac{1}{r}\frac{\partial h}{\partial r} = \frac{S}{T}\frac{\partial h}{\partial t} \tag{A-30}$$

where in consistent units:

> h = hydraulic head differential (at radius r and time t), L
> r = radius from well center, L
> t = elapsed time, T
> S = formation storativity
> T = formation transmissivity, L^2/T.

This equation describes nonsteady, radial flow of groundwater.

The solution to this equation utilized for analysis of slug-test (or DST flow-period) data is presented in the form of curves of $[H/H_o]$ (Figure A-5) and $[(H_o-H)/H_o]$ (Figure A-6) versus the dimensionless time parameter β for each of several values of α, where in consistent units:

$$\beta = Tt/r_c^2 \tag{A-31}$$

$$\alpha = r_s^2 S/r_c^2 \tag{A-32}$$

and

> H_o = initial (maximum) head differential, L
> H = head differential at time t, L
> t = time elapsed since test began, T
> r_s = radius of borehole, L
> r_c = inside radius of tubing string, L.

Plots of the quantities $[H/H_o]$ and $[(H_o-H)/H_o]$ versus t are made on semilog and log-log paper, respectively, of the same scale as the type curves. Semilog plotting and type curves are best used when a minimum of about
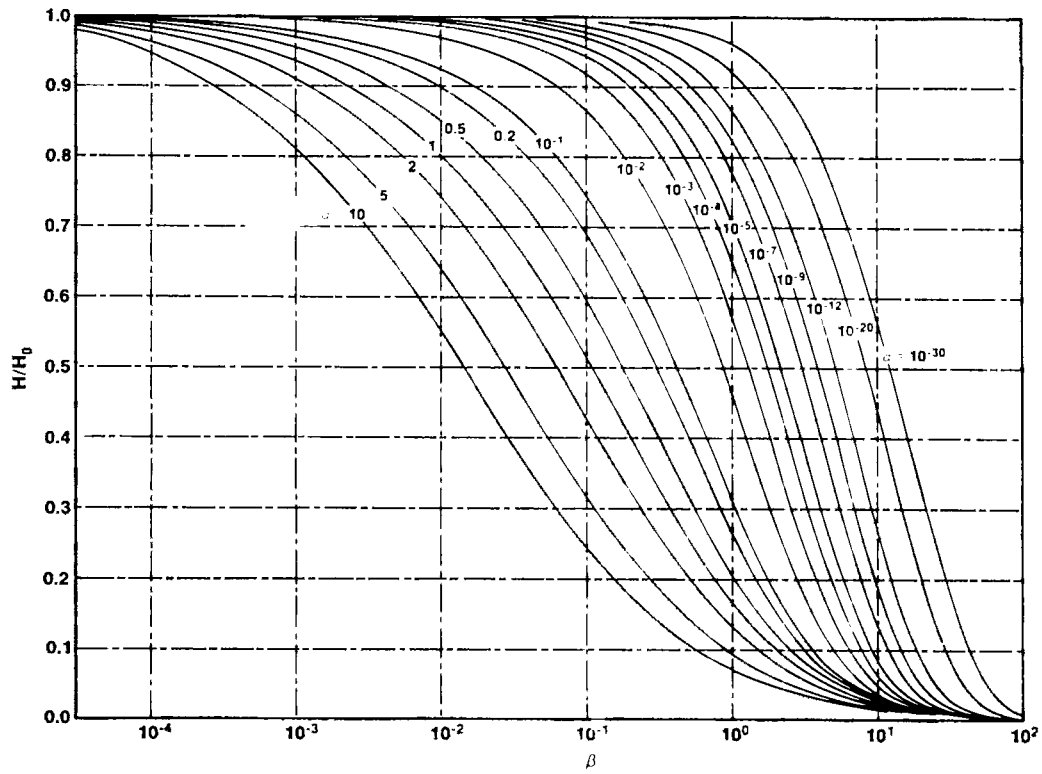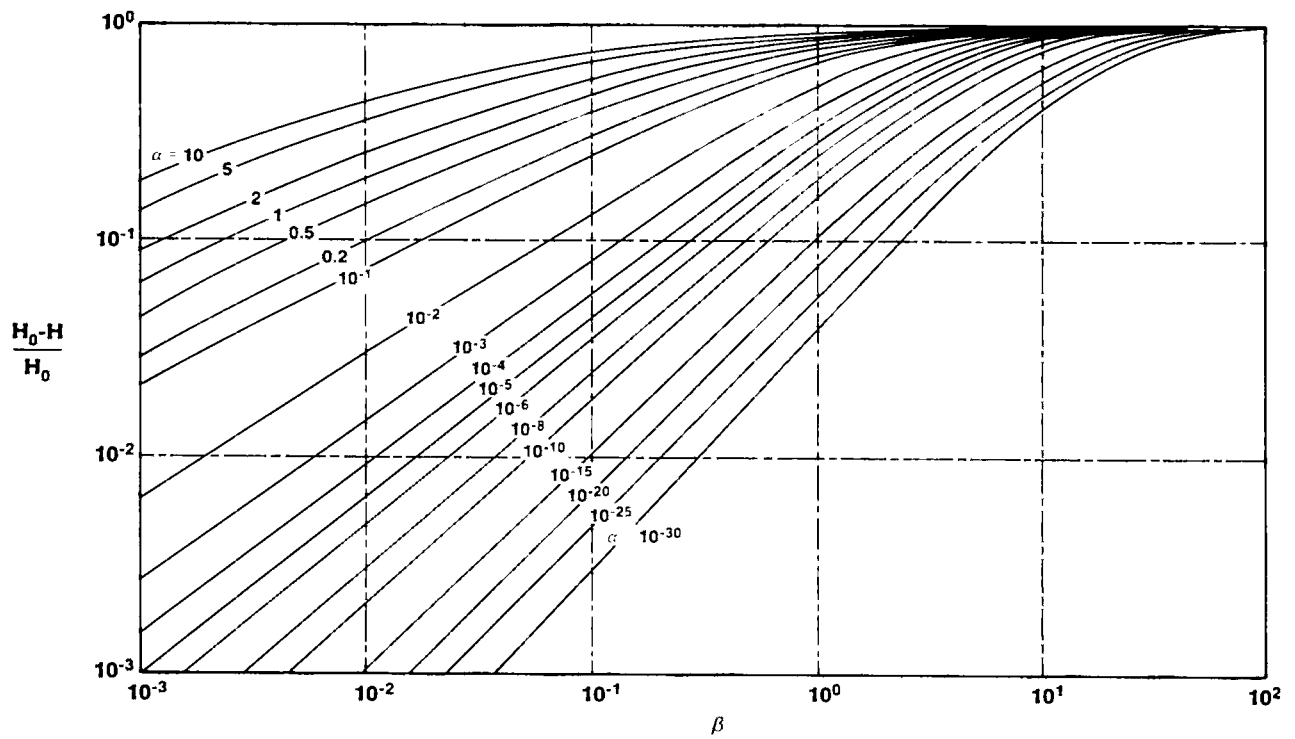
Figure A-5.   Semilog Slug-Test Type Curves

Figure A-6.   Early-Time Log-Log Slug-Test Curves

seventy percent recovery has occurred. For lesser degrees of recovery, log-log plotting techniques provide a more definitive type-curve match (Ramey et al., 1975). The type curves are placed over the test-data plots and translated horizontally with the horizontal axes coincident until the best possible match between the data and one of the type curves is achieved. In this position an arbitrary match point is chosen, and the corresponding values of α and β are read from the type curve, and t is read from the data plot. The transmissivity (T) is then calculated from the following rearrangement of Eq (A-31), using the coordinates of the match point:

$$T = \frac{r_c^2 \beta}{t} \qquad \text{(A-33)}$$

The vertically averaged hydraulic conductivity, K, can be calculated from:

$$K = T/b \qquad \text{(A-34)}$$

where: b = thickness of tested interval, L.

When static formation pressures are unknown, they may be approximated from flow-period or slug tests in the following manner. A log-log plot of $(H_o-H)/H_o$ versus elapsed time is prepared, using a "best-guess" value of the static formation pressure to calculate H_o and H. At late time, the data should become asymptotic to the $(H_o-H)/H_o$ value of 1.0. If the data become asymptotic to a lower value, the "best-guess" static formation pressure estimate was too high and should be revised downward. If the data exceed the $(H_o-H)/H_o$ value of 1.0, the estimate was too low and should be revised upward. In general, Horner extrapolations of buildup data, when possible, provide greater resolution in estimating static formation pressures than do slug-test interpretations.

A.3   PRESSURE-PULSE TEST ANALYSIS

Pressure-pulse tests were first described by Bredehoeft and Papadopulos (1980). The solution technique is very similar to that developed by Cooper et al. (1967) for slug tests. The only difference between the two methods is that in a slug test the water level changes in a tubing string of radius r_c, while in a pressure-pulse test water is only compressed in an isolated interval of the borehole. Analytically, the solution technique for pressure-pulse tests is the same as that derived for slug tests with the r_c^2 terms in Eqs (A-31), (A-32), and (A-33) replaced by $V_w C_w \rho_w g/\pi$, where in consistent units:

V_w = volume of water within the pressurized section of the system, L^3
C_w = compressibility of water, LT^2/M
ρ_w = density of water, M/L^3
g = gravitational acceleration, L/T^2.

With this substitution, and subject to the constraint that $\alpha \leq 0.1$ [see Eq (A-32)], the analysis proceeds as described above under Section A.2, Slug-Test Analysis.

A.4 INTERPRET WELL-TEST INTERPRETATION CODE

Manual type-curve fitting is a time-consuming process limited by the published type curves available, and by the degree of resolution/differentiation obtainable in manual curve fitting. The pumping-test and buildup analyses presented in this report were not performed manually, but by using the well-test analysis code INTERPRET developed by A.C. Gringarten and Scientific Software-Intercomp (SSI). INTERPRET is a proprietary code that uses analytical solutions. It can be leased from SSI.

INTERPRET can analyze drawdown (flow) and recovery (buildup) tests in single-porosity, double-porosity, and fractured media. It incorporates the analytical techniques discussed above, and additional techniques discussed in Gringarten et al. (1974), Bourdet and Gringarten (1980), and Gringarten (1984). Rather than relying on a finite number of drawdown type curves, INTERPRET calculates the precise drawdown or buildup type curve corresponding to the match point and data point selected by the user.

After type-curve selection, INTERPRET simulates the test with the chosen parameters so that the user can see how good the match truly is. Through an iterative parameter-adjustment process, the user fine-tunes the simulation until satisfied with the results. Log-log and semilog (Horner and dimensionless Horner) plotting techniques are employed in a cross-checking procedure to ensure consistency of the final model with the data in every respect. Once the final model is selected, INTERPRET calculates final parameter values. Analyses obtained using INTERPRET have been verified by manual calculations.

In addition to standard type-curve analysis, INTERPRET allows the incorporation of constant-pressure and no-flow boundaries in analysis, using the theory of superposition and image wells discussed by Ferris et al. (1962). A constant-pressure boundary can be simulated by adding a recharge (image) well to the model. A no-flow boundary can be simulated by adding a discharge (image) well to the model. Drawdowns and rises from multiple discharge and recharge wells are additive.

In INTERPRET, an image well (either discharge or recharge) is included by specifying a dimensionless distance for the image well from the production well, and by using the line-source solution of Theis (1935) to calculate the drawdown or recovery caused by that well at the production well. Theis (1935) derived an exponential integral (Ei) solution for drawdown caused by a line-source well in a porous medium:

$$p_D = -0.5 \, Ei(-r_D^2/4t_D) \tag{A-35}$$

where:

$$\frac{t_D}{r_D^2} = \frac{0.000264 \, kht}{\phi \mu c_t hr^2} \tag{A-36}$$

The terms p_D and t_D are defined by Eqs (A-1) and (A-2), respectively; other terms are as defined above in Section A.1.1.

160

The dimensionless distance from the production well to the image well is related to the "actual" distance to the image well, r_i, by the following:

$$r_i = r_w \sqrt{C_D D_D}$$

where: D_D = dimensionless distance

and other terms are as defined above. The actual hydraulic boundary is then half of the distance from the production well to the image well.

DISTRIBUTION:

U. S. Department of Energy (5)
Office of Civilian Radioactive Waste Management
Office of Geologic Repositories
Forrestal Building
Washington, DC 20585
   Stephen H. Kale - RW-20
      Associate Director
   T. H. Isaacs - RW-20
      Deputy Associate Director
   James C. Bresee - RW-22
      Director, Repository
        Coordination Div.
   Ralph Stein - RW-23
      Director, Engineering &
        Geotechnology
   James P. Knight - RW-24
      Director, Siting, Licensing
        and Quality Assurance

U. S. Department of Energy (3)
Albuquerque Operations Office
P.O. Box 5400
Albuquerque, NM 87185
   R. G. Romatowski
   J. E. Bickel
   D. G. Jackson
      Public Affairs Division

U. S. Department of Energy/AL
Attn: National Atomic Museum Librarian
P.O. Box 5400
Albuquerque, NM 87185

U. S. Department of Energy (6)
WIPP Project Office (Carlsbad)
P.O. Box 3090
Carlsbad, NM 88221
   J. Tillman
   A. Hunt
   T. Lukow (2)
   V. Daub
   B. Young

U. S. Department of Energy, SRPO (4)
Salt Repository Project Office
110 N. 25 Mile Avenue
Hereford, TX 79045
   J. O. Neff
   R. Wunderlich
   G. Appel
   R. Wu

U. S. Department of Energy
Research & Technical Support Division
P.O. Box E
Oak Ridge, TN 37830
   D. E. Large

U. S. Department of Energy
Richland Operations Office
Nuclear Fuel Cycle & Production
   Division
P.O. Box 500
Richland, WA 99352
   R. E. Gerton

U. S. Department of Energy (5)
Office of Defense Waste and
   Transportation Management
Washington, DC 20545
   G. Daly ———— DP-121
   M. Duff ———— DP-121
   A. Follett ——— DP-121
   J. Mather ——— DP-121

U. S. Department of Energy (2)
Idaho Operations Office
Fuel Processing and Waste
   Management Division
785 DOE Place
Idaho Falls, ID 83402

U. S. Department of Energy (4)
Savannah River Operations Office
Waste Management Project Office
P.O. Box A
Aiken, SC 29801
    S. Cowan
    W. J. Brumley
    J. R. Covell
    D. Fulmer

U. S. Nuclear Regulatory Commission (4)
Division of Waste Management
Mail Stop 623SS
Washington, DC 20555
    M. Bell
    H. Miller
    J. Philip
    NRC Library

U. S. Geological Survey
Branch of Regional Geology
MS913, Box 25046
Denver Federal Center
Denver, CO 80225
    R. Snyder

U. S. Geological Survey (2)
Water Resources Division
Suite 200
4501 Indian School, NE
Albuquerque, NM. 87110
    C. Peters
    P. Davies

State of New Mexico (3)
Environmental Evaluation Group
P.O. Box 968
Santa Fe, NM 87503
    R. H. Neill, Director

NM Department of Energy & Minerals
P.O. Box 2770
Santa Fe, NM 87501
    K. LaPlante, Librarian

New Mexico Bureau of Mines
   and Mineral Resources (2)
Socorro, NM 87801
    F. E. Kottolowski, Director
    J. Hawley

Battelle Pacific Northwest Laboratories (6)
Battelle Boulevard
Richland, WA 99352
    D. J. Bradley
    J. Relyea
    R. E. Westerman
    S. Bates
    H. C. Burkholder
    L. Pederson

Battelle Memorial Institute (13)
Project Management Division
P.O. Box 2360
Hereford, TX 79045
    ONWI Library
    W. Carbiener, General Manager (3)
    V. Adams
    S. Gupta
    J. Kirchner
    A. LaSala
    T. Naymik
    W. Newcomb
    A. Razem
    O. Swanson
    J. Treadwell

Bechtel Inc. (2)
P.O. Box 3965
45-11-B34
San Francisco, CA 94119
    E. Weber
    H. Taylor

New Mexico State Engineers Office
District II, 909 E. Second
P.O. Box 1717
Roswell, NM 88201
    A. Mason

INTERA Technologies, Inc. (9)
6580 Austin Center Blvd., #300
Austin, TX 78731
    G. E. Grisak
    J. F. Pickens
    G. J. Saulnier
    V. A. Kelley
    A. Haug
    A. M. LaVenue
    M. Reeves
    T. L. Cauffman
    Library

INTERA Technologies, Inc.
P.O. Box 2123
Carlsbad, NM 88221
    W. Stensrud

IT Corporation (3)
P.O. Box 2078
Carlsbad, NM 88221
    R. McKinney
    M. Crawley
    D. Deal

IT Corporation (3)
Suite 306
2340 Alamo, SE
Albuquerque, NM 87106
    W. E. Coons
    S. Niou
    J. Myers

RE/SPEC, Inc.
P.O. Box 725
Rapid City, SD 57709
    P. F. Gnirk

RE/SPEC, Inc.
P.O. Box 14984
Albuquerque, NM 87191
    S. W. Key

SAIC
101 Convention Center Dr.
Las Vegas, NV 89109
    G. Dymmel

Systems, Science, and Software (2)
Box 1620
La Jolla, CA 92038
    E. Peterson
    P. Lagus

University of Arizona
Department of Nuclear Engineering
Tucson, AZ 85721
    J. G. McCray

University of New Mexico (2)
Geology Department
Albuquerque, NM 87131
    D. G. Brookins
    Library

The Pennsylvania State University
Materials Research Laboratory
University Park, PA 16802
    D. Roy

Texas A&M University
Center of Tectonophysics
College Station, TX 77840
    J. Handin

University of Texas at El Paso
Department of Geological Sciences
El Paso, TX 79968
    D. W. Powers

Westinghouse Electric Corporation (7)
P.O. Box 2078
Carlsbad, NM 88221
    Library
    W. Moffitt
    V. DeJong
    W. Chiquelin
    T. Dillon
    V. Likar
    R. Kehrman

National Academy of Sciences,
  WIPP Panel:

Dr. Konrad B. Krauskopf, Chairman
Department of Geology
Panama Street
Stanford University
Stanford, CA 94305

Dr. Frank L. Parker
Department of Environmental and
    Water Resources Engineering
Vanderbilt University
Nashville, TN 37235

Dr. John O. Blomeke
Oak Ridge National Laboratory
P.O. Box X
Oak Ridge, TN 37830

Dr. John D. Bredehoeft
Western Region Hydrologist
Water Resources Division
U. S. Geological Survey
345 Middlefield Road
Menlo Park, CA 94025

Dr. Karl P. Cohen
928 N. California Avenue
Palo Alto, CA 94303

Dr. Fred M. Ernsberger
250 Old Mill Road
Pittsburgh, PA 15238

Dr. Rodney C. Ewing
Department of Geology
University of New Mexico
200 Yale, NE
Albuquerque, NM 87131

Dr. Charles Fairhurst
Department of Civil and Mineral Engineering
University of Minnesota
500 Pillsbury Dr. SE
Minneapolis, MN 55455

Dr. William R. Muehlberger
Department of Geological Sciences
University of Texas at Austin
P.O. Box 7909
Austin, TX 78712

Dr. D'Arcy A. Shock
233 Virginia
Ponca City, OK 74601

Dr. Peter B. Meyers, Staff Director
National Academy of Sciences
Committee on Radioactive Waste Management
2101 Constitution Avenue
Washington, DC 20418

Ms. Remi Langum
Staff Officer
Board on Radioactive Waste Management
GF462
2101 Constitution Avenue
Washington, D.C. 20418

Hobbs Public Library
509 N. Ship Street
Hobbs, NM 88248
      M. Lewis, Librarian

New Mexico Tech
Martin Speere Memorial Library
Campus Street
Socorro, NM 87810

New Mexico State Library
P.O. Box 1629
Santa Fe, NM 87503
      I. Vollenhofer

Zimmerman Library
University of New Mexico
Albuquerque, NM 87131
      Z. Vivian

WIPP Public Reading Room
Atomic Museum
Kirtland East AFB
Albuquerque, NM 87185
      G. Schreiner

WIPP Public Reading Room
Carlsbad Municipal Library
101 S. Halagueno St.
Carlsbad, NM 88220
    L. Hubbard, Head Librarian

Thomas Brannigan Library
106 W. Hadley St.
Las Cruces, NM 88001
    D. Dresp, Head Librarian

Roswell Public Library
301 N. Pennsylvania Avenue
Roswell, NM 88201
    N. Langston

Svensk Karnbransleforsorjning AB
Project KBS
Karnbranslesakerhet
Box 5864
10248 Stockholm, SWEDEN
    F. Karlsson

Institut fur Tieflagerung (4)
Theodor-Heuss-Strasse 4
D-3300 Braunschweig
FEDERAL REPUBLIC OF GERMANY
    K. Kuhn

Bundesanstalt fur Geowissenschaften
    und Rohstoffe
Postfach 510 153
3000 Hannover 51
FEDERAL REPUBLIC OF GERMANY
    M. Langer

Hahn-Mietner-Institut fur Kernforschung
 Glienicker Strasse 100
100 Berlin 39
FEDERAL REPUBLIC OF GERMANY
    W. Lutze

Bundesministerium fur Forschung und
    Technologie
Postfach 200 706
5300 Bonn 2
FEDERAL REPUBLIC OF GERMANY
    Rolf-Peter Randl

Physikalisch-Technische Bundesanstalt
Postfach 33 45
D-3300 Braunschweig
FEDERAL REPUBLIC OF GERMANY
    P. Brenneke

Kernforschug Karlsruhe
Postfach 3640
7500 Karlsruhe
FEDERAL REPUBLIC OF GERMANY
    K. D. Closs

Attomic Energy of Canada, Ltd. (4)
Whiteshell Nuclear Research Establishment
Pinewa, Manitoba, CANADA
ROE 1L0
    P. Haywood
    J. Tait
    C. C. Davison
    D. Stevenson

Studiecentrum Voor Kernenergie (1)
Centre D'Energie Nucleaire
SCK/CEN
Boeratang 200
B-2400 Mol
BELGIUM
    A. Bonne

Ontario Hydro Research Lab
800 Kipling Avenue
Toronto, Ontario, CANADA
M8Z 5S4
    D. K. Mukerjee

Centre D'Etudes Nucleaires
    De La Vallee Rhone
CEN/VALRHO
S.D.H.A. BP 171
30205 Bagnols-Sur-Ceze
FRANCE
    C. Sombret

OECD Nuclear Energy Agency
Division of Radiation Protection
    and Waste Management
38, Boulevard Suchet
75016 Paris, FRANCE
    J-P Olivier

Nationale Genossenschaft fur die
Lagerung Radioaktiver Abfalle (3)
Parkstrasse 23
CH5401 Baden
SWITZERLAND
P. Hufschmied
C. McCombie
M. Thury

Argonne National Laboratory
9700 South Cass Avenue
Argonne, IL 60439
D. Hambeley

Brookhaven National Laboratory
Associated Universities, Inc.
Upton, NY 11973
P. W. Levy, Senior Scientist

Los Alamos National Laboratory
Los Alamos, NM 87545
B. Erdal, CNC-11

Oak Ridge National Laboratory (4)
Box Y
Oak Ridge, TN 37830
R. E. Blanko
E. Bondietti
C. Claiborne
G. H. Jenks

Oak Ridge National Laboratory
Building 2001
Ecological Sciences Information Center
P.O. Box X
Oak Ridge, TN 37830
C. S. Fore

Rockwell International
Rocky Flats Plant
Golden, CO 80401
C. E. Wickland

Rockwell International (3)
Atomics International Division
Rockwell Hanford Operations
P.O. Box 800
Richland, WA 99352
J. Nelson (HWVP)
P. Salter
W. W. Schultz

National Ground Water Information Center
6375 Riverside Drive
Dublin, OH 43017
J. Bix

Sandia Internal:

1510	J. W. Nunziato		6331	A. L. Jensen
1520	C. W. Peterson		6331	S. J. Lambert
1521	R. D. Krieg		6331	K. L. Robinson
1521	H. S. Morgan		6331	M. D. Siegel
3141	S. A. Landenberger (5)		6332	L. D. Tyler
3151	W. L. Garner (3)		6332	J. C. Stormont
3154-1	C. H. Dalin, For: DOE/OSTI (8)		6332	Sandia WIPP Central Files (2)
6000	D. L. Hartley			(700HIND)
6230	W. C. Luth		6333	T. M. Schultheis
6232	W. R. Wawersik		6334	D. R. Anderson
6233	T. M. Gerlach		6334	K. Brinster
6253	D. A. Northrup		6334	L. Brush
6253	N. R. Warpinski		6334	R. L. Hunter
6300	R. W. Lynch		6334	M. G. Marietta
6310	T. O. Hunter		7100	C. D. Broyles
6312	F. W. Bingham		7110	J. D. Plimpton
6313	T. Blejwas		7120	M. J. Navratil
6314	J. R. Tillerson		7125	R. L. Rutter
6315	S. Sinnock		7125	J. T. McIlmoyle
6330	W. D. Weart		7130	J. O. Kennedy
6331	A. R. Lappin		7133	O. Burchett
6331	R. L. Beauheim		7133	J. W. Mercer
6331	D. J. Borns		7135	P. D. Seward
6331	M. M. Gonzales		8524	P. W. Dean (SNLL Library)